

# Bayesian MCMC Approach to the Multicomponent Volatility Jump augmented Models

Ahmed Djeddi

Doctor of Philosophy

University of York

Economics

July 2022



## Abstract

GARCH-MIDAS model of Engle et al. (2013) describes the volatility of daily returns as the product of a short term volatility component  $g_t$ , modelled by a Unit GARCH(1,1), and a long term component volatility  $\tau_t$  which is modelled by macroeconomic variable(s) which are observed at a lower frequency. This model has been applied extensively in volatility modelling using Maximum Likelihood Estimation (MLE) Method despite that little is known about its finite sample properties. In this thesis, we fill this gap, and extend it to other models such as EGARCH-MIDAS, and stochastic volatility models such as SVL-MIDAS and Heston-MIDAS models and their jump augmented versions to capture the leverage effect and the impact of rare events.

Results of our first contribution indicate that in sample and out sample performance of GARCH type MIDAS models depend on the specification  $g_t$  whereas  $\hat{\tau}_t$  is not sensitive to the choice of  $g_t$ ; our simulation and empirical studies suggest that whenever EGARCH(1,1), say, outperforms GARCH(1,1), EGARCH-MIDAS outperforms GARCH-MIDAS; and MLE estimate of GARCH-MIDAS, and EGARCH-MIDAS are not consistent when the returns series contain spikes or its volatility is highly persistent. These results led us to our second main contribution of estimating their parameters and those of their Jump augmented versions using Bayesian approach by overcoming the complexity of their posterior distributions by applying Metropolis Hasting simulation method. Our simulation and empirical studies indicate that our MCMC algorithms successfully capture the jump component and produce accurate estimates when MLE fails. Based on the findings of our first two contributions and the recognized out-performance of stochastic volatility models over GARCH type models, we developed SV-MIDAS, SVL-MIDAS, and Heston-MIDAS with their jump augmented extensions.

Our MCMC algorithms can be extended to more complex multicomponent volatility models to be considered in our future work.



## Acknowledgements

I am deeply indebted to my supervisors Professor Yongcheol Shin and Dr Paola Zerilli for their patience, guidance, and for having introduced me to MIDAS models and Stochastic Volatility models which were valuable for formulating my initial vague research proposal of developing new volatility models. I would like to thank Professor Shin for being so generous with his time in mentoring me to become rigorous by providing solid theoretical justification. I would like to thank Dr Paola Zerilli for having pushed me to deepen my knowledge on Bayesian methods by answering her long list of requests. In sum, I feel fortunate to have been supervised by Professor Yongcheol Shin and Dr Paola Zerilli.

I would like also to thank Professor Laura Coroneo for the helpful suggestions, useful discussions, and encouragement.

I would like to thank the Department of Economics and related studies for having given me the opportunity to gain a teaching experience as a Graduate Teaching Assistant.

Finally, I would like to thank my wife Fettouma for her understanding and moral support. My thanks go to my parents for having believed in me, and for their generous financial support.

Ahmed Djeddi,  
York,  
July 2022.



## **Declaration**

I declare that this thesis is a presentation of original work and I am the sole author. This work has not previously been presented for an award at this, or any other, University. All sources are acknowledged as References.





# Contents

<b>List of tables</b>	<b>xi</b>
<b>List of figures</b>	<b>xiii</b>
<b>1 Introduction</b>	<b>1</b>
1.1 Motivations and Scopes . . . . .	1
1.2 The summary of Chapter 2 . . . . .	3
1.3 The summary of Chapter 3 . . . . .	4
1.4 The summary of Chapter 4 . . . . .	5
<b>2 Asymmetric GARCH-MIDAS Models</b>	<b>7</b>
2.1 Introduction . . . . .	7
2.2 GARCH-MIDAS Models . . . . .	10
2.2.1 Symmetric GARCH-MIDAS model . . . . .	10
2.2.2 Asymmetric GJR-GARCH-MIDAS model . . . . .	12
2.3 The EGARCH-MIDAS Model . . . . .	13
2.3.1 Identification of the volatility components . . . . .	14
2.3.2 Statistical properties of GJR-GARCH-MIDAS and EGARCH-MIDAS . . . . .	15
2.4 QML Estimation . . . . .	17
2.5 Simulation study . . . . .	18
2.6 Empirical Application . . . . .	23
2.6.1 Benchmark estimation results . . . . .	24
2.6.2 In-sample fit comparison . . . . .	26
2.6.3 Out of sample forecast performance . . . . .	29
2.6.4 Conclusion . . . . .	31
2.7 Appendix 1 . . . . .	32
2.7.1 Proof of Propositions 1 and 2 . . . . .	32
2.7.2 Descriptive statistics of stock market returns and macroeconomic variables . . . . .	37
<b>3 Bayesian MCMC Approach to Asymmetric GARCH-MIDAS Models with Jump Components</b>	<b>45</b>
3.1 Introduction . . . . .	45
3.2 Generalised GARCH and EGARCH MIDAS Models . . . . .	47
3.2.1 MCMC algorithm for GJR-GARCH-MIDAS . . . . .	51
3.2.2 MCMC algorithm for EGARCH-MIDAS models . . . . .	55
3.3 Monte Carlo Simulation . . . . .	56
3.3.1 Experiment 1: the DGP with no jump components . . . . .	56

3.3.2	Experiment 2: the DGP with jump components . . . . .	59
3.4	Empirical Application . . . . .	60
3.4.1	Benchmark estimation results . . . . .	61
3.4.2	In-sample fit comparison . . . . .	63
3.4.3	Out of sample forecast performance . . . . .	64
3.4.4	Conclusion . . . . .	67
3.5	Appendix 2 . . . . .	67
3.5.1	Derivation of the proposal density of Alternative GARCH-MIDAS models . . . . .	67
3.5.2	Empirical results . . . . .	74
<b>4</b>	<b>Bayesian MCMC Approach to Heston-SV-MIDAS Models with Jump</b>	<b>83</b>
4.1	Introduction . . . . .	83
4.2	The Models . . . . .	85
4.2.1	Bayesian Estimation of SV-MIDAS models . . . . .	88
4.2.2	Prior and posterior distributions of the parameters of SV-L-MIDAS . . . . .	89
4.2.3	Estimation of the Heston-MIDAS model . . . . .	93
4.2.4	SVL-MIDAS, and Heston-MIDAS models with jump component . . . . .	95
4.2.5	Bayes Factor Analysis . . . . .	97
4.3	Monte Carlo Simulation . . . . .	98
4.4	Empirical Application . . . . .	102
4.4.1	Benchmark estimation results . . . . .	103
4.4.2	In-sample fit comparison . . . . .	104
4.4.3	Bayes factor analysis . . . . .	106
4.4.4	Out-Sample fit comparison . . . . .	107
4.5	Conclusion . . . . .	109
4.6	Appendix 3 . . . . .	109
4.6.1	Posteriors of parameter of Heston-MIDAS Models with no Jump component . . . . .	109
4.6.2	Posterior distribution of parameters of SVL-MIDAS Model with no Jump Component . . . . .	117
4.6.3	Posterior distribution of the parameters $(\mu_z, \sigma_z, \lambda)$ of Jump component for SVL-MIDAS-J and Heston-MIDAS-J . . . . .	119
4.6.4	Empirical Results . . . . .	122
<b>5</b>	<b>Conclusions</b>	<b>123</b>
5.1	Conclusions . . . . .	123
	<b>References</b>	<b>127</b>

## List of Tables

2.5.1 QML estimation results for DGP constructed by GARCH-MIDAS . . . . .	20
2.5.2 QML estimation results for DGP constructed by GARCH-MIDAS . . . . .	21
2.5.3 QML estimation results for DGP constructed by GJR-GARCH-MIDAS . . . . .	22
2.5.4 QML estimation results for DGP constructed by EGARCH-MIDAS . . . . .	23
2.6.1 QML estimation results for SP500 using IP growth . . . . .	25
2.6.2 The summary of QML estimation results . . . . .	27
2.6.3 The ranking of macroeconomic variables . . . . .	28
2.6.4 QLIKE loss of daily total volatility forecast . . . . .	30
2.6.5 RMSE loss of daily total volatility forecast . . . . .	31
2.7.1 Summary statistics of daily returns . . . . .	37
2.7.2 Parameter Estimates of Standard Models . . . . .	37
2.7.3 Estimation results for GARCH-MIDAS models using local macroeconomic variables . . . . .	38
2.7.4 Estimation results for GARCH-MIDAS models using cross-country macroeconomic variables . . . . .	38
2.7.5 QLIKE LOSS Daily Forecast . . . . .	39
2.7.6 RMSE LOSS all forecast . . . . .	42
3.3.1 MCMC and QML estimates for GARCH-MIDAS . . . . .	58
3.3.2 MCMC and QML estimates for GJR-GARCH-MIDAS . . . . .	58
3.3.3 MCMC and QML estimates for EGARCH-MIDAS . . . . .	58
3.3.4 MCMC and QML estimates for GARCH-MIDAS-J . . . . .	59
3.3.5 MCMC and QML estimates for GJR-GARCH-MIDAS-J . . . . .	60
3.3.6 MCMC estimates for EGARCH-MIDAS-J . . . . .	60
3.4.1 MCMC and QML estimates of benchmark models . . . . .	62
3.4.2 MCMC Estimates of Jump-augmented MIDAS models . . . . .	63
3.4.3 The summary of Bayesian MCMC estimation results . . . . .	64
3.4.4 QLIKE LOSS of daily volatility forecast . . . . .	66
3.4.5 RMSE LOSS of daily volatility forecast . . . . .	66
3.5.1 Estimation results of GARCH-MIDAS models for the period: 9.2000-8.2019 . . . . .	76
3.5.2 MCMC and QML Estimates for the period: 4.2000-8.2021 . . . . .	77
3.5.3 QML Estimates of the models when MCMC estimates are used as initial values . . . . .	78
3.5.4 RMSE LOSS function 2000-2019 . . . . .	79
3.5.5 QLIKE LOSS function 2000-2019 . . . . .	80
3.5.6 and MCMC estimates of GARCH-MIDAS -DGP GARCH-MIDAS-J . . . . .	81
3.5.7 QML and MCMC estimates of GJR-GARCH-MIDAS - DGP GJR-GARCH-MIDAS-J . . . . .	81
3.5.8 QML and MCMC estimates of EGARCH-MIDAS - DGP EGARCH-MIDAS-J . . . . .	81
4.2.1 Jeffreys's scale of evidence for Bayes Factors . . . . .	97
4.3.1 Bayesian MCMC estimates of the SV-L-MIDAS model . . . . .	100

---

4.3.2 Bayesian MCMC estimates of the Heston-MIDAS model . . . . .	101
4.3.3 Bayesian MCMC estimates of the SV-L-MIDAS-J model . . . . .	102
4.3.4 Bayesian MCMC estimates of the Heston-MIDAS-J model . . . . .	102
4.4.1 Parameter estimates of SV models . . . . .	103
4.4.2 Parameter estimates of Heston models . . . . .	104
4.4.3 MCMC parameter estimates of Heston-MIDAS models - $OP_{OPEC}$ . . . . .	104
4.4.4 MCMC parameter estimates of SV-L-MIDAS models - $OP_{OPEC}$ . . . . .	104
4.4.5 Estimation results of the impact of economic indicators on WTI returns volatility . . . . .	106
4.4.6 log Bayes factor results . . . . .	107
4.4.7 RMSE LOSS of daily volatility forecast . . . . .	108
4.4.8 QLIKE LOSS of daily volatility forecast . . . . .	109
4.6.1 Bayesian MCMC Estimates of SV-MIDAS, SVL-MIDAS and their jump augmented extensions	122
4.6.2 Bayesian MCMC Estimates of General Heston-MIDAS and its jump augmented extension . .	122

## List of Figures

2.1	Beta Weighting function . . . . .	12
2.2	Beta Weighting function . . . . .	20
2.3	Long term volatility component of SP500 . . . . .	26
2.4	Returns data of the indices in the period 2000-2020 . . . . .	36
2.5	Movement of the macroeconomic variables of all countries . . . . .	36
3.1	Crude Oil WTI daily data for the period 2000-2021 . . . . .	61
3.2	Plot of Beta weighting function . . . . .	71
3.3	Crude Oil WTI daily Price for the period 2000-2021 . . . . .	74
3.4	Industrial production of US and China, and CFNAI . . . . .	75
3.5	Effective Exchange rate of US and China . . . . .	75
3.6	GEPU, EPU of US, EPU of China, and EPU of Russia . . . . .	75
3.7	Global Oil Production, OPEC Oil Production, OPEC Oil supply . . . . .	75



## 1.1 Motivations and Scopes

It is challenging to model and forecast the (unobservable) time-varying volatility of asset returns because it requires us to jointly capture the salient features of the return volatility. Several models have been proposed in the literature to capture the four stylised facts; (i) volatility is time varying; (ii) it tends to clustered over time; (iii) the distribution of returns is asymmetric; and (iv) it possesses a high kurtosis.

Two most popular volatility models are GARCH model proposed by Engle (1982) and Bollerslev (1986), and the stochastic volatility (SV) model advanced by Taylor (1986). These models have been successful in addressing the time-varying and clustering patterns of financial time series. However, they failed to capture large skewness/asymmetry and kurtosis of asset returns. A number of simulation and empirical studies demonstrated that ignoring these issues may result in misleading parameter estimates (violating the stationarity condition) as well as IGARCH effect (extremely high persistence), e.g. Feng (2004), Ausan and Galeano (2007), Choudhry and Wu (2008), Liu and Hung (2010), Ewing and Malik (2017), Men et al. (2017) and Lin (2018)

To capture the asymmetric impact of the returns on volatility, GARCH models were extended by including a leverage component, e.g. GJR-GHARCH(1,1) by EGARCH(1,1) by Nelson (1991), Glosten et al. (1993), Log-GARCH(1,1) by Francq et al. (2013) and TARCH(1,1) by Zakoian (1994). Harvey and Shephard (1996) developed the SV-L model, which captures the leverage effect via the correlation between return innovation and volatility innovation, see also Heston (1993).

Several extensions have also been proposed to capture the large kurtosis of the financial data. The most popular approach aims to model the return innovation by the long-tail distributions such as t-distribution, GED distribution or a mixture of two normal distributions, e.g. Nelson (1991), Bai et al. (2003), Men et al. (2017) and Chen et al. (2020). Another popular approach suggests adding jump components by assuming that the occurrence of rare events is governed by a Bernoulli process while the magnitude of the jump follows a normal distribution with a relatively large variance, e.g. the extended Heston Model by Bates (2001). On the contrary, it has

not been popular to add a jump component in GARCH models mainly due to the intractability of the maximum likelihood estimation especially when the number of parameters becomes very large. Occasional shifts and structural breaks in volatility of returns have also been investigated using Switching Regime GARCH and SV models, e.g. Zou and Chen (2013), Mota et al. (2014) and Abi Jaber (2019).

The GARCH and SV models tend to produce highly persistent or integrated volatility, which could be caused by the presence of structural breaks or rare events. This is known as IGARCH effect, which led to the development of non-parametric multiplicative component volatility models. They aim to transform the return series into stationary series that could be modelled by asymmetric GARCH model with a smaller persistence, e.g. Feng (2004).

Following this research trend, we aim to develop the multiplicative volatility components model of the form,  $\sigma_t^2 = \tau_t g_t$ , where  $\tau_t$  is the long term volatility component and  $g_t$  captures the short term dynamic volatility component. The short term component is usually modelled by GARCH(1,1) or GJR-GARCH(1,1) with unconditional mean of one. Nonparametric and deterministic models were proposed for modelling the long term component, e.g. Feng (2004), Engle and Rangel (2008), Hafner and Linton (2010), Amado and Teriasvirta (2013), Engle et al. (2013), and Han and Kristensen (2015). For example, Engle and Rangel (2008) assumed that  $\tau_t$  is deterministic, and proposed estimating it non-parametrically using the SPLINE-GARCH model. Koo and Linton (2015) proposed estimating  $\tau_t$  by applying the kernel method to the realised volatility. Han and Kristensen (2015) considered  $\tau_t = f(x_t)$  where  $f(\cdot)$  is a polynomial function of order 1 and  $x_t$  is a random variable. The main advantage of this multiplicative model lies in that the scaled returns become stationary such that the unsatisfactory IGARCH effects can be avoided by fitting GARCH model to the scaled returns.

In principle,  $\tau_t$  should be modelled as a function of the overall economic environment rather than a specific financial variable. Notice that many macroeconomic variables, such as industrial production and inflation rate, are observed at a lower frequency (monthly or quarterly). In this regard, Engle et al. (2013) proposed the GARCH-MIDAS model where  $\tau_t$  is modelled using the MIDAS regression which can deal with the data with mixed frequency. Since then, GARCH-MIDAS models have been popular in many empirical studies, so as to identify the impacts of macroeconomic conditions on the total volatility of asset returns, e.g. Alsheikhmubarak and Giouvris (2017), Conrad et al. (2018), Yu et al. (2018), Lin and Chang (2020), Fang et al. (2020) and You and Liu (2020).

Following this research trend, Chapter 2 reviews the main properties of the GARCH-MIDAS processes and develops the EGARCH-MIDAS model to deal with the leverage effects. In Chapter 3, we develop the jump-augmented GJR-GARCH-MIDAS and EGARCH-MIDAS models that can also capture the large kurtosis of the returns. We then propose the Bayesian MCMC estimation approach, because the Maximum Likelihood estimation becomes intractable in this case. Finally, Chapter 4 presents the MIDAS extension to the SV model, called the SV-MIDAS



model with and without jump component. The proposed Heston-MIDAS Model is expected to shed further lights on the implication of the popular Heston Model in option pricing.

## 1.2 The summary of Chapter 2

In Section 2.2 we review the GARCH-MIDAS model proposed by Engle et al. (2013). The total volatility is specified by  $\sigma_t^2 = g_t \tau_t$  where the short-term volatility,  $g_t$  is assumed to follow a Unit GARCH(1,1) process  $g_t = (1 - \alpha - \beta) + \alpha \frac{(r_{t-1} - \mu)^2}{\tau_t} + \beta g_{t-1}$  with  $E(g_t) = 1$ , and the long-term volatility is modelled by  $\log \tau_t = m + \theta \sum_{k=1}^K w_k(\omega) X_{t-k}$  where  $w_k(\omega)$ 's for  $k = 1, \dots, K$ , are smoothing weights and  $X_t$  is a macroeconomic variable. The parameters  $(\alpha, \beta, m, \theta, \omega)$  are jointly estimated using Quasi Maximum Likelihood (QML) method. Recently, this model has been applied to investigating the impact of macroeconomic variables on the return volatility for several stock market indices and commodities.

In Section 2.3 we develop the EGARCH-MIDAS model as a competing model to the existing GJR-GARCH-MIDAS model advanced by Conrad and Kleen (2020). However, it is not straightforward to impose the necessary condition,  $E(g_t) = 1$ , unlike in GJR-GARCH-MIDAS, because its intercept is not easily expressed as a function of other parameters. We overcome this drawback by using the  $MA(\infty)$  representation of EGARCH(1,1) from which  $E(g_t)$  can be expressed as an exponentially decaying infinite series whose element can be expressed as a function of other parameters. We have also proposed the scaling approach by comparing the sample mean of the average of the short term volatility estimate obtained by considering  $\alpha_0$  as a parameter, scaled by its average, which is a good estimate of the unconditional mean  $E(g_t)$ .

In Section 2.4, we show that EGARCH-MIDAS model produces a larger kurtosis and a longer memory of the autocorrelations  $\rho(k)$  of the return squared than those of EGARCH(1,1). These are desired properties for capturing the observed large kurtosis and long memory of returns.

Despite the growing literature on the GARCH-MIDAS model, to date, there has been a lack of studies that rigorously investigate statistical properties, the finite sample performance of the QML estimator and the robustness with respect to the model misspecification. To fill this gap we have conducted a comprehensive simulation study in Section 2.5. The main findings are summarised as follows: First, QMLE can produce accurate parameter estimates and identify the long- and short-term volatility components only if the numerical method used for maximizing the log-likelihood achieves a global maximum. Second, the fit of the total volatility depends on the correct model specification of the short term component,  $g_t$ , though the estimation of the long term component  $\tau_t$  seems to be rather insensitive. In particular, for EGARCH-MIDAS, the scaling modification is necessary to produce the accurate estimate of the long term volatility.

In Section 2.6, we analyse the time-varying volatility patterns of the seven stock market indices (SP500, NASDAQ, CAC40, DAX, FTSE100, NIKKEI, and HANGSENG) over the period Jan 2000-Aug 2019, but also evaluate the relative performance of GARCH-MIDAS, GJR-GARCH-

MIDAS and EGARCH-MIDAS in terms of in-sample fit and out of sample forecasting. Our main findings are summarised as follows: According to  $\Delta\text{BIC}$  and RMSE, EGARCH-MIDAS is the preferred model for SP500, NASDAQ, CAC40, DAX, FTSE100 and NIKKEI whereas GJR-GARCH-MIDAS is the preferred model for HANGSENG. Furthermore, the global indicator, Chicago Fed National Activity index  $CFNAI$  turns out to be the most influential variable affecting the long-term volatility for all seven indices. This highlights the dominant position of the US financial market. We next assess the forecasting performance of alternative models using RMSE and QLIKE loss functions, and find that EGARCH-MIDAS outperforms both GJR-GARCH-MIDAS and GARCH-MIDAS for almost all cases considered. In practice, we recommend to incorporate the leverage effect in the short term volatility component to improve the fit of the total volatility as well as the forecasting power.

### 1.3 The summary of Chapter 3

In Section 3.2 we develop the general class of (asymmetric) GARCH-MIDAS models by adding a jump component in the return equation to capture dynamics of rare events. The occurrence of a rare event is usually modelled by incorporating a component of the form,  $b_t z_t$  where  $b_t$  is an indicator of a rare event/jump with probability  $\kappa$ . We assume that  $b_t$  follows a Bernoulli distribution with a parameter,  $\kappa$  i.e.  $P(b_t = 1) = \kappa$ , and  $P(b_t = 0) = 1 - \kappa$ . The size of jump,  $z_t$  is assumed to follow a normal distribution,  $N(\mu_z, \sigma_z^2)$ .

In Section 3.3 we propose the Bayesian MCMC methodology to estimating asymmetric GARCH-MIDAS models with jump components, and describe how draws are simulated from the posterior distributions. We derive the closed form of posterior distributions by using uninformative prior distributions for E/GARCH parameters, normal priors for the two regression parameters of the long term component  $\tau_t$ , and normal prior with large variance and uniform prior for the weighting function  $w(\omega)$  which controls the smoothness of  $\tau_t$ . Since the posteriors are not conjugate, we adopt the Metropolis-Hasting (MH) Method and the Griddy-Gibbs method for simulating draws from the posterior distributions. To implement the MH method, we derive the 2nd order Taylor expansion of the posterior distributions of all the parameters, and deduce the associated normal proposal distribution, from which draws from the complex posteriors are obtained using acceptance/rejection method. The MCMC estimate is close to the QML counterpart if the number of iterations/updates is sufficiently large (Markov Chain Monte Carlo theorem). The precision of the MCMC estimate does not depend on the complexity or dimension of the model, since the joint density can be expressed as the product of marginal densities by Bayes theorem. The additional parameters only increase the number of iterations. This is a main advantage over the QML estimation that becomes intractable as the dimension of the parameters rises.

In Section 3.4 we confirm the validity of the MCMC approach via a comprehensive simulation study. First, when the simulated data do not contain outliers, both MCMC and QML estimates are relatively accurate for GARCH-MIDAS model while MCMC produces more precise

estimate of the leverage effects than QML for GJR-GARCH-MIDAS and EGARCH-MIDAS models. However, when the simulated data contain jump components, QML estimates become unreliable or computationally infeasible. Still, the proposed MCMC can be easily conducted and produce relatively satisfactory estimates. This demonstrates that the Bayesian MCMC estimation is indeed appealing for estimating asymmetric GARCH-MIDAS model with jump components because the distributions of the parameters can be estimated by simulation without assuming the normality distribution.

In Section 3.5 we address the important issues of leverage effects and rare events jointly by applying the jump-augmented asymmetric GARCH-MIDAS models to an analysis of time-varying volatility patterns of WTI daily returns over the period 9/2000-8/2019. We also evaluate the relative performance of GARCH-MIDAS-J, GJR-GARCH-MIDAS-J and EGARCH-MIDAS-J models in terms of in-sample fit and out of sample forecast performance. To examine the impacts of macroeconomic conditions on the long-run volatility, we consider a range of macroeconomic indicators for US, China, Russia, Saudi Arabia and OPEC.

In sum, we document evidence that the joint modelling of the leverage effect, the long term volatility and rare events through jump will be important in capturing the salient time-varying volatility patterns of the daily WTI returns and improving the forecasting power. BIC convincingly selects MIDAS models with jump components over MIDAS models without jump components. The jump augmented MIDAS models produced significant long term coefficients ( $\theta$ ) with predicted signs for all macroeconomic variables. Overall, EGARCH-MIDAS-J is the most preferred model. Furthermore, we find that the most influential variable is the  $OP_{OPEC}$ , that explains 43.5% of the total volatility for WTI returns. This highlights the dominant position of OPEC in the global oil industry. Finally, in terms of RMSE and QLIKE loss functions, EGARCH-MIDAS-J outperforms both GJR-GARCH-MIDAS-J and GARCH-MIDAS-J for almost all cases considered.

## 1.4 The summary of Chapter 4

Continuous time stochastic volatility (SV) models have been popular for modeling volatility of high frequency returns. We focus on the discrete versions, mainly the SV, SV with leverage (SV-L), and the Heston Models, where the asymmetry/leverage effect is incorporated via the correlation between the return and the volatility innovations. A number of studies showed that the SV model with normal errors outperforms GARCH model with normal or t-distribution, e.g. Carnero et al. (2003), Broto and Ruiz (2004) and Men et al. (2016).

Following the research trend in the GARCH-MIDAS literature, we develop the SV-MIDAS models by applying the multi-component volatility model. We also consider the extensions with leverage effects and jump components.

We then propose the Bayesian MCMC estimation method, because the conventional QML esti-

mation tend to produce the misleading results. Furthermore, the QML will be unable to estimate the SV-MIDAS model with leverage effects and jump components. We show that the posteriors of parameters of the SV-MIDAS model are conjugate. In particular, we estimate the parameters of the long term volatility component using the Metropolis-Hasting method while we evaluate posteriors for the short term volatility using the Random Walk method. We employ the Griddy-Gibbs method for simulating the correlation between between the return and the volatility innovations.

Eraker (2003) listed the Bayesian MCMC estimation approach advantages over other estimation methods employed for stochastic volatility models as follows: Bayesian MCMC approach estimates the latent volatility, jump times, and jumps sizes, accounts for estimation risk, Bayesian MCMC approach have superior sampling properties over other estimation approaches, and the Bayesian MCMC approach is computationally efficient as we can test its accuracy through Monte Carlo simulation experiments.

Our Simulation study confirms the reliability of our Bayesian MCMC estimation approach which is important for two reasons. First, due to time discretization of the models from continuous time to discrete time, we need to make sure that it does not lead to biases in the parameter estimates. Second, methods for estimating MIDAS type models and multivariate jump models are not well developed and it is important to verify that we can reliably estimate the parameters for the sample size.

In the empirical study, we model WTI returns using the proposed SV-MIDAS models and their jump augmented extensions by employing 10 economic indicators known for their impact on WTI returns volatility. Our results suggest that Heston-MIDAS-J, SVL-MIDAS-J are the favoured models according to DIC, and Bayes factor analysis. Also, we note that unlike the Heston model (benchmark), Heston-MIDAS was able to detect a negative leverage effect comparable to SVL-MIDAS model.

## Asymmetric GARCH-MIDAS Models

### 2.1 Introduction

In the seminal paper, Engle et al. (2013) advanced the GARCH-MIDAS model, which incorporates macroeconomic determinants due to their important role in explaining asset price volatility, e.g. Chen et al. (1986), Engle et al. (2008), Clements (2007), and Campbell and Diebold (2009). The total volatility,  $\sigma_t$  is expressed as the product of a short term volatility component,  $g_t$  and a long term volatility component  $\tau_t$ .  $g_t$  is modelled by a unit-variance GARCH(1,1) process whilst  $\tau_t$  is assumed to be a function of the low-frequency macroeconomic variables. This is estimated by the MIDAS regression (Ghysels et al. (2006)) that can handle the data with the mixed frequency. The use of unit-variance GARCH(1,1) for modelling the short term volatility component  $g_t$  enables us to identify the two volatility components separately and ensure that the long term volatility is equal to the total volatility in the long run. Furthermore, GARCH-MIDAS can be regarded as generalisation of the switching regime GARCH model (Bauwens et al. (2006)), which is shown to outperform GARCH, because GARCH-MIDAS can be expressed as GARCH with time varying intercept as a function of  $\tau_t$  and thus macroeconomic variable.

The GARCH-MIDAS model is a fully parametric multiplicative volatility component model. Sachs (2004), Feng(2004), and Rangle and Engle (2008) developed the semi-parametric models where  $g_t$  is modelled by GARCH(1,1) and  $\tau_t$  is estimated using a non-parametric curve fitting such as the kernel or spline method. First, GARCH-MIDAS can capture complex volatility dynamics with a relatively small number of parameters that can be estimated by the quasi maximum likelihood (QML) method. On the other hand, the semi-parametric models are estimated using a two-step procedure, where GARCH parameters are estimated based on a nonparametric estimate of  $\tau_t$ .

GARCH-MIDAS models have been extensively used for investigating whether macroeconomic variables exert significant impacts on the return volatility of financial assets. Asgharian et al. (2013) applied GARCH-MIDAS to the SP500 daily returns over the period January 1991–June 2008, using monthly data of 7 macroeconomic variables, and documented that GARCH-MIDAS outperforms GARCH(1,1) in predicting the long term volatility. Using the implied volatility index of FTSE 100 during April 2000–December 2015, Alsheikhmubarak and Giouvriss (2017) found that London 3 months Inter Bank and unemployment rate have a significant impact on the implied volatility index. Conrad et al. (2018) applied GARCH-MIDAS to estimating the long

term and short term volatility components of crypto currencies using SP500 realised volatility and Baltic dry index as a proxy of risk. Their results indicate that SP500 realised volatility (Baltic dry index) has a negative (positive) and significant impact on the long term component of Bitcoin volatility. Yu et al. (2018) observed that the hot money (change in foreign exchange reserves minus foreign direct investment minus trade and service balance) has significantly positive impact on the long term volatility of the Chinese stock market over the period 2000-2016. Lin and Chang (2020) applied GARCH-MIDAS to studying the impacts of equity, bulk shipping, commodity, currency, and crude oil markets on the United States Oil Fund (USO) and BlackRock World Energy Fund A2 (BGF) during July 2014–April 2020. Afees and Gupta (2020) found that oil supply shocks have significant impacts on stock markets volatility of BRICS (Brazil, Russia, India, China, and South Africa) except China and South Africa, while economics activity, oil consumption, and oil inventory demand shocks have significant impacts on BRICS stock markets except China. You and Liu (2020) applied GARCH-MIDAS model to forecasting daily exchange rate volatility by monthly monetary fundamentals.

To capture the leverage effect of the volatility, Conrad and Loch (2015) and Conrad and Kleen (2019) developed the GJR-GARCH-MIDAS model, which assumes unit-variance GJR-GARCH(1,1) model for the short term volatility. Goldman and Shen (2018) advanced the Spline-GTARCH model as an extension of Spline-GARCH of Engle and Rangel (2008) where the long term component is estimated by spline curve fitting and the short term component is modelled by unit-variance GTARCH(1,1).

As a main contribution, we develop the EGARCH-MIDAS model, which describes the dynamics of the short term volatility component in a different way from GJR-GARCH: GARCH can be expressed as an  $AR(\infty)$  process whereas EGARCH is represented by an  $MA(\infty)$  process. This approach is also motivated by the outperformance of EGARCH over GJR-GARCH as documented in several empirical studies, e.g. Awartani and Corradi (2005), Lin (2018), Chong et al. (1999), Teresiene (2009), and Naimy (2018). We show that the EGARCH-MIDAS process can produce the larger kurtosis than the EGARCH process. However, unlike GARCH, GJR-GARCH, and GTARCH models, it is not straightforward to derive the unit-variance EGARCH model, especially if we are interested in volatility forecasts that are evaluated using both  $g_t$  and  $\tau_t$  at the end point of the sample. We overcome this issue and derive the expression for the volatility forecast using the  $MA(\infty)$  representation of EGARCH which enables us to express its unconditional mean  $E(g_t)$  from which we can express the intercept  $\alpha_0$  as a function of the other parameters to achieve  $E(g_t) = 1$ .<sup>1</sup>

Despite the growing literature on the GARCH-MIDAS model, to date, there has been a lack of studies that rigorously investigate statistical properties, the finite sample performance of the QML estimator and the robustness with respect to the model misspecification. To fill this gap we have conducted a comprehensive simulation study. The main findings are summarised as

<sup>1</sup>Borup and Jakobson (2019) proposed the realised EGARCH-MIDAS. But, they bypass the identifiability issue by simply imposing that the intercept is zero.

follows: First, QMLE can produce accurate parameter estimates and identify the long- and short-term volatility components only if the numerical method used for maximising the log-likelihood achieves a global maximum.<sup>2</sup> Second, the fit of the total volatility depends on the correct model specification of the short term component,  $g_t$ , though the estimation of the long term component  $\tau_t$  seems to be rather insensitive. In practice, we recommend to incorporate the leverage effect in the short term volatility component to improve the fit of the total volatility.

We aim to analyse the time-varying volatility patterns of the seven stock market indices (SP500, NASDAQ, CAC40, DAX, FTSE100, NIKKEI, and HANGSENG) over the period Jan 2000-Aug 2019, but also evaluate the relative performance of GARCH-MIDAS, GJR-GARCH-MIDAS and EGARCH-MIDAS in terms of in-sample fit and out of sample forecasting. To investigate the impacts of macroeconomic conditions on the long-run volatility, we consider a range of macroeconomic variables.

Our main findings are summarised as follows: Both GJR-GARCH-MIDAS and EGARCH-MIDAS outperform GARCH-MIDAS, highlighting the importance of the leverage effects in practice. Furthermore, according to  $\Delta BIC$  and RMSE, EGARCH-MIDAS is the preferred model for SP500, NASDAQ, CAC40, DAX, FTSE100 and NIKKEI whereas GJR-GARCH-MIDAS is the preferred model for HANGSENG. In terms of the in-sample fit using BIC for EGARCH-MIDAS, GJRGARCH-MIDAS, and GARCH-MIDAS models, we find that the global indicator, Chicago Fed National Activity index  $CFNAI$  turns out to be the most influential variable affecting the long-term volatility for all seven indices. This highlights the dominant position of the US financial market. The second-most influential variable is the country-specific Industrial production ( $IP$ ) growth.

We next assess the forecasting performance of GJR-GARCH-MIDAS and EGARCH-MIDAS against GARCH-MIDAS as a benchmark model, using  $CFNAI$  and  $IP$  growth as the macroeconomic variable forecasting the long term volatility. In terms of RMSE and QLIKE loss functions, we find that EGARCH-MIDAS outperforms both GJR-GARCH-MIDAS and GARCH-MIDAS for almost all cases considered.

This Chapter is organized as follows: Section 2 provides an overview of GARCH-MIDAS and GJRGARCH-MIDAS models. In Section 3 we develop the EGACRH-MIDAS model and discuss the theoretical properties of the three models with a focus on the kurtosis and the autocorrelation function. In Section 4 we discuss the estimation of the models using QML method. Section 5 reports the main simulation results. Section 6 presents the empirical findings. Section 7 concludes.

---

<sup>2</sup>We strongly recommend the use of *simulanneal.m* of MATLAB. On the contrary, the popular *fmin.m* function tends to converge to a local maximum in which case a constant long term volatility stays outside the range of the realised volatility.

## 2.2 GARCH-MIDAS Models

Since the seminal work by Bollerslev(1986), a plethora of GARCH models have been proposed for modelling the volatility of asset returns, assuming that the generating process of the returns is stationary whose volatility reverts to a constant in the long run. However, empirical evidence suggests that complex volatility dynamics can be better described by the component model or two factor volatility model (Engle and Lee (1999), Adrian and Rosenberg (2008) and Conrad and Kleen (2020)). One class of the models is the multiplicative component model that describes the conditional volatility as a product of short-run and long-run components. In this section we present an overview on the multiplicative volatility component model, called the GARCH-MIDAS model by Engle et al. (2013), and its extension, the GJR-GARCH-MIDAS model by Conrad and Loch (2015) that can capture the leverage effect.

### 2.2.1 Symmetric GARCH-MIDAS model

Let  $r_{i,t}$  denote the return on day  $i$  of month (or quarter)  $t$ . Then, the GARCH-MIDAS model can be described by

$$r_{i,t} = \mu + \sqrt{\tau_t} g_{i,t} \varepsilon_{i,t} \quad i = 1, \dots, n_t \quad t = 1, \dots, N \quad (2.2.1)$$

$$g_{i,t} = \alpha_0 + \alpha \frac{(r_{i-1,t} - \mu)^2}{\tau_t} + \beta g_{i-1,t} \quad (2.2.2)$$

$$\tau_t = m + \theta \sum_{k=1}^K w(k, \omega_1, \omega_2) x_{t-k} \quad (2.2.3)$$

We note:

- a)  $n_t$  is the number of days in month  $t$ ,  $N$  is the number of months spanning the data, and conditional on information of day  $(i-1)$ ,  $\varepsilon_{i,t}$ 's are independently and identically normally distributed with mean 0 and variance 1.
- b)  $\{x_t\}_{t=1, \dots, N}$  are the values of an explanatory variable  $X$ , and  $w(k, \omega_1, \omega_2)$  is a weighting function whose shape is controlled by its parameters  $\omega_1$  and  $\omega_2$ , and  $K$  is the number of past values of  $x_t$ 's which are fed in the long term component,  $\tau_t$ . Conrad and Schienle (2018) assumes that  $\sum_{k=1}^K w(k, \omega_1, \omega_2) x_{t-k}$  is not degenerate for any  $(\omega_1, \omega_2)$  to ensure that  $\tau_t$  is non-constant with probability one unless  $\theta = 0$ . In empirical studies,  $X$  is taken as the realized volatility,  $RV$ , or a macroeconomic variable such as inflation rate or industrial production growth rate (Engle et al. (2013), and Conrad and Loch (2015)).
- c) The parameters  $\alpha$ , and  $\beta$  are positive and satisfy  $\alpha + \beta < 1$  to ensure stationary of the short term component  $g_{i,t}$ .  $\alpha_0$  is constrained to be equal to  $1 - \alpha - \beta$  to ensure that  $E(g_{i,t}) = 1$  such that the total volatility coincides with  $\tau_t$  in the long run.
- d) The parameters  $m$  and  $\theta$  are restricted to be positive to ensure non-negativity of  $\tau_t$ . In practice this restriction can be waived by replacing (2.2.3) by



$$\log(\tau_t) = m + \theta \sum_{k=1}^K w(k, \omega_1, \omega_2) x_{t-k} \quad (2.2.4)$$

In existing empirical studies,  $K$  is chosen to span past 1, 2, or 3 years, which correspond to  $K = 12, 24, 36$  for monthly macroeconomic variables. The weighting function,  $w(k, \omega_1, \omega_2)$  is given by the exponential, exponential Almon lag or the beta-weight specification given by

$$w(k, \omega_1, \omega_2) = \frac{\left(\frac{k}{K+1}\right)^{\omega_1-1} \left(1 - \frac{k}{K+1}\right)^{\omega_2-1}}{\sum_{j=1}^K \left(\frac{j}{K+1}\right)^{\omega_1-1} \left(1 - \frac{j}{K+1}\right)^{\omega_2-1}} \quad \text{for } k = 1, \dots, K \quad (2.2.5)$$

The advantage of using a parametric weighting function in (2.2.5) is to uniquely determine the  $K$  weights from  $\omega_1$  and  $\omega_2$ . But,  $w(k, \omega_1, \omega_2)$  is not necessarily a decreasing function of  $k$ , implying that values of macroeconomic variables far from  $x_t$  have more influence than its nearest values as shown in Fig.2.1(a).<sup>3</sup> To ensure a decreasing beta-weighting function in (2.2.5), we restrict  $\omega_1 = 1$  and  $\omega_2 > 1$  for every  $K$ . In other words, the weighting function has one parameter  $\omega = \omega_2$  and reduces to

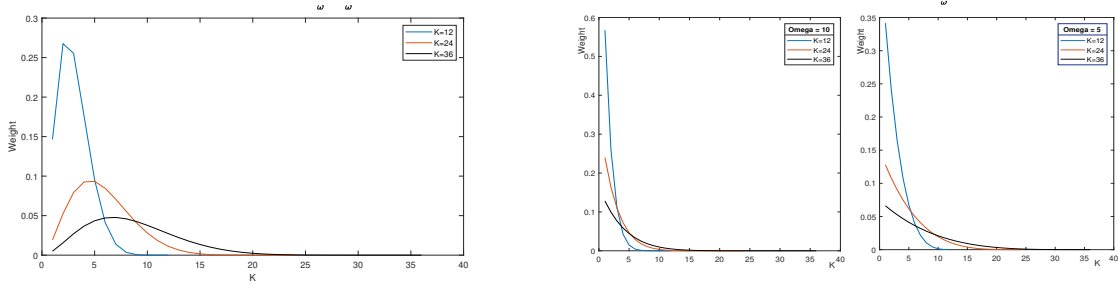
$$w(k, \omega) = \frac{\left(1 - \frac{k}{K+1}\right)^{\omega-1}}{\sum_{j=1}^K \left(1 - \frac{j}{K+1}\right)^{\omega-1}} \quad (2.2.6)$$

which produces the equal weights if  $\omega = 1$  i.e.  $w(k) = \frac{1}{K}$

Since  $K$  can be selected reasonably large ( $K = 36$ ) by the user, the lag length  $K$  is not considered as a parameter. If we want to determine an optimal  $K$ , we suggest to estimate the model for a range of values of  $K$  and choose the value for which higher values lead to no significant gain in BIC or log-likelihood value (see also the simulation and empirical sections). Fig.2.1(b) illustrates its impact for different values of  $\omega$ . The distribution of the weights seems to depend on the value of  $K$ : The weights of  $X_{t-1}$  and  $X_{t-2}$  represent about 86% and 12% respectively for  $K = 12$  and  $\omega_2 = 24$ . For  $K = 60$  and  $\omega_2 = 24$ , their weights becomes about 33% and 32%, respectively.

<sup>3</sup>This unusual pattern was justified by Conrad and Loch(2015) and Amendola et al. (2017) for real state data.

Figure 2.1: Beta Weighting function

(a)  $\omega_1 = 3, \omega_2 = 10, K = (12, 24, 36)$ (b)  $\omega_1 = 1, \omega_2 = (5, 10), K = (12, 24, 36)$ 

Note: Figure (a) shows the impact of not restricting  $\omega_1 = 1$ , where weighting function is not necessarily a decreasing function for different monthly values for  $K$ . Figure (b) shows the impact of restricting to  $\omega_1 = 1$ , to ensure a decreasing weighting function for different monthly values for  $K$

## 2.2.2 Asymmetric GJR-GARCH-MIDAS model

Conard and Loch (2015) and Conrad and Kleen (2018) developed the GJR-GARCH-MIDAS model to jointly capture the volatility clustering and the leverage effect by assuming the short term component,  $g_t$  follows the GJR-GARCH(1,1) model by Glosten et al. (1993). The GJR-GARCH-MIDAS model is given by

$$r_{i,t} = \mu + \sqrt{\tau_t} g_{i,t} \varepsilon_{i,t} \quad i = 1, \dots, n_t \quad t = 1, \dots, T \quad (2.2.7)$$

$$g_{i,t} = \alpha_0 + \alpha \frac{(r_{i-1,t} - \mu)^2}{\tau_t} + \gamma \frac{(r_{i-1,t} - \mu)^2}{\tau_t} 1_{[r_{i-1,t} - \mu < 0]} + \beta g_{i-1,t} \quad (2.2.8)$$

$$\log(\tau_t) = m + \theta \sum_{k=1}^K w(k, \omega_1, \omega_2) x_{t-k} \quad (2.2.9)$$

The parameters  $\alpha$  and  $\beta$  are positive and the presence of leverage effect is detected by the positive sign of  $\gamma$ . Then,  $g_{i,t}$  is weakly stationary if  $0 < \alpha + \beta + \gamma/2 < 1$ .<sup>4</sup>

To identify the 2 components,  $\tau_t$  and  $g_{i,t}$ , Conrad and Kleen (2018) restricted the intercept  $\alpha_0$  to be equal to  $1 - \alpha - \beta - \frac{\gamma}{2}$  such that  $E(g_{i,t}) = 1$ , to ensure that the unconditional variance  $\text{var}(r_{i,t}) = E(\tau_t)$ . They investigated the in-sample and forecasting performance via simulations, and found that it outperforms both GARCH(1,1) model and the Heterogeneous Autoregressive (HAR) model of Corsi (2009). But, they also found that the estimate of  $\theta$  depends on the value of  $K$ . Surprisingly, they did not provide the comparison with GARCH-MIDAS model and GJR-GARCH(1,1).

Goldman and Shen (2018) proposed the Spline-GTARCH model, as an extension of Spline-GARCH model by Engle and Rangel (2008), where the long term component is estimated using the spline curve fitting and the short term component is modelled by unit-variance GTARCH(1,1)

<sup>4</sup>More accurately, Goldman and Shen (2018) imposed  $0 < \alpha + \beta + \phi \gamma < 1$  to ensure that  $g_{i,t}$  is weakly stationary where  $\phi$  is the percentage of observations in the regime with negative innovations ( $\varepsilon_{i,t} < 0$ ). In practice, without the loss of generality,  $\phi$  is replaced by  $1/2$ .

model:

$$g_t = \omega + a(r_{t-1} - \mu)^2 + \gamma(r_{t-1} - \mu)^2 I_{(r_{t-1} - \mu < 0)} + \beta g_{t-1} + \delta g_{t-1} I_{(r_{t-1} - \mu < 0)} \quad (2.2.10)$$

Therefore, we define GTARCH-MIDAS by

$$\begin{aligned} r_{i,t} &= \mu + \sqrt{\tau_t} g_{i,t} \varepsilon_{i,t} \\ g_{i,t} &= \alpha_0 + \alpha \frac{(r_{i-1,t} - \mu)^2}{\tau_t} + \gamma \frac{(r_{i-1,t} - \mu)^2}{\tau_t} I_{(r_{i-1,t} - \mu < 0)} + \beta g_{i-1,t} + \delta g_{i-1,t} I_{(r_{i-1,t} - \mu < 0)} \\ \log(\tau_t) &= m + \theta \sum_{k=1}^K w(k, \omega_1, \omega_2) x_{t-k} \end{aligned}$$

where  $\alpha_0 = 1 - \alpha - \beta - (\gamma + \delta)/2$ . The parameters  $\gamma$  and  $\delta$  create the asymmetric response of volatility to negative shocks. Goldman and Shen (2018) claim that GTARCH captures the leverage effect better than GJR-GARCH as it produces a non-negligible  $\alpha$ . It also nests both GARCH-MIDAS and GJR-GARCH-MIDAS.

## 2.3 The EGARCH-MIDAS Model

The EGARCH(1,1) model by Nelson (1991) is the first approach to model the volatility as a function of the returns rather than the squared returns (appropriate for modelling the data possessing outliers). Moreover, it incorporates the leverage effect but does not nest GARCH(1,1), unlike GJR-GARCH. The moments structure differs between EGARCH and GJR-GARCH models. EGARCH is more suitable for modelling a long-memory financial data (the sample autocorrelation of the squared returns does not decay exponentially as it is the case for GJR-GARCH). Several studies found that EGARCH fits financial data better than GARCH models (e.g. Anyfantaki and Demos (2016), Cuervo et al. (2014), Heynen et al. (1994), Lumsdaine (1995)).

Following this research trend we now develop the EGARCH-MIDAS model given by

$$r_{i,t} = \mu + \sqrt{\tau_t} g_{i,t} \varepsilon_{i,t} \quad i = 1, \dots, n_t \quad t = 1, \dots, T \quad (2.3.1)$$

$$\log(g_{i,t}) = \alpha_0 + \gamma \varepsilon_{i-1,t} + \alpha \{ |\varepsilon_{i-1,t}| - E(|\varepsilon_{i-1,t}|) \} + \beta \log(g_{i-1,t}) \quad (2.3.2)$$

$$\log(\tau_t) = m + \theta \sum_{k=1}^K w(k, \omega_1, \omega_2) x_{t-k} \quad (2.3.3)$$

where  $\alpha_0, \alpha, \gamma$  are real,  $|\beta| < 1$  to ensure stationarity of the EGARCH component, and  $\varepsilon_{i,t}$ 's are iid with mean 0 and variance 1.

If we assume  $\varepsilon_{i,t}$ 's are iid  $N(0, 1)$ , we can show that  $E(|\varepsilon_{i,t}|) = \sqrt{\frac{2}{\pi}}$ , and replacing  $\varepsilon_{i,t}$  by

$\frac{r_{i,t}-\mu}{\sqrt{\tau_t}g_{i,t}}$  in equation (2.3.2) we get:

$$\log(g_{i,t}) = \alpha_0 + \beta \log(g_{i-1,t}) + \gamma \frac{(r_{i-1,t} - \mu)}{\sqrt{\tau_t}g_{i-1,t}} + \alpha \left( \frac{|r_{i-1,t} - \mu|}{\sqrt{\tau_t}g_{i-1,t}} - \sqrt{\frac{2}{\pi}} \right) \quad (2.3.4)$$

It is clear that the impact of  $\varepsilon_{i-1,t}$  on  $\log(g_{i,t})$  is  $(\alpha + \gamma) \frac{\varepsilon_{i-1,t}}{\sqrt{\tau_t}g_{i-1,t}}$  in the presence of good news ( $\frac{(r_{i-1,t}-\mu)}{\sqrt{\tau_t}g_{i-1,t}} > 0$ ) whereas it becomes  $(\alpha - \gamma) \frac{\varepsilon_{i-1,t}}{\sqrt{\tau_t}g_{i-1,t}}$  in the presence of bad news ( $\frac{(r_{i-1,t}-\mu)}{\sqrt{\tau_t}g_{i-1,t}} < 0$ ). Hence, if  $\gamma < 0$ , then a leverage effect is present (bad news have a larger impact than good news). From (2.3.4), it is clear that we do not impose positivity restrictions on the parameters of the short term component since  $\log(g_{i,t})$  is not restricted to be positive.

Despite the outperformance of EGARCH over GJR-GARCH documented in several studies, it is not straightforward to identify the two volatility components,  $\tau_t$  and  $g_{i,t}$  in EGARCH-MIDAS model. We next discuss two approaches to overcome this identification issue.

### 2.3.1 Identification of the volatility components

Unlike the GJR-GARCH-MIDAS model, it is not straightforward to translate  $E(g_{i,t}) = 1$  into a simple relation between the parameters  $\alpha_0, \gamma, \alpha$ , and  $\beta$  of the short term component in (2.3.2) or (2.3.4) due to Jensen inequality i.e.  $E(\log(Y)) > \log(E(Y))$ , i.e. for EGARCH, we have  $E(\log(g_{i,t})) > 0$ . We can overcome this issue by expressing  $E(g_{i,t})$  as series or by using Central Limit Theorem, as follows:

**MA( $\infty$ ) representation of the EGARCH short term component:** The first method for identifying the two volatility components is to use the infinite series approximation of  $E(g_{i,t})$  given by (Nelson (1991) and Kyriakopoulou (2015)):

$$E(g_{i,t}) = e^{\frac{\alpha_0 - \alpha \sqrt{\frac{2}{\pi}}}{1 - \beta}} \prod_{i=0}^{\infty} [e^{0.5\beta^{2i}\delta_1^2} \Phi(\beta^i \delta_1) + e^{0.5\beta^{2i}\delta_2^2} \Phi(\beta^i \delta_2)] \quad (2.3.5)$$

where  $\delta_1 = \alpha + \gamma$ ,  $\delta_2 = \alpha - \gamma$ , and  $\Phi(x) = \int_{-\infty}^x \frac{1}{\sqrt{2\pi}} e^{-\frac{x^2}{2}} dx$ .

Using the fact that  $\frac{r_{i,t}-\mu}{\tau_t}$  is EGARCH, we can easily check that (2.3.5) is also valid for the short term component,  $g_{i,t}$ , of EGARCH-MIDAS. Then,  $E(g_{i,t}) = 1$  or equivalently  $\log(E(g_{i,t})) = 0$  is satisfied when:

$$0 = \frac{\alpha_0 - \alpha \sqrt{\frac{2}{\pi}}}{(1 - \beta)} + \log\left(\prod_{i=1}^{\infty} [e^{0.5\beta^{2i}\delta_1^2} \Phi(\beta^i \delta_1) + e^{0.5\beta^{2i}\delta_2^2} \Phi(\beta^i \delta_2)]\right)$$

$$\alpha_0 = \alpha \sqrt{\frac{2}{\pi}} - (1 - \beta) \sum_{i=0}^{\infty} \log(e^{0.5\beta^{2i}\delta_1^2} \Phi(\beta^i \delta_1) + e^{0.5\beta^{2i}\delta_2^2} \Phi(\beta^i \delta_2)) \quad (2.3.6)$$

As  $i$  increases, the terms,  $\beta^{2i}\delta_1^2, \beta^i\delta_1, \beta^{2i}\delta_2^2, \beta^i\delta_2$  will decrease to 0. Hence, we can truncate the infinite series because the  $i$ th element of the series tends to  $\log(1)$  as both  $e^{0.5\beta^{2i}\delta_1^2}\Phi(\beta^i\delta_1)$  and  $e^{0.5\beta^{2i}\delta_2^2}\Phi(\beta^i\delta_2)$  will tend to  $\Phi(0) = 0.5$ .

We note that estimating  $\alpha_0$  by  $\alpha\sqrt{2/\pi}$  (ignoring the series term) leads to a small bias of about 0.05 for various beta values in the range  $[0.83, 0.99]$ . Similar graphs were obtained when the leverage parameter  $\gamma$  is positive. Hence, we conjecture that restricting the intercept to  $\alpha_0 = \alpha\sqrt{2/\pi}$  will produce a unit-variance EGARCH short term component.

**Central Limit Theorem application:** We estimate EGARCH-MIDAS by treating  $\alpha_0$  as a free parameter i.e.

$$\log(\hat{g}_{i,t}) = \hat{\alpha}_0 + \hat{\beta} \log(\hat{g}_{i-1,t}) + \hat{\gamma} \frac{(r_{t-1} - \hat{\mu})}{\sqrt{\hat{\tau}_t \hat{g}_{i-1,t}}} + \hat{\alpha} \left( \frac{|r_{t-1} - \hat{\mu}|}{\sqrt{\hat{\tau}_t \hat{g}_{i-1,t}}} - \sqrt{\frac{2}{\pi}} \right)$$

or equivalently

$$\hat{g}_{i,t} = e^{\hat{\alpha}_0} e^{\hat{\beta} \log(\hat{g}_{i-1,t}) + \hat{\gamma} \frac{(r_{t-1,t} - \hat{\mu})}{\sqrt{\hat{\tau}_t \hat{g}_{i-1,t}}} + \hat{\alpha} \left( \frac{|r_{t-1,t} - \hat{\mu}|}{\sqrt{\hat{\tau}_t \hat{g}_{i-1,t}}} - \sqrt{\frac{2}{\pi}} \right)} \quad (2.3.7)$$

and we normalize  $\hat{g}_{i,t}$ 's by their sample mean,  $\bar{g}$ , i.e. the mean of  $\hat{g}_{i,t}^* = \hat{g}_{i,t}/\bar{g}$  tends to 1 in the long run. From (2.3.7), the normalisation reduces to normalizing the intercept  $\hat{\alpha}_0$  by  $\bar{g}$  while the other parameters remain unchanged. Hence, the unit EGARCH component is:

$$\log(\hat{g}_{i,t}) = (\hat{\alpha}_0 - \log(\bar{g})) + \hat{\beta} \log(\hat{g}_{i-1,t}) + \hat{\gamma} \frac{(r_{i-1,t} - \hat{\mu})}{\sqrt{\hat{\tau}_t \hat{g}_{i-1,t}}} + \hat{\alpha} \left( \frac{|r_{i-1,t} - \hat{\mu}|}{\sqrt{\hat{\tau}_t \hat{g}_{i-1,t}}} - \sqrt{\frac{2}{\pi}} \right)$$

Finally, to keep the total volatility estimate unchanged, we multiply  $\hat{\tau}_t$  by  $\bar{g}$  which is equivalent to multiplying the long term component parameter estimates  $\hat{m}$  and  $\hat{\theta}$  by  $\bar{g}$ . Since  $\bar{g}$  is positive, the scaling does not affect the sign of the important parameter  $\hat{\theta}$  in the economic interpretation of the impact of macroeconomic variable.

## 2.3.2 Statistical properties of GJR-GARCH-MIDAS and EGARCH-MIDAS

### Kurtosis of GJR-GARCH-MIDAS and EGARCH-MIDAS

Similar to GJR-GARCH-MIDAS (Conrard and Klein (2019)), EGARCH-MIDAS model produces a larger kurtosis than the standard EGARCH when the macroeconomic variable has a significant impact on the long term volatility. This property is desired as most of return series have large sample kurtosis.

**Proposition 1:** *The kurtosis  $K$  of GJR-GARCH-MIDAS and EGARCH-MIDAS is greater than the kurtosis their nested standard model. More precisely, they satisfy:*

GJRGARCH-MIDAS:

$$K_{GJRM} = \frac{E(\tau_t^2)}{E^2(\tau_t)} K_{GJR} > K_{GJR}$$

## EGARCH-MIDAS

$$K_{EGM} = \frac{E(\tau_t^2)}{E^2(\tau_t)} K_{EG} > K_{EG}$$

where  $K_{GJRM}$  is the kurtosis of GJRGARCH-MIDAS,  $K_{EGM}$  is the kurtosis of EGARCH-MIDAS,  $K_{GJR}$  is the kurtosis of standard GJRGARCH(1,1),  $K_{EG}$  is the kurtosis of standard EGARCH(1,1). See Appendix 1.

## Long memory of EGARCH-MIDAS

Several extensions of GARCH model were developed to capture the long memory of volatility measured by the autocorrelation of the squared returns, denoted  $\rho_2(k)$ . GJR-GARCH(1,1) fails to capture this stylised fact due to its the exponential rate of decay. Camero (2004) discussed the relationship between kurtosis, persistence, and first order autocorrelation,  $\rho_2(1)$  for GARCH(1,1) and EGARCH(1,1). Unlike GARCH, the decay rate of  $\rho_2(1)$  of EGARCH does not depend on  $\beta$ , but on the other parameters  $\alpha_0$ ,  $\alpha$ , and  $\gamma$ . From Conrard and Klein (2019), it is easily seen that the implied  $\rho_2(k)$  of GJR-GARCH-MIDAS model can be expressed as a linear combination of the autocorrelation of  $\tau_t$  and  $g_t$ . We show that this result can also be applied to EGARCH-MIDAS model.

**Proposition 2:** *Under general regular conditions of stationarity  $0 < |\beta| < 1$  for EGARCH-MIDAS,  $0 < \alpha < 1$ ,  $0 < \beta < 1$ , and  $0 < \alpha + \beta + \frac{\gamma}{2} < 1$  for GJR-GARCH-MIDAS, the autocorrelation function of squared returns for GJR-GARCH-MIDAS and EGARCH-MIDAS is given by:*

$$\rho_2(k) = \rho_2^\tau(k) \frac{\text{var}(\tau_t)}{\text{var}((r_t - \mu)^2)} + \rho_2^g(k) \frac{(\rho_2^\tau(k) \text{var}(\tau_t) + E^2(\tau_t)) \text{var}(g_t \varepsilon_t^2)}{\text{var}((r_t - \mu)^2)} \quad (2.3.8)$$

where  $\rho_2^\tau(k)$  and  $\rho_2^g(k)$  are the autocorrelation of squared  $\tau_t$ s and  $g_t$ . See Appendix 1.

We note that when  $\tau_t$  is constant ( $\theta = 0$ ) i.e. the macroeconomic variable has no impact on the total volatility, (2.3.8) reduces to  $\rho_2(k) = \rho_2^g(k)$  whereas when  $\tau_t$  is a slowly varying stationary process,  $\rho_2^\tau(k)$  is large, the first term of the right hand side measure by how much  $\rho_2^g(k)$  will be shifted away from the x-axis when  $\rho_2^g(k)$  decays to 0. Hence, (E)GJR-GARCH-MIDAS models are appealing for modelling returns having long memory.

## GJR-GARCH and EGARCH with time varying intercepts

We can show that GJR-GARCH-MIDAS model is equivalent to GJR-GARCH(1,1) model with a time varying intercept  $\alpha_0$ . By multiplying both sides of  $g_{i,t}$  in (2.2.8) by  $\tau_t$ , we express the total volatility,  $\sigma_{i,t}^2 = \tau_t g_{i,t}$ , of GJR-GARCH-MIDAS as

$$\sigma_{i,t}^2 = \tau_t \left(1 - \alpha - \beta - \frac{\gamma}{2}\right) + \tau_t \alpha \frac{(r_{i-1,t} - \mu)^2}{\tau_t} + \tau_t \gamma \frac{(r_{i-1,t} - \mu)^2}{\tau_t} I_{(r_{i-1,t} - \mu < 0)} + \tau_t \beta g_{i-1,t}$$

$$\sigma_{i,t}^2 = \tau_t(1 - \alpha - \beta - \frac{\gamma}{2}) + \alpha(r_{i-1,t} - \mu)^2 + \gamma(r_{i-1,t} - \mu)^2 I_{(r_{i-1,t} - \mu < 0)} + \beta \sigma_{i-1,t}^2 \quad (2.3.9)$$

where the last equality is obtained by assuming that  $(i-1)^{th}$  and  $i^{th}$  days belong to the same month  $t$ . This shows that GJR-GARCH-MIDAS model is more general than the switching-regime GJR-GARCH model, where we usually have the 2 or 3 regime-dependent intercepts.

Similarly, we show that EGARCH-MIDAS is EGARCH(1,1) with time varying intercept: Using (2.3.4),  $\sigma_{i,t}^2$ , can be expressed as

$$\sigma_{i,t}^2 = \tau_t e^{\alpha_0} e^{\beta \log(g_{i-1,t}) + \gamma \frac{(r_{i-1,t} - \mu)}{\sqrt{\tau_t g_{i-1,t}}} + \alpha \left( \frac{|r_{i-1,t} - \mu|}{\sqrt{\tau_t g_{i-1,t}}} - \sqrt{\frac{2}{\pi}} \right)}$$

Since  $\tau_t = e^{\log(\tau_t)}$ , and  $\sigma_{i-1,t} = \sqrt{\tau_t g_{i-1,t}}$ , the above equality becomes:

$$\begin{aligned} \sigma_{i,t}^2 &= e^{\log(\tau_t)} e^{\alpha_0} e^{\beta \log(\frac{\sigma_{i-1,t}^2}{\tau_t}) + \gamma \frac{(r_{i-1,t} - \mu)}{\sqrt{\sigma_{i-1,t}}} + \alpha \left( \frac{|r_{i-1,t} - \mu|}{\sqrt{\sigma_{i-1,t}}} - \sqrt{\frac{2}{\pi}} \right)} \\ \sigma_{i,t}^2 &= e^{\alpha_0 + (1-\beta) \log(\tau_t)} e^{\beta \log(\sigma_{i-1,t}) + \gamma \frac{(r_{i-1,t} - \mu)}{\sqrt{\sigma_{i-1,t}}} + \alpha \left( \frac{|r_{i-1,t} - \mu|}{\sqrt{\sigma_{i-1,t}}} - \sqrt{\frac{2}{\pi}} \right)} \end{aligned}$$

Hence,

$$\log(\sigma_{i,t}^2) = (\alpha_0 + (1-\beta) \log(\tau_t)) + \gamma \frac{(r_{i-1,t} - \mu)}{\sqrt{\sigma_{i-1,t}}} + \alpha \left( \frac{|r_{i-1,t} - \mu|}{\sqrt{\sigma_{i-1,t}}} - \sqrt{\frac{2}{\pi}} \right) + \beta \log(\sigma_{i-1,t}^2) \quad (2.3.10)$$

The above specification is that of EGARCH(1,1) with time varying intercept  $\alpha_0 + (1-\beta) \log(\tau_t) = \alpha_0 + (1-\beta)(m + \theta \sum_{k=1}^K w(k, \omega) X_{t-k})$

## 2.4 QML Estimation

We apply the the quasi-maximum likelihood (QML) method to estimate the parameters of GJR-GARCH-MIDAS and EGARCH-MIDAS models. For the three model specifications given by (2.2.1-2.2.3), (2.2.7-2.2.9) and (2.3.1-2.3.3), it is not straightforward to derive a density of  $\mathbf{r} = \{r_{i,t}\}_{i=1, \dots, n_t, t=1, \dots, N}$  since the distribution of volatility components,  $g_{i,t}$  and  $\tau_t$ , are unknown.

Assuming the conditional normality of  $\varepsilon_{i,t}$ , the likelihood function is given by

$$\log(L(\mathbf{r} | \Theta)) = -\frac{T}{2} \log(2\pi) - \frac{1}{2} \sum_{t=1}^N \sum_{i=1}^{n_t} \log(\tau_t g_{i,t}) - \frac{1}{2} \sum_{t=1}^N \sum_{i=1}^{n_t} \frac{(r_{i,t} - \mu)^2}{\tau_t g_{i,t}} \quad (2.4.1)$$

where  $T = \sum_{t=1}^N n_t$  and  $\Theta$  is the vector of parameters, i.e.  $\Theta = (\mu, \alpha, \beta, m, \theta, \omega)$  for GARCH-MIDAS,  $\Theta = (\mu, \alpha, \beta, \gamma, m, \theta, \omega)$  for GJR-GARCH-MIDAS, and  $\Theta = (\mu, \alpha_0, \beta, \gamma, \alpha, m, \theta, \omega)$  for EGARCH-MIDAS.

Since the estimation of the long term component,  $\tau_t$  requires  $t > K$ , we maximise:

$$\log(L(\mathbf{r} | \Theta)) = -\frac{T}{2} \log(2\pi) - \frac{1}{2} \sum_{t=1}^N \sum_{i=K+1}^{n_i} \log(\tau_t g_{i,t}) - \frac{1}{2} \sum_{t=1}^N \sum_{i=K+1}^{n_i} \frac{(r_{i,t} - \mu)^2}{\tau_t g_{i,t}} \quad (2.4.2)$$

The QML estimator of  $\Theta$  is then obtained by maximising  $\log(L(\mathbf{r} | \Theta))$ .

The QML can be estimated using the numerical algorithm such as the popular *fmincon.m* built in the MATLAB function. Via simulations, we find that this function tends to produce a local maximum instead of the global one. Thus, we highly recommend the use of *simulannealbnd.m* function, especially when *fmincon.m* produces a unusually large estimate of the Beta weighting function,  $\omega$ . As the covariance matrix of QML estimate is more complex than the inverse of an information matrix, the parameters are estimated numerically from Gradient and Hessian. However, GJR-GARCH-MIDAS and EGARCH-MIDAS models introduce more parameters because we need to estimate the long term volatility component. Notice however that if the number of parameters is more than 7, then the QML tends to become unreliable, see Nakatsuma (2000), Ardia et al. (2008) and Takaishi (2011).

Consistency and asymptotic normality of QMLE have been derived by Lee and Hanson (1994) for GJR-GARCH(1,1) and Kyriakoupoulou (2014) for EGARCH(1,1). However, it is still challenging to derive the relevant asymptotic theory for GJR-GARCH-MIDAS and EGARCH-MIDAS. Wang and Ghysels (2014) provided the proof for the GARCH-MIDAS model only if the long term volatility is estimated using the realised volatility rather than macroeconomic variables. The main issue is how to deal with stochastic macroeconomic variables that are observed at a different frequency (month or quarter). Assuming that macroeconomic variable is observed at the same daily frequency, Conrad and Kleen (2019) are able to provide the asymptotic theory for GJR-GARCH-MIDAS. Given the existing consistency and asymptotic normality of the EGARCH estimator, we conjecture that the approach by Conrad and Kleen (2019) can be employed to derive the asymptotic theory for EGARCH-MIDAS.

It is still challenging to derive the relevant asymptotic theory for GJR-GARCH-MIDAS and EGARCH-MIDAS, though most existing studies simply assume that the QML estimator is normally distributed asymptotically. We leave this for future work, but evaluate the validity of the QML estimator via simulations in the next section.

## 2.5 Simulation study

We investigate the finite sample performance of the QML estimator. To make the simulation design realistic, we construct the DGP in a data-oriented manner as follows:

First, we generate a sample of 240 monthly observations for an artificial macroeconomic vari-



able, which is assumed to follow an AR(1) process (e.g. Conrad and Kleen (2021)):

$$x_t = \varphi x_{t-1} + \varepsilon_t, \quad \varepsilon_t \sim N(0, 1), \quad t = 1, \dots, 240$$

where we set  $\varphi = 0.95$  and  $x_0 = 0$ . Second, we generate the long term component  $\tau_t$  by

$$\log(\tau_t) = m + \theta \sum_{k=1}^K w(k, \omega) x_{t-k}$$

where we set  $K = 24$ ,  $\omega = 5$  and  $w(k, \omega)$  is the Beta weighting function given in (2.2.6).<sup>5</sup> For parameter values, we set  $m = 0.1$  and consider several values of  $\theta = \{-0.8, -0.4, -0.2, 0, 0.2, 0.4, 0.8\}$ . Third, we generate the daily observations of the unit-variance short-term component,  $g_{i,t}$  for each month  $t$  and for  $i = 1, \dots, 22$  as follows:

$$\text{GARCH-MIDAS: } g_{i,t} = (1 - \alpha - \beta) + \alpha \frac{(r_{i-1,t} - \mu)^2}{\tau_t} + \beta g_{i-1,t};$$

$$\text{GJR-GARCH-MIDAS: } g_{i,t} = (1 - \alpha - \beta - \frac{\gamma}{2}) + \alpha \frac{(r_{i-1,t} - \mu)^2}{\tau_t} + \gamma \frac{(r_{i-1,t} - \mu)^2}{\tau_t} 1_{[r_{i-1,t} - \mu < 0]} + \beta g_{i-1,t};$$

$$\text{EGARCH-MIDAS: } \log(g_{i,t}) = \alpha \sqrt{\frac{2}{\pi}} + \alpha \left\{ \frac{|r_{i-1,t} - \mu|}{\sqrt{\tau_t g_{i-1,t}}} - \sqrt{\frac{2}{\pi}} \right\} + \gamma \frac{r_{i-1,t} - \mu}{\sqrt{\tau_t g_{i-1,t}}} + \beta g_{i-1,t}$$

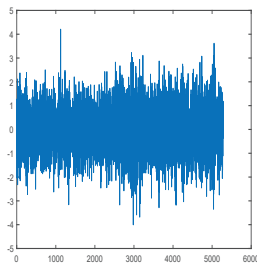
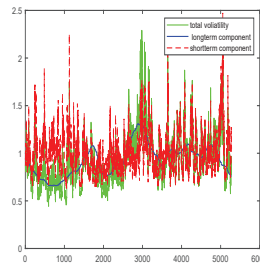
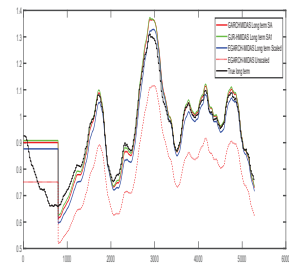
where the parameters of the models are chosen, and initial values  $r_{0,1}$  and  $g_{0,1}$  are chosen to enable us to simulate recursively/sequentially  $g_{i,t}$  and  $r_{i,t}$  because  $g_{i,t}$  requires the value of  $r_{i-1,t}$  and computation of  $r_{i,t}$  requires the value of  $g_{i,t}$ . Finally, we generate the daily returns by  $r_{i,t} = \mu + \sqrt{\tau_t g_{i,t}} \varepsilon_{i,t}$ , where we set  $\mu = 0$ , draw  $\varepsilon_t$  randomly from  $N(0, 1)$ , and we set the initial values at  $r_{0,1} = 0$ , and  $g_{0,1} = 1$ .

We first depict the simulated return data generated by GARCH-MIDAS in Fig.2.2(a) and the total volatility together with the long-term component,  $\tau_t$  and the short-term component,  $g_{i,t}$  in Fig.2.2(b), and Table 2.5.1 reports the QML estimates for three models.

EGARCH-MIDAS and GJR-GARCH-MIDAS correctly reject the absence of the leverage effect whilst the three models produce similar estimates of  $\tau_t$ . In Fig.2.2(c) we showed that the long term component,  $\hat{\tau}_t$  estimated by three models are relatively close to the true one. In particular, we find that only the scaling procedure for EGARCH-MIDAS can produce accurate estimates of  $\tau_t$  whereas unscaled EGARCH-MIDAS (with  $\alpha_0$  being estimated) tends to significantly underestimate the long term component.

<sup>5</sup>Due to  $K$  lagged values, we generated  $240 + K$  samples for  $x_t$ .

Figure 2.2: Beta Weighting function

(a) simulated daily re-  
turns(b) simulated volatility  
component(c) simulated long term  
component

Note: Figure (a) shows the simulated daily return using GARCH-MIDAS; Figure (b) shows simulated total volatility, short term component of the total volatility and the long term component of the volatility; Figure (c) shows the true, and simulated long term component of the volatility using GARCH-MIDAS, GJR-GARCH-MIDAS, and EGARCH-MIDAS.

Table 2.5.1: QML estimation results for DGP constructed by GARCH-MIDAS

Model	Parameters							Fit statistic			RMSE		
	$\mu$	$\alpha$	$\beta$	$\gamma$	$\theta$	$\omega$	m	BIC	LOG-L	TV	LV	SV	
True value	0	0.05	0.9	0	-0.3	5	-0.1						
G-MIDAS	0.010 (0.013)	0.053 (0.009)	0.899 (0.020)		-0.358 (0.083)	4.943 (2.688)	-0.113 (0.046)	12409	-6178	0.019	0.028	0.022	
GJR-MIDAS	0.009 (0.014)	0.053 (0.011)	0.898 (0.020)	0.000 (0.012)	-0.349 (0.083)	5.347 (3.06)	-0.104 (0.047)	12417	-6178	0.019	0.025	0.02	
EG-MIDAS	0.01 (0.005)	0.106 (0.007)	0.953 (0.001)	0.001 (0.003)	-0.363 (0.020)	4.422 (0.556)	-0.14 (0.079)	12432	-6181	0.0598	0.038	0.069	
EG-MIDAS-U	0.01 (0.463)	0.107 (0.033)	0.953 (0.007)	0.001 (0.009)	-0.347 (0.078)	4.241 (1.702)	-0.294 (0.859)	12432	-6181	0.059	0.164	0.215	

Note: The table reports the parameter estimates of GARCH-MIDAS (2.2.1-2.2.3), GJR-GARCH-MIDAS (2.2.7-2.2.9), and EGARCH-MIDAS (2.3.1-2.3.3). We provide the results for monthly long term components. The parameter estimates standard deviations are reported in brackets. The parameter estimates are based on 20 years of observations. The long term component is assumed to depend on  $K=24$  monthly observations. The covariate  $X_t$  is modeled as an AR(1) process.  $BIC = -2\text{LOG}L + p\log(T)$  where  $p$  is the number of parameters of the model,  $T$  is number of returns, and LOGL is the Log-Likelihood.

## Simulation results

Table 2.5.2 reports the QML estimation results for GARCH-MIDAS, GJR-GARCH-MIDAS and EGARCH-MIDAS models when the data is generated by GARCH-MIDAS. We also present the fit of the model using AIC, BIC and logL, as well as RMSEs of the total, long term, and short term volatility. As described above, we use numerical algorithm, *simunealbd.m* in Matlab to minimise any chance of convergence to the local maximum instead of the global maximum. QML estimates for GARCH-MIDAS are pretty close to the true values in most cases considered. Not surprisingly, GARCH-MIDAS is the best fitting model in terms of BIC while displaying the smallest RMSEs of the total, long term, and short term volatility in all cases. Further, QML estimates for GJR-GARCH-MIDAS look more or less consistent and clearly indicate that the leverage coefficient is insignificant.

In Table 2.5.3 we present the QML estimation results when the data are generated from GJR-

GARCH-MIDAS. QML estimates for GJR-GARCH-MIDAS are pretty accurate, including the leverage coefficient and the long-run parameter,  $\theta$ . GJR-GARCH-MIDAS is the best fitting model, but also producing much smaller RMSEs than GARCH-MIDAS and EGARCH-MIDAS.

The QML estimation results are then reported in Table 2.5.4 when the data are generated from EGARCH-MIDAS. QML estimates for EGARCH-MIDAS are mostly close to the true values. Now, EGARCH-MIDAS is the best fitting model while displaying much smaller RMSEs than other models in all cases.<sup>6</sup>

Table 2.5.2: QML estimation results for DGP constructed by GARCH-MIDAS

Model	Parameters									Fit			Fit	
	$\theta$	$\mu_0$	$\alpha_0$	$\beta_{0.9}$	$\gamma$	$\alpha_{0.07}$	$\theta$	$\omega_5$	m 0.1	BIC	log $-L$	TV	LV	SV
G-MIDAS	-0.2	0.001 (0.014)	0.031	0.898 (0.013)		0.069 (0.008)	-0.209 (0.141)	5.112 (60.980)	0.086 (0.084)	12772.06	-6360.31	0.056	0.113	0.087
	-0.4	-0.001 (0.014)	0.031	0.899 (0.013)		0.069 (0.008)	-0.384 (0.148)	5.19 (0.637)	0.097 (0.088)	12800.77	-6374.67	0.065	0.15	0.114
	0.4	-0.002 (0.014)	0.032	0.897 (0.014)		0.07 (0.009)	0.391 (0.138)	5.129 (0.449)	0.101 (0.081)	12906.33	-6427.45	0.062	0.127	0.093
	-0.8	0.002 (0.014)	0.028	0.899 (0.013)		0.071 (0.008)	-0.789 (0.170)	5.253 (0.674)	0.106 (0.118)	12967.62	-6458.11	0.103	0.288	0.231
	0.8	-0.006 (0.013)	0.028	0.901 (0.013)		0.069 (0.008)	0.753 (0.167)	5.321 (0.844)	0.103 (0.108)	12799.16	-6373.87	0.091	0.238	0.191
GJR-MIDAS	-0.2	-0.001 (0.014)	0.030	0.899 (0.013)	0.005 (0.013)	0.067 (0.010)	-0.192 (0.144)	5.068 (27.137)	0.090 (0.088)	12780.94	-6360.47	0.059	0.119	0.0941
	-0.4	-0.002 (0.014)	0.030	0.899 (0.013)	0.006 (0.012)	0.066 (0.010)	-0.347 (0.151)	5.155 (0.519)	0.097 (0.094)	12860.25	-6400.12	0.072	0.151	0.120
	0.4	-0.003 (0.014)	0.032	0.897 (0.013)	0.006 (0.013)	0.067 (0.011)	0.381 (0.141)	5.105 (0.383)	0.104 (0.085)	12915.23	-6427.62	0.069	0.144	0.104
	-0.8	0.006 (0.014)	0.025	0.902 (0.012)	0.005 (0.012)	0.068 (0.010)	-0.773 (0.183)	5.161 (0.639)	0.122 (0.158)	12979.64	-6459.82	0.118	0.318	0.207
	0.8	-0.002 (0.014)	0.027	0.902 (0.012)	0.004 (0.012)	0.068 (0.010)	0.769 (0.166)	5.163 (0.475)	0.123 (0.112)	12833.39	-6374.19	0.099	0.280	0.183
EG-MIDAS	-0.2	-0.003 (0.821)	0.057 (0.202)	0.968 (0.007)	0.006 (0.501)	0.144 (0.250)	-0.189 (0.092)	5.055 (10.517)	0.084 (1.002)	12799.60	-6365.52	0.122	0.121	0.165
	-0.4	-0.008 (0.748)	0.048 (0.203)	0.968 (0.007)	0.004 (0.465)	0.143 (0.256)	-0.381 (0.093)	5.187 (0.688)	0.087 (0.196)	12828.59	-6380.01	0.127	0.147	0.204
	0.4	-0.001 (0.742)	0.084 (0.260)	0.968 (0.007)	0.003 (0.529)	0.145 (0.317)	0.384 (0.088)	5.138 (0.664)	0.083 (0.220)	12936.40	-6433.91	0.136	0.158	0.215
	-0.8	0.002 (0.723)	0.039 (0.211)	0.971 (0.005)	0.001 (0.505)	0.147 (0.268)	-0.788 (0.107)	5.236 (0.705)	0.112 (0.127)	12999.25	-6465.34	0.179	0.323	0.287
	0.8	-0.001 (0.713)	0.011 (0.311)	0.971 (0.006)	0.001 (0.616)	0.144 (0.383)	0.760 (0.097)	5.278 (0.803)	0.096 (0.234)	12857.35	-6384.39	0.158	0.273	0.247

Note: Note: This table reports the simulation results of QMLE approach when the data generating process is GARCH-MIDAS. G-MIDAS, GJR-MIDAS, and EG-MIDAS refer to GARCH-MIDAS (2.2.1-2.2.3), GJR-GARCH-MIDAS (2.2.7-2.2.9), and EGARCH-MIDAS (2.3.1-2.3.3) respectively. TV, LV, and SV, refer to total volatility, Long-term component, and Short-term component respectively. We provide the results for monthly long term components. The parameter estimates standard deviations are reported in brackets. The parameter estimates are based on 20 years of observations. The long term component is assumed to depend on  $K=24$  monthly observations. The covariate  $X_t$  is modeled as an AR(1) process.  $BIC = -2\text{LOGL} + p\log(T)$  where  $p$  is the number of parameters of the model,  $T$  is number of returns, and LOGL is the Log-Likelihood.

<sup>6</sup>We have conducted the additional simulation using the EGARCH-MIDAS DGP with a very high volatility persistence with  $\beta = 0.99$ . Both GARCH-MIDAS and GJR-GARCH-MIDAS tend to estimate the long term component,  $\tau$ , incorrectly (the estimates of  $\theta$  are insignificant too). We also obtained  $\hat{\alpha} + \hat{\beta} = 0.9987$  for GARCH-MIDAS and  $\hat{\alpha} + \hat{\beta} + \frac{\hat{\gamma}}{2} > 1$  (1.006) for GJR-GARCH-MIDAS, both of which violate the stationary condition. In this case only EGARCH-MIDAS can produce relatively correct estimates. These results are available upon request.

Table 2.5.3: QML estimation results for DGP constructed by GJR-GARCH-MIDAS

Model	Parameters									Fit			RMSE	
True values	$\theta$	$\mu_0$	$\alpha_0$	$\beta_{0.9}$	$\gamma_{0.06}$	$\alpha_{0.05}$	$\theta$	$\omega_5$	m 0.1	BIC	$\log -L$	TV	LV	SV
G-MIDAS	-0.2	0.013 (0.013)	0.021	0.894 (0.011)		0.978 (0.008)	-0.218 (0.181)	5.129 (47.524)	0.078 (0.129)	12442.29	-6195.43	0.168	0.168	0.228
	-0.4	0.013 (0.013)	0.021	0.895 (0.011)		0.083 (0.009)	-0.371 (0.175)	5.121 (0.476)	0.111 (0.142)	12551.31	-6249.94	0.178	0.219	0.241
	0.4	0.013 (0.013)	0.021	0.894 (0.011)		0.084 (0.009)	0.386 (0.174)	5.107 (0.493)	0.094 (0.135)	12532.74	-6240.65	0.179	0.182	0.229
	-0.8	0.012 (0.012)	0.019	0.895 (0.011)		0.085 (0.008)	-0.778 (0.214)	5.237 (0.715)	0.093 (0.164)	12518.55	-6233.56	0.217	0.208	0.202
	0.8	0.011 (0.013)	0.02	0.896 (0.011)		0.083 (0.008)	0.781 (0.201)	5.168 (0.642)	0.111 (0.154)	12692.65	-6320.61	0.218	0.263	0.237
GJR-MIDAS	-0.2	0.001 (0.013)	0.022	0.899 (0.011)	0.058 (0.013)	0.049 (0.009)	-0.202 (0.173)	5.077 (85.086)	0.092 (0.126)	12429.38	-6184.69	0.072	0.162	0.161
	-0.4	0.001 (0.013)	0.021	0.900 (0.011)	0.060 (0.013)	0.049 (0.009)	-0.384 (0.177)	5.091 (0.427)	0.099 (0.138)	12538.99	-6239.50	0.079	0.213	0.146
	0.4	0.001 (0.013)	0.016	0.898 (0.011)	0.061 (0.013)	0.050 (0.009)	0.391 (0.175)	5.075 (0.272)	0.095 (0.131)	12519.49	-6229.75	0.078	0.163	0.136
	-0.8	0.001 (0.013)	0.018	0.901 (0.011)	0.057 (0.013)	0.052 (0.009)	-0.786 (0.217)	5.081 (0.494)	0.091 (0.177)	12509.60	-6224.80	0.115	0.199	0.163
	0.8	-0.001 (0.013)	0.018	0.901 (0.011)	0.057 (0.013)	0.051 (0.009)	0.739 (0.196)	5.129 (0.577)	0.110 (0.154)	12681.79	-6310.89	0.105	0.253	0.155
EG-MIDAS	-0.2	-0.002 (3.002)	0.022 (0.350)	0.978 (0.002)	-0.038 (0.009)	0.162 (0.434)	-0.189 (0.101)	5.196 (43.296)	0.118 (1.107)	12457.62	-6194.52	0.182	0.172	0.366
	-0.4	-0.002 (0.860)	0.037 (0.234)	0.978 (0.003)	-0.040 (0.011)	0.163 (0.293)	-0.367 (0.117)	5.035 (0.611)	0.089 (0.271)	12565.28	-6248.35	0.174	0.252	0.412
	0.4	-0.002 (0.979)	0.052 (0.441)	0.977 (0.003)	-0.040 (0.011)	0.163 (0.547)	0.387 (0.104)	5.084 (0.566)	0.077 (0.211)	12544.60	-6238.02	0.181	0.185	0.352
	-0.8	-0.003 (1.107)	0.058 (0.346)	0.981 (0.002)	-0.037 (0.009)	0.166 (0.435)	-0.777 (0.126)	5.149 (0.789)	0.081 (0.258)	12535.80	-6233.61	0.215	0.224	0.424
	0.8	-0.004 (0.953)	0.047 (0.280)	0.981 (0.002)	-0.038 (0.009)	0.164 (0.346)	0.759 (0.127)	5.161 (0.682)	0.089 (0.202)	12708.98	-6320.20	0.2145	0.525	0.451

Note: Note: This table reports the simulation results of QMLE approach when the data generating process is GJR-GARCH-MIDAS. G-MIDAS, GJR-MIDAS, and EG-MIDAS refer to GARCH-MIDAS (2.2.1-2.2.3), GJR-GARCH-MIDAS (2.2.7-2.2.9), and EGARCH-MIDAS (2.3.1-2.3.3) respectively. TV, LV, and SV, refer to total volatility, Long-term component, and Short-term component respectively. We provide the results for monthly long term components. The parameter estimates standard deviations are reported in brackets. The parameter estimates are based on 20 years of observations. The long term component is assumed to depend on  $K=24$  monthly observations. The covariate  $X_t$  is modeled as an AR(1) process.  $BIC = -2LOGL + p \log(T)$  where  $p$  is the number of parameters of the model,  $T$  is number of returns, and LOGL is the Log-Likelihood.

Table 2.5.4: QML estimation results for DGP constructed by EGARCH-MIDAS

Model	Parameters									Fit			RMSE		
	True values	$\theta$	$\mu_0$	$\alpha_0$	$\beta_{0.95}$	$\gamma_{-0.1}$	$\alpha_{0.04}$	$\theta$	$\omega_5$	m 0.1	BIC	$\log-L$	TV	LV	SV
G-MIDAS	-0.2	0.025 (0.016)	0.056	0.893 (0.022)			0.049 (0.008)	-0.213 (0.056)	5.322 (0.708)	0.145 (0.045)	13971.2	-6959.88	0.369	0.197	0.399
	-0.4	0.025 (0.016)	0.054	0.896 (0.021)			0.049 (0.008)	-0.407 (0.058)	5.533 (6.917)	0.128 (0.047)	14024.11	-6986.34	0.406	0.181	0.400
	0.4	0.0240 (0.016)	0.052	0.898 (0.020)			0.048 (0.008)	0.392 (0.067)	5.415 (2.403)	0.119 (0.054)	14081.18	-7014.87	0.413	0.214	0.455
	-0.8	0.022 (0.015)	0.039	0.912 (0.016)			0.047 (0.007)	-0.783 (0.108)	5.681 (34.207)	0.138 (0.117)	14009.54	-6979.05	0.614	0.219	0.753
	0.8	0.022 (0.015)	0.042	0.908 (0.017)			0.049 (0.007)	0.786 (0.091)	5.693 (2.036)	0.108 (0.900)	13906.79	-6927.68	0.579	0.236	0.617
GJR-MIDAS	-0.2	0.006 (0.016)	0.049	0.901 (0.015)	0.098 (0.014)	0.006 (0.009)	-0.195 (0.063)	5.111 (0.4248)	0.127 (0.0601)	13883.29	-6911.65	0.222	0.189	0.342	
	-0.4	0.005 (0.016)	0.048	0.902 (0.015)	0.098 (0.014)	0.001 (0.009)	-0.401 (0.064)	5.256 (2.764)	0.119 (0.067)	13935.76	-6937.88	0.249	0.190	0.374	
	0.4	0.004 (0.016)	0.049	0.904 (0.015)	0.098 (0.014)	0.001 (0.009)	0.407 (0.061)	5.115 (2.229)	0.127 (0.056)	13988.17	-6964.08	0.246	0.244	0.299	
	-0.8	0.007 (0.015)	0.041	0.908 (0.013)	0.096 (0.013)	0.002 (0.008)	-0.796 (0.086)	5.427 (5.155)	0.143 (0.084)	13857.13	-6896.41	0.398	0.197	0.430	
	0.8	0.006 (0.015)	0.043	0.906 (0.013)	0.098 (0.013)	0.001 (0.008)	0.802 (0.078)	5.496 (1.649)	0.119 (0.078)	13753.92	-6844.81	0.378	0.238	0.636	
EG-MIDAS	-0.2	-0.001 (1.586)	0.079 (0.884)	0.953 (0.014)	-0.095 (1.471)	0.0394 (1.014)	-0.192 (0.041)	5.223 (0.892)	0.114 (0.171)	13857.66	-6894.54	0.117	0.181	0.191	
	-0.4	0.001 (1.809)	0.028 (0.824)	0.946 (0.013)	-0.093 (0.018)	0.046 (0.973)	-0.404 (0.041)	5.268 (1.434)	0.113 (2.208)	13919.6	-6925.52	0.161	0.168	0.235	
	0.4	-0.001 (1.079)	0.008 (0.427)	0.952 (0.013)	-0.097 (0.014)	0.043 (0.512)	0.397 (0.042)	5.451 (1.318)	0.112 (1.443)	13967.97	-6949.7	0.149	0.183	0.156	
	-0.8	0.003 (1.419)	0.005 (0.581)	0.957 (0.012)	-0.095 (0.019)	0.055 (0.693)	-0.798 (0.056)	5.296 (1.074)	0.114 (2.012)	13898.92	-6915.17	0.254	0.175	0.175	
	0.8	0.001 (1.211)	-0.011 (0.457)	0.956 (0.014)	-0.096 (0.018)	0.055 (0.519)	0.796 (0.061)	5.693 (1.579)	0.119 (2.099)	13794.74	-6863.09	0.258	0.205	0.245	

Note: This table reports the simulation results of QMLE approach when the data generating process is EGARCH-MIDAS. G-MIDAS, GJR-MIDAS, and EG-MIDAS refer to GARCH-MIDAS (2.2.1-2.2.3), GJR-GARCH-MIDAS (2.2.7-2.2.9), and EGARCH-MIDAS (2.3.1-2.3.3) respectively. TV, LV, and SV, refer to total volatility, Long-term component, and Short-term component respectively. We provide the results for monthly long term components. The parameter estimates standard deviations are reported in brackets. The parameter estimates are based on 20 years of observations. The long term component is assumed to depend on  $K=24$  monthly observations. The covariate  $X_t$  is modeled as an AR(1) process.  $BIC = -2LOGL + p \log(T)$  where  $p$  is the number of parameters of the model,  $T$  is number of returns, and LOGL is the Log-Likelihood.

In sum, we establish that the finite sample performance of the QML estimator is relatively satisfactory in all cases considered. In particular, for EGARCH-MIDAS, the scaling modification is necessary in producing the accurate estimate of the long term and the total volatility. According to BIC and RMSE, the accuracy of the total volatility will be improved when we use the correct specification of the short term volatility component. Moreover, we find that the long term volatility component is similarly estimated across the different specifications of the short term volatility component.

## 2.6 Empirical Application

Most existing empirical studies, using GARCH-MIDAS or GJR-GARCH-MIDAS, focus mainly on investigating whether the impacts of (selected) macroeconomic variables on the total and the long term volatility of the stock market indices are significant, e.g. Asgharian et al. (2013), Alsheikhmubarak and Giouvris (2017), Conrad et al. (2018), and Lin and Chang (2020).

We aim to analyse the time-varying volatility patterns of the seven stock market indices (SP500, NASDAQ, CAC40, DAX, FTSE100, NIKKEI, and HSE), but also evaluate the relative performance of GARCH-MIDAS, GJR-GARCH-MIDAS and EGARCH-MIDAS in terms of in-sample fit and out of sample forecasting performance over the period Jan 2000-Aug 2019. To investigate the impacts of macroeconomic conditions on the long-run volatility, we consider a range of macroeconomic variables. First, we employ the country-specific macroeconomic variables: industrial production (*IP*), economic policy uncertainty (*EPU*), effective exchange rate (*EER*), inflation rate (*IN*) and unemployment rate (*UR*). Next, we consider the global macro indicators: global economic policy uncertainty (*GEPU*) and Chicago Fed national activity index (*CFNI*). For *IP*, *EPU*, *EER*, *GEPU* and *FPU*, we use the growth rate which is constructed by  $100\log(X_t/X_{t-1})$ .

We report the descriptive statistics for the 7 stock market returns over the period Jan 2000-Aug 2019 in Table 2.7.1 in Appendix 1. We observe the large sample skewness, providing a support for including the leverage component in the volatility model. We note that adding the sub-period from Jan 2020 to Aug 2020, significantly increased the skewness and kurtosis of the returns for US and European indices but not for NIKKEI and HANGSENG. During the COVID19 pandemic period the largest fall in returns occurred for the U.S. and European indices whilst returns for NIKKEI and HANGSENG fell less severely, see Fig.2.4.

We display the observations of the macroeconomic variables in Fig.2.5 in Appendix 1. Each series tends to co-move, and captures the impacts of the major events such as Asian boom in early 2000s, the Iraqi war in 2003, the global financial crisis in 2008, the sharp oil price decrease in 2014, and the covid-19 pandemic. From Panel B of Table 2.7.1, we note that covid-19 pandemic does not change the overall correlation pattern. The correlations between the US and European indices range between 0.43 and 0.57. On the other hand the correlations between the US and Asian indices are much smaller (0.12–0.19) whilst those between European and Asian indices range between 0.26 and 0.37.

### 2.6.1 Benchmark estimation results

We first present the estimation results for GARCH(1,1), GJR-GARCH(1,1) and EGARCH(1,1) models in Table 2.7.2 in Appendix 1. We find that both GJR-GARCH(1,1) and EGARCH(1,1) models produce a significant leverage effect for all indices.<sup>7</sup>  $\Delta$ BIC statistic also favors GJR-GARCH(1,1) over GARCH(1,1) for all indices.<sup>8</sup> Overall, both  $\Delta$ BIC and RMSE select EGARCH(1,1) as the preferred specification. We also obtained similar conclusions for the data over 2000-2020 including the ongoing pandemic period.

<sup>7</sup>Likelihood ratio (LR) test strongly rejects the null hypothesis,  $\gamma = 0$  at the 1% significance level where  $\gamma$  is the leverage parameter.

<sup>8</sup>According to Kass and Raftery (1995),  $\Delta$ BIC is the difference between the BIC values of two competing models where the data strongly (weakly) favours the model of interest if  $\Delta$ BIC is greater than 6 (between 2 and 6).

We next report the estimation results for the SP500 index with IP growth selected as a determinant of the long term volatility component in Table 2.6.1. This application is the same as that analysed by Conrad and Kleen (2020), who applied only GJR-GARCH-MIDAS. Our results using MATLAB code produce QML estimates of GJR-GARCH-MIDAS close to those of Conrad and Kleen(2019), who obtained the estimates using R. Furthermore, the proposed scaling procedure for EGARCH-MIDAS seems to work successfully for identifying the two volatility components:  $\hat{\tau}_t$ s estimated by GJR-GARCH-MIDAS and EGARCH-MIDAS are relatively close to each other, see Fig. 3.1.

Comprehensive estimation results for all seven indices and seven macroeconomic variables are reported in Tables 2.7.3–2.7.4 in Appendix 1, where we present the QML estimates, BIC, logL, RMSE and a volatility ratio defined by  $VR = var(\log(\hat{\tau}_t))/var(\log(\hat{\tau}_t\hat{g}_t))$ .<sup>9</sup> Both GJR-GARCH-MIDAS and EGARCH-MIDAS confirm the presence of a leverage effect in volatility for all seven indices.<sup>10</sup> Furthermore, the short term volatility is highly persistent across three models. Next, the size of the long run estimate,  $\hat{\theta}$ , is qualitatively similar across the 3 models, though  $\hat{\theta}$  by GARCH-MIDAS becomes insignificant, suggesting that the standard error of  $\hat{\theta}$  depends on the correct specification of  $g_t$ .<sup>11</sup> Overall, according to  $\Delta$ BIC and RMSE, EGARCH-MIDAS is the preferred model for SP500, NASDAQ, CAC40, DAX, FTSE100 and NIKKEI whereas GJR-GARCH-MIDAS is the preferred model for HANGSENG.

Table 2.6.1: QML estimation results for SP500 using IP growth

Model	$\hat{\mu}$	$\hat{\alpha}_0$	$\hat{\alpha}$	$\hat{\beta}$	$\hat{\gamma}$	Per	$\hat{\theta}$	$\hat{\omega}$	$\hat{m}$	BIC	LOGL	RMSE	VR
GARCH	0.060 (0.008)	0.020 (0.001)	0.100 (0.002)	0.884 (0.003)		0.985				27567.39	-13765.22	6.77	
G-MIDAS	0.063 (0.01)	0.02 (0.005)	0.111 (0.003)	0.869 (0.004)		0.980	-0.637 (0.123)	5.323 (1.504)	0.293 (0.0843)	25306.33	-12625.45	6.76	7.58
GJRGARCH	0.034 (0.016)	0.02 (0.004)	0.02 (0.007)	0.899 (0.008)	0.123 (0.007)	0.981				25482.28	-12718.21	6.66	
GJR-MIDAS	0.035 (0.009)	0.024 (0.006)	0.013 (0.004)	0.893 (0.004)	0.140 (0.005)	0.976	-0.673 (0.112)	8.638 (2.348)	0.1052 (0.0638)	23212.51	-11574.15	7.44	8.71
GJR-MIDAS(CK)		0.02 (0.008)	0.019 (0.006)	0.903 (0.005)	0.113 (0.007)	0.977	-0.650 (0.161)	8.271 (1.782)	0.074 (0.089)	29211	-14573		10.63
EGARCH	0.03 (0.015)	0.002 (0.002)	0.145 (0.010)	0.978 (0.003)	-0.099 (0.006)	0.978				25434.48	-12694.31	6.5	
EG-MIDAS	0.030 (0.020)	0.000 (0.000)	0.148 (0.001)	0.974 (0.000)	-0.1104 (0.002)	0.974	-0.527 (0.097)	9.888 (3.495)	0.0548 (0.0873)	23179.41	-11553.01	6.26	5.90

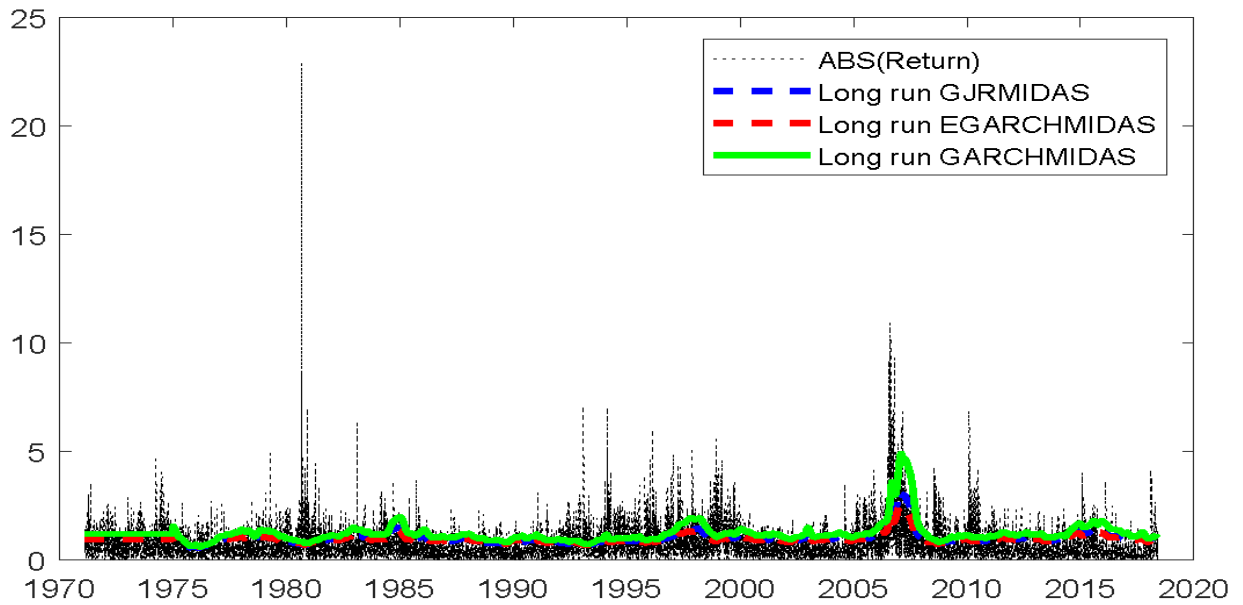
Notes: G-MIDAS, GJR-MIDAS, GJR-MIDAS(CK), and EG-MIDAS refer to GARCH-MIDAS (2.2.1-2.2.3), GJR-GARCH-MIDAS(2.2.7-2.2.9), GJR-GARCH-MIDAS by Conrad and Kleen (2020), and EGARCH-MIDAS(2.3.1-2.3.3) respectively. This table reproduce QML estimates of GJR-GARCH-MIDAS by Conrad and Kleen (2020). Standard errors are given in brackets.  $BIC = -2LOGL + p\log(T)$  where  $p$  is the number of parameters of the model,  $T$  is number of observations, and LOGL is the log-likelihood of the model. BIC in CK is computed using  $p = 6$  ( $\mu$  is not estimated) instead of  $p = 7$  for GJR-GARCH-MIDAS. Persistence, per is computed by  $[\hat{\alpha} + \hat{\beta}, \hat{\alpha} + \hat{\beta} + \hat{\gamma}/2, \hat{\beta}]$  for GARCH-MIDAS, GJR-GARCH-MIDAS and EGARCH-MIDAS models.

<sup>9</sup>Following the literature, we first set the range of  $\omega$ , say [1,50]. It is well-established (e.g. Engle et al. (2013)) that the estimation algorithm tends to result in a local-maximum if  $\omega$  is estimated at near boundary (close to 1 or 50). To ensure that QML estimates do not correspond to a local-maximum, we repeat the numerical estimation using the additional 12 intervals of  $\omega$  in [1, 4], [4, 8], [8, 12], ..., [44, 50] together with [1, 50], and select the estimate that produces the largest LOGL.

<sup>10</sup>The likelihood ratio test for the null,  $\gamma = 0$  strongly rejects GARCH-MIDAS against GJRGARCH-MIDAS for all indices and macroeconomic variables.

<sup>11</sup>This may cast doubt upon the statistical independence between  $\hat{g}_t$  and  $\hat{\tau}_t$  derived by Wang and Ghyeles (2014)

Figure 2.3: Long term volatility component of SP500



Note: The long term volatility component,  $\tau_t$ , is estimated respectively by GARCH-MIDAS, GJR-GARCH-MIDAS and EGARCH-MIDAS models..

## 2.6.2 In-sample fit comparison

In Table 2.6.2 we report the in-sample fit performance of alternative GARCH-MIDAS models, where we reproduce the long term estimate,  $\hat{\theta}$ , VR and BIC from Table 2.7.3 in Appendix 1. We summarise the main findings as follows:

First, according to BIC, EGARCH-MIDAS is the preferred model for SP500, NASDAQ, CAC40, DAX and NIKKEI whilst GJR-GARCH-MIDAS is the preferred model for HANGSENG across all macroeconomic variables. For FTSE100 we obtained mixed results: EGARCH-MIDAS is preferred for *IP*, *EER*, *GEP* and GJR-GARCH-MIDAS is preferred for *IN*, *EPU*, *CFNI*.

Second, the long term estimates,  $\hat{\theta}$ , produced by GJR-GARCH-MIDAS and EGARCH-MIDAS, are mostly significant with predicted signs while those from GARCH-MIDAS tend to be insignificant. IP growth has a significant counter-cyclical impact for all 7 indices. We also observe a significant negative impact of EER growth on the volatility for all indices except for HANGSENG showing a positive impact, which may reflect the Chinese governments policy to keep Yuan low to boost their exports (Li and Moosa (2017) and Anisul (2021)). Interestingly, *CFNAI*, measuring an overall financial market condition in the US, produced a highly significant counter-cyclical impact on the volatility for all seven indices.

Third, we evaluate the relative importance of each macroeconomic variable by employing VR that measures the fraction of the total volatility explained by the long term component. Focusing on EGARCH-MIDAS estimation results, we find that the most influential variable is the global financial market condition proxied by *CFNAI*, that explains 27.5% of the total volatility for SP500 while covering between 15%-34% of the total volatility for the other indices. This



highlights the dominant position of the US financial market. The second-most influential variable is IP growth, that explains 12.8% of the total volatility for SP500 while covering between 5%-13% of the total volatility for the other indices.<sup>12</sup>

Fourth, we find a mixed evidence on the impacts of EPU and GEPU. EGARCH-MIDAS produces a significant positive impact of EPU (GEPU) for SP500, NASDAQ, CAC40 and NIKKEI (HANGSENG). On the other hand, GJR-GARCH-MIDAS presents a positive significant impact of EPU for CAC40, FTSE and NIKKEI and a positive significant impact of GEPU only for FTSE100. In terms of VR, EPU tends to be more influential than GEPU for SP500, NASDAQ, CAC40 and NIKKEI whilst the reverse is true for FTSE and HANGSENG.

Table 2.6.2: The summary of QML estimation results

Macro	Model	SP500			NASDAQ			CAC40			DAX			FTSE			NIKKEI			HSE		
		$\hat{\theta}$	VR	BIC	$\hat{\theta}$	VR	BIC	$\hat{\theta}$	VR	BIC	$\hat{\theta}$	VR	BIC	$\hat{\theta}$	VR	BIC	$\hat{\theta}$	VR	BIC	$\hat{\theta}$	VR	BIC
IP	GM	-1.08 <sup>a</sup>	22.7%	11701	-0.858 <sup>a</sup>	19.20%	13473	-1.375 <sup>a</sup>	13.6%	14073	0.092	1.3%	14203	-1.353 <sup>a</sup>	12.2%	12171	0.123	3.9%	14312	-0.068 <sup>c</sup>	0.8%	13644
	GJRM	-1.038 <sup>a</sup>	16.3%	11521	-0.807 <sup>a</sup>	15.20%	13344	-1.263 <sup>a</sup>	10.7%	13870	-0.445 <sup>a</sup>	5.7%	14059	-1.87 <sup>a</sup>	11.5%	11982	-0.548 <sup>a</sup>	7.2%	14234	-0.06 <sup>c</sup>	0.8%	13601
	EGM	-1.207 <sup>a</sup>	12.8%	11504	-0.716 <sup>a</sup>	11.80%	13328	-1.058 <sup>a</sup>	9.8%	13826	-0.404 <sup>a</sup>	5.6%	14051	-1.952 <sup>a</sup>	13.3%	11981	-0.396 <sup>a</sup>	6.8%	14206	-0.729 <sup>b</sup>	4.9%	13611
UR	GM	0.096 <sup>a</sup>	4.2%	11708	0.035	0.7%	13483	-0.144	1.7%	14083	0.006	0%	14208	0.147 <sup>a</sup>	6.3%	12173	0.125 <sup>c</sup>	2.7%	14313	-0.338	0.4%	13650
	GJRM	0.111 <sup>a</sup>	5.0%	11524	0.057 <sup>b</sup>	1.8%	13354	0.142 <sup>b</sup>	1.7%	13883	0.011	0.1%	14064	0.14 <sup>a</sup>	5.4%	11991	0.214 <sup>a</sup>	7.6%	14229	-0.269	0.6%	13604
	EGM	0.153 <sup>a</sup>	9.5%	11512	0.088 <sup>a</sup>	4.3%	13343	-0.15 <sup>a</sup>	1.6%	13847	0.032 <sup>a</sup>	1%	14059	0.182 <sup>a</sup>	9.5%	11991	0.127 <sup>a</sup>	2.8%	14212	0.6 <sup>a</sup>	1.2%	13616
In	GM	-0.078	1.1%	11713	0.134 <sup>a</sup>	2.1%	13481	0.149	1.3%	14082	0.301 <sup>b</sup>	3.3%	14205	0.243 <sup>a</sup>	4.5%	12176	-0.102	2.2%	14313	0.078 <sup>c</sup>	4.9%	13648
	GJRM	-0.122 <sup>a</sup>	2.5%	11533	0.117 <sup>a</sup>	1.4%	13355	0.14 <sup>c</sup>	1%	13884	-0.254 <sup>a</sup>	4.2%	14060	0.309 <sup>a</sup>	6.7%	11988	-0.159 <sup>a</sup>	5%	14234	-0.08 <sup>c</sup>	2.9%	13603
	EGM	-0.078 <sup>a</sup>	1.2%	11532	0.149 <sup>a</sup>	2.3%	13347	-0.127 <sup>a</sup>	1.6%	13847	-0.207 <sup>a</sup>	3%	14055	0.36 <sup>a</sup>	9.6%	11990	-0.07 <sup>c</sup>	1.1%	14214	0.114 <sup>a</sup>	5.7%	13613
EER	GM	-0.142	0.3%	11713	-0.266 <sup>c</sup>	1.4%	13482	-2.075 <sup>a</sup>	8.4%	14077	0.102	0.3%	14206	0.055	0.6%	12179	-0.321 <sup>a</sup>	5.7%	14310	0.168 <sup>a</sup>	4.9%	13637
	GJRM	-0.225 <sup>b</sup>	2.5%	11531	-0.48 <sup>a</sup>	5.3%	13349	-1.885 <sup>a</sup>	5.7%	13876	-0.377	1.2%	14061	-0.235 <sup>a</sup>	2.4%	11998	-0.434 <sup>a</sup>	32%	14215	0.471 <sup>a</sup>	4.8%	13600
	EGM	-0.095 <sup>a</sup>	1%	11529	-0.376 <sup>a</sup>	2.5%	13346	-1.271 <sup>a</sup>	2.7%	13844	-1.073 <sup>a</sup>	2.2%	14056	-0.531 <sup>a</sup>	7.9%	11993	-0.147 <sup>a</sup>	5.3%	14209	0.589 <sup>a</sup>	11.3%	13606
EPU	GM	0.124 <sup>a</sup>	5.0%	11708	0.006 <sup>c</sup>	0.6%	13481	0.061 <sup>b</sup>	3.3%	14079	0.003	0.4%	14205	0.079 <sup>a</sup>	6.5%	12171	0.162 <sup>a</sup>	15.4%	14301	0	0%	13650
	GJRM	-0.007	0.1%	11537	-0.018	1.1%	13354	0.051 <sup>b</sup>	1.8%	13882	-0.01	1%	14061	0.055 <sup>a</sup>	3%	11996	0.134 <sup>a</sup>	9.5%	14228	0	0%	13605
	EGM	0.261 <sup>a</sup>	18.9%	11488	0.171 <sup>a</sup>	11.2%	13329	0.084 <sup>a</sup>	4.8%	13838	-0.004	0.3%	14059	-0.004	0.1%	12005	0.147 <sup>a</sup>	11.7%	14199	0.004	0.1%	13617
GEPU	GM	-0.011	0.7%	11712	-0.02	1.3%	13481	-0.004	0.1%	14083	0.005	0.4%	14206	0.086 <sup>a</sup>	3%	12176	0.006	0.8%	14312	0.006	0.8%	13645
	GJRM	-0.013	1.1%	11533	-0.027	3.2%	13349	-0.013	0.9%	13882	-0.015	1%	14061	0.078 <sup>a</sup>	2.3%	11998	-0.035	1.9%	14238	-0.015	0.3%	13604
	EGM	0.151 <sup>a</sup>	6.9%	11517	-0.017	2.1%	13341	0.09 <sup>a</sup>	2.9%	13844	-0.006	0.4%	14057	0.154 <sup>a</sup>	9.4%	11991	-0.015	0.6%	14214	0.08 <sup>a</sup>	3.6%	13613
CFNAI	GM	-1.193 <sup>a</sup>	40.4%	11669	-0.947 <sup>a</sup>	33.7%	13458	-0.985 <sup>a</sup>	30%	14057	-0.935 <sup>a</sup>	28.1%	14187	-1.066 <sup>a</sup>	34.5%	12143	-0.755 <sup>a</sup>	26%	14298	-0.974 <sup>a</sup>	39.1%	13629
	GJRM	-1.191 <sup>a</sup>	34.4%	11489	-0.933 <sup>a</sup>	28.8%	13326	-0.933 <sup>a</sup>	22.4%	13856	-0.899 <sup>a</sup>	19.6%	14043	-1.034 <sup>a</sup>	28.9%	11951	-0.732 <sup>a</sup>	18.9%	14220	-1.035 <sup>a</sup>	39.2%	13577
	EGM	-1.046 <sup>a</sup>	27.5%	<b>11462</b>	-0.819 <sup>a</sup>	22.4%	<b>13304</b>	-0.87 <sup>a</sup>	15.2%	<b>13817</b>	-0.796 <sup>a</sup>	15.2%	<b>14036</b>	-0.983 <sup>a</sup>	26.2%	<b>11960</b>	-0.724 <sup>a</sup>	19.3%	<b>14191</b>	-0.907 <sup>a</sup>	33.7%	13585

Notes: a, b, and c represent 1%, 5%, and 10% significance level. GM, GJRM and EGM refer to GARCH-MIDAS, GJR-GARCH-MIDAS and EGARCH-MIDAS.  $VR = var(\log(\hat{\tau}_t))/var(\log(\hat{\tau}_t\hat{g}_t))$  measures the fraction of the total volatility explained by the long term component.  $BIC = -2LOGL + plog(T)$ , where LOGL is the log-likelihood of the model,  $p$  is the number of parameters, and  $T$  is the number of observations. For each index the smallest BIC is highlighted in bold.

Finally, we present the ranking of 7 macroeconomic variables in terms of the in-sample fit using BIC for for EGARCH-MIDAS, GJRGARCH-MIDAS, and GARCH-MIDAS models in Table 2.6.3. First of all, the global indicator, *CFNAI* is considered the most influential macroeconomic variable affecting the total and the long-term volatility of all seven indices for all models. Next, we find that the second-most influential variable is country-specific *IP* growth followed by *EER* growth and *IN*.

<sup>12</sup>Notice that DAX and NIKKEI are the least influenced by *IP* in terms of their low values of VR (5–6%). This may be due to the high quality of German and Japanese products whose demand is less affected during recession as their economies seem to recover quickly after crisis periods (Wink et al. (2018) and Marin (2018)).

Table 2.6.3: The ranking of macroeconomic variables

Index	Rank	G-MIDAS		GJR-MIDAS		EG-MIDAS	
		Macro	BIC	Macro	BIC	Macro	BIC
SP500	1	<i>CFNAI</i>	11669	<i>CFNAI</i>	11489	<i>CFNAI</i>	11462
	2	<i>IP</i>	11700	<i>IP</i>	11521	<i>FPU</i>	11474
	3	<i>EPU</i>	11708	<i>UR</i>	11524	<i>EPU</i>	11487
	4	<i>UR</i>	11708	<i>EER</i>	11532	<i>IP</i>	11504
	5	<i>GEPU</i>	11712	<i>GEPU</i>	11533	<i>GEPU</i>	11517
	6	<i>IN</i>	11713	<i>INF</i>	11533	<i>EER</i>	11530
	7	<i>EER</i>	11714	<i>EPU</i>	11537	<i>IN</i>	11532
NASDAQ	1	<i>CFNAI</i>	13458	<i>CFNAI</i>	13326	<i>CFNAI</i>	13304
	2	<i>IP</i>	13473	<i>IP</i>	13344	<i>FPU</i>	13313
	3	<i>GEPU</i>	13481	<i>GEPU</i>	13349	<i>IP</i>	13328
	4	<i>EPU</i>	13481	<i>EER</i>	13350	<i>EPU</i>	13329
	5	<i>IEER</i>	13482	<i>UR</i>	13354	<i>GEPU</i>	13341
	6	<i>IN</i>	13483	<i>EPU</i>	13354	<i>EER</i>	13346
	7	<i>UR</i>	13483	<i>IN</i>	13355	<i>IN</i>	13347
CAC40	1	<i>CFNAI</i>	14057	<i>CFNAI</i>	13856	<i>CFNAI</i>	13817
	2	<i>IP</i>	14073	<i>IP</i>	13870	<i>IP</i>	13826
	3	<i>EER</i>	14078	<i>EER</i>	13877	<i>EPU</i>	13838
	4	<i>EPU</i>	14079	<i>EPU</i>	13882	<i>EER</i>	13844
	5	<i>IN</i>	14082	<i>GEPU</i>	13882	<i>GEPU</i>	13844
	6	<i>UR</i>	14083	<i>UR</i>	13883	<i>UR</i>	13847
	7	<i>GEPU</i>	14083	<i>IN</i>	13884	<i>IN</i>	13847
DAX	1	<i>CFNAI</i>	14187	<i>CFNAI</i>	14043	<i>CFNAI</i>	14036
	2	<i>IP</i>	14203	<i>IP</i>	14059	<i>IP</i>	14051
	3	<i>IN</i>	14205	<i>IN</i>	14060	<i>IN</i>	14055
	4	<i>EPU</i>	14205	<i>EPU</i>	14061	<i>EPU</i>	14056
	5	<i>GEPU</i>	14206	<i>GEPU</i>	14061	<i>GEPU</i>	14057
	6	<i>UR</i>	14208	<i>UR</i>	14064	<i>UR</i>	14059
	7	<i>EER</i>	14208	<i>EER</i>	14065	<i>EER</i>	14059
FTSE100	1	<i>CFNAI</i>	12143	<i>CFNAI</i>	11951	<i>CFNAI</i>	11960
	2	<i>IP</i>	12171	<i>IP</i>	11982	<i>IP</i>	11981
	3	<i>EPU</i>	12171	<i>IN</i>	11988	<i>IN</i>	11990
	4	<i>UR</i>	12173	<i>UR</i>	11991	<i>UR</i>	11991
	5	<i>GEPU</i>	12176	<i>EPU</i>	11996	<i>GEPU</i>	11991
	6	<i>IN</i>	12176	<i>EER</i>	11998	<i>EER</i>	11994
	7	<i>EER</i>	12179	<i>GEPU</i>	11998	<i>EPU</i>	12005
NIKKEI	1	<i>CFNAI</i>	14298	<i>CFNAI</i>	14220	<i>CFNAI</i>	14191
	2	<i>EPU</i>	14301	<i>EER</i>	14215	<i>EER</i>	14199
	3	<i>EER</i>	14311	<i>EPU</i>	14228	<i>EPU</i>	14206
	4	<i>IP</i>	14312	<i>UR</i>	14229	<i>UR</i>	14212
	5	<i>GEPU</i>	14312	<i>IP</i>	14234	<i>IP</i>	14212
	6	<i>UR</i>	14313	<i>IN</i>	14234	<i>IN</i>	14214
	7	<i>IN</i>	14313	<i>GEPU</i>	14239	<i>GEPU</i>	14214
HSE	1	<i>CFNAI</i>	13629	<i>CFNAI</i>	13577	<i>CFNAI</i>	13585
	2	<i>EER</i>	13637	<i>EER</i>	13600	<i>EER</i>	13606
	3	<i>IP</i>	13644	<i>IP</i>	13601	<i>IP</i>	13611
	4	<i>GEPU</i>	13645	<i>IN</i>	13603	<i>IN</i>	13613
	5	<i>IN</i>	13648	<i>GEPU</i>	13604	<i>GEPU</i>	13613
	6	<i>UR</i>	13650	<i>UR</i>	13605	<i>UR</i>	13616
	7	<i>EPU</i>	13650	<i>EPU</i>	13605	<i>EPU</i>	13617

Notes: This table ranks five country-specific macroeconomic variables, (*IP*, *IN*, *UR*, *EPU*, *EER*) and two global indicators (*CFNAI*, *GEPU*). BIC values are obtained from Tables 2.7.3–2.7.4.

### 2.6.3 Out of sample forecast performance

Forecasting evaluation is a main tool for comparing the performance of alternative volatility models. We consider two popular measures of forecasting performance, RMSE(k) and QLIKE(k) given by

$$RMSE(k) = \sqrt{\frac{\sum_{i=1}^N \{\sigma_{T+i+k}^2 - \hat{\sigma}_{T+i+k}^2\}^2}{N}}$$

$$QLIKE(k) = \frac{\sum_{i=1}^N \left\{ \frac{\sigma_{T+i+k}^2}{\hat{\sigma}_{T+i+k}^2} - \log\left(\frac{\sigma_{T+i+k}^2}{\hat{\sigma}_{T+i+k}^2}\right) - 1 \right\}}{N}$$

where  $\hat{\sigma}_{T+i+k}^2$  is the  $k$ -day ahead forecast of the total volatility,  $\sigma_{T+i+k}^2 = \tau_{T+k} g_{T+i+k}$ , that is estimated using in-sample observations ending on day  $T+i$  for GJR-GARCH-MIDAS and EGARCH-MIDAS models. Since the daily volatility is unknown, we proxy it by the daily average of 5 min intraday volatility.<sup>13</sup> For comparing forecasting performance of models, as done in the literature, we eliminate the impact of the last day,  $T$ , of the in-sample by applying the rolling window principle,  $N$  times, to the in-sample, and we compute the  $k$ -day forecasts for each in-sample ending on  $T+1, T+2, \dots, T+N$ . The  $k$ -day forecast is the average of the  $N$  forecasts. In Appendix we discuss how to compute the  $k$ -day ahead volatility forecast based on the  $i$ th in-sample observations,  $\{r_1, \dots, r_{T+i}\}$ , using an analytic formula and a simulation Carlo Method.<sup>14</sup> We assess the forecasting performance of GJR-GARCH-MIDAS and EGARCH-MIDAS against GARCH-MIDAS as a benchmark model. We compute QLIKE (RMSE) loss as the ratio of QLIKE (RMSE) of GJRM and EGM to QLIKE (RMSE) of GARCH-MIDAS, and select the model with the smallest QLIKE (RMSE) loss as the preferred specification.

Tables 2.6.4–2.6.5 report RMSE and QLIKE losses for the  $k$ -day ahead forecast of the total volatility with  $k = [1, 5, 10, 15, 20]$  using in-sample period, 03/1/2000 to 31/7/2019. We consider *CFNAI* and *IP* growth as the macroeconomic variable respectively when forecasting the long term volatility because both were found to be most influential in terms of the in-sample fit. Panel A in Table 2.6.4 reports QLIKE loss results when using *CFNAI*. For all forecast horizons, EGARCH-MIDAS outperforms both GJR-GARCH-MIDAS and GARCH-MIDAS for all indices except FTSE100 in which case GARCH-MIDAS is preferred. From Panel B using *IP* growth, we observe qualitatively similar results except that GARCH-MIDAS outperforms over a longer horizon, e.g.  $k \geq 15$  for HANGSENG. Next, we turn to RMSE loss results in Table 2.6.5. From Panel A using *CFNAI*, EGARCH-MIDAS is the clear winner for all indices and across all horizons. From Panel B using *IP* growth, we still observe that EGARCH-MIDAS outperforms both GJR-GARCH-MIDAS and GARCH-MIDAS for all indices, though at the longer horizon ( $k = 20$ ) the forecasting performance of GARCH-MIDAS becomes very close to that of EGARCH-MIDAS for CAC40, DAX and NIKKEI.

<sup>13</sup>Paton (2011) showed that RMSE and QLIKE are invariant so long as the true but unknown volatility is proxied by an unbiased estimate.

<sup>14</sup>We use the analytic method to compute RMSE and QLIKE to substantially save the computation time as both analytic and simulation methods produce quite similar values.

Overall, we confirm the best out-of-sample forecasting performance for EGARCH-MIDAS, which suggest the importance of explicitly modelling the leverage effect in the short-term volatility.<sup>15</sup> Furthermore, from Tables 2.7.5-2.7.6 in Appendix, we find that QLIKE favours EGARCH-MIDAS 977 times, GJRGARCH-MIDAS 302 times, and GARCH-MIDAS 149 times whereas RMSE favours EGARCH-MIDAS 1054 times, GJRGARCH-MIDAS 291 times, and GARCH-MIDAS 99 times across all seven indices and seven macroeconomic variables.

Table 2.6.4: QLIKE loss of daily total volatility forecast

Panel A: QLIKE loss of GJRM and EGM against GARCH-MIDAS using CFNAI						
Index	Model	Horizon				
		1	5	10	15	20
SP500	GJR-MIDAS	0.932	0.954	0.979	0.988	1.011
	EG-MIDAS	0.834	0.865	0.892	0.909	0.939
NASDAQ	GJR-MIDAS	0.999	0.944	0.961	0.959	0.925
	EG-MIDAS	0.918	0.875	0.891	0.894	0.869
CAC40	GJR-MIDAS	0.877	0.914	0.939	0.978	0.967
	EG-MIDAS	0.869	0.872	0.892	0.947	0.926
DAX	GJR-MIDAS	0.877	0.896	0.914	0.981	0.981
	EG-MIDAS	0.861	0.855	0.874	0.939	0.939
FTSE100	GJR-MIDAS	1.015	0.982	1.008	1.046	1.001
	EG-MIDAS	1.032	0.983	1.038	1.068	1.046
NIKKEI	GJR-MIDAS	0.948	0.964	0.937	0.932	0.921
	EG-MIDAS	0.902	0.914	0.886	0.904	0.899
HSE	GJR-MIDAS	0.967	0.985	0.993	0.999	1.001
	EG-MIDAS	0.966	0.965	0.975	0.984	0.991
Panel B: QLIKE loss of GJRM and EGM against GARCH-MIDAS using IP growth						
Index	Model	Horizon				
		1	5	10	15	20
SP500	GJR-MIDAS	0.859	0.885	0.914	0.919	0.948
	EG-MIDAS	0.799	0.821	0.858	0.849	0.872
NASDAQ	GJR-MIDAS	0.985	0.941	0.960	0.958	0.907
	EG-MIDAS	0.9316	0.8921	0.906	0.903	0.856
CAC40	GJR-MIDAS	0.873	0.938	0.964	1.018	1.017
	EG-MIDAS	0.876	0.881	0.903	0.971	0.955
DAX	GJR-MIDAS	0.883	0.917	0.941	1.007	1.006
	EG-MIDAS	0.877	0.879	0.899	0.968	0.970
FTSE100	GJR-MIDAS	1.025	0.999	1.028	1.053	1.001
	EG-MIDAS	1.030	0.983	1.037	1.062	1.015
NIKKEI	GJR-MIDAS	0.992	0.994	0.993	1.019	1.029
	EG-MIDAS	0.907	0.926	0.903	0.920	0.929
HSE	GJR-MIDAS	0.974	0.987	0.995	1.002	1.006
	EG-MIDAS	0.969	0.971	0.986	1.006	1.025

Note: Panel A reports QLIKE loss of the  $k$ -day total volatility forecast for  $k = 1, 5, 10, 15, 20$  when CFNAI is used as a macroeconomic variable when forecasting the long term volatility. QLIKE loss is the ratio of QLIKE of GJR-GARCH-MIDAS and EGARCH-MIDAS to QLIKE of GARCH-MIDAS. The preferred model is the one with the smallest QLIKE loss. Panel B reports QLIKE loss using IP growth as a macroeconomic variable.

<sup>15</sup>This additional evidence is more or less in line with the previous empirical findings on forecasting superiority of GARCH over GJR-GARCH and GARCH, e.g. Awartani and Corradi (2005), Lin (2018) and Naimy (2018).

Table 2.6.5: RMSE loss of daily total volatility forecast

Panel A: RMSE loss of GJRM and EGM using CFNAI with respect to GARCH-MIDAS						
Index	Model	Horizon				
		1	5	10	15	20
SP500	GJR-GARCH-MIDAS	0.972	0.942	0.963	0.965	0.965
	EGARCH-MIDAS	0.936	0.905	0.910	0.903	0.906
NASDAQ	GJR-GARCH-MIDAS	0.966	0.937	0.957	0.953	0.941
	EGARCH-MIDAS	0.935	0.911	0.915	0.906	0.913
CAC40	GJR-GARCH-MIDAS	0.982	1.026	1.047	1.074	1.076
	EGARCH-MIDAS	0.949	0.935	0.953	0.976	0.971
DAX	GJR-GARCH-MIDAS	0.968	0.984	1.006	1.031	1.026
	EGARCH-MIDAS	0.959	0.949	0.971	0.999	0.998
FTSE 100	GJR-GARCH-MIDAS	1.003	1.003	0.988	0.988	0.973
	EGARCH-MIDAS	0.977	0.957	0.959	0.967	0.963
NIKKEI	GJR-GARCH-MIDAS	0.978	0.972	0.991	0.979	0.972
	EGARCH-MIDAS	0.978	0.957	0.979	0.976	0.967
HSE	GJR-GARCH-MIDAS	0.974	0.976	0.976	0.974	0.973
	EGARCH-MIDAS	0.974	0.957	0.961	0.959	0.963
Panel B: QLIKE loss of GJRM and EGM using IP with respect to GARCH-MIDAS						
Index	Model	Horizon				
		1	5	10	15	20
SP500	GJR-GARCH-MIDAS	0.975	0.952	0.974	0.981	0.984
	EGARCH-MIDAS	0.941	0.906	0.909	0.879	0.831
NASDAQ	GJR-GARCH-MIDAS	0.968	0.944	0.966	0.962	0.953
	EGARCH-MIDAS	0.940	0.919	0.922	0.907	0.895
CAC40	GJR-GARCH-MIDAS	0.986	1.054	1.093	1.144	1.164
	EGARCH-MIDAS	0.952	0.942	0.969	0.982	0.998
DAX	GJR-GARCH-MIDAS	0.986	1.042	1.098	1.163	1.184
	EGARCH-MIDAS	0.972	0.980	0.983	0.994	0.999
FTSE100	GJR-GARCH-MIDAS	1.002	1.003	0.990	0.989	0.972
	EGARCH-MIDAS	0.980	0.954	0.960	0.965	0.960
NIKKEI	GJR-GARCH-MIDAS	0.968	0.957	0.971	0.948	0.949
	EGARCH-MIDAS	0.985	0.969	0.993	0.992	0.997
HSE	GJR-GARCH-MIDAS	0.974	0.973	0.974	0.973	0.975
	EGARCH-MIDAS	0.974	0.959	0.970	0.962	0.966

Notes: Panel A reports the RMSE loss of the  $k$ -day total volatility forecast for  $k=[1,5,10,15,20]$  when CFNAI is used. RMSE loss is the ratio of RMSE of GJR-GARCH-MIDAS and EGARCH-MIDAS to RMSE of GARCH-MIDAS. The preferred model is the one with smallest RMSE loss. Panel B reports the RMSE loss using macroeconomic variable  $IP$ .

## 2.6.4 Conclusion

Following a growing popularity of the GARCH-MIDAS model, we have developed the EGARCH-MIDAS model and demonstrated that the QML estimation can produce relatively accurate estimates. We have also compared the relative performance of the EGARCH-MIDAS model against the GJR-GARCH-MIDAS model advanced by Conrad and Kleen (2020) in terms of in-sample fit and out of sample forecasting performance. Employing the seven stock market index

returns (SP500, NASDAQ, CAC40, DAX, FTSE100, NIKKEI, and HANGSENG) and seven macroeconomic variables over the period Jan 2000-Aug 2019, we find that EGARCH-MIDAS outperforms GJR-GARCH-MIDAS in almost all cases considered.

Due to pervasive evidence on outlying events observed in the financial market, we expect that an inclusion of the jump component will improve the performance of the GARCH models. In the next Chapter, we aim to develop the Bayesian estimation method for estimating GJR-GARCH-MIDAS and EGARCH-MIDAS model with jump components.

## 2.7 Appendix 1

### 2.7.1 Proof of Propositions 1 and 2

#### i) Proof of Proposition 1

We first derive the kurtosis of EGARCH and EGARCH-MIDAS models. Using  $r_t = \mu + \sqrt{\tau_t} g_t \varepsilon_t$ ,  $E(g_t) = 1$ ,  $\varepsilon_t \sim iidN(0,1)$ ,  $E((r_t - \mu)^2) = E(\tau_t)$ , the kurtosis of the returns can be expressed as

$$K = \frac{E((r_t - \mu)^4)}{E^2((r_t - \mu)^2)} = \frac{var((r_t - \mu)^2) + E^2((r_t - \mu)^2)}{E^2((r_t - \mu)^2)} = \frac{var((r_t - \mu)^2) + E^2(\tau_t)}{E^2(\tau_t)} \quad (2.7.1)$$

where  $E^2(X)$  denotes  $(E(X))^2$ . Rewriting  $var((r_t - \mu)^2)$  in terms of the volatility components:

$$var((r_t - \mu)^2) = E(\tau_t^2 g_t^2 \varepsilon_t^4) - E^2(\tau_t) = E(\tau_t^2) E(g_t^2) E(\varepsilon_t^4) - E^2(\tau_t) \quad (2.7.2)$$

and replacing  $var((r_t - \mu)^2)$  by the right hand side, the kurtosis of the multiplicative volatility model is formulated by

$$K = \frac{E(\tau_t^2)}{E^2(\tau_t)} E(g_t^2) E(\varepsilon_t^4) \quad (2.7.3)$$

By nonnegativity of  $var(\tau_t)$ , we have:  $E(\tau_t^2) > E^2(\tau_t)$ , which leads to:

$$K > E(g_t^2) E(\varepsilon_t^4) \quad (2.7.4)$$

where the right hand side is the kurtosis of the nested MIDAS model with constant  $\tau_t$ , i.e. EGARCH or GJR-GARCH model with unrestricted intercepts.

The kurtosis of GARCH-MIDAS, GJR-GARCH-MIDAS, and EGARCH-MIDAS models is larger than that their nested standard model, i.e.  $K_{(GJR)GARCH-MIDAS} > K_{(GJR)GARCH}$ , and  $K_{EGARCH-MIDAS} > K_{EGARCH}$ , where we have (see Hu et al.(2002)):

$$K_{EGARCH} = 3e^{(\delta_1^2/(1-\beta^2))} \prod_{i=1}^{\infty} \frac{\Phi(2\delta_1\beta^{i-1}) + e^{-8\gamma\alpha\beta^{2(i-1)}}\Phi(2\delta_2\beta^{i-1})}{(\Phi(\delta_1\beta^{i-1}) + e^{-2\gamma\alpha\beta^{2(i-1)}}\Phi(\delta_2\beta^{i-1}))^2} \quad (2.7.5)$$

where  $\delta_1 = \alpha + \gamma$ ,  $\delta_2 = \alpha - \gamma$  and  $\Phi(x) = \int_{-\infty}^x \frac{1}{\sqrt{2\pi}} e^{-x^2/2} dx$

Using corollary 4.2 of Hu et al. (2002), which states that  $K_{EGARCH} > 3$ , it is easily seen that

$$\prod_{i=1}^{\infty} \frac{\Phi(2\delta_1\beta^{i-1}) + e^{-8\gamma\alpha\beta^{2(i-1)}}\Phi(2\delta_2\beta^{i-1})}{(\Phi(\delta_1\beta^{i-1}) + e^{-2\gamma\alpha\beta^{2(i-1)}}\Phi(\delta_2\beta^{i-1}))^2} > 1$$

If  $\alpha = 0$ , i.e.  $\delta_1 = -\delta_2$ , the  $i^{\text{th}}$  element of the series is equal to 1. Hence, (2.7.5) reduces to  $K_{EGM} = 3e^{(\delta_1^2/(1-\beta^2))}$ . On the other hand, if  $\alpha \neq 0$ , (2.7.5) cannot be simplified and the product series does not converge to 1.

## ii) Proof of Proposition 2

Without loss of generality assuming that  $\mu = 0$ , the autocorrelation of squared returns at lag  $k$  is given by

$$\rho_2(k) = \text{corr}(r_t^2, r_{t-k}^2) = \frac{E(r_t^2 r_{t-k}^2) - E(r_t^2)E(r_{t-k}^2)}{\sqrt{\text{var}(r_t^2)\text{var}(r_{t-k}^2)}} \quad (2.7.6)$$

Plugging  $r_t^2 = \tau_t g_t \varepsilon_t^2$  and using the stationarity of  $r_t$  and unit-variance  $g_t$ ,  $E(g_t) = 1$ , the slow varying property of  $\tau_t$  (among the months and it is constant in each month), and independence between the two volatility components, we can rewrite (2.7.6) as

$$\rho_2(k) = \frac{E(\tau_t \tau_{t-k})E(g_t \varepsilon_t^2 g_{t-k} \varepsilon_{t-k}^2) - E(\tau_t)E(\tau_{t-k})}{\text{var}(r_t^2)}$$

By adding and subtracting  $E(\tau_t \tau_{t-k})$  in the numerator,  $\rho_2(k)$  will be expressed as

$$\rho_2(k) = \frac{E(\tau_t \tau_{t-k}) - E(\tau_t)E(\tau_{t-k})}{\text{var}(r_t^2)} + \frac{E(\tau_t \tau_{t-k})E(g_t \varepsilon_t^2 g_{t-k} \varepsilon_{t-k}^2) - 1}{\text{var}(r_t^2)} \quad (2.7.7)$$

Replacing 1 by  $E(g_t)E(g_{t-k})$  (Conrard and Kleen (2019)) and using the fact that  $\text{cov}(\tau_t, \tau_{t-k}) = \rho_2^\tau(k)\text{var}(\tau_t)$ , (2.7.7) can be re-written as:

$$\rho_2(k) = \rho_2^\tau(k) \frac{\text{var}(\tau_t)}{\text{var}(r_t^2)} + \frac{E(\tau_t \tau_{t-k})E(g_t \varepsilon_t^2 g_{t-k} \varepsilon_{t-k}^2) - E(g_t)E(g_{t-k})}{\text{var}(r_t^2)} \quad (2.7.8)$$

Using the independence between  $g_t$  and  $\varepsilon_t$ , and  $E(\varepsilon_t^2) = 1$ , (2.7.8) becomes:

$$\rho_2(k) = \rho_2^\tau(k) \frac{\text{var}(\tau_t)}{\text{var}(r_t^2)} + \frac{E(\tau_t \tau_{t-k})\text{cov}(g_t \varepsilon_t^2, g_{t-k} \varepsilon_{t-k}^2)}{\text{var}(r_t^2)}$$

Using  $E(\tau_t \tau_{t-k}) = \rho_2^\tau(k)\text{var}(\tau_t) + E^2(\tau_t)$ , and  $\text{cov}(g_t \varepsilon_t^2, g_{t-k} \varepsilon_{t-k}^2) = \rho_2^g(k)\text{var}(g_t \varepsilon_t^2)$ , we get the desired result as long as the short term component is stationary with unit-variance.

$$\rho_2(k) = \rho_2^\tau(k) \frac{\text{var}(\tau_t)}{\text{var}(r_t^2)} + \rho_2^g(k) \frac{\text{var}(g_t \varepsilon_t^2)(\rho_2^\tau(k)\text{var}(\tau_t) + E^2(\tau_t))}{\text{var}(r_t^2)} \quad (2.7.9)$$

$$\rho_2^g(k) = (\alpha + \beta + \gamma/2)^{k-1} \frac{\alpha(1 - (\alpha + \frac{\gamma}{2})\beta + \beta^2)}{1 - 2(\alpha + \frac{\gamma}{2})\beta + \beta^2} \text{ for GJR-GARCH.}$$

### Analytic formula

Using in-sample observations,  $\{r_1, \dots, r_T\}$ , we estimate the total volatility by  $\hat{\sigma}_t^2 = \hat{\tau}_t \hat{g}_t$ . Then, it is easily seen that  $\hat{\sigma}_{T+k}^2 = E(\sigma_{T+k}^2 | \hat{\sigma}_T^2)$ . Notice that  $\hat{\tau}_{T+k} = \hat{\tau}_T$  if the day,  $k$  belongs to  $T$ th month since there is no extra information from monthly macroeconomic variable. Therefore,

$$\hat{\sigma}_{T+k}^2 = \hat{\tau}_T E(g_{T+k} | \hat{g}_T, \hat{\tau}_T) \quad (2.7.10)$$

where  $E(g_{T+k} | \hat{g}_T, \hat{\tau}_T)$  is the  $k$ -day ahead forecast of the short term component,  $g_t$ . If the  $k$ th day falls in another month, then  $\hat{\sigma}_{T+k}^2 = E(\tau_{T+k} | \hat{\tau}_T) E(g_{T+k} | \hat{g}_T, \hat{\tau}_T)$  and  $E(\tau_{T+k} | \hat{\tau}_T)$  can be obtained using the predicted value of  $X$  from its generating AR(1) process. Due to a high persistence of the long term component,  $\tau_t$ , it is argued to be  $E(\tau_{T+k} | \hat{\tau}_T) = \hat{\tau}_T$ . Hence, forecasting  $\sigma_t^2$  is computed using (2.7.10) for every  $k$  and every month. That is, the forecast of  $\hat{\sigma}_t^2$  reduces to forecasting the short term component.

### GARCH-MIDAS and GJR-GARCH-MIDAS models:

The forecast of the short term component can be evaluated analytically as follows:

1. The 1-day ahead forecast is computed using (1.2.8) for GJR-GARCH and (1.2.2) for GARCH-MIDAS with  $\hat{\gamma} = 0$ :

$$g_{T+1|T} = 1 - (\hat{\alpha} + \hat{\beta} + \hat{\gamma}/2) + \hat{\alpha} \frac{(r_T - \hat{\mu})^2}{\hat{\tau}_T} + \frac{1}{2} \hat{\gamma} \frac{(r_T - \hat{\mu})^2}{\hat{\tau}_T} I_{(r_T - \hat{\mu}) < 0} + \hat{\beta} \hat{g}_T \quad (2.7.11)$$

2. The  $k$ -day forecast can be obtained recursively by

$$g_{T+k|T} = 1 + (\hat{\alpha} + \hat{\beta} + \hat{\gamma}/2)^{k-1} (g_{T+1|T} - 1) \quad (2.7.12)$$

As  $k$  increases,  $g_{T+k|T}$  will tend to 1 if  $\hat{\alpha} + \hat{\beta} + \hat{\gamma}/2 < 1$ . Therefore, the forecast of the total volatility will tend to  $\hat{\tau}_{T+k}$ .

### EGARCH-MIDAS model:

The  $k$ -day ahead forecast,  $\hat{\sigma}_{T+k}^2$  of the total volatility can be computed using (2.7.10). However, it is not straightforward to derive the  $k$ -day forecast of EGARCH(1,1) short term component because of its log specification. Thus, we use Tsay's (2002) formula as follows:

1. The 1-day ahead forecast can be computed from the 1-day ahead forecast of  $\log(g_t)$  given in (2.3.4):

$$\log(g_{T+1|T}) = \hat{\alpha}_0^* + \hat{\gamma} \frac{(r_T - \hat{\mu})}{\sqrt{\hat{\tau}_T \hat{g}_T}} + \hat{\alpha} \left( \frac{|r_T - \hat{\mu}|}{\sqrt{\hat{\tau}_T \hat{g}_T}} - \sqrt{\frac{2}{\pi}} \right) + \hat{\beta} \log(\hat{g}_T) \quad (2.7.13)$$



where  $\hat{\alpha}_0^* = \hat{\alpha}_0 + (1 - \beta) \log(\tau_T)$ . Thus

$$g_{T+1|T} = e^{\hat{\alpha}_0^* + \hat{\gamma} \frac{(r_T - \hat{\mu})}{\sqrt{\hat{\tau}_T \hat{g}_T} + \hat{\alpha} \left( \frac{|r_T - \hat{\mu}|}{\sqrt{\hat{\tau}_T \hat{g}_T} - \sqrt{\frac{2}{\pi}}} \right) + \hat{\beta} \log(\hat{g}_T)} \quad (2.7.14)$$

2. The k-day forecast can be computed recursively by (see Tsay (2002))<sup>16</sup>:

$$g_{T+k|T} = g_{T+k-1|T}^{\hat{\beta}} e^{\hat{\alpha}_0^* - \alpha \sqrt{\frac{2}{\pi}} \{e^{0.5 \hat{\delta}_1^2} \Phi(\hat{\delta}_1) + e^{0.5 \hat{\delta}_2^2} \Phi(\hat{\delta}_2)\}} \quad (2.7.15)$$

where  $\hat{\delta}_1 = \hat{\alpha} + \hat{\gamma}$ ,  $\hat{\delta}_2 = \hat{\alpha} - \hat{\gamma}$ , and  $\Phi(x)$  is cdf of  $N(0,1)$ .

$$e^{E(\log(g_{T+1|T}))} \leq E(g_{T+1|T}) = E(e^{\log(g_{T+1|T})}) = E(g_{T+1|T})$$

### Monte Carlo Method

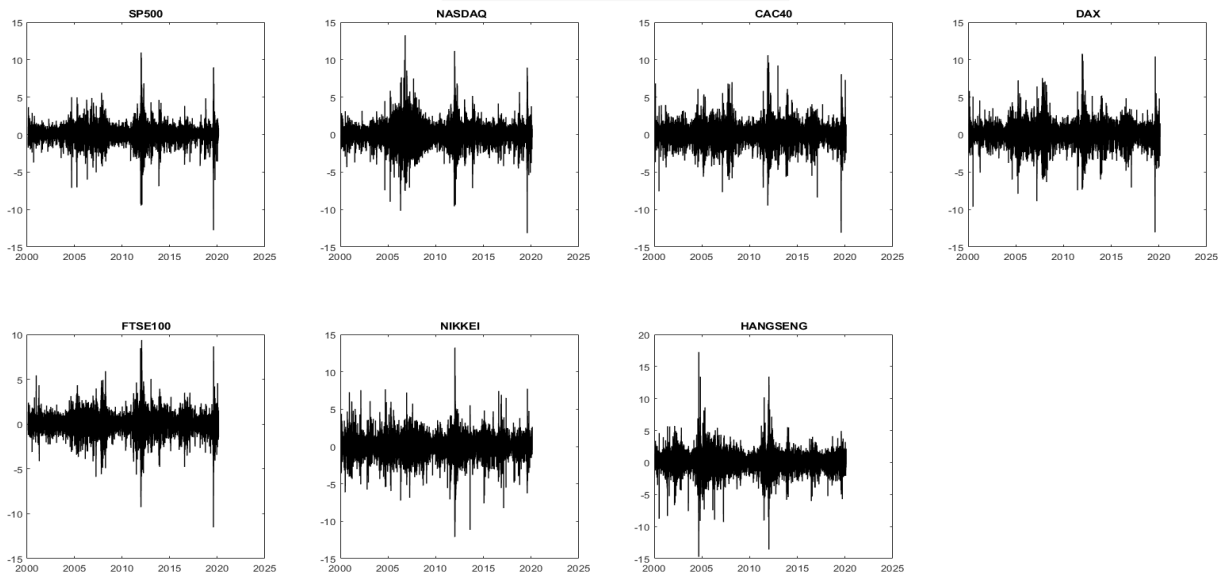
Alternatively, we can employ the Monte Carlo method. It consists of simulating  $B$  paths of the k-day ahead forecast as follows: For each path  $j = 1, \dots, B$ :

1. Simulate  $r_{T+1|T}^{(j)}$  from  $N(\hat{\mu}, \tau_T \hat{g}_{T+1|T})$  where  $\hat{g}_{T+1|T}^{(j)}$  is computed using (2.7.11) for GJR-GARCH-MIDAS and (2.7.14) for EGARCH-MIDAS.
2. Simulate  $r_{T+2|T}^{(j)}$  from  $N(\hat{\mu}, \tau_T \hat{g}_{T+2|T})$  where  $\hat{g}_{T+2|T}^{(j)}$  is computed using  $r_{T+1|T}^{(j)}$  and  $\hat{g}_{T+1|T}$ .
3. Continue the iteration and simulate  $r_{T+k|T}^{(j)}$ ,  $\hat{g}_{T+k|T}$  and  $\sigma_{T+k|T}^2$ .

If  $k$  is large, one can update  $\tau_T$  by  $\tau_{T+k|T}$  which can be computed by including monthly forecasts  $\hat{X}_{T+22l}$ s such that  $22l < k$  for monthly data (period=22 days) in the long-term volatility model (2.3). The simulated forecast of  $\sigma_{T+k|T}^2$  and  $\hat{g}_{T+k|T}$  are estimated by the sample average of the  $B$  forecasts.

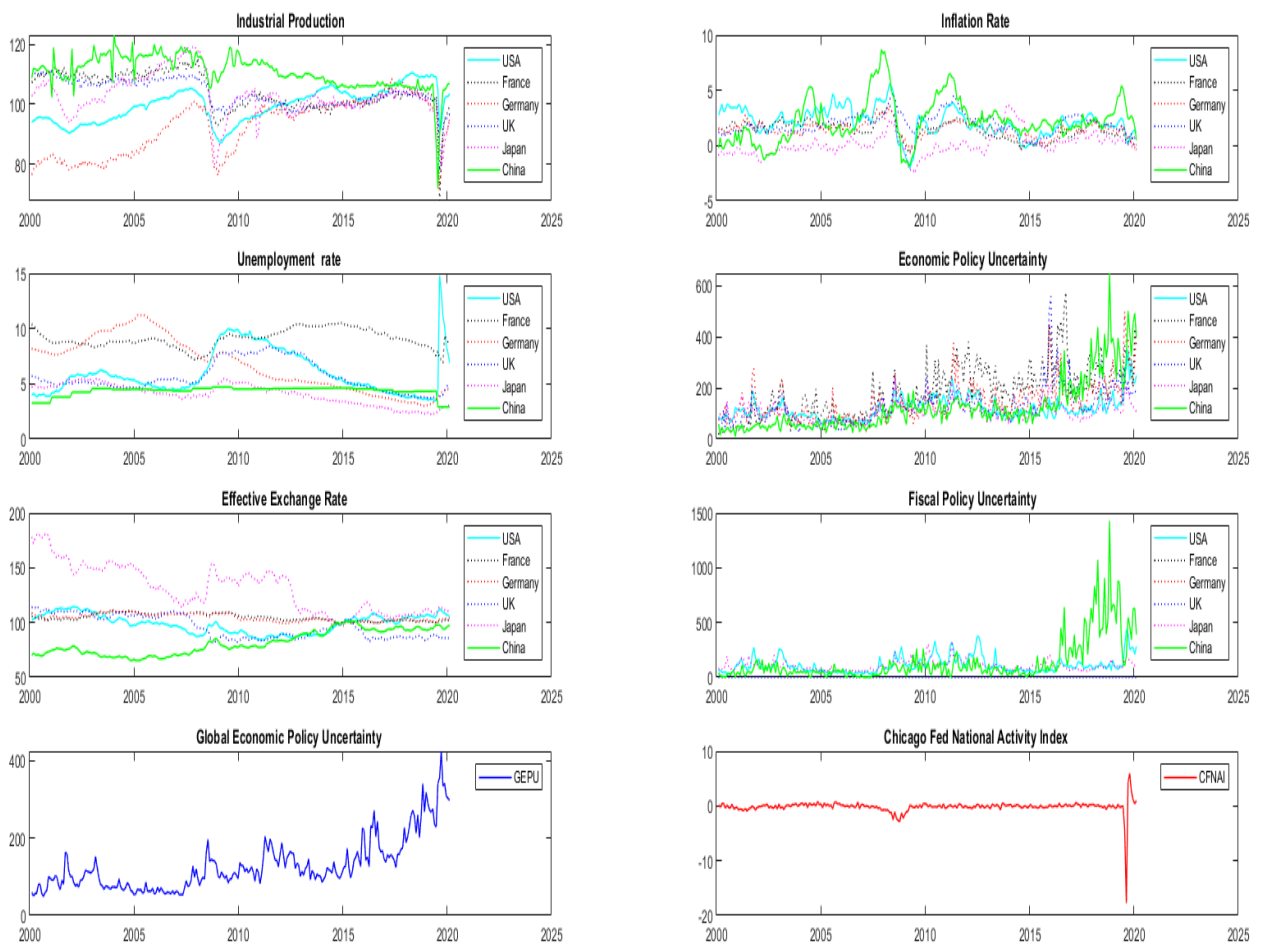
<sup>16</sup>Tsay (2002) derived (2.7.15) using  $E(e^X) = \int e^x f(x) dx$  to overcome the Jensen's inequality since  $e^x$  is convex.

Figure 2.4: Returns data of the indices in the period 2000-2020



Note: This Figure shows the daily return data of SP500, NASDAQ, CAC40, DAX, FTSE100, NIKKEI, and HANGSENG for the period 2000-2020

Figure 2.5: Movement of the macroeconomic variables of all countries



Note: This Figure shows the monthly movements of the macroeconomic indicators of each country for the period 2000-2020.

### 2.7.2 Descriptive statistics of stock market returns and macroeconomic variables

Table 2.7.1: Summary statistics of daily returns

**Panel A: Descriptive statistics of returns**

Index	Jan 2000-August 2019					Jan 2000-August 2020						
	Mean	Std.	Kurtosis	Skewness	Min.	Max.	Mean	Std.	Kurtosis	Skewness	Min.	Max.
SP500	0.015	1.193	11.648	-0.221	-9.470	10.957	0.017	1.256	14.070	-0.389	-12.765	10.957
NASDAQ	0.014	1.562	9.007	0.001	-10.168	13.255	0.020	1.598	9.749	-0.123	-13.149	13.255
CAC40	0.000	1.413	8.267	-0.040	-9.472	10.595	-0.003	1.445	9.324	-0.216	-13.098	10.595
DAX	0.012	1.459	7.685	-0.066	-8.875	10.797	0.012	1.491	8.822	-0.174	-13.055	10.797
FTSE100	0.003	1.141	9.835	-0.162	-9.266	9.384	-0.001	1.180	11.293	-0.344	-11.512	9.384
NIKKEI	0.002	1.492	9.467	-0.425	-12.111	13.235	0.003	1.498	9.359	-0.387	-12.111	13.235
HSE	0.011	1.455	11.140	-0.072	-13.582	13.407	0.008	1.456	10.832	-0.089	-13.582	13.407

**Panel B: Correlation between daily returns**

Index	Jan. 2000- Aug. 2019							Index	Jan. 2000-Aug. 2020						
	SP500	NASDQ	CAC40	DAX	FTSE	NIK	HSE		SP500	NASDQ	CAC40	DAX	FTSE	NIK	HSE
SP500	1.00	0.88	0.53	0.57	0.52	0.14	0.19	SP	1.00	0.88	0.52	0.56	0.50	0.13	0.18
NASDAQ	0.88	1.00	0.47	0.52	0.44	0.13	0.18	NASD	0.88	1.00	0.46	0.51	0.43	0.12	0.18
CAC40	0.53	0.47	1.00	0.87	0.84	0.30	0.35	CAC	0.52	0.46	1.00	0.87	0.83	0.28	0.34
DAX	0.57	0.52	0.87	1.00	0.79	0.27	0.34	DAX	0.56	0.51	0.87	1.00	0.78	0.26	0.33
FTSE100	0.52	0.44	0.84	0.79	1.00	0.30	0.37	FTSE	0.50	0.43	0.83	0.78	1.00	0.29	0.36
NIKKEI	0.14	0.13	0.30	0.27	0.30	1.00	0.48	NIK	0.13	0.12	0.28	0.26	0.29	1.00	0.48
HSE	0.19	0.18	0.35	0.34	0.37	0.48	1.00	HANG	0.18	0.18	0.34	0.33	0.36	0.48	1.00

Notes: Panel A reports Descriptive statistics of returns in percentage for the periods Jan-2000 to August-2019, and Jan-2000 to August-2020. Panel B reports the correlation between the returns of the indices for the two periods.

### A1.3 Parameter estimates of the models

#### i) Parameter estimates of GJR-GARCH(1,1) and EGARCH(1,1) models

Table 2.7.2: Parameter Estimates of Standard Models

Index	Period	GARCH						GJR-GARCH						EGARCH										
		$\hat{\mu}$	$\hat{\alpha}_0$	$\hat{\beta}$	$\hat{\alpha}$	BIC	logL	RMSE	$\hat{\mu}$	$\hat{\alpha}_0$	$\hat{\beta}$	$\hat{\alpha}$	$\hat{\gamma}$	BIC	logL	RMSE	$\hat{\mu}$	$\hat{\alpha}_0$	$\hat{\beta}$	$\hat{\alpha}$	$\hat{\gamma}$	BIC	logL	RMSE
SP500	2000-2019	0.06	0.022	0.866	0.114	11696.9	-5831.7	4.17	0.023	0.023	0.878	0.000	0.194	11521	-5739.5	4.05	0.027	-0.002	0.972	0.147	-0.156	<b>11509.2</b>	-5733.6	4.07
	2000-2020	0.064	0.024	0.853	0.128	12543.4	-6254.8	5.09	0.027	0.024	0.873	0.016	0.174	12406.8	-6182.3	4.98	0.03	0.001	0.972	0.175	-0.135	<b>12395.8</b>	-6176.8	4.99
NASD	2000-2019	0.074	0.029	0.887	0.094	13466	-6716.2	4.36	0.036	0.033	0.892	0.003	0.16	13340.1	-6649.1	4.26	0.031	0.008	0.973	0.127	-0.129	<b>13324.7</b>	-6641.4	4.28
	2000-2020	0.077	0.031	0.879	0.102	14392	-7179.1	5.29	0.039	0.031	0.897	0.01	0.14	14282.2	-7120	5.21	0.032	0.011	0.973	0.149	-0.115	<b>14278</b>	-7117.9	5.22
CAC40	2000-2019	0.056	0.023	0.886	0.103	14066.1	-7016.2	5.01	0.01	0.026	0.893	0.000	0.185	13868.2	-6913.1	4.88	0.001	0.007	0.979	0.11	-0.151	<b>13825.3</b>	-6891.6	4.85
	2000-2020	0.056	0.027	0.878	0.11	14994	-7480	5.69	0.01	0.027	0.893	0.000	0.186	14784.3	-7371	5.6	0	0.008	0.979	0.113	-0.154	<b>14728.9</b>	-7343.3	5.51
DAX	2000-2019	0.072	0.023	0.9	0.088	14190.3	-7078.3	4.97	0.031	0.025	0.911	0.000	0.144	14045.5	-7001.8	4.83	0.024	0.009	0.98	0.12	-0.112	<b>14032.9</b>	-6995.4	4.84
	2000-2020	0.072	0.024	0.897	0.091	15148.3	-7557.2	5.79	0.029	0.025	0.913	0.000	0.141	14985.6	-7471.7	5.65	0.023	0.01	0.98	0.12	-0.117	<b>14964.3</b>	-7461	5.63
FTSE	2000-2019	0.039	0.017	0.879	0.107	12163.4	-6064.9	3.53	0.002	0.019	0.897	0.000	0.167	11986.5	-5972.2	3.41	0.003	-0.001	0.983	0.116	-0.119	<b>11982.3</b>	-5970	3.43
	2000-2020	0.037	0.018	0.873	0.113	13091.7	-6528.8	4.17	0	0.019	0.897	0.000	0.167	12904.3	-6430.9	4.07	-0.007	0.001	0.982	0.117	-0.123	<b>12887</b>	-6422.3	4.06
NIKKEI	2000-2019	0.059	0.042	0.871	0.111	14297.4	-7132	5.9	0.027	0.055	0.868	0.04	0.127	14222.7	-7090.4	5.78	0.02	0.024	0.961	0.2	-0.102	<b>14188.9</b>	-7073.5	5.84
	2000-2020	0.061	0.044	0.869	0.113	15115.9	-7541.1	5.91	0.027	0.055	0.868	0.036	0.133	15025.4	-7491.6	5.78	0.02	0.024	0.962	0.197	-0.105	<b>14991.8</b>	-7474.9	5.84
HSE	2000-2019	0.048	0.016	0.934	0.056	13633.3	-6799.9	6.06	0.027	0.022	0.929	0.022	0.065	<b>13588.4</b>	-6773.3	5.9	0.028	0.009	0.985	0.121	-0.052	13591.7	-6774.9	5.93
	2000-2020	0.044	0.016	0.933	0.057	14500.1	-7233.2	5.97	0.023	0.023	0.93	0.02	0.067	<b>14448.1</b>	-7203	5.81	0.024	0.01	0.984	0.121	-0.054	14452.9	-7205.4	5.84

Standard deviations are given between brackets.  $\hat{\alpha}_0$  of GJR-GARCH is extremely small as recognised in the literature. For each index the smallest BIC value is given in bold. GARCH model is given by:  $r_t = \mu + \sqrt{g_t}\epsilon_t$   $g_t = \alpha_0 + \alpha(r_{t-1} - \mu)^2 + \beta g_{t-1}$ , GJR-GARCH model is given by:  $r_t = \mu + \sqrt{g_t}\epsilon_t$   $g_t = \alpha_0 + \alpha(r_{t-1} - \mu)^2 + \gamma(r_{t-1} - \mu)^2 1_{[r_{t-1} - \mu < 0]}$   $+\beta g_{t-1}$ , and EGARCH model is given by:  $r_t = \mu + \sqrt{e^{g_t}}\epsilon_t$   $\log(g_t) = \alpha_0 + \beta \log(g_{t-1}) + \gamma \frac{(r_{t-1} - \mu)}{\sqrt{g_{t-1}}} + \alpha \left( \frac{|r_{t-1} - \mu|}{\sqrt{g_{t-1}}} - \sqrt{\frac{2}{\pi}} \right)$

ii) Parameter estimates of GJR-GARCH-MIDAS and EGARCH-MIDAS models

Table 2.7.3: Estimation results for GARCH-MIDAS models using local macroeconomic variables

Table with columns for INDEX, MACRO, GARCH-MIDAS, GJR-GARCH-MIDAS, and EGARCH-MIDAS. Each model section includes parameters (alpha, beta, gamma, delta, omega) and their estimates with standard errors and significance markers.

Notes: Parameter estimates of GARCH-MIDAS, GJR-GARCH-MIDAS, and EGARCH-MIDAS models are reported for seven macroeconomic country specific variables (DPI,IN,UR,EPU,EER,FPU, and CFNAI) for the period 2000/1 based on monthly observations reaching as far as 2019, with the lag length K = 24. Estimation of GARCH-MIDAS, GJR-GARCH-MIDAS, and EGARCH-MIDAS employs daily return data starting in 2000/1. a, b, and c indicate significance at the 1%, 5%, and 10% level respectively. BIC is the Bayesian information criterion and LogL is the log-likelihood function. VR, the volatility ratio, is calculated on monthly basis.

Table 2.7.4: Estimation results for GARCH-MIDAS models using cross-country macroeconomic variables

Table with columns for INDEX, MACRO, GARCH-MIDAS, GJR-GARCH-MIDAS, and EGARCH-MIDAS. Each model section includes parameters (alpha, beta, gamma, delta, omega) and their estimates with standard errors and significance markers.

Notes: Parameter estimates of GARCH-MIDAS, GJR-GARCH-MIDAS, and EGARCH-MIDAS models are reported for seven macroeconomic country specific variables (EPU\_Global, EER\_FR, EER\_RU, EER\_UK, EER\_JPN, EER\_CH, FPU\_JPN, DPI\_US, NAI, EER\_US, FPU\_US) for the period 2000/1 based on monthly observations reaching as far as 2019, with the lag length K = 24. Estimation of GARCH-MIDAS, GJR-GARCH-MIDAS, and EGARCH-MIDAS employs daily return data starting in 2000/1. a, b, and c indicate significance at the 1%, 5%, and 10% level respectively. BIC is the Bayesian information criterion and LogL is the log-likelihood function. VR, the volatility ratio, is calculated on monthly basis.

## A1.4 Forecast Results

Table 2.7.5: QLIKE LOSS Daily Forecast

Index	Macro	Model	1	5	10	15	20	25	30	35	40	45	50	55	60	66	
SP500	IP	G-MIDAS	0.039	0.040	0.042	0.041	0.041	0.039	0.037	0.035	0.035	0.043	0.052	0.094	0.151	0.171	
		GJR-MIDAS	0.033	0.035	0.038	0.038	0.039	0.040	0.037	0.035	0.034	0.042	0.052	0.096	0.158	0.181	
		EG-MIDAS	0.031	0.033	0.036	0.035	0.036	0.037	0.034	0.031	0.031	0.041	0.053	0.107	0.180	0.209	
	IN	G-MIDAS	0.036	0.037	0.040	0.038	0.038	0.038	0.036	0.034	0.034	0.043	0.054	0.098	0.160	0.184	
		GJR-MIDAS	0.032	0.034	0.038	0.037	0.038	0.039	0.036	0.033	0.032	0.041	0.052	0.099	0.165	0.190	
		E-MIDAS	0.032	0.034	0.036	0.035	0.036	0.038	0.038	0.035	0.033	0.061	0.098	0.251	0.445	0.492	
	UR	G-MIDAS	0.036	0.035	0.038	0.035	0.033	0.036	0.036	0.034	0.035	0.072	0.112	0.284	0.508	0.605	
		GJR-MIDAS	0.032	0.034	0.037	0.036	0.036	0.036	0.034	0.031	0.030	0.042	0.058	0.123	0.215	0.254	
		EGARCH-MIDAS	0.032	0.034	0.037	0.035	0.035	0.036	0.034	0.031	0.030	0.043	0.058	0.124	0.213	0.249	
	EPU	G-MIDAS	0.036	0.037	0.040	0.039	0.039	0.038	0.036	0.035	0.035	0.043	0.053	0.097	0.159	0.183	
		GJR-MIDAS	0.032	0.034	0.038	0.037	0.038	0.038	0.036	0.033	0.032	0.041	0.052	0.100	0.167	0.192	
		E-MIDAS	0.031	0.034	0.037	0.038	0.040	0.041	0.039	0.036	0.036	0.042	0.050	0.086	0.137	0.157	
	GEPUS	G-MIDAS	0.037	0.038	0.040	0.039	0.039	0.038	0.036	0.034	0.034	0.043	0.053	0.096	0.156	0.180	
		GJR-MIDAS	0.033	0.035	0.038	0.037	0.038	0.038	0.036	0.033	0.032	0.041	0.052	0.098	0.162	0.187	
		E-MIDAS	0.031	0.034	0.037	0.037	0.039	0.040	0.038	0.035	0.035	0.041	0.047	0.076	0.117	0.132	
	EER	G-MIDAS	0.036	0.037	0.040	0.038	0.038	0.037	0.035	0.034	0.034	0.043	0.054	0.102	0.168	0.196	
		GJR-MIDAS	0.032	0.034	0.037	0.036	0.037	0.038	0.035	0.032	0.032	0.041	0.052	0.100	0.169	0.197	
		E-MIDAS	0.032	0.034	0.037	0.037	0.038	0.039	0.036	0.033	0.033	0.043	0.053	0.098	0.160	0.182	
	FPUUS	G-MIDAS	0.036	0.037	0.040	0.038	0.038	0.038	0.036	0.034	0.034	0.043	0.053	0.098	0.159	0.183	
		GJR-MIDAS	0.032	0.034	0.037	0.037	0.038	0.039	0.036	0.034	0.033	0.041	0.051	0.095	0.158	0.183	
		E-MIDAS	0.030	0.033	0.036	0.036	0.037	0.038	0.036	0.034	0.033	0.042	0.053	0.099	0.163	0.185	
	CFNAI	G-MIDAS	0.037	0.039	0.041	0.039	0.039	0.038	0.036	0.034	0.034	0.042	0.052	0.097	0.158	0.174	
		GJR-MIDAS	0.035	0.037	0.040	0.039	0.039	0.040	0.036	0.033	0.032	0.040	0.050	0.096	0.158	0.180	
		E-MIDAS	0.031	0.033	0.036	0.036	0.037	0.037	0.035	0.032	0.031	0.039	0.048	0.092	0.152	0.173	
	FPUJPN	G-MIDAS	0.036	0.038	0.040	0.040	0.040	0.040	0.038	0.037	0.037	0.044	0.053	0.091	0.146	0.170	
		GJR-MIDAS	0.033	0.035	0.038	0.038	0.039	0.040	0.037	0.035	0.034	0.041	0.050	0.089	0.146	0.172	
		E-MIDAS	0.031	0.033	0.036	0.036	0.037	0.038	0.035	0.033	0.033	0.039	0.046	0.080	0.132	0.157	
	EERCH	G-MIDAS	0.036	0.037	0.039	0.038	0.037	0.037	0.035	0.033	0.033	0.043	0.054	0.102	0.170	0.200	
		GJR-MIDAS	0.032	0.034	0.037	0.037	0.038	0.038	0.036	0.033	0.032	0.042	0.053	0.103	0.171	0.197	
		E-MIDAS	0.031	0.033	0.036	0.036	0.037	0.038	0.036	0.032	0.032	0.040	0.050	0.093	0.152	0.177	
	NASDAQ	IP	G-MIDAS	0.028	0.030	0.032	0.032	0.035	0.037	0.036	0.036	0.036	0.043	0.050	0.078	0.122	0.132
			GJR-MIDAS	0.027	0.028	0.031	0.031	0.032	0.034	0.033	0.032	0.033	0.039	0.047	0.076	0.122	0.134
			E-MIDAS	0.026	0.027	0.029	0.029	0.030	0.032	0.031	0.030	0.031	0.037	0.044	0.072	0.115	0.127
		IN	G-MIDAS	0.028	0.029	0.032	0.031	0.034	0.037	0.036	0.035	0.035	0.043	0.050	0.080	0.127	0.141
			GJR-MIDAS	0.027	0.027	0.030	0.030	0.031	0.033	0.032	0.031	0.032	0.039	0.046	0.078	0.127	0.142
			E-MIDAS	0.026	0.027	0.030	0.029	0.031	0.033	0.032	0.031	0.032	0.038	0.045	0.072	0.114	0.126
		UR	G-MIDAS	0.028	0.028	0.031	0.029	0.030	0.034	0.036	0.035	0.036	0.065	0.090	0.204	0.365	0.392
			GJR-MIDAS	0.026	0.027	0.030	0.029	0.030	0.032	0.031	0.030	0.030	0.039	0.048	0.086	0.145	0.163
			E-MIDAS	0.025	0.026	0.029	0.028	0.029	0.031	0.031	0.029	0.030	0.039	0.048	0.084	0.140	0.154
		EPU	GARCH-MIDAS	0.028	0.029	0.032	0.031	0.034	0.036	0.035	0.035	0.035	0.043	0.050	0.081	0.127	0.140
			GJR-MIDAS	0.027	0.027	0.031	0.030	0.031	0.033	0.032	0.031	0.031	0.039	0.046	0.076	0.124	0.136
			E-MIDAS	0.026	0.027	0.031	0.031	0.033	0.034	0.034	0.033	0.034	0.039	0.045	0.067	0.103	0.114
		GEPUS	G-MIDAS	0.028	0.030	0.032	0.032	0.035	0.037	0.036	0.035	0.035	0.043	0.050	0.080	0.126	0.138
			GJR-MIDAS	0.027	0.027	0.031	0.030	0.031	0.033	0.032	0.031	0.031	0.039	0.046	0.076	0.124	0.137
			E-MIDAS	0.026	0.027	0.030	0.030	0.031	0.033	0.032	0.031	0.032	0.038	0.044	0.069	0.107	0.116
		EER	G-MIDAS	0.027	0.029	0.032	0.031	0.033	0.036	0.035	0.035	0.035	0.043	0.050	0.083	0.134	0.148
			GJR-MIDAS	0.026	0.027	0.030	0.029	0.030	0.032	0.031	0.030	0.031	0.039	0.047	0.083	0.139	0.156
			E-MIDAS	0.026	0.026	0.029	0.029	0.030	0.032	0.032	0.031	0.032	0.039	0.047	0.077	0.123	0.134
FPUUS		G-MIDAS	0.028	0.029	0.032	0.031	0.034	0.036	0.035	0.035	0.035	0.043	0.050	0.080	0.126	0.138	
		GJR-MIDAS	0.027	0.027	0.031	0.030	0.031	0.033	0.032	0.031	0.032	0.039	0.046	0.076	0.123	0.136	
		E-MIDAS	0.026	0.027	0.030	0.030	0.031	0.033	0.033	0.032	0.033	0.039	0.046	0.073	0.115	0.125	
CFNAI		G-MIDAS	0.028	0.030	0.033	0.032	0.035	0.037	0.037	0.037	0.037	0.044	0.050	0.080	0.125	0.133	
		GJR-MIDAS	0.028	0.029	0.032	0.031	0.032	0.034	0.033	0.032	0.032	0.039	0.046	0.077	0.123	0.134	
		E-MIDAS	0.026	0.027	0.029	0.029	0.030	0.032	0.031	0.030	0.031	0.039	0.047	0.084	0.138	0.149	
FPUJPN		G-MIDAS	0.028	0.030	0.032	0.032	0.035	0.038	0.037	0.037	0.037	0.044	0.051	0.078	0.121	0.134	
		GJR-MIDAS	0.027	0.028	0.031	0.031	0.032	0.034	0.033	0.033	0.033	0.040	0.046	0.074	0.118	0.133	
		E-MIDAS	0.026	0.027	0.030	0.030	0.032	0.034	0.033	0.032	0.033	0.039	0.045	0.071	0.111	0.124	
EERCH		G-MIDAS	0.028	0.029	0.032	0.031	0.033	0.036	0.035	0.035	0.035	0.043	0.050	0.082	0.130	0.144	
		GJR-MIDAS	0.026	0.027	0.030	0.030	0.031	0.033	0.032	0.031	0.032	0.040	0.048	0.081	0.132	0.146	
		E-MIDAS	0.026	0.026	0.029	0.029	0.030	0.032	0.032	0.031	0.032	0.039	0.046	0.076	0.120	0.131	

Notes: The table reports the QLIKE LOSS daily forecasts for 1-day ahead forecast to 3-month ahead volatility forecasts for GARCH-MIDAS, GJR-GARCH-MIDAS, and EGARCH-MIDAS using all macroeconomic variables.

Index	Macro	Model	1	5	10	15	20	25	30	35	40	45	50	55	60	66	
CAC40	IP	G-MIDAS	0.033	0.033	0.035	0.037	0.040	0.040	0.038	0.037	0.036	0.039	0.042	0.056	0.085	0.100	
		GJR-MIDAS	0.029	0.031	0.034	0.038	0.040	0.041	0.039	0.039	0.038	0.041	0.043	0.053	0.073	0.081	
		E-MIDAS	0.029	0.029	0.032	0.036	0.038	0.038	0.037	0.037	0.037	0.039	0.041	0.051	0.074	0.084	
	IN	G-MIDAS	0.033	0.033	0.035	0.038	0.040	0.040	0.038	0.037	0.037	0.040	0.043	0.056	0.083	0.096	
		GJR-MIDAS	0.029	0.031	0.034	0.039	0.041	0.041	0.040	0.040	0.040	0.043	0.045	0.054	0.070	0.073	
		E-MIDAS	0.029	0.029	0.032	0.036	0.038	0.038	0.037	0.037	0.037	0.040	0.042	0.052	0.074	0.083	
	UR	G-MIDAS	0.034	0.033	0.037	0.038	0.038	0.038	0.034	0.034	0.037	0.047	0.050	0.082	0.155	0.199	
		GJR-MIDAS	0.029	0.031	0.034	0.039	0.040	0.041	0.039	0.039	0.039	0.043	0.045	0.055	0.073	0.078	
		E-MIDAS	0.029	0.029	0.032	0.037	0.038	0.039	0.037	0.037	0.037	0.040	0.042	0.052	0.072	0.081	
	EPU	G-MIDAS	0.033	0.033	0.035	0.038	0.040	0.040	0.038	0.037	0.037	0.040	0.043	0.056	0.083	0.095	
		GJR-MIDAS	0.029	0.030	0.033	0.037	0.039	0.040	0.038	0.037	0.037	0.040	0.043	0.054	0.077	0.086	
		E-MIDAS	0.029	0.029	0.032	0.036	0.037	0.037	0.036	0.036	0.036	0.038	0.041	0.052	0.079	0.090	
	GEPU	G-MIDAS	0.033	0.033	0.035	0.038	0.040	0.040	0.038	0.037	0.037	0.040	0.043	0.056	0.082	0.093	
		GJR-MIDAS	0.029	0.032	0.035	0.039	0.041	0.041	0.040	0.040	0.040	0.043	0.045	0.053	0.069	0.073	
		E-MIDAS	0.029	0.029	0.032	0.037	0.039	0.040	0.039	0.039	0.039	0.041	0.043	0.052	0.071	0.078	
	EER	G-MIDAS	0.033	0.033	0.035	0.038	0.040	0.040	0.038	0.037	0.037	0.040	0.043	0.055	0.081	0.094	
		GJR-MIDAS	0.029	0.031	0.034	0.039	0.041	0.042	0.040	0.040	0.040	0.044	0.046	0.053	0.068	0.071	
		E-MIDAS	0.029	0.029	0.032	0.037	0.038	0.038	0.037	0.037	0.037	0.040	0.041	0.049	0.066	0.073	
	EER <sub>US</sub>	G-MIDAS	0.033	0.033	0.035	0.038	0.040	0.041	0.038	0.038	0.038	0.041	0.043	0.056	0.081	0.093	
		GJR-MIDAS	0.029	0.031	0.035	0.039	0.041	0.041	0.040	0.039	0.040	0.043	0.045	0.053	0.070	0.074	
		E-MIDAS	0.029	0.029	0.032	0.037	0.039	0.039	0.038	0.038	0.038	0.040	0.042	0.052	0.072	0.080	
	IP <sub>US</sub>	G-MIDAS	0.038	0.040	0.043	0.044	0.040	0.042	0.033	0.031	0.046	0.061	0.064	0.097	0.196	0.235	
		GJR-MIDAS	0.029	0.030	0.033	0.036	0.037	0.038	0.035	0.034	0.034	0.038	0.042	0.058	0.094	0.109	
		E-MIDAS	0.029	0.029	0.031	0.035	0.035	0.035	0.033	0.032	0.032	0.036	0.040	0.058	0.098	0.118	
	CFNAI	G-MIDAS	0.033	0.033	0.036	0.038	0.041	0.041	0.039	0.038	0.038	0.040	0.042	0.054	0.079	0.089	
		GJR-MIDAS	0.029	0.030	0.034	0.037	0.040	0.040	0.038	0.038	0.037	0.040	0.041	0.051	0.072	0.080	
		E-MIDAS	0.028	0.029	0.032	0.036	0.038	0.038	0.037	0.037	0.036	0.039	0.040	0.051	0.073	0.084	
	FPU <sub>JPN</sub>	G-MIDAS	0.032	0.033	0.036	0.038	0.041	0.042	0.040	0.039	0.039	0.042	0.044	0.055	0.078	0.090	
		GJR-MIDAS	0.029	0.031	0.034	0.039	0.041	0.041	0.040	0.040	0.040	0.043	0.045	0.054	0.071	0.074	
		E-MIDAS	0.029	0.030	0.033	0.038	0.040	0.040	0.039	0.040	0.039	0.041	0.043	0.052	0.071	0.080	
	EER <sub>CH</sub>	G-MIDAS	0.033	0.033	0.035	0.037	0.039	0.040	0.037	0.036	0.036	0.039	0.042	0.056	0.086	0.103	
		GJR-MIDAS	0.029	0.031	0.034	0.039	0.041	0.042	0.040	0.039	0.039	0.042	0.044	0.054	0.073	0.079	
		E-MIDAS	0.029	0.029	0.032	0.036	0.037	0.037	0.036	0.036	0.035	0.038	0.040	0.051	0.076	0.088	
	DAX	IP	G-MIDAS	0.028	0.028	0.029	0.032	0.034	0.034	0.034	0.034	0.032	0.036	0.037	0.067	0.071	0.082
			GJR-MIDAS	0.025	0.026	0.028	0.032	0.034	0.035	0.034	0.035	0.035	0.038	0.040	0.061	0.062	0.067
			E-MIDAS	0.025	0.025	0.026	0.031	0.033	0.033	0.033	0.033	0.034	0.036	0.037	0.060	0.062	0.069
IN		GHMIDAS	0.028	0.028	0.029	0.031	0.033	0.034	0.033	0.033	0.032	0.035	0.037	0.071	0.075	0.088	
		GJR-MIDAS	0.025	0.026	0.027	0.032	0.033	0.034	0.033	0.033	0.034	0.038	0.039	0.062	0.064	0.071	
		E-MIDAS	0.024	0.024	0.026	0.030	0.032	0.032	0.031	0.032	0.032	0.035	0.036	0.061	0.064	0.074	
UR		G-MIDAS	0.028	0.028	0.029	0.029	0.031	0.033	0.031	0.031	0.032	0.044	0.047	0.144	0.172	0.230	
		GJR-MIDAS	0.025	0.026	0.027	0.031	0.033	0.033	0.033	0.033	0.034	0.038	0.039	0.064	0.067	0.074	
		E-MIDAS	0.024	0.024	0.026	0.031	0.033	0.034	0.035	0.036	0.036	0.041	0.043	0.076	0.080	0.091	
EPU		G-MIDAS	0.028	0.028	0.029	0.031	0.033	0.034	0.033	0.033	0.031	0.035	0.037	0.072	0.077	0.090	
		GJR-MIDAS	0.025	0.026	0.027	0.031	0.033	0.033	0.032	0.033	0.034	0.037	0.039	0.063	0.065	0.073	
		E-MIDAS	0.024	0.024	0.026	0.030	0.032	0.032	0.031	0.032	0.032	0.035	0.037	0.064	0.068	0.078	
GEPU		G-MIDAS	0.028	0.028	0.029	0.031	0.033	0.034	0.033	0.033	0.032	0.036	0.037	0.071	0.075	0.088	
		GJR-MIDAS	0.025	0.026	0.027	0.032	0.033	0.034	0.033	0.033	0.034	0.038	0.039	0.063	0.064	0.071	
		E-MIDAS	0.024	0.025	0.026	0.030	0.032	0.033	0.032	0.033	0.033	0.036	0.038	0.066	0.068	0.077	
EER		G-MIDAS	0.028	0.028	0.029	0.031	0.033	0.033	0.032	0.032	0.031	0.035	0.037	0.073	0.078	0.093	
		GJR-MIDAS	0.025	0.026	0.027	0.032	0.033	0.034	0.033	0.034	0.034	0.038	0.039	0.062	0.063	0.070	
		E-MIDAS	0.024	0.024	0.026	0.030	0.032	0.032	0.032	0.032	0.033	0.036	0.038	0.065	0.069	0.079	
EER <sub>US</sub>		G-MIDAS	0.028	0.028	0.029	0.031	0.033	0.034	0.033	0.033	0.032	0.036	0.038	0.076	0.081	0.096	
		GJR-MIDAS	0.025	0.026	0.027	0.031	0.033	0.034	0.033	0.034	0.034	0.038	0.039	0.063	0.065	0.072	
		E-MIDAS	0.024	0.024	0.026	0.030	0.032	0.033	0.032	0.033	0.033	0.036	0.037	0.063	0.065	0.074	
IP <sub>US</sub>		G-MIDAS	0.033	0.033	0.039	0.039	0.038	0.039	0.032	0.030	0.040	0.055	0.057	0.163	0.220	0.317	
		GJR-MIDAS	0.024	0.025	0.026	0.029	0.030	0.031	0.030	0.029	0.029	0.036	0.038	0.083	0.092	0.112	
		E-MIDAS	0.024	0.023	0.024	0.028	0.029	0.029	0.028	0.028	0.028	0.034	0.036	0.082	0.091	0.114	
CFNAI		G-MIDAS	0.028	0.028	0.029	0.032	0.034	0.034	0.033	0.033	0.031	0.035	0.036	0.069	0.073	0.084	
		GJR-MIDAS	0.025	0.025	0.027	0.031	0.033	0.033	0.033	0.033	0.032	0.036	0.037	0.067	0.070	0.081	
		E-MIDAS	0.024	0.024	0.026	0.030	0.032	0.032	0.031	0.032	0.032	0.035	0.036	0.063	0.066	0.077	
FPU <sub>JPN</sub>		G-MIDAS	0.028	0.028	0.029	0.032	0.034	0.035	0.034	0.034	0.033	0.037	0.038	0.069	0.074	0.086	
		GJR-MIDAS	0.025	0.026	0.027	0.031	0.033	0.034	0.033	0.033	0.034	0.038	0.039	0.063	0.065	0.072	
		E-MIDAS	0.025	0.025	0.026	0.030	0.032	0.033	0.032	0.033	0.033	0.036	0.037	0.063	0.066	0.077	
EER <sub>CH</sub>		G-MIDAS	0.028	0.028	0.029	0.031	0.032	0.033	0.032	0.032	0.030	0.035	0.036	0.074	0.081	0.097	
		GJR-MIDAS	0.025	0.026	0.027	0.031	0.033	0.034	0.033	0.033	0.034	0.038	0.039	0.063	0.065	0.072	
		E-MIDAS	0.024	0.024	0.025	0.029	0.031	0.031	0.030	0.030	0.031	0.034	0.035	0.063	0.068	0.081	

Notes: The table reports the QLIKE LOSS daily forecasts for 1-day ahead forecast to 3-month ahead volatility forecasts for GARCH-MIDAS, GJR-GARCH-MIDAS, and EGARCH-MIDAS using all macroeconomic variables.

Index	Macro	Model	1	5	10	15	20	25	30	35	40	45	50	55	60	66	
FTSE100	IP	G-MIDAS	0.031	0.032	0.034	0.036	0.037	0.037	0.038	0.036	0.035	0.035	0.036	0.038	0.049	0.077	
		GJR-MIDAS	0.032	0.032	0.035	0.038	0.037	0.036	0.037	0.035	0.034	0.034	0.034	0.036	0.050	0.079	
		E-MIDAS	0.032	0.032	0.035	0.038	0.038	0.037	0.038	0.036	0.035	0.035	0.036	0.037	0.048	0.073	
	IN	G-MIDAS	0.032	0.033	0.034	0.036	0.036	0.036	0.037	0.035	0.034	0.035	0.035	0.038	0.050	0.081	
		GJR-MIDAS	0.033	0.033	0.036	0.038	0.037	0.036	0.037	0.034	0.033	0.034	0.035	0.037	0.052	0.084	
		E-MIDAS	0.032	0.032	0.035	0.038	0.037	0.036	0.037	0.034	0.034	0.033	0.034	0.035	0.047	0.072	
	UR	G-MIDAS	0.034	0.034	0.036	0.036	0.036	0.035	0.035	0.033	0.033	0.037	0.037	0.044	0.060	0.120	
		GJR-MIDAS	0.034	0.033	0.036	0.038	0.036	0.035	0.035	0.033	0.032	0.033	0.034	0.038	0.058	0.101	
		E-MIDAS	0.033	0.032	0.035	0.037	0.035	0.034	0.035	0.034	0.033	0.033	0.035	0.040	0.067	0.117	
	EPU	G-MIDAS	0.032	0.032	0.034	0.036	0.036	0.036	0.037	0.035	0.034	0.035	0.035	0.037	0.049	0.079	
		GJR-MIDAS	0.033	0.033	0.036	0.038	0.037	0.036	0.036	0.034	0.033	0.034	0.035	0.037	0.053	0.085	
		E-MIDAS	0.032	0.031	0.035	0.037	0.036	0.036	0.036	0.034	0.033	0.033	0.034	0.035	0.048	0.074	
	GEPUS	G-MIDAS	0.031	0.032	0.034	0.036	0.037	0.036	0.037	0.036	0.035	0.035	0.036	0.038	0.049	0.077	
		GJR-MIDAS	0.033	0.033	0.036	0.038	0.037	0.036	0.036	0.034	0.033	0.034	0.034	0.037	0.051	0.082	
		E-MIDAS	0.032	0.032	0.036	0.039	0.038	0.038	0.038	0.036	0.035	0.035	0.036	0.036	0.046	0.066	
	EER	G-MIDAS	0.032	0.033	0.034	0.036	0.036	0.036	0.037	0.035	0.034	0.035	0.036	0.039	0.051	0.084	
		GJR-MIDAS	0.033	0.033	0.036	0.038	0.037	0.036	0.037	0.034	0.033	0.034	0.035	0.038	0.055	0.090	
		E-MIDAS	0.032	0.032	0.036	0.038	0.037	0.037	0.037	0.035	0.034	0.034	0.035	0.037	0.051	0.080	
	EER <sub>US</sub>	G-MIDAS	0.032	0.033	0.034	0.036	0.036	0.036	0.037	0.035	0.035	0.035	0.036	0.038	0.049	0.079	
		GJR-MIDAS	0.033	0.033	0.036	0.038	0.037	0.036	0.037	0.034	0.033	0.034	0.035	0.037	0.052	0.085	
		E-MIDAS	0.033	0.032	0.036	0.039	0.037	0.037	0.037	0.035	0.034	0.034	0.035	0.037	0.049	0.075	
	IP <sub>US</sub>	GH-MIDAS	0.034	0.041	0.042	0.037	0.038	0.036	0.032	0.030	0.028	0.027	0.032	0.041	0.052	0.112	
		GJR-MIDAS	0.034	0.034	0.036	0.038	0.036	0.035	0.035	0.033	0.031	0.033	0.034	0.038	0.059	0.104	
		E-MIDAS	0.032	0.031	0.034	0.036	0.035	0.034	0.035	0.033	0.032	0.033	0.034	0.037	0.057	0.096	
	CFNAI	G-MIDAS	0.031	0.032	0.034	0.035	0.036	0.036	0.037	0.035	0.034	0.034	0.035	0.037	0.051	0.081	
		GJR-MIDAS	0.032	0.032	0.034	0.037	0.036	0.036	0.036	0.034	0.033	0.033	0.034	0.036	0.050	0.082	
		E-MIDAS	0.032	0.032	0.035	0.038	0.038	0.038	0.039	0.037	0.036	0.035	0.037	0.040	0.059	0.097	
	FPU <sub>JPN</sub>	G-MIDAS	0.031	0.032	0.034	0.036	0.037	0.037	0.038	0.037	0.036	0.036	0.037	0.039	0.050	0.078	
		GJR-MIDAS	0.033	0.033	0.036	0.038	0.037	0.036	0.037	0.034	0.033	0.034	0.035	0.037	0.052	0.084	
		E-MIDAS	0.032	0.032	0.036	0.039	0.038	0.038	0.039	0.036	0.036	0.035	0.036	0.037	0.048	0.074	
	EER <sub>CH</sub>	G-MIDAS	0.032	0.033	0.034	0.035	0.036	0.035	0.036	0.034	0.034	0.034	0.035	0.038	0.052	0.087	
		GJR-MIDAS	0.033	0.033	0.035	0.038	0.036	0.036	0.036	0.033	0.032	0.033	0.034	0.037	0.053	0.088	
		E-MIDAS	0.033	0.032	0.035	0.038	0.037	0.036	0.037	0.034	0.033	0.033	0.034	0.036	0.049	0.077	
	NIKKEI	IP	G-MIDAS	0.037	0.036	0.039	0.039	0.038	0.036	0.035	0.034	0.039	0.046	0.050	0.057	0.057	
			GJR-MIDAS	0.034	0.033	0.036	0.035	0.034	0.032	0.033	0.031	0.032	0.036	0.043	0.049	0.058	0.060
			E-MIDAS	0.034	0.033	0.035	0.036	0.035	0.032	0.033	0.032	0.031	0.034	0.038	0.041	0.045	0.047
		IN	G-MIDAS	0.037	0.036	0.039	0.038	0.037	0.035	0.036	0.034	0.033	0.037	0.043	0.047	0.053	0.054
			GJR-MIDAS	0.034	0.034	0.036	0.035	0.034	0.032	0.033	0.032	0.031	0.035	0.041	0.045	0.052	0.054
			E-MIDAS	0.033	0.033	0.035	0.035	0.034	0.032	0.032	0.032	0.031	0.035	0.039	0.043	0.049	0.051
		UR	G-MIDAS	0.037	0.035	0.038	0.037	0.036	0.034	0.035	0.033	0.033	0.037	0.045	0.049	0.057	0.059
			GJR-MIDAS	0.033	0.033	0.035	0.034	0.032	0.030	0.030	0.029	0.030	0.036	0.045	0.051	0.063	0.067
			E-MIDAS	0.033	0.032	0.034	0.034	0.033	0.030	0.031	0.030	0.030	0.034	0.041	0.046	0.055	0.057
		EPU	G-MIDAS	0.037	0.037	0.041	0.041	0.041	0.038	0.039	0.038	0.037	0.040	0.045	0.048	0.053	0.054
			GJR-MIDAS	0.036	0.036	0.038	0.037	0.036	0.034	0.035	0.034	0.033	0.037	0.042	0.046	0.052	0.054
			E-MIDAS	0.033	0.033	0.036	0.036	0.035	0.033	0.034	0.033	0.032	0.035	0.040	0.044	0.050	0.051
		GEPUS	G-MIDAS	0.037	0.036	0.039	0.038	0.037	0.035	0.036	0.034	0.033	0.038	0.044	0.048	0.054	0.055
			GJR-MIDAS	0.034	0.033	0.036	0.035	0.034	0.032	0.032	0.031	0.031	0.035	0.041	0.045	0.052	0.054
			E-MIDAS	0.033	0.033	0.035	0.035	0.034	0.032	0.032	0.032	0.031	0.034	0.039	0.043	0.048	0.049
EER <sub>US</sub>		G-MIDAS	0.037	0.036	0.039	0.038	0.037	0.035	0.036	0.035	0.034	0.038	0.044	0.048	0.054	0.055	
		GJR-MIDAS	0.034	0.034	0.036	0.036	0.034	0.032	0.033	0.032	0.032	0.035	0.041	0.046	0.052	0.054	
		E-MIDAS	0.033	0.033	0.035	0.036	0.035	0.032	0.033	0.032	0.032	0.036	0.042	0.046	0.052	0.053	
FPU <sub>JPN</sub>		G-MIDAS	0.038	0.038	0.042	0.042	0.042	0.040	0.041	0.039	0.038	0.041	0.045	0.048	0.053	0.053	
		GJR-MIDAS	0.036	0.036	0.039	0.039	0.038	0.035	0.037	0.035	0.034	0.037	0.042	0.046	0.051	0.052	
		E-MIDAS	0.034	0.034	0.036	0.037	0.036	0.034	0.035	0.035	0.034	0.037	0.040	0.044	0.048	0.050	
IP <sub>US</sub>		G-MIDAS	0.041	0.038	0.038	0.038	0.035	0.040	0.037	0.037	0.042	0.061	0.098	0.124	0.161	0.218	
		GJR-MIDAS	0.033	0.033	0.035	0.034	0.032	0.030	0.031	0.029	0.030	0.035	0.045	0.051	0.062	0.066	
		E-MIDAS	0.033	0.032	0.034	0.034	0.033	0.030	0.030	0.029	0.030	0.033	0.040	0.044	0.053	0.057	
CFNAI		G-MIDAS	0.037	0.036	0.040	0.039	0.038	0.036	0.037	0.035	0.034	0.038	0.043	0.047	0.052	0.052	
		GJR-MIDAS	0.035	0.035	0.037	0.037	0.035	0.033	0.034	0.032	0.032	0.035	0.041	0.045	0.051	0.053	
		E-MIDAS	0.033	0.033	0.035	0.035	0.034	0.032	0.033	0.032	0.031	0.034	0.039	0.043	0.049	0.050	
EER <sub>CH</sub>		G-MIDAS	0.037	0.035	0.038	0.038	0.037	0.034	0.035	0.034	0.033	0.037	0.043	0.048	0.055	0.057	
		GJR-MIDAS	0.036	0.036	0.038	0.035	0.034	0.032	0.032	0.031	0.031	0.035	0.041	0.046	0.055	0.058	
		E-MIDAS	0.033	0.032	0.034	0.034	0.032	0.030	0.031	0.030	0.030	0.033	0.039	0.044	0.052	0.055	
HANGSENG		IP	G-MIDAS	0.037	0.035	0.034	0.033	0.032	0.033	0.030	0.030	0.028	0.029	0.029	0.032	0.038	0.043
			GJR-MIDAS	0.036	0.034	0.034	0.033	0.032	0.033	0.030	0.030	0.030	0.030	0.031	0.032	0.036	0.039
			E-MIDAS	0.036	0.034	0.033	0.033	0.033	0.033	0.030	0.030	0.030	0.030	0.031	0.032	0.036	0.039
		IN	G-MIDAS	0.037	0.035	0.034	0.033	0.032	0.033	0.030	0.030	0.029	0.029	0.029	0.031	0.036	0.040
			GJR-MIDAS	0.036	0.034	0.034	0.033	0.032	0.033	0.029	0.029	0.028	0.028	0.029	0.032	0.038	0.043
			E-MIDAS	0.036	0.034	0.033	0.032	0.032	0.032	0.029	0.029	0.029	0.029	0.029	0.031	0.034	0.036
		UR	G-MIDAS	0.037	0.035	0.034	0.033	0.032	0.033	0.030	0.030						

Table 2.7.6: RMSE LOSS all forecast

Index	Macro	Model	1	5	10	15	20	25	30	35	40	45	50	55	60	66	
SP500	IP	G-MIDAS	0.215	0.178	0.188	0.149	0.117	0.119	0.123	0.122	0.125	0.371	0.543	1.817	3.193	3.430	
		GJR-MIDAS	0.209	0.169	0.184	0.146	0.115	0.113	0.116	0.112	0.113	0.352	0.525	1.753	3.087	3.322	
		E-MIDAS	0.202	0.161	0.171	0.131	0.098	0.098	0.103	0.100	0.100	0.345	0.516	1.721	3.030	3.261	
	IN	G-MIDAS	0.215	0.178	0.189	0.149	0.116	0.117	0.121	0.120	0.123	0.372	0.544	1.819	3.195	3.433	
		GJR-MIDAS	0.210	0.170	0.186	0.149	0.118	0.115	0.117	0.114	0.114	0.354	0.527	1.754	3.088	3.324	
		E-MIDAS	0.203	0.164	0.176	0.139	0.109	0.109	0.117	0.114	0.113	0.357	0.533	1.737	3.047	3.278	
	UR	G-MIDAS	0.222	0.185	0.194	0.150	0.111	0.113	0.122	0.123	0.129	0.392	0.569	1.851	3.230	3.470	
		GJR-MIDAS	0.209	0.167	0.181	0.140	0.103	0.099	0.103	0.098	0.098	0.352	0.530	1.759	3.096	3.333	
		E-MIDAS	0.202	0.161	0.170	0.128	0.092	0.092	0.099	0.095	0.095	0.346	0.519	1.725	3.035	3.267	
	EPU	G-MIDAS	0.215	0.178	0.190	0.150	0.117	0.118	0.122	0.120	0.123	0.372	0.544	1.818	3.194	3.433	
		GJR-MIDAS	0.210	0.170	0.186	0.149	0.117	0.113	0.115	0.111	0.111	0.353	0.527	1.754	3.089	3.324	
		E-MIDAS	0.203	0.168	0.184	0.157	0.139	0.142	0.147	0.145	0.147	0.355	0.519	1.713	3.019	3.249	
	GEPUS	G-MIDAS	0.215	0.179	0.190	0.150	0.116	0.116	0.120	0.119	0.123	0.372	0.544	1.818	3.194	3.432	
		GJR-MIDAS	0.211	0.172	0.187	0.150	0.118	0.114	0.115	0.112	0.112	0.353	0.526	1.753	3.088	3.323	
		E-MIDAS	0.203	0.166	0.182	0.153	0.134	0.136	0.139	0.136	0.138	0.350	0.512	1.707	3.011	3.239	
	EER	G-MIDAS	0.215	0.177	0.188	0.147	0.112	0.112	0.116	0.115	0.117	0.371	0.544	1.820	3.197	3.436	
		GJR-MIDAS	0.210	0.170	0.185	0.148	0.115	0.111	0.113	0.109	0.109	0.353	0.526	1.754	3.089	3.325	
		E-MIDAS	0.203	0.164	0.177	0.141	0.112	0.112	0.117	0.113	0.114	0.349	0.517	1.720	3.027	3.257	
	FPU <sub>US</sub>	G-MIDAS	0.215	0.178	0.189	0.149	0.115	0.116	0.120	0.119	0.122	0.371	0.544	1.819	3.195	3.433	
		GJR-MIDAS	0.209	0.169	0.185	0.149	0.120	0.118	0.120	0.116	0.116	0.354	0.526	1.752	3.087	3.322	
		E-MIDAS	0.201	0.162	0.175	0.142	0.118	0.121	0.126	0.122	0.121	0.350	0.519	1.717	3.024	3.255	
	CFNAI	G-MIDAS	0.215	0.178	0.187	0.145	0.110	0.112	0.117	0.115	0.117	0.369	0.541	1.819	3.194	3.430	
		GJR-MIDAS	0.209	0.167	0.180	0.140	0.106	0.105	0.109	0.106	0.106	0.350	0.523	1.753	3.088	3.322	
		E-MIDAS	0.201	0.161	0.170	0.131	0.100	0.102	0.107	0.105	0.105	0.342	0.512	1.716	3.023	3.254	
	FPU <sub>JPN</sub>	G-MIDAS	0.215	0.180	0.192	0.156	0.129	0.131	0.136	0.137	0.141	0.376	0.545	1.816	3.191	3.429	
		GJR-MIDAS	0.211	0.171	0.187	0.151	0.122	0.120	0.122	0.120	0.122	0.353	0.524	1.750	3.084	3.320	
		E-MIDAS	0.202	0.163	0.176	0.140	0.112	0.112	0.116	0.115	0.118	0.343	0.509	1.710	3.017	3.249	
	EER <sub>CH</sub>	G-MIDAS	0.215	0.177	0.187	0.145	0.109	0.110	0.114	0.112	0.114	0.370	0.544	1.820	3.197	3.436	
		GJR-MIDAS	0.210	0.170	0.186	0.149	0.118	0.115	0.118	0.114	0.113	0.355	0.528	1.755	3.090	3.325	
		E-MIDAS	0.203	0.163	0.174	0.136	0.105	0.105	0.109	0.106	0.107	0.345	0.514	1.717	3.024	3.255	
	NASDAQ	IP	G-MIDAS	0.269	0.211	0.220	0.186	0.143	0.150	0.155	0.152	0.156	0.413	0.541	1.756	3.261	3.396
			GJR-MIDAS	0.261	0.200	0.213	0.179	0.136	0.141	0.145	0.140	0.141	0.391	0.521	1.693	3.154	3.289
			E-MIDAS	0.253	0.194	0.203	0.169	0.128	0.134	0.138	0.132	0.134	0.380	0.507	1.654	3.086	3.218
		IN	G-MIDAS	0.269	0.211	0.219	0.183	0.137	0.144	0.148	0.146	0.149	0.411	0.541	1.757	3.264	3.401
			GJR-MIDAS	0.261	0.199	0.212	0.177	0.132	0.137	0.140	0.135	0.136	0.390	0.521	1.693	3.155	3.291
			E-MIDAS	0.254	0.195	0.206	0.174	0.136	0.143	0.148	0.143	0.145	0.385	0.510	1.654	3.085	3.218
UR		GH-MIDAS	0.274	0.215	0.223	0.186	0.134	0.144	0.152	0.152	0.159	0.435	0.574	1.789	3.299	3.439	
		GJR-MIDAS	0.260	0.197	0.210	0.174	0.124	0.129	0.133	0.127	0.127	0.390	0.524	1.697	3.161	3.297	
		E-MIDAS	0.253	0.192	0.201	0.165	0.121	0.128	0.134	0.128	0.129	0.384	0.514	1.661	3.094	3.228	
EPU		G-MIDAS	0.270	0.211	0.220	0.185	0.138	0.145	0.149	0.146	0.150	0.412	0.542	1.757	3.264	3.400	
		GJR-MIDAS	0.261	0.200	0.214	0.180	0.133	0.138	0.140	0.134	0.135	0.389	0.520	1.692	3.154	3.289	
		E-MIDAS	0.255	0.201	0.216	0.190	0.163	0.171	0.176	0.172	0.176	0.392	0.513	1.649	3.078	3.210	
GEPUS		G-MIDAS	0.270	0.212	0.221	0.185	0.138	0.145	0.148	0.146	0.151	0.412	0.542	1.757	3.263	3.400	
		GJR-MIDAS	0.263	0.202	0.216	0.181	0.134	0.137	0.139	0.134	0.136	0.390	0.520	1.692	3.154	3.289	
		E-MIDAS	0.256	0.200	0.213	0.183	0.147	0.153	0.157	0.154	0.157	0.387	0.510	1.650	3.080	3.211	
EER		G-MIDAS	0.269	0.210	0.218	0.182	0.133	0.140	0.144	0.141	0.145	0.411	0.543	1.759	3.266	3.404	
		GJR-MIDAS	0.260	0.198	0.211	0.175	0.127	0.131	0.134	0.128	0.129	0.390	0.523	1.696	3.158	3.295	
		E-MIDAS	0.254	0.196	0.207	0.175	0.137	0.145	0.149	0.144	0.147	0.388	0.515	1.658	3.089	3.221	
FPU <sub>US</sub>		G-MIDAS	0.270	0.211	0.220	0.185	0.139	0.146	0.150	0.147	0.152	0.412	0.542	1.757	3.263	3.400	
		GJR-MIDAS	0.261	0.201	0.215	0.181	0.136	0.140	0.142	0.136	0.138	0.390	0.521	1.692	3.153	3.289	
		E-MIDAS	0.253	0.196	0.209	0.181	0.150	0.159	0.164	0.159	0.160	0.390	0.515	1.654	3.084	3.216	
CFNAI		G-MIDAS	0.270	0.212	0.220	0.184	0.137	0.144	0.149	0.146	0.148	0.410	0.539	1.756	3.263	3.396	
		GJR-MIDAS	0.261	0.199	0.211	0.175	0.129	0.134	0.138	0.134	0.134	0.389	0.518	1.693	3.155	3.289	
		E-MIDAS	0.252	0.193	0.201	0.167	0.125	0.132	0.139	0.135	0.135	0.384	0.514	1.662	3.094	3.226	
FPU <sub>JPN</sub>		G-MIDAS	0.270	0.215	0.226	0.195	0.157	0.166	0.171	0.171	0.178	0.421	0.547	1.756	3.261	3.398	
		GJR-MIDAS	0.262	0.202	0.217	0.185	0.144	0.149	0.152	0.149	0.152	0.393	0.522	1.691	3.152	3.288	
		E-MIDAS	0.255	0.199	0.212	0.182	0.148	0.154	0.159	0.157	0.160	0.388	0.512	1.653	3.084	3.217	
EER <sub>CH</sub>		G-MIDAS	0.269	0.211	0.219	0.183	0.136	0.143	0.147	0.144	0.148	0.412	0.543	1.758	3.265	3.402	
		GJR-MIDAS	0.261	0.200	0.214	0.181	0.137	0.142	0.145	0.139	0.141	0.393	0.524	1.695	3.157	3.292	
		E-MIDAS	0.254	0.196	0.207	0.175	0.137	0.144	0.149	0.144	0.147	0.387	0.514	1.657	3.087	3.220	
EER <sub>CH</sub>		GJR-MIDAS	0.035	0.035	0.037	0.037	0.035	0.033	0.034	0.032	0.032	0.035	0.041	0.045	0.051	0.053	
		E-MIDAS	0.033	0.033	0.035	0.035	0.034	0.032	0.033	0.032	0.031	0.034	0.039	0.043	0.049	0.050	
		G-MIDAS	0.037	0.035	0.038	0.038	0.037	0.034	0.035	0.034	0.033	0.037	0.043	0.048	0.055	0.057	
		GJR-MIDAS	0.036	0.036	0.038	0.035	0.034	0.032	0.032	0.031	0.031	0.035	0.041	0.046	0.055	0.058	
		E-MIDAS	0.033	0.032	0.034	0.034	0.032	0.030	0.031	0.030	0.030	0.033	0.039	0.044	0.052	0.055	
		G-MIDAS	0.037	0.035	0.038	0.038	0.037	0.034	0.035	0.034	0.033	0.037	0.043	0.048	0.055	0.057	

Notes: The table reports the RMSE LOSS daily forecasts for 1-day ahead forecast to 3-month ahead volatility forecasts for GARCH-MIDAS, GJR-GARCH-MIDAS, and EGARCH-MIDAS using all macroeconomic variables.



Index	Macro	Model	1	5	10	15	20	25	30	35	40	45	50	55	60	66	
CAC40	IP	GARCHMIDAS	0.271	0.201	0.201	0.198	0.197	0.217	0.212	0.209	0.212	0.310	0.357	1.160	2.721	2.927	
		GJR-MIDAS	0.267	0.212	0.220	0.227	0.229	0.246	0.238	0.229	0.229	0.319	0.360	1.110	2.607	2.805	
		E-MIDAS	0.257	0.189	0.195	0.198	0.198	0.213	0.208	0.205	0.210	0.295	0.335	1.080	2.550	2.749	
	IN	G-MIDAS	0.271	0.202	0.204	0.201	0.201	0.222	0.215	0.212	0.218	0.315	0.362	1.160	2.719	2.924	
		GJR-MIDAS	0.269	0.218	0.231	0.243	0.251	0.270	0.265	0.258	0.263	0.353	0.394	1.118	2.605	2.797	
		E-MIDAS	0.258	0.190	0.197	0.201	0.201	0.217	0.212	0.208	0.214	0.301	0.342	1.082	2.551	2.748	
	UR	G-MIDAS	0.270	0.198	0.195	0.188	0.184	0.206	0.199	0.197	0.203	0.312	0.364	1.168	2.728	2.942	
		GJR-MIDAS	0.268	0.216	0.229	0.239	0.245	0.264	0.258	0.249	0.252	0.345	0.388	1.119	2.608	2.803	
		E-MIDAS	0.258	0.191	0.198	0.203	0.204	0.220	0.215	0.212	0.219	0.304	0.344	1.082	2.549	2.746	
	EPU	G-MIDAS	0.271	0.203	0.204	0.202	0.202	0.222	0.216	0.214	0.219	0.316	0.363	1.160	2.719	2.924	
		GJR-MIDAS	0.267	0.209	0.216	0.221	0.222	0.238	0.230	0.220	0.220	0.313	0.356	1.112	2.613	2.813	
		EH-MIDAS	0.257	0.187	0.191	0.193	0.191	0.207	0.201	0.198	0.202	0.290	0.333	1.083	2.556	2.755	
	GEPU	G-MIDAS	0.272	0.203	0.205	0.202	0.202	0.222	0.216	0.213	0.219	0.316	0.363	1.159	2.718	2.922	
		GJR-MIDAS	0.270	0.219	0.232	0.243	0.249	0.268	0.261	0.253	0.259	0.350	0.390	1.116	2.604	2.796	
		E-MIDAS	0.259	0.195	0.205	0.213	0.216	0.233	0.229	0.227	0.233	0.314	0.353	1.083	2.548	2.744	
	EER	G-MIDAS	0.271	0.202	0.203	0.201	0.200	0.220	0.214	0.212	0.217	0.313	0.360	1.158	2.717	2.922	
		GJR-MIDAS	0.270	0.220	0.235	0.248	0.256	0.276	0.272	0.266	0.272	0.361	0.403	1.119	2.602	2.793	
		E-MIDAS	0.258	0.190	0.197	0.202	0.203	0.219	0.213	0.209	0.218	0.302	0.339	1.076	2.542	2.736	
	EER <sub>US</sub>	G-MIDAS	0.271	0.203	0.205	0.204	0.204	0.225	0.219	0.217	0.223	0.318	0.365	1.160	2.718	2.922	
		GJR-MIDAS	0.269	0.217	0.230	0.241	0.247	0.266	0.260	0.252	0.256	0.346	0.388	1.116	2.605	2.798	
		E-MIDAS	0.258	0.192	0.200	0.206	0.208	0.224	0.220	0.217	0.224	0.307	0.347	1.082	2.548	2.745	
	IP <sub>US</sub>	G-MIDAS	0.271	0.204	0.208	0.207	0.205	0.230	0.215	0.201	0.203	0.321	0.378	1.182	2.747	2.954	
		GJR-MIDAS	0.264	0.203	0.207	0.207	0.205	0.221	0.210	0.198	0.195	0.297	0.344	1.115	2.620	2.825	
		E-MIDAS	0.256	0.181	0.181	0.178	0.173	0.190	0.184	0.181	0.183	0.278	0.325	1.087	2.563	2.767	
	CFNAI	G-MIDAS	0.271	0.203	0.204	0.202	0.202	0.222	0.218	0.217	0.220	0.312	0.357	1.157	2.717	2.920	
		GJR-MIDAS	0.266	0.208	0.213	0.217	0.218	0.233	0.226	0.220	0.220	0.307	0.347	1.107	2.609	2.808	
		E-MIDAS	0.258	0.189	0.194	0.197	0.196	0.211	0.207	0.205	0.208	0.292	0.332	1.080	2.551	2.750	
	FPU <sub>JP</sub>	G-MIDAS	0.272	0.206	0.210	0.210	0.212	0.232	0.229	0.229	0.236	0.326	0.372	1.159	2.715	2.920	
		GJR-MIDAS	0.269	0.216	0.229	0.240	0.247	0.266	0.261	0.253	0.257	0.347	0.388	1.116	2.605	2.798	
		E-MIDAS	0.262	0.202	0.212	0.220	0.223	0.238	0.236	0.237	0.245	0.320	0.358	1.084	2.549	2.747	
	EER <sub>CH</sub>	G-MIDAS	0.270	0.200	0.199	0.195	0.193	0.213	0.207	0.205	0.208	0.306	0.354	1.159	2.721	2.928	
		GJR-MIDAS	0.268	0.213	0.222	0.230	0.233	0.250	0.242	0.232	0.233	0.323	0.364	1.110	2.606	2.803	
		E-MIDAS	0.257	0.187	0.191	0.192	0.190	0.205	0.200	0.197	0.201	0.288	0.329	1.081	2.553	2.754	
	DAX	IP	G-MIDAS	0.235	0.197	0.207	0.203	0.206	0.230	0.228	0.225	0.229	0.354	0.401	2.625	2.695	3.084
			GJR-MIDAS	0.232	0.205	0.227	0.237	0.244	0.265	0.264	0.260	0.266	0.372	0.417	2.514	2.576	2.961
			E-MIDAS	0.228	0.193	0.210	0.215	0.219	0.237	0.235	0.235	0.239	0.343	0.384	2.466	2.528	2.907
		IN	G-MIDAS	0.234	0.195	0.204	0.199	0.201	0.225	0.222	0.219	0.222	0.351	0.398	2.628	2.698	3.088
			GJR-MIDAS	0.230	0.201	0.221	0.228	0.233	0.253	0.250	0.244	0.246	0.359	0.405	2.515	2.578	2.965
			E-MIDAS	0.225	0.187	0.201	0.203	0.205	0.223	0.220	0.218	0.221	0.332	0.374	2.466	2.529	2.911
		UR	G-MIDAS	0.234	0.192	0.198	0.188	0.185	0.214	0.211	0.206	0.209	0.356	0.407	2.641	2.716	3.114
			GJR-MIDAS	0.230	0.201	0.221	0.227	0.232	0.252	0.250	0.243	0.246	0.361	0.407	2.518	2.582	2.970
			E-MIDAS	0.225	0.192	0.217	0.236	0.255	0.286	0.301	0.316	0.337	0.440	0.500	2.500	2.566	2.947
		EPU	G-MIDAS	0.234	0.195	0.204	0.199	0.200	0.224	0.221	0.218	0.221	0.351	0.399	2.628	2.699	3.089
			GJR-MIDAS	0.228	0.200	0.220	0.227	0.232	0.252	0.249	0.241	0.244	0.359	0.406	2.517	2.580	2.968
			E-MIDAS	0.226	0.188	0.202	0.203	0.205	0.223	0.221	0.219	0.223	0.335	0.377	2.470	2.534	2.916
GEPU		G-MIDAS	0.234	0.196	0.205	0.201	0.203	0.227	0.225	0.222	0.225	0.353	0.401	2.627	2.697	3.088	
		GJR-MIDAS	0.232	0.204	0.224	0.231	0.236	0.255	0.252	0.246	0.249	0.364	0.409	2.517	2.579	2.966	
		E-MIDAS	0.226	0.191	0.207	0.212	0.216	0.235	0.234	0.233	0.235	0.344	0.388	2.472	2.536	2.916	
EER		G-MIDAS	0.234	0.195	0.203	0.197	0.198	0.223	0.219	0.216	0.219	0.350	0.398	2.628	2.699	3.090	
		GJR-MIDAS	0.230	0.202	0.223	0.231	0.237	0.257	0.254	0.248	0.252	0.364	0.410	2.514	2.577	2.964	
		E-MIDAS	0.226	0.188	0.204	0.208	0.212	0.231	0.229	0.228	0.232	0.343	0.387	2.472	2.536	2.917	
EER <sub>US</sub>		G-MIDAS	0.234	0.194	0.203	0.197	0.199	0.225	0.223	0.220	0.223	0.353	0.401	2.630	2.700	3.092	
		GJR-MIDAS	0.230	0.202	0.223	0.230	0.236	0.257	0.255	0.249	0.253	0.365	0.411	2.517	2.580	2.967	
		E-MIDAS	0.226	0.188	0.203	0.207	0.210	0.229	0.228	0.226	0.229	0.339	0.381	2.469	2.532	2.912	
IP <sub>US</sub>		G-MIDAS	0.238	0.197	0.212	0.206	0.207	0.236	0.228	0.210	0.213	0.365	0.420	2.655	2.731	3.121	
		GJR-MIDAS	0.225	0.189	0.202	0.199	0.197	0.217	0.212	0.202	0.200	0.333	0.380	2.532	2.600	2.993	
		E-MIDAS	0.222	0.177	0.186	0.181	0.178	0.199	0.197	0.193	0.193	0.321	0.366	2.480	2.547	2.932	
CFNAI		G-MIDAS	0.235	0.196	0.204	0.199	0.200	0.224	0.222	0.219	0.221	0.349	0.394	2.627	2.696	3.085	
		GJR-MIDAS	0.227	0.193	0.205	0.205	0.206	0.224	0.221	0.216	0.215	0.334	0.378	2.528	2.593	2.980	
		E-MIDAS	0.225	0.186	0.198	0.199	0.200	0.217	0.215	0.213	0.215	0.327	0.369	2.471	2.534	2.915	
FPU <sub>JP</sub>		G-MIDAS	0.236	0.200	0.210	0.207	0.210	0.234	0.233	0.232	0.237	0.360	0.407	2.626	2.696	3.087	
		GJR-MIDAS	0.229	0.201	0.221	0.228	0.233	0.253	0.251	0.244	0.246	0.361	0.406	2.517	2.580	2.967	
		E-MIDAS	0.229	0.193	0.208	0.211	0.213	0.230	0.228	0.228	0.232	0.340	0.382	2.470	2.534	2.915	
EER <sub>CH</sub>		G-MIDAS	0.233	0.193	0.200	0.193	0.194	0.218	0.215	0.212	0.214	0.347	0.395	2.629	2.701	3.093	
		GJR-MIDAS	0.230	0.202	0.223	0.231	0.236	0.256	0.254	0.247	0.250	0.363	0.410	2.516	2.579	2.966	
		E-MIDAS	0.224	0.183	0.195	0.194	0.194	0.212	0.208	0.205	0.208	0.324	0.366	2.469	2.534	2.917	

Notes: The table reports the RMSE LOSS daily forecasts for 1-day ahead forecast to 3-month ahead volatility forecasts for GARCH-MIDAS, GJR-GARCH-MIDAS, and EGARCH-MIDAS using all macroeconomic variables.

Index	Macro	Model	1	5	10	15	20	25	30	35	40	45	50	55	60	66	
FTSE100	IP	G-MIDAS	0.210	0.186	0.187	0.188	0.188	0.188	0.195	0.195	0.195	0.200	0.211	0.301	0.949	2.097	
		GJR-MIDAS	0.211	0.187	0.186	0.186	0.183	0.181	0.188	0.185	0.184	0.189	0.200	0.285	0.913	2.022	
		E-MIDAS	0.206	0.178	0.180	0.181	0.180	0.179	0.186	0.184	0.184	0.190	0.200	0.280	0.891	1.974	
	IN	G-MIDAS	0.210	0.185	0.186	0.186	0.185	0.185	0.185	0.191	0.192	0.191	0.196	0.207	0.300	0.949	2.099
		GJR-MIDAS	0.211	0.186	0.185	0.185	0.182	0.180	0.187	0.184	0.181	0.188	0.200	0.287	0.915	2.023	
		E-MIDAS	0.205	0.176	0.179	0.180	0.179	0.177	0.184	0.183	0.182	0.189	0.200	0.280	0.892	1.974	
	UR	G-MIDAS	0.213	0.184	0.185	0.182	0.180	0.179	0.186	0.188	0.188	0.198	0.207	0.309	0.960	2.115	
		GJR-MIDAS	0.210	0.184	0.183	0.182	0.177	0.175	0.182	0.180	0.177	0.185	0.196	0.287	0.918	2.028	
		E-MIDAS	0.204	0.173	0.174	0.172	0.170	0.168	0.177	0.178	0.178	0.181	0.194	0.284	0.901	1.987	
	EPU	G-MIDAS	0.210	0.185	0.186	0.185	0.184	0.184	0.191	0.191	0.191	0.195	0.205	0.298	0.948	2.097	
		GJR-MIDAS	0.211	0.186	0.186	0.186	0.182	0.180	0.186	0.183	0.180	0.189	0.200	0.287	0.915	2.024	
		E-MIDAS	0.205	0.176	0.177	0.177	0.176	0.174	0.182	0.181	0.180	0.185	0.195	0.278	0.893	1.978	
	GEPU	G-MIDAS	0.210	0.186	0.187	0.187	0.187	0.188	0.194	0.194	0.194	0.199	0.211	0.301	0.948	2.096	
		GJR-MIDAS	0.212	0.187	0.187	0.186	0.182	0.180	0.187	0.183	0.181	0.190	0.200	0.287	0.915	2.023	
		E-MIDAS	0.207	0.181	0.184	0.188	0.188	0.188	0.194	0.192	0.191	0.198	0.209	0.283	0.889	1.970	
	EER	G-MIDAS	0.211	0.186	0.187	0.186	0.185	0.185	0.191	0.192	0.191	0.197	0.208	0.302	0.951	2.100	
		GJR-MIDAS	0.211	0.187	0.186	0.186	0.183	0.181	0.188	0.185	0.182	0.190	0.202	0.290	0.917	2.025	
		E-MIDAS	0.206	0.177	0.179	0.181	0.179	0.177	0.185	0.184	0.183	0.190	0.202	0.284	0.895	1.979	
	EER <sub>US</sub>	G-MIDAS	0.211	0.186	0.187	0.186	0.186	0.186	0.192	0.192	0.191	0.197	0.208	0.300	0.948	2.097	
		GJR-MIDAS	0.211	0.186	0.186	0.185	0.182	0.180	0.186	0.182	0.180	0.188	0.199	0.287	0.915	2.023	
		E-MIDAS	0.205	0.176	0.178	0.179	0.178	0.176	0.183	0.181	0.181	0.189	0.199	0.281	0.894	1.977	
	IP <sub>US</sub>	G-MIDAS	0.200	0.181	0.182	0.183	0.183	0.186	0.186	0.187	0.183	0.188	0.203	0.311	0.951	2.106	
		GJR-MIDAS	0.210	0.184	0.182	0.181	0.177	0.174	0.182	0.179	0.177	0.184	0.196	0.288	0.919	2.029	
		E-MIDAS	0.204	0.173	0.173	0.173	0.171	0.168	0.177	0.177	0.176	0.182	0.194	0.282	0.900	1.986	
	CFNAI	G-MIDAS	0.210	0.184	0.184	0.183	0.182	0.182	0.191	0.192	0.192	0.194	0.205	0.298	0.951	2.100	
		GJR-MIDAS	0.211	0.185	0.182	0.181	0.177	0.176	0.184	0.183	0.182	0.185	0.196	0.284	0.915	2.025	
		E-MIDAS	0.205	0.176	0.177	0.177	0.176	0.173	0.183	0.184	0.183	0.185	0.200	0.285	0.900	1.986	
	FPU <sub>JPN</sub>	G-MIDAS	0.211	0.187	0.189	0.189	0.190	0.190	0.198	0.199	0.200	0.204	0.216	0.303	0.950	2.097	
		GJR-MIDAS	0.211	0.186	0.185	0.185	0.182	0.180	0.187	0.183	0.180	0.188	0.199	0.287	0.915	2.023	
		E-MIDAS	0.210	0.184	0.186	0.188	0.187	0.185	0.193	0.193	0.194	0.198	0.208	0.285	0.893	1.976	
	EER <sub>CH</sub>	G-MIDAS	0.210	0.184	0.185	0.183	0.182	0.182	0.189	0.189	0.188	0.193	0.204	0.299	0.951	2.101	
		GJR-MIDAS	0.210	0.185	0.184	0.183	0.179	0.178	0.184	0.182	0.179	0.186	0.197	0.286	0.916	2.025	
		E-MIDAS	0.205	0.175	0.177	0.178	0.176	0.174	0.181	0.180	0.180	0.186	0.198	0.280	0.894	1.980	
	NIKKEI	IP	G-MIDAS	0.177	0.176	0.190	0.196	0.199	0.213	0.218	0.221	0.330	0.509	0.808	1.032	1.357	1.400
			GJR-MIDAS	0.171	0.168	0.185	0.186	0.189	0.202	0.201	0.204	0.311	0.485	0.775	1.000	1.324	1.370
			E-MIDAS	0.174	0.170	0.189	0.194	0.199	0.214	0.217	0.222	0.310	0.470	0.743	0.962	1.275	1.317
		IN	G-MIDAS	0.176	0.175	0.188	0.192	0.197	0.210	0.214	0.218	0.325	0.503	0.801	1.025	1.350	1.395
			GJR-MIDAS	0.172	0.169	0.186	0.188	0.191	0.203	0.204	0.206	0.309	0.481	0.769	0.993	1.315	1.359
			E-MIDAS	0.172	0.168	0.185	0.188	0.193	0.208	0.209	0.214	0.310	0.474	0.750	0.970	1.285	1.328
		UR	G-MIDAS	0.175	0.172	0.184	0.186	0.190	0.202	0.203	0.206	0.320	0.502	0.805	1.030	1.358	1.404
			GJR-MIDAS	0.169	0.164	0.178	0.176	0.177	0.188	0.185	0.185	0.302	0.481	0.776	1.003	1.330	1.376
			E-MIDAS	0.170	0.164	0.179	0.179	0.181	0.194	0.192	0.194	0.300	0.471	0.755	0.977	1.295	1.339
		EPU	G-MIDAS	0.182	0.189	0.210	0.222	0.235	0.251	0.261	0.269	0.360	0.525	0.811	1.031	1.352	1.396
			GJR-MIDAS	0.176	0.178	0.198	0.204	0.211	0.223	0.228	0.231	0.325	0.490	0.773	0.995	1.315	1.359
			E-MIDAS	0.176	0.174	0.194	0.201	0.208	0.223	0.227	0.232	0.321	0.481	0.755	0.973	1.287	1.329
		GEPU	G-MIDAS	0.176	0.174	0.188	0.192	0.198	0.210	0.215	0.220	0.327	0.504	0.803	1.026	1.352	1.397
			GJR-MIDAS	0.171	0.168	0.184	0.186	0.188	0.200	0.201	0.203	0.308	0.480	0.768	0.992	1.314	1.358
			E-MIDAS	0.172	0.167	0.185	0.188	0.192	0.208	0.209	0.214	0.309	0.473	0.749	0.969	1.282	1.324
EER <sub>US</sub>		G-MIDAS	0.176	0.175	0.189	0.193	0.199	0.212	0.217	0.222	0.329	0.506	0.804	1.027	1.353	1.397	
		GJR-MIDAS	0.172	0.170	0.187	0.189	0.194	0.206	0.208	0.211	0.313	0.483	0.770	0.994	1.315	1.359	
		E-MIDAS	0.172	0.169	0.188	0.194	0.200	0.218	0.221	0.227	0.321	0.484	0.759	0.978	1.292	1.333	
FPU <sub>JPN</sub>		G-MIDAS	0.187	0.197	0.222	0.240	0.256	0.274	0.288	0.299	0.383	0.541	0.820	1.037	1.355	1.398	
		GJR-MIDAS	0.181	0.186	0.209	0.220	0.230	0.244	0.251	0.257	0.342	0.501	0.777	0.997	1.314	1.357	
		E-MIDAS	0.179	0.180	0.204	0.216	0.227	0.245	0.252	0.260	0.341	0.493	0.760	0.975	1.285	1.327	
IP <sub>US</sub>		G-MIDAS	0.173	0.170	0.179	0.175	0.178	0.192	0.188	0.190	0.328	0.524	0.846	1.066	1.396	1.449	
		GJR-MIDAS	0.169	0.164	0.179	0.177	0.178	0.189	0.186	0.186	0.303	0.481	0.776	1.003	1.329	1.375	
		E-MIDAS	0.170	0.163	0.178	0.177	0.179	0.191	0.188	0.191	0.297	0.467	0.750	0.973	1.292	1.338	
CFNAI		G-MIDAS	0.178	0.178	0.193	0.199	0.205	0.216	0.220	0.224	0.329	0.504	0.801	1.023	1.348	1.390	
		GJR-MIDAS	0.174	0.173	0.191	0.195	0.199	0.210	0.211	0.213	0.312	0.482	0.768	0.991	1.312	1.356	
		E-MIDAS	0.174	0.171	0.189	0.194	0.198	0.211	0.212	0.216	0.309	0.472	0.749	0.969	1.283	1.325	
EER <sub>CH</sub>		G-MIDAS	0.175	0.173	0.185	0.187	0.191	0.202	0.203	0.206	0.318	0.499	0.800	1.026	1.354	1.400	
		GJR-MIDAS	0.171	0.167	0.183	0.183	0.185	0.195	0.194	0.195	0.304	0.478	0.769	0.995	1.319	1.365	
		E-MIDAS	0.171	0.164	0.179	0.179	0.179	0.192	0.189	0.190	0.296	0.466	0.750	0.973	1.291	1.336	
HSE		IP	G-MIDAS	0.311	0.278	0.275	0.272	0.288	0.322	0.273	0.269	0.267	0.275	0.289	0.424	0.635	0.781
			GJR-MIDAS	0.304	0.271	0.268	0.265	0.281	0.315	0.263	0.260	0.259	0.267	0.279	0.409	0.615	0.757
			E-MIDAS	0.303	0.267	0.267	0.267	0.287	0.320	0.278	0.280	0.283	0.291	0.307	0.421	0.611	0.743
		IN	G-MIDAS	0.312	0.279	0.276	0.273	0.288	0.321	0.271	0.268	0.267	0.274	0.288	0.421	0.629	0.774
			GJR-MIDAS	0.303	0.271	0.268	0.264	0.280	0.314	0.262	0.260	0.259	0.267	0.279	0.409	0.615	0.757
			E-MIDAS	0.303	0.266	0.265	0.263	0.279	0.311	0.264	0.263	0.261	0.268	0.281	0.403	0.595	0.725
		UR	G-MIDAS	0.312	0.279	0.276	0.273	0.288	0.321	0.272	0						

# Bayesian MCMC Approach to Asymmetric GARCH-MIDAS Models with Jump Components

## 3.1 Introduction

If the presence of outliers/rare events is ignored in standard GARCH models, then QML estimates tend to produce very high persistence close to IGARCH effects. Liu et al. (2019) argued that if structural breaks were ignored, then the volatility persistence of GARCH models would be overestimated such that the estimates are often close to the parameter boundaries that violate stationarity of the volatility. To accommodate structure breaks or rare events, the t-distribution and the generalized error distribution were imposed on innovations by Bollerslev (1987) and Nelson (1991) whereas Bai et al. (2003) employed a mixture of two zero mean normal distributions.

In the GARCH-MIDAS literature non-normal innovations have not been explicitly considered though violation of normality assumption may lead to inconsistency of QML estimates. Another weakness of the QML method lies in that when estimating the complex models with a large number of parameters, the QML estimation may result in the convergence to a local maximum instead of the global maximum of the likelihood function (Conrad and Kleen (2019)). Since the likelihood function for GARCH-MIDAS models is maximised via a constrained optimisation to ensure non-negativity and stationarity of the volatility, the optimal properties of MLE do not necessarily hold. Moreover, it is hard to obtain the global maximum, especially if the true parameter values are close to the boundary of the parameter space and/or the short term volatility component is nearly non-stationary.

As a main contribution, we propose Bayesian MCMC methodology to estimating asymmetric GARCH-MIDAS models that also include jump components, which are supposed to capture the presence of rare events.<sup>1</sup> In the Bayesian approach, each parameter  $\Theta_i$  is regarded as a random variable with a known prior distribution  $\pi(\Theta_i)$ , from which we derive the posterior distribution,  $p(\Theta_i | \Theta_{-i}, \mathbf{r})$  where  $\mathbf{r}$  denotes returns data and  $\Theta_{-i}$  is the set of the other parameters.

<sup>1</sup>The MCMC approach has not been popular for estimating standard GARCH models because the posterior distributions of the parameters cannot be expressed as known families of distribution. To overcome this difficulty, Ardia (2008), Takaishi (2011), Bauwens and Lubrano (1998), Vontros et al. (2000), and Nakatsuma (2000) apply a Metropolis Hasting simulation method which consists of approximating (complex) posterior distributions by normal or Gamma distributions, from which it is straightforward to apply the simulation method.

We then construct the MCMC estimate, denoted  $\hat{\Theta}_i$ , as the sample mean of a large number of draws from  $p(\Theta_i | \Theta_{-i}, \mathbf{r})$ .

The MCMC estimate is close to the QML counterpart if the number of iterations/updates is sufficiently large (Markov Chain Monte Carlo theorem). More importantly, the precision of the MCMC estimate for GARCH-MIDAS models does not depend on the complexity or dimension of the model, since the joint density can be expressed as a function of marginal densities by Bayes theorem.<sup>2</sup> Addition of a parameter in the model will only increase the number of iterations to reach convergence. This is a main advantage over the QML estimation that becomes intractable as the dimension of the parameters rises. Furthermore, we can obtain credible intervals for the parameter estimates from the empirical distributions of the large simulated samples.

We confirm the validity of the MCMC approach via a comprehensive simulation study. First, when the simulated data do not contain outliers, both MCMC and QML estimates are relatively accurate for GARCH-MIDAS model while MCMC produces more precise estimate of the leverage effect than QML for GJR-GARCH-MIDAS and EGARCH-MIDAS models. However, when the simulated data contain jump components, we find that QML estimates become unreliable or computationally infeasible. Still, the proposed MCMC estimates can be easily conducted and are relatively satisfactory.

We aim to address the important issues of leverage effect and rare events by applying the jump-augmented asymmetric GARCH-MIDAS models to an analysis of time-varying volatility patterns of WTI daily returns over the period 09/2000-8/2019. We also evaluate the relative performance of GARCH-MIDAS-J, GJR-GARCH-MIDAS-J and EGARCH-MIDAS-J models in terms of in-sample fit and out of sample forecast performance. To examine the impacts of macroeconomic conditions on the long-run volatility, we consider a range of macroeconomic indicators for US, China, Russia and OPEC.

In sum, we document evidence that the inclusion of the leverage effect, the long term volatility, and rare events through jump will be important in capturing the salient time-varying volatility patterns of the daily WTI returns. BIC convincingly selects MIDAS models with jump components over MIDAS models without jump components. The jump augmented MIDAS models produced significant long term coefficients ( $\theta$ ) with predicted signs for all macroeconomic variables. Overall, EGARCH-MIDAS-J is the most preferred model. When evaluating the relative importance of each macroeconomic variable by employing VR that measures the fraction of the total volatility explained by the long term component, we find that the most influential variable is the  $OP_{OPEC}$ , that explains 43.5% of the total volatility for WTI returns. This highlights the dominant position of the OPEC in the global oil industry. Finally, in terms of RMSE and QLIKE loss functions, we find that EGARCH-MIDAS-J outperforms both GJR-GARCH-MIDAS-J and

---

<sup>2</sup>In the past when the computing power was limited, the Bayesian approach is criticised mainly because it requires proper prior distributions of the parameters. Nowadays, the selection of the prior distributions and the initial parameter estimates are no longer crucial as long as they are non-informative, i.e. close to the uniform distribution on the support of the parameters.

GARCH-MIDAS-J for almost all cases considered.

This chapter is organised as follows. Section 2 presents the general class of GARCH-MIDAS models with leverage effects and jump components. In Section 3, we describe the Bayesian MCMC estimation using the Metropolis-Hasting and Adaptive approach. Section 4 presents the comprehensive simulation results. Section 5 provides the main empirical findings for WTI returns. Section 6 concludes.

## 3.2 Generalised GARCH and EGARCH MIDAS Models

In this section, we develop the general class of GARCH-MIDAS models by adding a jump component in the return equation to capture dynamics of rare events. The occurrence of a rare event is usually modelled by incorporating a component of the form,  $b_t z_t$  where  $b_t$  is an indicator of a rare event/jump of size,  $z_t$  with probability  $\kappa$ . We assume that  $b_t$  follows a Bernoulli distribution with a parameter,  $\kappa$  i.e.  $P(b_t = 1) = \kappa$ , and  $P(b_t = 0) = 1 - \kappa$  where  $\kappa$  is usually less than 0.1. The size  $z_t$  is considered as an observation from a random variable that follows a normal distribution,  $N(\mu_z, \sigma_z^2)$ .

Rare events can be incorporated either in the return equation, in the specification of the short term volatility or the long term volatility.<sup>3</sup> We consider only the case where the jump component  $b_t z_t$  is included in the return equation, i.e.

$$r_t = \mu_t + b_t z_t + \sigma_t \varepsilon_t \quad (3.2.1)$$

where  $\mu_t$  is either set to a constant intercept  $\mu$ , or a function of the volatility components, i.e.

$$\mu_t = \mu + \lambda_1 g_t + \lambda_2 \tau_t$$

where  $g_t$  and  $\tau_t$  are the short term and long term volatility components for  $\sigma_t = \sqrt{g_t \tau_t}$ , and  $\varepsilon_t \sim N(0, 1)$ .

We assume that  $\tau_t$  is modelled by:

$$\log(\tau_t) = m + \theta \sum_{k=1}^K w_k X_{t-k} \quad (3.2.2)$$

where  $w_k$  is defined by:

$$w_k = \frac{(1 - \frac{k}{K})^\omega}{\sum_{k=1}^K (1 - \frac{k}{K})^\omega} \quad k = 1, \dots, K$$

satisfying  $\sum_{k=1}^K w_k = 1$ ,  $X$  is the macroeconomic variable, and  $K$  is chosen by the user where its

<sup>3</sup>In the literature, the jump component was included only in the return equation for GARCH models whereas it was included in both the return and volatility equations for stochastic volatility models.

typical values are 12, 24, or 36.

Then, the GARCH-MIDAS Jump augmented model can be expressed as:

$$r_t = \mu + e_t \tag{3.2.3}$$

$$e_t = b_t z_t + \sqrt{g_t \tau_t} \varepsilon_t \tag{3.2.4}$$

$$\log(\tau_t) = m + \theta \sum_{k=1}^K w_k X_{t-k} \tag{3.2.5}$$

where  $\varepsilon_t \sim N(0, 1)$ . We then consider the three different models for the short term volatility,  $g_t$  that follows unit-variance GARCH(1,1), unit-variance GJR-GARCH(1,1) or unit-variance EGARCH(1,1) (see Chapter 2):

**Unit-variance GARCH(1,1):**

$$g_t = \alpha_0 + \alpha \frac{(r_{t-1} - \mu_{t-1})^2}{\tau_{t-1}} + \beta g_{t-1} \tag{3.2.6}$$

where  $\alpha_0 = 1 - \alpha - \beta$ ,  $\alpha > 0$ ,  $0 < \beta < 1$ , and  $0 < \alpha + \beta < 1$

**Unit-variance GJR-GARCH(1,1):**

$$g_t = \alpha_0 + \alpha \frac{(r_{t-1} - \mu_{t-1})^2}{\tau_{t-1}} + \gamma \frac{(r_{t-1} - \mu_{t-1})^2}{\tau_{t-1}} 1_{(r_{t-1} - \mu_{t-1} < 0)} + \beta g_{t-1} \tag{3.2.7}$$

where  $\alpha_0 = 1 - \alpha - \beta - \frac{\gamma}{2}$ ,  $\alpha > 0$ ,  $0 < \beta < 1$ ,  $\gamma > 0$ , and  $0 < \alpha + \beta + \frac{\gamma}{2} < 1$ .

**Scaled EGARCH(1,1):**

$$\log(g_t) = c_0 + \alpha \left( \frac{|r_{t-1} - \mu_{t-1}|}{g_{t-1} \tau_{t-1}} - \sqrt{\frac{2}{\pi}} \right) + \gamma \left( \frac{r_{t-1} - \mu_{t-1}}{\sqrt{g_{t-1} \tau_{t-1}}} \right) + \beta \log(g_{t-1}) \tag{3.2.8}$$

where  $0 < \beta < 1$ , and  $c_0$  is chosen as a function of the parameters of EGARCH(1,1), so that  $E(g_t) = 1$  for identifiability purpose. In Bayesian estimation, we use the scaling technique proposed in chapter 2 i.e.  $c_0 = \alpha \sqrt{\frac{\pi}{2}}$ .

The general model (3.2.1-3.2.5) nests GARCH-MIDAS, GJR-GARCH-MIDAS and EGARCH-MIDAS models by fixing  $b_t = 0$ , and  $\lambda_1 = \lambda_2 = 0$ . We estimate the parameters of GARCH-MIDAS jump augmented model using (3.2.3) instead of (3.2.1) to avoid the usage of the following specification of  $g_t$  of EGARCH-MIDAS:

$$\log(g_t) = c_0 + \alpha \left( \frac{|r_{t-1} - \mu_{t-1} - b_{t-1} z_{t-1}|}{g_{t-1} \tau_{t-1}} - \sqrt{\frac{2}{\pi}} \right) + \gamma \left( \frac{r_{t-1} - \mu_{t-1} - b_{t-1} z_{t-1}}{\sqrt{g_{t-1} \tau_{t-1}}} \right) + \beta \log(g_{t-1}) \tag{3.2.9}$$

If we use (3.2.9),  $(b_t, z_t)$  are drawn from their posteriors for each  $t$  which require the necessity

of updating  $\log(g_t)$  from time  $t$  to  $T$  in each MCMC iteration which is time consuming (Nakajima (2012), and Chen and Grant (2016)). This is also the case when the specification of  $g_t$  is GARCH, or GJR-GARCH.

The use of (3.2.4) simplifies the estimation procedure since (3.2.1) can be expressed as

$$r_t = \mu_t + e_t$$

where  $e_t$  follows a mixture of  $N(0, \sigma_t^2)$  and  $N(\mu_z, \sigma_t^2 + \sigma_z^2)$  with mixing parameter  $\kappa$ , whose density is given by<sup>4</sup>

$$f_e(x) = \frac{\kappa}{\sqrt{2\pi(\sigma_t^2 + \sigma_z^2)}} e^{-\frac{(x-\mu_z)^2}{2(\sigma_t^2 + \sigma_z^2)}} + \frac{1-\kappa}{\sqrt{2\pi\sigma_t^2}} e^{-\frac{x^2}{2\sigma_t^2}}$$

This can be derived by noting that (3.2.4) can be written as:

$$\begin{aligned} e_t = b_t z_t + \sqrt{g_t \tau_t} \varepsilon_t &= \begin{cases} \sqrt{g_t \tau_t} \varepsilon_t & \text{if } b_t = 0 \\ z_t + \sqrt{g_t \tau_t} \varepsilon_t & \text{if } b_t = 1 \end{cases} \\ &= \begin{cases} N(0, g_t \tau_t) & \text{with probability } 1 - \kappa \\ N(\mu_z, g_t \tau_t + \sigma_z^2) & \text{with probability } \kappa \end{cases} \end{aligned}$$

where  $z_t \sim N(\mu_z, \sigma_z^2)$ ,  $\varepsilon_t \sim N(0, 1)$ , and assuming the size  $z_t$  of the jump is independent of  $\varepsilon_t$ .

To sum, it is almost impossible to estimate the general GARCH-MIDAS models, (3.2.3-3.2.6) by the QMLE due to the large number of parameters,  $6 + 2(p + 1)$  parameters (more than 7) for GARCH-MIDAS-J, and more importantly the parameters of GARCH(1,1) with mixture normal are estimated using the iterative Expected Maximum (EM) algorithm which is sensitive to the initial values (Lee and Lee (2009)) and time consuming. This led to its estimation using MCMC algorithm (Ausin and Galeano (2007)).

### The Bayesian MCMC Estimation

In Bayesian estimation, the parameter vector  $\Theta \in R^d$  of a given model is considered as a random variable having a density  $\pi(\Theta)$ , called the prior density. This distribution represents our prior belief about the value of  $\Theta$ . Using Bayes theorem, the conditional density  $p(\Theta | \mathbf{r})$  can be expressed as

$$p(\Theta | \mathbf{r}) = \frac{p(\mathbf{r}, \Theta)}{p(\mathbf{r})} = \frac{L(\mathbf{r} | \Theta)\pi(\Theta)}{\int_{\Theta} L(\mathbf{r} | \Theta)\pi(\Theta)d\Theta} \quad (3.2.10)$$

where  $L(\mathbf{r} | \Theta)$  is the likelihood function.  $p(\Theta | \mathbf{r})$  is called the posterior density of  $\Theta$ , repre-

<sup>4</sup>When the innovation of standard GARCH(1,1) model follows the mixture normal distribution, the model is called a mixture GARCH model, see Ausin and Galeano (2007).

senting our knowledge about the parameter  $\Theta$  after having observed  $\mathbf{r}$ . The Bayesian estimate,  $\hat{\Theta}$  is  $E(\Theta | \mathbf{r})$ , which is defined by:

$$\hat{\Theta} = \int_{\Theta} \Theta p(\Theta | \mathbf{r}) d\Theta \tag{3.2.11}$$

If  $d = \dim \Theta$  is large, then  $\hat{\Theta}$  cannot be computed analytically from (3.2.11) because, in general,  $p(\Theta | \mathbf{r})$  cannot be expressed in a close form despite that  $\int_{\Theta} L(\mathbf{r} | \Theta) \pi(\Theta) d\Theta$  is constant with respect to  $\Theta$ , i.e.

$$p(\Theta | \mathbf{r}) \propto L(\mathbf{r} | \Theta) \pi(\Theta) \tag{3.2.12}$$

We can overcome this technical difficulty by estimating  $\hat{\Theta}$  by the sample mean of simulated samples from its posterior density. Thus, Bayesian estimation reduces to an evaluation of the sample mean of draws  $\Theta^{(j)}$  from  $p(\Theta | \mathbf{r})$ , where  $\Theta^{(j)}$  is the simulated value of  $\Theta$  in iteration  $j$ . Note that  $\Theta^{(j)}$ 's can be simulated using the MCMC algorithm, irrespective of the complexity of  $p(\Theta | \mathbf{r})$  as long as the likelihood function  $L(\mathbf{r} | \Theta)$  is well-defined on the parameter space of  $\Theta$ .

The MCMC algorithm updates  $p(\Theta | \mathbf{r})$  iteratively from updated value of  $L(\mathbf{r} | \Theta)$ . More explicitly, it consists of the following iterative steps:

- (i) Choose initial parameter values, denoted  $\Theta^{(0)}$ , and any starting values of the data, for  $t = 0$ , that are necessary to compute  $L(\mathbf{r} | \Theta^{(0)})$ .
- (ii) Draw  $\Theta^{(j)}$  from  $p(\Theta | \mathbf{r}) \propto L(\mathbf{r} | \Theta^{(j-1)}) \pi(\Theta)$

We repeat step (ii) a large number of times  $N$ .

When  $\Theta$  is a high-dimensional parameter vector, it is useful to group the  $d$  parameters of the model in  $m$  subgroups, i.e.  $\Theta = (\Theta_1, \Theta_2, \dots, \Theta_m)$  where  $d = \sum_{i=1}^m d_i$ ,  $d_i = \dim \Theta_i$ , and step ii) will be expanded into  $m$  steps: Each  $\Theta_i^{(j)}$  is simulated separately from its low-dimensional posterior density,  $p(\Theta_i | \Theta_{-i}^{(j-1)}, \mathbf{r})$ . In other words, step (ii) of the MCMC algorithm is expanded into  $m$  steps where the  $i$ th step consists of simulating  $\Theta_i$  from  $p(\Theta_i | \Theta_{-i}, \mathbf{r})$  and each  $\hat{\Theta}_i$  is computed using:

$$\hat{\Theta}_i = \frac{\sum_{j=n_b+1}^N \Theta_i^{(j)}}{N - n_b} \tag{3.2.13}$$

where  $N$  is the number of iterations and we usually set  $n_b = \frac{N}{2}$  to eliminate the impact of the initial value of  $\hat{\Theta}_i^{(0)}$ . Tierney (1994) showed that  $(\hat{\Theta}_1, \hat{\Theta}_2, \dots, \hat{\Theta}_m)$  is a Markov chain and consistently estimates the  $d$ -dimensional  $\Theta$ . Notice that when some individual elements of  $\Theta$  are estimated as a subgroup, it improves the speed of the MCMC algorithm.

In sum, the Bayesian MCMC methodology reduces mainly to simulating  $\Theta_i$ 's from their posterior densities assuming that the other parameters  $\Theta_{-i}$ 's are equal to their draws in the previous iteration. This approach is popular for estimating complex models even if the posterior densities  $p(\Theta_i | \Theta_{-i}, \mathbf{r})$  do not belong to a known family of densities, We next provide the detailed



MCMC algorithms for GJR-GARCH-MIDAS, and EGARCH-MIDAS models with and without jump component.

### 3.2.1 MCMC algorithm for GJR-GARCH-MIDAS

Consider the GJR-GARCH-MIDAS model given by

$$r_t = \mu + \sqrt{g_t \tau_t} \varepsilon_t \quad (3.2.14)$$

$$\log(\tau_t) = m + \theta \sum_{k=1}^K w_k X_{t-k} \quad (3.2.15)$$

$$g_t = \alpha_0 + \alpha \frac{(r_{t-1} - \mu)^2}{\tau_{t-1}} + \gamma \frac{(r_{t-1} - \mu)^2}{\tau_{t-1}} 1_{(r_{t-1} - \mu < 0)} + \beta g_{t-1} \quad (3.2.16)$$

where  $\alpha > 0$ ,  $0 < \beta < 1$ ,  $0 < \alpha + \beta + \frac{\gamma}{2} < 1$ ,  $\alpha_0 = 1 - \alpha - \beta - \frac{\gamma}{2}$ ,  $w_k = \frac{(1 - \frac{k}{K})^\omega}{\sum_{k=1}^K (1 - \frac{k}{K})^\omega}$  for  $k = 1, \dots, K$ ,  $\sum_{k=1}^K w_k = 1$ , and we assume  $\varepsilon_t \sim N(0, 1)$ . It nests GARCH-MIDAS model by imposing  $\gamma = 0$ .

Let  $\Theta = \{\mu, \boldsymbol{\theta}_s, \boldsymbol{\theta}_L, \omega\}$  where  $\boldsymbol{\theta}_s = \{\alpha, \beta, \gamma\}$  are the parameters of the short-term component,  $g_t$ ,  $\boldsymbol{\theta}_L = \{m, \theta\}$  are the parameters of the long-term component,  $\tau_t$ , and  $\omega$  is the parameter of the weighting function  $w_k$ . Assuming  $\varepsilon_t \sim N(0, 1)$ , the likelihood function,  $L(\mathbf{r} | \Theta)$ , and the posterior density,  $p(\Theta | \mathbf{r})$ , can be expressed as

$$L(\mathbf{r} | \Theta) = \left(\frac{1}{\sqrt{2\pi}}\right)^T \prod_{t=1}^T \frac{1}{\sqrt{g_t \tau_t}} e^{-\frac{(r_t - \mu)^2}{2g_t \tau_t}} \quad (3.2.17)$$

$$p(\Theta | \mathbf{r}) \propto L(\mathbf{r} | \Theta) \pi(\Theta) \quad (3.2.18)$$

To implement the MCMC algorithm for estimating  $\Theta$  from the returns data  $\mathbf{r} = \{r_0, r_1, \dots, r_T\}$  and initial parameter estimates,  $\Theta^{(0)}$ , we consider the following prior distributions,  $\pi(\cdot)$ 's for the individual elements in  $\Theta$ :

$$\mu \sim N(0, 1)$$

$$(\alpha, \beta) \sim LN_2(0, I_2) \mathbf{1}_{(0 < \alpha + \beta + \gamma/2 < 1)}$$

$$\gamma | (\alpha, \beta) \sim N(0, 1) \mathbf{1}_{(0 < \alpha + \beta + \gamma/2 < 1)}$$

$$\boldsymbol{\theta}_L = (m, \theta) \sim N_2(0, \Sigma_{\tau 1}); \quad \omega \sim N(10, 20^2) \mathbf{1}_{(1 < \omega < 50)}$$

where  $I_2$  is an identity matrix,  $\mathbf{1}_{(\cdot)}$  is an indicator function,  $LN_2$  denotes a bivariate log-normal distribution, i.e.  $(\log \alpha, \log \beta) \sim N_2(0, I_2) \mathbf{1}_{(\alpha + \beta + \gamma/2 < 1)}$ , and  $N_p(d, \Sigma)$  represents a  $p$ -dimensional multivariate normal distribution with mean  $d$  and variance  $\Sigma$ . Chen and Grant (2016) employed the above prior distributions of  $\mu$ ,  $(\alpha, \beta)$  and  $\gamma$  for GARCH(1,1) and GJR-GARCH(1,1) whereas Ardia (2008) and Nakatsuma (2000) used common uniform and normal prior distributions for  $(\alpha, \beta)$ . We prefer to use the log-normal prior to deal with non-negativity of  $(\alpha, \beta)$  respectively.

We summarise the MCMC algorithms for estimating GJR-GARCH-MIDAS as follows:

1. Choose initial estimates of parameter, denoted  $\Theta^{(0)} = (\mu^{(0)}, \theta_s^{(0)}, \theta_L^{(0)}, \omega^{(0)})$ ;
2. Draw  $\mu^{(1)}$  from  $p(\mu | \Theta_{-\mu}, \mathbf{r})$  where  $\Theta_{-\mu} = (\omega^{(0)}, \theta_s^{(0)}, \theta_L^{(0)})$ ;
3. Draw  $\omega^{(1)}$  from  $p(\omega | \Theta_{-\omega}, \mathbf{r})$  where  $\Theta_{-\omega} = (\mu^{(1)}, \theta_s^{(0)}, \theta_L^{(0)})$ ;
4. Draw  $\theta_L^{(1)}$  from  $p(\theta_L | \Theta_{-\theta_L}, \mathbf{r})$  where  $\Theta_{-\theta_L} = (\mu^{(1)}, \omega^{(1)}, \theta_s^{(0)})$ ;
5. Draw  $\theta_s^{(1)}$  from  $p(\theta_s | \Theta_{-\theta_s}, \mathbf{r})$  where  $\Theta_{-\theta_s} = (\mu^{(1)}, \omega^{(1)}, \theta_L^{(1)})$ .

Repeat steps 2 to 5 a large number of times,  $N$ , by resetting initial estimates,  $\Theta_i^{(0)}$ , by  $\Theta^{(j-1)}$ .  $\Theta_{-i}$  denotes the updated values of all the elements of  $\Theta$  excluding  $\Theta_i$ , and each posterior distribution  $p(\Theta_i | \Theta_{-i}, \mathbf{r})$  is computed using (3.2.12). However,  $p(\Theta_i | \Theta_{-i}, \mathbf{r})$  does not belong to a known family, for any choice of the prior distribution  $\pi(\Theta_i)$ , which led us to use Metropolis-Hasting method for drawing  $\mu, \theta_s, \theta_L$ , and  $\omega$ . Then, we obtain the MCMC estimate,  $\hat{\Theta}_i$  as the sample mean of the truncated simulated draws,  $\{\Theta_i^{(n_b+1)}, \dots, \Theta_i^{(N)}\}$  by (3.2.13).

Using (3.2.17-3.2.18) and the above prior densities, we derive in Appendix 2, the posterior densities of the individual elements of  $\Theta_i$ :

$$p(\mu | \Theta_{-\mu}, \mathbf{r}) \propto \left( \prod_{t=1}^T \frac{1}{\sqrt{g_t \tau_t}} \right) e^{-\frac{1}{2} \{ \mu^2 (1 + \sum_{t=1}^T \frac{1}{g_t \tau_t}) - 2\mu \sum_{t=1}^T \frac{r_t}{g_t \tau_t} + \sum_{t=1}^T (\frac{r_t}{g_t \tau_t})^2 \}} \quad (3.2.19)$$

For convenience, draws of  $\theta_s = (\alpha, \beta, \gamma)$  are obtained from draws of  $\theta_s^* = (\gamma_1, \gamma_2, \gamma)$  where  $\gamma_1 = \log(\alpha)$ , and  $\gamma_2 = \log(\beta)$ , by expressing the short-term component in (3.2.16) as:

$$g_t = 1 - e^{\gamma_1} - e^{\gamma_2} - \frac{\gamma}{2} + e^{\gamma_1} \frac{(r_{t-1} - \mu)^2}{\tau_{t-1}} + \gamma \frac{(r_{t-1} - \mu)^2}{\tau_{t-1}} 1_{(r_{t-1} - \mu < 0)} + e^{\gamma_2} g_{t-1}$$

Then,

$$p(\theta_s^* | \Theta_{-\theta_s^*}, \mathbf{r}) \propto \left( \prod_{t=1}^T \frac{1}{\sqrt{g_t \tau_t}} \right) e^{-\frac{1}{2} \{ \sum_{t=1}^T \frac{(r_t - \mu)^2}{g_t \tau_t} + \theta_s^{*'} \theta_s^* \}} \quad (3.2.20)$$

$$p(\gamma | \Theta_{-\gamma}, \mathbf{r}) \propto \left( \prod_{t=1}^T \frac{1}{\sqrt{g_t \tau_t}} \right) e^{-\frac{1}{2} \{ \sum_{t=1}^T \frac{(r_t - \mu)^2}{g_t \tau_t} + \gamma^2 \}} \quad (3.2.21)$$

Similarly, the posterior densities of the parameters of the long term component  $(\theta_L, \omega)$  are:

$$p(\theta_L | \Theta_{-\theta_L}, \mathbf{r}) \propto \left( \prod_{t=1}^T \frac{1}{\sqrt{g_t \tau_t}} \right) e^{-\frac{1}{2} \{ \sum_{t=1}^T \frac{(r_t - \mu)^2}{g_t \tau_t} + \theta_L' \theta_L \}} \quad (3.2.22)$$

$$p(\omega | \Theta_{-\omega}, \mathbf{r}) \propto \left( \prod_{t=1}^T \frac{1}{\sqrt{g_t \tau_t}} \right) e^{-\frac{1}{2} \left\{ \sum_{t=1}^T \frac{(r_t - \mu)^2}{g_t \tau_t} + \frac{(\omega - 10)^2}{20^2} \right\}} \quad (3.2.23)$$

Notice however that the posterior density,  $p(\mu | \Theta_{-\mu}, \mathbf{r})$  in (3.2.19), cannot be expressed as a normal density because  $g_t$  is a function of  $\mu$ , and  $(\prod_{t=1}^T \frac{1}{\sqrt{g_t \tau_t}})$  or  $(1 + \sum_{t=1}^T \frac{1}{g_t \tau_t})$  is not a constant. Indeed, this issue also applies to all other parameters. Simulations from the posterior densities (3.2.19-3.2.23) can be conducted using Random walk, Metropolis Hastings method (Chib and Greenberg (1995)) or the Adaptive MCMC approach, which approximate the posterior densities by known densities such as Normal densities so that we can easily update posterior distributions in each iteration. In this regard, we propose approximating the posteriors density by normal density, denoted  $q(\Theta_i)$  with mean  $\mu_{\Theta_i}^*$  and variance  $\Sigma_{\Theta_i}^*$ . Hence, we expect that the parameters  $\mu_{\Theta_i}^*$  and  $\Sigma_{\Theta_i}^*$  of the proposal density  $q(\Theta_i)$  are equal to the mean and variance of the posterior density  $p(\Theta_i | \Theta_{-i}, \mathbf{r})$ . Using the 2nd order Taylor expansion of  $p(\Theta_i | \Theta_{-i}^{(j-1)}, \mathbf{r})$ , we have:

$$\mu_{\Theta_i}^* = \tilde{\Theta}_i + \Sigma_{\Theta_i}^* \frac{\partial \log(p(\Theta_i | \Theta_{-i}^{(j-1)}, \mathbf{r}))}{\partial \Theta_i} \Big|_{\Theta_i = \tilde{\Theta}_i} \quad (3.2.24)$$

$$\Sigma_{\Theta_i}^* = - \frac{\partial \log(p(\Theta_i | \Theta_{-i}^{(j-1)}, \mathbf{r}))}{\partial \Theta_i \partial \Theta_j'} \Big|_{\Theta_i = \tilde{\Theta}_i} \quad (3.2.25)$$

where  $\tilde{\Theta}_i$  is the mode of  $p(\Theta_i | \Theta_{-i}^{(j-1)}, \mathbf{r})$ . If  $\Theta_i$  is uni-variate,  $\mu_{\Theta_i}^*$ , and  $\Sigma_{\Theta_i}^*$  are the mean and the variance of the proposal uni-variate normal density. See Appendix 2 for analytic details.

In the  $j$ th iteration of the MCMC algorithm, a simulated value  $\Theta_i^*$  from  $q(\Theta_i)$  is regarded as a draw  $\Theta_i^{(j)}$  from  $p(\Theta_i | \Theta_{-i}^{(j-1)}, \mathbf{r})$  if it passes the following Acceptance rejection test:

1. Accept  $\Theta_i^*$  as a draw from  $p(\Theta_i | \Theta_{-i}^{(j-1)}, \mathbf{r})$ , i.e.  $\Theta_i^{(j)} = \Theta_i^*$ , with probability  $\kappa$  where

$$\kappa = \min \left\{ \frac{p(\Theta_i^* | \Theta_{-i}^{(j-1)}, \mathbf{r}) q(\Theta_i^{(j-1)})}{p(\Theta_i^{(j-1)} | \Theta_{-i}^{(j-1)}, \mathbf{r}) q(\Theta_i^*)}, 1 \right\}$$

2. If  $\Theta_i^*$  is rejected, then we set:  $\Theta_i^{(j)} = \Theta_i^{(j-1)}$ .

Smith and Roberts (1993) discusses the asymptotic properties of the final simulated sample,  $\{\Theta_i^{(n_b)}, \dots, \Theta_i^{(N)}\}$ , as a representative sample from  $p(\Theta_i | \Theta_{-i}, \mathbf{r})$ , under mild regularity conditions, and therefore  $\hat{\Theta}$  is a consistent estimator of  $\Theta$ . They also considered MCMC algorithm as the stochastic analogue of the EM algorithm where expectations and maxima are replaced random draws.

If the computation of  $\mu_{\Theta_i}^*$  and  $\Sigma_{\Theta_i}^*$  using (3.2.24-3.2.25), is rather tedious, then draws from the posterior density  $p(\Theta_i | \Theta_{-i}, \mathbf{r})$  can be simulated using the Random Walk (RW) or Adaptive Random Walk (ARW) approach. RW simulates the new candidate  $\Theta_i^*$  by perturbing the current

value,  $\Theta_i^{(j-1)}$  using the following bootstrap technique:

$$\Theta_i^* = \Theta_i^{(j-1)} + cN_{d_i}(\mathbf{0}, I_{d_i}) \quad (3.2.26)$$

where  $d_i$  is the dimension of  $\Theta_i$  and  $c$  is a tuning parameter selected by the user to ensure that the rate of acceptance of  $\Theta_i^*$ 's is more than 40%. ARW is similar to RW except that the tuning parameter  $c$  is updated such that the variance,  $cI_{d_i}$  is equal to the sample variance of the previous draws  $\{\Theta_i^{(nb)}, \dots, \Theta_i^{(j-1)}\}$ , where the update is done, for example, every 100 or 200 iterations.

Roberts and Rosenthal (2009) advanced the following adaptive proposal,  $q(\Theta_i)$ :

$$q(\Theta_i | \Theta_i^{(0)}, \Theta_i^{(1)}, \dots, \Theta_i^{(j-1)}) = \begin{cases} N_{d_i}(\Theta^{(j-1)}, 0.1^2 I_{d_i}/d_i) & \text{if } j \leq 2d_i \\ (1 - \delta)N_{d_i}(\Theta^{(j-1)}, cov(\Theta^{(0)}, \Theta^{(1)}, \dots, \Theta^{(j-1)})2.38^2/d_i) \\ + \delta N_{d_i}(\Theta^{(j-1)}, 0.1^2 I_{d_i}/d_i) & \text{if } j > 2d_i \end{cases}$$

where the scaling factor,  $2.38^2$  is applied to optimise the mixing properties of the Metropolis search for the Gaussian proposals (Gelman, Roberts, and Gilks 1996).  $q(\Theta_i)$  is a mixture of two normal distributions with a mixing parameter  $\delta$  when the number of iterations exceed  $2d$ . Following Roberts and Rosenthal (2009) we set  $\delta = 0.05$ . The second component,  $N_{d_i}(\Theta^{(j-1)}, 0.1^2 I_{d_i}/d_i)$  would prevent us from generating singular covariance matrix due to some problematic values of  $Cov(\Theta^{(0)}, \Theta^{(1)}, \dots, \Theta^{(j-1)})$ . Notice that the Adaptive step is applied only to the burn-in draws. After burn-in, we then fix the value of the covariance matrix and use a normal proposal to continue the Metropolis Hastings step for  $\Theta$ .

For jump augmented models illustrated in (3.2.1) or (3.2.4), we add two more steps to the MCMC algorithm; namely, simulating from the posterior density of the mixing parameter  $\kappa$  using uniform prior  $[0, 0.15]$  for  $\kappa$ , and from the posterior density of the parameter vector  $(\mu_z, \sigma_z^2)$  of the jump size using normal prior  $N_2(0, 100)$  for  $(\mu_z, \log(\sigma_z^2))$ . Hence, the MCMC algorithm for GJR-GARCH-MIDAS with jump combines steps 1 to 5 with the following two additional steps:

6. Draw  $\kappa^{(1)}$  from  $p(\kappa | \Theta_{-\kappa}, \mathbf{r})$  where  $\Theta_{-\kappa} = (\mu^{(1)}, \theta_s^{(1)}, \theta_L^{(1)}, \omega^{(1)}, \mu^{(0)}, \sigma_z^{2(0)})$
7. Draw  $(\mu_z^{(1)}, \sigma_z^{2(1)})$  from  $p(\mu_z, \sigma_z^2 | \Theta_{-\mu_z, \sigma_z^2}, \mathbf{r})$  where  $\Theta_{-\mu_z, \sigma_z^2} = (\mu^{(1)}, \theta_s^{(1)}, \theta_L^{(1)}, \omega^{(1)}, \kappa^{(1)})$

Then, we repeat steps 1 to 7 a large number of times, and obtain the MCMC estimate,  $\hat{\Theta}_i$ , by (3.2.13).

The posterior distributions of all parameters can be derived using (3.2.18). Since the conditional density of the  $r_t$  is a mixture of two normal densities, we replace the likelihood function in (3.2.17) by

$$L(\mathbf{r} | \Theta) \propto \prod_{t=1}^T \left\{ \frac{(1 - \kappa)}{\sqrt{g_t \tau_t}} e^{-\frac{(r_t - \mu)^2}{2g_t \tau_t}} + \frac{\kappa}{\sqrt{\sigma_z^2 + g_t \tau_t}} e^{-\frac{(r_t - \mu - \mu_z)^2}{2(\sigma_z^2 + g_t \tau_t)}} \right\} \quad (3.2.27)$$

### 3.2.2 MCMC algorithm for EGARCH-MIDAS models

Consider the jump-augmented EGARCH-MIDAS model given by

$$r_t = \mu + e_t \quad (3.2.28)$$

$$\log(\tau_t) = m + \theta \sum_{k=1}^K w_k X_{t-k} \quad (3.2.29)$$

$$\log(g_t) = c_0 + \alpha \left( \frac{|r_{t-1} - \mu_{t-1}|}{g_{t-1} \tau_{t-1}} - \sqrt{\frac{2}{\pi}} \right) + \gamma \left( \frac{r_{t-1} - \mu_{t-1}}{\sqrt{g_{t-1} \tau_{t-1}}} \right) + \beta \log(g_{t-1}) \quad (3.2.30)$$

where  $0 < \beta < 1$ ,  $c_0$ ,  $\alpha$ ,  $\gamma$ ,  $\mu$ ,  $m$ , and  $\theta$ 's are real. We assume  $e_t$  is the mixture of  $N(0, \tau_t g_t)$  and  $N(\mu_z, \tau_t g_t + \sigma_z^2)$  with mixing parameter  $\kappa$ , and  $c_0 = \alpha \sqrt{\frac{2}{\pi}}$  to ensure that  $g_t$  is scaled EGARCH(1,1). EGARCH-MIDAS-J nests EGARCH-MIDAS model by imposing  $b_t = 0$  for all  $t$  or  $\kappa = 0$ .

Define  $\Theta = (\mu, \boldsymbol{\theta}_s, \boldsymbol{\theta}_L, \boldsymbol{\omega})$  where  $\boldsymbol{\theta}_s = (\alpha, \log(\beta), \gamma)$  are the parameters of the short-term component  $g_t$ ,  $\boldsymbol{\theta}_L = (m, \theta)$  are the parameters of the long-term component,  $\tau_t$ , and  $\boldsymbol{\omega}$  is the parameter of the weighting function  $w_k$ .<sup>5</sup>

The MCMC algorithms for EGARCH-MIDAS and EGARCH-MIDAS-J models are the same as those of GJR-GARCH-MIDAS and GJR-GARCH-MIDAS-J models, except that we need to use the following prior density of  $\boldsymbol{\theta}_s$ :

$$\boldsymbol{\theta}_s = (\alpha, \log(\beta), \gamma) \sim N_3(\mathbf{0}, I_3) 1_{(0 < \beta < 1)}$$

We summarise the MCMC algorithms for estimating EGARCH-MIDAS as follows:

1. Choose initial estimates of the parameters  $\Theta_{EGM}^{(0)} = (\mu^{(0)}, \boldsymbol{\theta}_s^{(0)}, \boldsymbol{\theta}_L^{(0)}, \boldsymbol{\omega}^{(0)})$ ;
2. Draw  $\mu^{(1)}$  from  $p(\mu | \Theta_{-\mu}, \mathbf{r})$  where  $\Theta_{-\mu} = (\boldsymbol{\omega}^{(0)}, \boldsymbol{\theta}_s^{(0)}, \boldsymbol{\theta}_L^{(0)})$ ;
3. Draw  $\boldsymbol{\omega}^{(1)}$  from  $p(\boldsymbol{\omega} | \Theta_{-\boldsymbol{\omega}}, \mathbf{r})$  where  $\Theta_{-\boldsymbol{\omega}} = (\mu^{(1)}, \boldsymbol{\theta}_s^{(0)}, \boldsymbol{\theta}_L^{(0)})$ ;
4. Draw  $\boldsymbol{\theta}_L^{(1)}$  from  $p(\boldsymbol{\theta}_L | \Theta_{-\boldsymbol{\theta}_L}, \mathbf{r})$  where  $\Theta_{-\boldsymbol{\theta}_L} = (\mu^{(1)}, \boldsymbol{\omega}^{(1)}, \boldsymbol{\theta}_s^{(0)})$ ;
5. Draw  $\boldsymbol{\theta}_s^{(1)}$  from  $p(\boldsymbol{\theta}_s | \Theta_{-\boldsymbol{\theta}_s}, \mathbf{r})$  where  $\Theta_{-\boldsymbol{\theta}_s} = (\mu^{(1)}, \boldsymbol{\omega}^{(1)}, \boldsymbol{\theta}_L^{(1)})$ .

For EGARCH-MIDAS-J model, we add two more steps:

6. Draw  $\kappa^{(1)}$  from  $p(\kappa | \Theta_{-\kappa}, \mathbf{r})$  where  $\Theta_{-\kappa} = (\mu^{(1)}, \boldsymbol{\theta}_s^{(1)}, \boldsymbol{\theta}_L^{(1)}, \boldsymbol{\omega}^{(1)}, \mu^{(0)}, \sigma_z^{2(0)})$
7. Draw  $(\mu_z^{(1)}, \sigma_z^{2(1)})$  from  $p(\mu_z, \sigma_z^2 | \Theta_{-\mu_z, \sigma_z^2}, \mathbf{r})$  where  $\Theta_{-\mu_z, \sigma_z^2} = (\mu^{(1)}, \boldsymbol{\theta}_s^{(1)}, \boldsymbol{\theta}_L^{(1)}, \boldsymbol{\omega}^{(1)}, \kappa^{(1)})$

Then, we repeat steps 1 to 5 or 1 to 7 a large number of times, and obtain the corresponding

<sup>5</sup>We can derive the log-likelihood functions for EGARCH-MIDAS and EGARCH-MIDAS with jump similarly to (3.2.17) and (3.2.27), respectively.

MCMC estimate,  $\hat{\Theta}_i$  by (3.2.13).

Similarly, to GARCH-MIDAS and GJR-GARCH-MIDAS, the posterior densities of the parameters of EGARCH-MIDAS cannot be expressed using known families of densities. In Appendix 2, we derive:

$$\begin{aligned}
 p(\mu \mid \Theta_{-\mu}, r) &\propto \left( \prod_{t=1}^T \frac{1}{\sqrt{g_t}} \right) e^{-\frac{1}{2} \left\{ \mu^2 \left( \sum_{t=1}^T \frac{1}{g_{t-1}} + \frac{1}{\sigma_0^2} \right) - 2\mu \left( \sum_{t=1}^T \frac{r_{t-1}}{g_{t-1}} - \mu_0 \right) \right\}} \\
 p(\boldsymbol{\theta}_s \mid \mu, \boldsymbol{\theta}_L, \boldsymbol{\omega}) &\propto \left( \prod_{t=1}^T \frac{1}{\sqrt{g_t \tau_t}} \right) e^{-\frac{1}{2} \sum_{t=1}^T \frac{(r_{t-1} - \mu)^2}{g_{t-1} \tau_{t-1}}} \pi(\boldsymbol{\theta}_s) \\
 p(\boldsymbol{\theta}_L \mid \mu, \boldsymbol{\theta}_s, \boldsymbol{\omega}) &\propto \left( \prod_{t=1}^T \frac{1}{\sqrt{g_t \tau_t}} \right) e^{-\frac{1}{2} \sum_{t=1}^T \frac{(r_{t-1} - \mu)^2}{g_{t-1} \tau_{t-1}}} \pi(\boldsymbol{\theta}_L) \\
 p(\boldsymbol{\omega} \mid \mu, \boldsymbol{\theta}_s, \boldsymbol{\theta}_L) &\propto \left( \prod_{t=1}^T \frac{1}{\sqrt{g_t \tau_t}} \right) e^{-\frac{1}{2} \sum_{t=1}^T \frac{(r_{t-1} - \mu)^2}{g_{t-1} \tau_{t-1}}} 1[0.50]p
 \end{aligned}$$

Since the term  $\prod_{t=1}^T \frac{1}{\sqrt{g_t \tau_t}}$  is a function of  $\boldsymbol{\theta}_s$ ,  $\boldsymbol{\theta}_L$ , and  $\boldsymbol{\omega}$ , the posteriors cannot be expressed as a multivariate normal density. Similarly the posterior of  $\mu$  cannot be expressed as a normal density because  $\prod_{t=1}^T \frac{1}{\sqrt{g_t}}$  is a function of  $\mu$ .

The posteriors of the parameters of the jump size  $z_t$ , and the mixture parameter  $\kappa$  are discussed in Appendix 2.

### 3.3 Monte Carlo Simulation

We conduct two experiments to investigate the finite sample performance of the Bayesian MCMC and QML estimators. To make the simulation design realistic, we construct the two data generating processes (DGP) with and without jump components in a data-oriented manner where  $r_t$  represents the value of the return on  $t^{th}$  day, for  $t = 1, \dots, T$ , of the simulated return data. For each  $t$ , we denote by  $n$ , for  $n = 1, \dots, N$ , the month to which day  $t$  belongs to, and we denote by  $i$ , for  $i = 1, \dots, 22$  working days, its index in the month. In other words, the day  $t$  is described by  $(i, n)$  i.e.  $t = 22(n - 1) + i$ .

#### 3.3.1 Experiment 1: the DGP with no jump components

First, we generate a sample of  $(180 + K)$  monthly observations with  $K = 24$  for an artificial macroeconomic variable,<sup>6</sup> which follows an AR(1) process (e.g. Conrad and Kleen (2021)):

$$x_n = \phi x_{n-1} + \varepsilon_n, \quad \varepsilon_n \sim N(0, 1), \quad n = 1, \dots, 180 + K$$

<sup>6</sup>we generate  $(180 + K)$  samples for  $x_n$  due to the  $K$  lagged values of  $x_n$  used in modelling  $\log \tau_n$ .

where we set  $\varphi = 0.95$  and  $x_0 = 0$ . Second, we generate the 180 monthly observations of the long term volatility,  $\tau_n$  by

$$\log(\tau_n) = m + \theta \sum_{k=1}^K w(k, \omega) x_{K+n-k} \quad n = 1, \dots, 180$$

where  $w(k, \omega)$  is the Beta weighting function. We set  $m = (-0.1, 0.1)$  and consider several values of  $\theta = (0.3, -0.45, 0.45, 0.6)$  and  $\omega = 10$ . Third, we generate the  $22 \times 180$  daily observations of the unit-variance short-term volatility,  $g_t = g_{i,n}$  by

$$\text{GARCH-MIDAS: } g_{i,n} = (1 - \alpha - \beta) + \alpha \frac{(r_{i-1,n} - \mu)^2}{\tau_n} + \beta g_{i-1,n};$$

$$\text{GJR-GARCH-MIDAS: } g_{i,n} = (1 - \alpha - \beta - \frac{\gamma}{2}) + \alpha \frac{(r_{i-1,n} - \mu)^2}{\tau_n} + \gamma \frac{(r_{i-1,n} - \mu)^2}{\tau_n} 1_{[r_{i-1,n} - \mu < 0]} + \beta g_{i-1,n};$$

$$\text{EGARCH-MIDAS: } \log(g_{i,n}) = \alpha \sqrt{\frac{2}{\pi}} + \alpha \left\{ \frac{|r_{i-1,n} - \mu|}{\sqrt{\tau_n g_{i-1,n}}} - \sqrt{\frac{2}{\pi}} \right\} + \gamma \frac{r_{i-1,n} - \mu}{\sqrt{\tau_n g_{i-1,n}}} + \beta g_{i-1,n}$$

We set the true values of the parameters as follow:  $(\alpha, \beta) = [(0.05, 0.92), (0.08, 0.9)]$  for GARCH-MIDAS,  $(\alpha, \beta, \gamma) = [(0.05, 0.85, 0.1), (0.08, 0.82, 0.1)]$  for GJR-GARCH-MIDAS, and  $(\alpha, \beta, \gamma) = [(0.03, 0.85, -0.1), (0.05, 0.9, -0.07), (0.05, 0.92, -0.04)]$  for EGARCH-MIDAS. Finally, we generate daily returns by  $r_{i,n} = \mu + \sqrt{\tau_n g_{i,n}} \varepsilon_t$ , where we set  $\mu = 0$  and draw  $\varepsilon_t$  randomly from  $N(0, 1)$ . To simulate  $r_{i,n}$  and  $g_{i,n}$  recursively, we set initial values,  $r_{0,1} = 0$  and  $g_{0,1} = 1$ .

Table 3.3.1 reports the simulation results when the DGP is generated by GARCH-MIDAS processes. We find that both MCMC and QML estimates are satisfactory and close to true parameter values, even though QML produces a biased estimate of  $\omega$  with a large standard error. Further, MCMC produces the smaller standard errors of the long term estimates ( $m$  and  $\theta$ ) than QML.

Table 3.3.2 presents the QML and Bayesian MCMC estimates when the DGP is GJR-GARCH-MIDAS. We obtain qualitatively similar results to those of Table 3.3.1. Further, MCMC produces more precise leverage coefficient,  $\gamma$  with the smaller standard error than QML.

Table 3.3.3 presents the QML and Bayesian estimates when the DGP is EGARCH-MIDAS. We also obtain qualitatively similar results to those of Tables 3.3.1 and 3.3.2. MCMC also produces more precise leverage coefficient,  $\gamma$  with the smaller standard error than QML. Further, the bias of QML estimate of the long term intercept,  $m$  becomes large with substantially large standard errors.

In sum, we establish that Bayesian MCMC can produce the relatively precise estimates for GARCH-MIDAS, GJR-GARCH-MIDAS and EGARCH-MIDAS models. In the current case where the persistence ( $\alpha + \beta$ ) is less than 0.98, we find that QML estimates are also satisfactory.

Table 3.3.1: MCMC and QML estimates for GARCH-MIDAS

	$\mu$	$\alpha$	$\beta$	m	$\theta$	$\omega$
TRUE	0	0.05	0.92	-0.1	0.3	10
QMLE	-0.001 (0.015)	0.049 (0.011)	0.911 (0.020)	-0.137 (0.079)	0.336 (0.081)	15.058 (19.105)
MCMC	-0.001 (0.028)	0.052 (0.009)	0.905 (0.020)	-0.128 (0.064)	0.331 (0.072)	10.329 (3.582)
TRUE	0	0.08	0.9	0.1	0.6	10
QMLE	0.003 (0.014)	0.079 (0.010)	0.898 (0.013)	0.116 (0.150)	0.595 (0.118)	13.631 (10.859)
MCMC	-0.001 (0.025)	0.080 (0.009)	0.899 (0.012)	0.104 (0.115)	0.606 (0.108)	10.417 (3.380)

Notes: This table reports the estimation results of GARCH-MIDAS (3.2.3-3.2.6) using Bayesian MCMC approach and QMLE approach when DGP is GARCH-MIDAS model with 250 replications. MCMC estimates are evaluated using 30,000 iterations with 10,000 burn-ins. Standard deviations are given in brackets.

Table 3.3.2: MCMC and QML estimates for GJR-GARCH-MIDAS

Parameter	$\mu$	$\alpha$	$\beta$	$\gamma$	m	$\theta$	$\omega$
True	0	0.05	0.85	0.1	-0.1	0.3	10
QMLE	0.001 (0.014)	0.045 (0.013)	0.845 (0.019)	0.124 (0.021)	-0.119 (0.089)	0.309 (0.081)	15.143 (22.649)
MCMC	0.003 (0.023)	0.054 (0.012)	0.855 (0.019)	0.097 (0.018)	-0.122 (0.063)	0.305 (0.072)	10.380 (3.291)
True	0	0.08	0.82	0.1	0.1	0.45	10
QMLE	0.002 (0.014)	0.076 (0.013)	0.814 (0.019)	0.111 (0.020)	0.108 (0.093)	0.452 (0.083)	17.052 (37.215)
MCMC	0.009 (0.023)	0.081 (0.012)	0.843 (0.019)	0.099 (0.018)	0.119 (0.065)	0.441 (0.065)	10.975 (3.351)

Notes: This table reports the estimation results of GJR-GARCH-MIDAS (3.2.14-3.2.16) model using Bayesian MCMC and QMLE approaches when DGP is GJR-GARCH-MIDAS with 250 replications. MCMC estimates are evaluated using 30,000 iterations with 10,000 burn-ins. Standard deviations are given in brackets.

Table 3.3.3: MCMC and QML estimates for EGARCH-MIDAS

	$\mu$	c	$\beta$	$\gamma$	$\alpha$	m	$\theta$	$\omega$
TRUE	0		0.85	-0.1	0.03	-0.1	0.45	10
QMLE	-0.013 (0.016)	0.002 (0.043)	0.863 (0.032)	-0.090 (0.029)	0.025 (0.020)	-0.064 (0.334)	0.466 (0.033)	12.574 (4.025)
MCMC	-0.011 (0.027)	0.013 (0.005)	0.838 (0.040)	-0.096 (0.016)	0.032 (0.023)	-0.093 (0.028)	0.461 (0.034)	9.778 (2.055)
TRUE	0		0.9	-0.07	0.05	-0.1	0.45	10
QMLE	0.015 (0.016)	0.001 (0.029)	0.888 (0.026)	-0.082 (0.023)	0.031 (0.016)	-0.101 (0.263)	0.463 (0.026)	13.102 (3.779)
MCMC	0.016 (0.021)	0.009 (0.003)	0.890 (0.023)	-0.073 (0.011)	0.051 (0.014)	-0.093 (0.060)	0.457 (0.056)	10.744 (2.774)
TRUE	0		0.92	-0.04	0.05	-0.1	0.3	10
QMLE	-0.005 (0.020)	0.001 (0.021)	0.906 (0.036)	-0.042 (0.015)	0.046 (0.018)	-0.073 (0.229)	0.298 (0.039)	13.749 (9.184)
MCMC	0.001 (0.031)	0.005 (0.003)	0.919 (0.041)	-0.041 (0.011)	0.059 (0.017)	-0.081 (0.044)	0.301 (0.044)	10.063 (3.214)

Notes: This table reports the estimation results of EGARCH-MIDAS (3.2.28-3.2.30) model using Bayesian MCMC and QMLE approaches when DGP is EGARCH-MIDAS with 250 replications. MCMC estimates are evaluated using 30,000 iterations with 10,000 burn-ins. Standard deviations are given in brackets.



### 3.3.2 Experiment 2: the DGP with jump components

We now generate daily return data with jump component as follows:

$$r_t = r_{i,n} = \mu + b_t z_t + \sigma_{i,n} \varepsilon_t \quad (3.3.1)$$

where  $b_t$  follows a Bernoulli distribution with rate  $\kappa$ , and  $z_t$  follows  $N(\mu_z, \sigma_z^2)$ . We consider  $\kappa = (3\%, 5\%, 8\%)$  and  $\sigma_z^2 = (9, 25, 36)$  to generate the low, medium, and high jumps.

Table 3.3.4 reports the simulation results when the data is generated from the GARCH-MIDAS-J model. Most of MCMC estimates are relatively close to the true parameter values. By contrast, QML estimates are significantly biased and misleading in almost all cases. It also produced an incorrect sign for the long-run coefficient,  $\theta$ .

Table 3.3.5 reports the simulation results when the data is generated from the GJR-GARCH-MIDAS-J model. MCMC estimates are relatively close to the true parameter values whilst QML estimates are significantly biased and misleading in almost all cases. Finally, Table 3.3.6 presents the simulation results when the data is generated from the EGARCH-MIDAS-J model.

In sum, in the case where GARCH-MIDAS models are subject to the jumps, we don't recommend the use of QML method that produces unreliable estimates or becomes computationally infeasible. On the contrary, the proposed MCMC estimates are relatively satisfactory and can be easily conducted.

Table 3.3.4: MCMC and QML estimates for GARCH-MIDAS-J

	$\mu$	$\alpha$	$\beta$	m	$\theta$	$\omega$	$\mu_z$	$\sigma_z^2$	$\kappa$
TRUE	0	0.08	0.9	0.1	0.6	10	-0.03	9	0.08
MCMC	-0.003 (0.045)	0.080 (0.003)	0.891 (0.004)	0.058 (0.058)	0.509 (0.053)	10.325 (3.841)	0.066 (0.124)	11.097 (1.704)	0.0744 (0.013)
QMLE	-0.009 (0.051)	0.095 (0.005)	0.958 (0.008)	0.044 (0.085)	0.262 (0.321)	20.562 (16.434)	-0.045 (0.047)	18.305 (17.011)	0.048 (0.089)
TRUE	0	0.05	0.92	0.1	0.3	10	-0.03	25	0.05
MCMC	-0.004 (0.042)	0.052 (0.001)	0.911 (0.001)	0.103 (0.001)	0.248 (0.002)	9.491 (3.339)	-0.041 (0.076)	27.376 (4.859)	0.044 (0.005)
QMLE	-0.004 (0.015)	0.120 (0.001)	0.899 (0.009)	0.003 (0.001)	-0.243 (0.006)	24.391 (30.039)	0.021 (0.048)	16.418 (6.958)	0.084 (0.009)
TRUE	0	0.08	0.85	-0.1	-0.45	10	-0.03	36	0.03
MCMC	-0.006 (0.040)	0.086 (0.001)	0.844 (0.001)	-0.130 (0.001)	-0.429 (0.001)	10.274 (3.386)	-0.039 (0.053)	38.658 (4.473)	0.024 (0.004)
QMLE	-0.006 (0.042)	0.094 (0.014)	0.893 (0.069)	0.432 (0.003)	0.323 (0.001)	18.509 (14.811)	-0.121 (0.074)	20.113 (6.745)	0.043 (0.006)

Notes: This table reports the estimation results of GARCH-MIDAS-J given by (3.3.1) and (3.2.5-3.2.6) using Bayesian MCMC approach and QMLE approach when DGP is GARCH-MIDAS-J with 250 replications. MCMC estimates are evaluated using 40,000 iterations with 15,000 burn-ins. Standard deviations are given in brackets.

Table 3.3.5: MCMC and QML estimates for GJR-GARCH-MIDAS-J

Parameter	$\mu$	$\alpha$	$\beta$	$\gamma$	m	$\theta$	$\omega$	$\mu_Z$	$\sigma_Z^2$	$\kappa$
TRUE	0	0.06	0.85	0.1	-0.1	0.3	10	-0.03	9	0.08
MCMC	-0.014 (0.03)	0.068 (0.001)	0.834 (0.003)	0.108 (0.004)	-0.137 (0.010)	0.323 (0.007)	10.043 (2.924)	-0.022 (0.055)	10.174 (2.444)	0.076 (0.013)
QMLE	0.002 (0.033)	0.080 (0.032)	0.903 (0.030)	0.142 (0.039)	-0.039 (0.088)	0.163 (0.051)	16.436 (14.531)	0.028 (0.045)	15.829 (3.242)	0.042 (0.082)
TRUE	0	0.05	0.85	0.1	-0.1	0.3	10	-0.03	25	0.05
MCMC	-0.036 (0.031)	0.033 (0.001)	0.851 (0.001)	0.106 (0.001)	-0.101 (0.001)	0.293 (0.001)	11.031 (3.051)	-0.026 (0.025)	26.562 (2.038)	0.047 (0.002)
QMLE	0.004 (0.044)	0.090 (0.042)	0.899 (0.071)	0.140 (0.093)	-0.034 (0.009)	-0.102 (0.074)	19.512 (20.902)	-0.004 (0.173)	18.190 (6.285)	0.027 (0.044)
TRUE	0	0.06	0.85	0.1	-0.1	-0.45	10	-0.03	36	0.03
MCMC	-0.019 (0.042)	0.032 (0.001)	0.847 (0.001)	0.091 (0.001)	-0.115 (0.001)	-0.428 (0.001)	11.071 (2.052)	-0.024 (0.009)	37.736 (2.196)	0.268 (0.014)
QMLE	0.003 (0.040)	0.0884 (0.003)	0.890 (0.041)	0.139 (0.039)	0.061 (0.093)	0.272 (0.071)	21.061 (24.080)	0.410 (0.005)	19.631 (3.970)	0.020 (0.004)

Notes: This table reports the estimation results of GJR-GARCH-MIDAS-J given by (3.3.1) and (3.2.15-3.2.16) using Bayesian MCMC approach and QMLE approach when DGP is by GJR-GARCH-MIDAS-J with 250 replications. MCMC estimates are evaluated using 40,000 iterations with 15,000 burn-ins. Standard deviations are given in brackets.

Table 3.3.6: MCMC estimates for EGARCH-MIDAS-J

	$\mu$	c	$\beta$	$\gamma$	$\alpha$	m	$\theta$	$\omega$	$\mu_Z$	$\sigma_z^2$	$\kappa$
True	0		0.9	-0.1	0.05	-0.1	0.4	10	-0.03	9	0.08
MCMC	-0.008 (0.009)	0.003 (0.004)	0.904 (0.013)	-0.108 (0.007)	0.046 (0.023)	-0.091 (0.031)	0.388 (0.044)	11.003 (3.119)	-0.029 (0.133)	10.050 (1.010)	0.077 (0.023)
True	0		0.9	-0.1	0.05	-0.1	0.4	5	-0.03	25	0.05
MCMC	-0.020 (0.014)	0.002 (0.003)	0.894 (0.014)	-0.098 (0.006)	0.056 (0.022)	-0.087 (0.029)	0.394 (0.039)	5.304 (1.09)	-0.031 (0.127)	25.572 (4.810)	0.048 (0.019)
True	0		0.9	-0.05	0.05	-0.1	-0.45	10	-0.03	36	0.03
MCMC	-0.051 (0.017)	0.010 (0.007)	0.899 (0.008)	-0.058 (0.004)	0.041 (0.003)	-0.126 (0.078)	-0.447 (0.038)	10.913 (1.022)	-0.031 (0.044)	37.041 (7.039)	0.029 (0.010)

Notes: This table reports the estimation results of EGARCH-MIDAS-J given by (3.3.1) and (3.2.29-3.2.30) using Bayesian MCMC approach when DGP is EGARCH-MIDAS-J with 250 replications. MCMC estimates are evaluated using 40,000 iterations with 15,000 burn-ins. Standard deviations are given in brackets.

### 3.4 Empirical Application

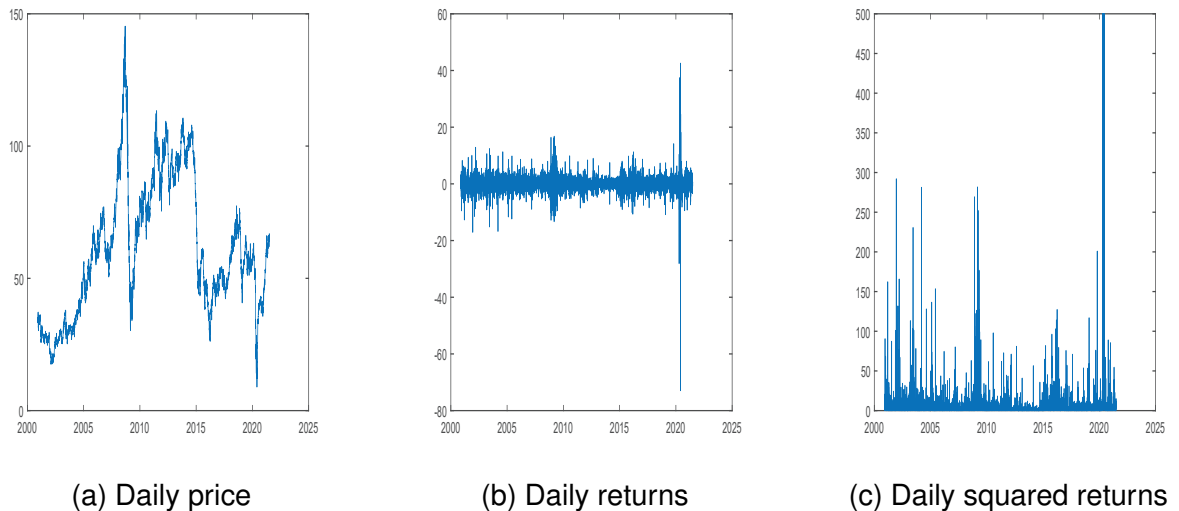
It is still difficult to find the best fitting econometric model for WTI returns and volatility. For example, Chen and Grant (2016) and Zerilli et al. (2019) applied stochastic volatility models whilst Wei et al. (2010) and Wang et al. (2016) applied factor models and standard GARCH. Recently, Pan et al. (2017), Razmi et al. (2020) and Yi et al. (2021) applied GARCH-MIDAS and Regime-Switching GARCH-MIDAS models, respectively.

We aim to address the important issues of leverage effects and rare events by applying the jump-augmented asymmetric GARCH-MIDAS models to an analysis of time-varying volatility patterns of WTI daily returns over the period 09/2000-8/2019. To examine the impacts of macroeconomic conditions on the long-run volatility, we consider a range of macroeconomic

variables: industrial production ( $IP$ ) of USA and China; economic policy uncertainty ( $EPU$ ) of USA and China; effective exchange rate ( $EER$ ) of USA and China; global economic policy uncertainty ( $GEPU$ ); OPEC oil production ( $OP_{OPEC}$ ), OPEC oil supply ( $OS_{OPEC}$ ), and global oil production ( $GOP$ ); Chicago Feds national activity index ( $CFNAI$ ) as a proxy of overall economic indicator. We use the growth rate constructed by  $100\log(X_t/X_{t-1})$ . We also evaluate the relative performance of GARCH-MIDAS-J, GJR-GARCH-MIDAS-J and EGARCH-MIDAS-J models in terms of in-sample fit and out of sample forecast performance.

In Fig.3.1(a) we observe that the daily price of WTI has been rather volatile, sharply decreasing a few times following the major adverse events in relation to the OPEC policy uncertainty, political instability, financial crises and economic recessions. Figs.3.1(b)-3.1(c) show that the returns series follows a stationary process while its volatility displays the time-varying clustering pattern with small, medium and large ranges of fluctuations, reflecting the impacts of global events such as Iraqi war in 2003, Global financial crisis during 2007/8, the shale oil exploration in 2014, and shortage of crude oil demand in 2020.

Figure 3.1: Crude Oil WTI daily data for the period 2000-2021



Note: Figure(a) illustrates the movement of WTI daily price in the period 2000-2021; Figure(b) shows the daily returns of WTI; Figure(c) show the the time-varying clustering pattern of small, medium, and large fluctuations.

In this empirical study, we attempt to capture the low, medium, and large levels of volatility by using macroeconomic variables in identifying the long term volatility component  $\tau_t$ . Figures 3.3-3.7 in Appendix 2, display a clear co-movement between WTI price and  $IP$  of USA and China,  $EER$  of China, Global Oil production and OPEC Oil production and supply.

### 3.4.1 Benchmark estimation results

Table 3.4.1 reports QMLE and Bayesian MCMC estimates of GARCH, GJR-GARCH, EGARCH, and their MIDAS counterparts where we use Global Economic Policy Uncertainty,  $GEPU$  as

the macroeconomic variable. For GARCH, GJR-GARCH, and EGARCH models. MCMC and QML produce estimates close to each other, in line with the simulation results. Leverage effects in GJR-GARCH and EGARCH are significant at the 1% level. Furthermore, BIC and RMSE suggest that EGARCH is the preferred model over GARCH and GJR-GARCH. Turning to MIDAS extensions, we find that the long-term coefficients ( $m$  and  $\theta$ ) are mostly significant and the fit of the model is significantly improved. Interestingly, the use of multiplicative volatility component model renders the magnitude of the leverage effect almost doubled while the persistence slightly reduced. Finally, BIC and RMSE suggest that EGARCH-MIDAS is the best fitting model.

**Table 3.4.1: MCMC and QML estimates of benchmark models**

Model	$\mu$	$\alpha_0$	$\alpha$	$\beta$	$\gamma$	Per	$m$	$\theta$	$\omega$	BIC	LOGL	RMSE
GARCH-Q	0.047 (0.028)	0.055 (0.009)	0.062 (0.004)	0.929 (0.005)		0.991				20770.7	-10368.4	13.809
GARCH-B	0.048 (0.028)	0.058 (0.013)	0.063 (0.006)	0.928 (0.007)		0.991				20771.1	-10368.6	13.808
G-MIDAS-B	0.039 (0.034)	0.032 (0.005)	0.122 (0.011)	0.846 (0.011)		0.968	1.997 (0.117)	0.046 (0.024)	8.032 (5.162)	19881.5	-9302.1	11.212
GJRGARCH-Q	0.017 (0.006)	0.049 (0.008)	0.027 (0.005)	0.937 (0.004)	0.052 (0.0287)	0.991				20744.5	-10351.0	13.804
GJRGARCH-B	0.022 (0.027)	0.049 (0.020)	0.029 (0.005)	0.937 (0.008)	0.051 (0.009)	0.991				20745.0	-10351.3	13.803
GJR-MIDAS-B	-0.015 (0.041)	0.028 (0.004)	0.055 (0.009)	0.859 (0.009)	0.117 (0.015)	0.972	2.049 (0.117)	0.054 (0.017)	8.161 (4.845)	19862.2	-9285.6	11.0
EGARCH-Q	0.005 (0.028)	0.024 (0.003)	0.111 (0.007)	0.987 (0.002)	-0.058 (0.005)	0.987				20717.5	-10337.6	13.717
EGARCH-B	-0.0025 (0.031)	0.025 (0.004)	0.114 (0.013)	0.986 (0.002)	-0.058 (0.004)	0.986				20717.7	-10337.6	13.716
EG-MIDAS-B	0.137 (0.002)	0.001 (0.003)	0.166 (0.013)	0.982 (0.003)	-0.093 (0.008)	0.982	2.022 (0.159)	0.011 (0.009)	13.089 (5.249)	19445.4	-9243.1	10.612

Notes: Q and B refer to QMLE and Bayesian MCMC estimates; G-MIDAS, GJR-MIDAS, and EG-MIDAS refer to GARCH-MIDAS, GJR-GARCH-MIDAS, and EGARCH-MIDAS respectively; Persistence, Per is  $\alpha + \beta$  for G-MIDAS (3.2.3-3.2.6),  $\alpha + \beta + \gamma/2$  for GJR-MIDAS (3.2.14-3.2.16), and  $\beta$  for EG-MIDAS (3.2.28-3.2.30);  $BIC = -2LOGL + p \log(T)$  where  $p$  is the number of parameters of the model, and  $T$  is number of observations; For MCMC estimation, BIC and RMSE are computed using the final estimates; LOGL is the log likelihood.

Table 3.4.2 presents the MCMC estimation results for the jump-augmented MIDAS models. The estimates of jump components ( $\mu_z$ ,  $\sigma_z^2$  and  $\kappa$ ) are all significant. However, GARCH-J, GJR-GARCH-J, and EGARCH-J produce an estimated mean of the jump size,  $\mu_z$  around -1.1, which seems to be odds with practice. With MIDAS extensions, the estimates of  $\mu_z$  are much smaller and reasonably close to zero while the fit of the model is significantly improved. In this case we find an occurrence rate at about 4.5% while  $\sigma_z^2$  are substantially larger. With jump components the leverage effects are still significant while the persistence is significantly reduced. BIC and RMSE convincingly select the jump-augmented MIDAS models over the jump-augmented standard model. Overall, we find that EGARCH-MIDAS-J is the best fitting model.

Table 3.4.2: MCMC Estimates of Jump-augmented MIDAS models

Model	$\mu$	$\alpha_0$	$\alpha$	$\beta$	$\gamma$	Per	M	$\theta$	$\omega$	$\mu_z$	$\sigma_z^2$	$\kappa$	BIC	LOGL	RMSE
GARCH-J	0.103 (0.029)	0.029 (0.001)	0.067 (0.001)	0.915 (0.001)		0.982				-1.098 (0.067)	12.585 (0.915)	0.067 (0.028)	21347.9	-10644.3	13.844
G-MIDAS-J	0.066 (0.043)	0.018	0.132 (0.001)	0.849 (0.001)		0.966	0.998 (0.001)	0.054 (0.001)	12.506 (3.929)	-0.009 (0.001)	28.741 (0.001)	0.045 (0.006)	19451.7	-9037.2	9.621
GJR-GARCH-J	0.036 (0.026)	0.035 (0.009)	0.025 (0.004)	0.939 (0.006)	0.041 (0.007)	0.985				-1.037 (0.138)	13.729 (2.175)	0.043 (0.042)	20560.2	-10246.2	13.832
GJR-MIDAS-J	0.034 (0.049)	0.044	0.039 (0.009)	0.867 (0.011)	0.101 (0.015)	0.956	0.806 (0.126)	0.069 (0.048)	3.365 (2.241)	-0.016 (0.001)	28.115 (0.001)	0.046 (0.009)	19447.4	-9020.7	9.262
EGARCH-J	0.059 (0.027)	0.004 (0.003)	0.097 (0.009)	0.992 (0.002)	-0.049 (0.003)	0.992				-1.295 (0.428)	16.438 (3.895)	0.051 (0.013)	20526.9	-10229.6	13.803
EG-MIDAS-J	0.133 (0.001)	0.001 (0.003)	0.165 (0.013)	0.981 (0.003)	-0.116 (0.008)	0.966	0.930 (0.157)	0.077 (0.009)	3.701 (5.197)	-0.029 (0.001)	31.429 (0.001)	0.044 (0.011)	19445.7	-9019.8	9.102

Notes: G-MIDAS-J, GJR-MIDAS-J, and EG-MIDAS-J refer to GARCH-MIDAS-J(3.3.1,3.2.5-3.2.6), GJR-GARCH-MIDAS-J(3.3.1, 3.2.15-3.2.16), and EGARCH-MIDAS-J (3.3.1, 3.2.29-3.2.30) respectively; Persistence, Per is  $\alpha + \beta$  for G-MIDAS-J,  $\alpha + \beta + \gamma/2$  for GJR-MIDAS-J, and  $\beta$  for EG-MIDAS-J;  $BIC = -2LOGL + plog(T)$  where  $p$  is the number of parameters of the model, and  $T$  is number of observations; For MCMC estimation, BIC and RMSE are computed using the final estimates; LOGL is the log likelihood.

In sum we document evidence that the joint modelling of the leverage effect, the long term volatility and rare events through jump will be important in capturing the salient time-varying volatility patterns of the daily WTI returns.

### 3.4.2 In-sample fit comparison

In Table 3.4.3 we summarise the in-sample estimation results for symmetric and asymmetric GARCH-MIDAS models and their jump-augmented extensions where we reproduce the long term estimate,  $\hat{\theta}$ , VR and BIC from Table 3.5.1 in Appendix 2. We summarise the main findings as follows:

First, BIC convincingly selects MIDAS models with jump components over MIDAS models without jump components. Overall, EGARCH-MIDAS-J is the most preferred model across all the 10 macroeconomic variables considered.

Second, the jump augmented MIDAS models produced significant long term coefficients ( $\theta$ ) with predicted signs for all macroeconomic variables. Focusing on EGARCH-MIDAS-J estimation results, they also tend to produce slightly large magnitudes than MIDAS models without jump components.

Third, we evaluate the relative importance of each macroeconomic variable by employing VR that measures the fraction of the total volatility explained by the long term component. Notice that jump-augmented MIDAS models produced a larger VR than MIDAS models without jump components, suggesting that if we ignore the presence of rare events of outliers, then the long term variance is likely to be under-estimated.<sup>7</sup> Focusing on EGARCH-MIDAS-J estimation results, we find that the most influential variable is the  $OP_{OPEC}$ , that explains 43.5% of the total volatility for WTI returns. The second-most influential variable is GOP growth, that explains 39.2% of the total volatility, followed by  $OS_{OPEC}$  (37%) and  $EER_{US}$  (36.3%). This highlights the dominant position of the OPEC in the global oil industry.

<sup>7</sup>We have conducted the additional simulation and found that the (downside) impacts of omitting jump components are substantial, Tables (3.5.6–3.5.8)

Table 3.4.3: The summary of Bayesian MCMC estimation results

Macro	GARCH-MIDAS			GARCH-MIDAS-J			GJR-GARCH-MIDAS			GJRGARCH-MIDAS-J			EGARCH-MIDAS			EGARCH-MIDAS-J		
	$\hat{\theta}$	BIC	VR	$\hat{\theta}$	BIC	VR	$\hat{\theta}$	BIC	VR	$\hat{\theta}$	BIC	VR	$\hat{\theta}$	BIC	VR	$\hat{\theta}$	BIC	VR
<i>IP<sub>US</sub></i>	-0.327 <sup>a</sup>	19866	15 %	-0.354 <sup>a</sup>	19487	25 %	-0.305 <sup>a</sup>	19851	17 %	-0.342 <sup>a</sup>	19478	29 %	-0.382 <sup>a</sup>	19477	18 %	-0.376 <sup>a</sup>	<b>19453</b>	31 %
<i>IP<sub>CH</sub></i>	-0.412 <sup>a</sup>	19859	14 %	-0.440 <sup>a</sup>	19505	19 %	-0.404 <sup>a</sup>	19858	16 %	-0.412 <sup>a</sup>	19455	23 %	-0.315 <sup>a</sup>	19453	17 %	-0.405 <sup>a</sup>	<b>19423</b>	24 %
<i>EER<sub>US</sub></i>	-0.834 <sup>a</sup>	19863	16 %	-0.883 <sup>a</sup>	19491	29 %	-0.838 <sup>a</sup>	19846	19 %	-0.794 <sup>a</sup>	19496	34 %	-0.794 <sup>a</sup>	19494	20 %	-0.874 <sup>a</sup>	<b>19485</b>	36 %
<i>EER<sub>CH</sub></i>	-0.339 <sup>a</sup>	19887	9 %	-0.364 <sup>a</sup>	19458	19 %	-0.372 <sup>a</sup>	19866	10 %	-0.393 <sup>a</sup>	19451	22 %	-0.237 <sup>a</sup>	19449	11 %	-0.432 <sup>a</sup>	<b>19429</b>	23 %
<i>GEP<sub>U</sub></i>	0.046 <sup>a</sup>	19882	11 %	0.054 <sup>a</sup>	19452	24 %	0.054 <sup>a</sup>	19862	13 %	0.070 <sup>b</sup>	19447	28 %	0.011 <sup>a</sup>	19449	14 %	0.077 <sup>a</sup>	<b>19445</b>	30 %
<i>EPU<sub>US</sub></i>	0.014 <sup>a</sup>	19884	14 %	0.015 <sup>a</sup>	19508	27 %	0.004	19863	16 %	0.137 <sup>a</sup>	19454	32 %	0.017	19452	17 %	0.150 <sup>a</sup>	<b>19418</b>	34 %
<i>EPU<sub>CH</sub></i>	-0.060 <sup>a</sup>	19886	8 %	-0.090 <sup>a</sup>	19450	15 %	-0.085 <sup>b</sup>	19863	10 %	-0.078 <sup>a</sup>	19452	18 %	0.039 <sup>a</sup>	19450	10 %	-0.086 <sup>a</sup>	<b>19413</b>	19 %
<i>GOP</i>	0.496 <sup>a</sup>	19883	17 %	0.670 <sup>a</sup>	19455	32 %	0.805 <sup>a</sup>	19860	20 %	0.866 <sup>a</sup>	19451	37 %	0.266 <sup>a</sup>	19449	21 %	0.953 <sup>a</sup>	<b>19430</b>	39 %
<i>OPOPEC</i>	0.243 <sup>a</sup>	19884	19 %	0.291 <sup>a</sup>	19500	35 %	0.381 <sup>a</sup>	19859	22 %	0.450 <sup>a</sup>	19465	41 %	0.120 <sup>b</sup>	19463	23 %	0.495 <sup>a</sup>	<b>19451</b>	44 %
<i>OSOPEC</i>	-0.038 <sup>c</sup>	19882	14 %	-0.070 <sup>a</sup>	19487	30 %	-0.064 <sup>a</sup>	19853	16 %	-0.075 <sup>b</sup>	19461	35 %	-0.067 <sup>b</sup>	19459	17 %	-0.083 <sup>b</sup>	<b>19449</b>	37 %

Notes:  $\hat{\theta}$  is the estimate of the impact of the macroeconomic variable on  $\tau_t$ ; a, b, and c indicate 1%, 5%, and 10% significance level;  $VR = var(\log(\hat{\tau}_t))/var(\log(\hat{\tau}_t\hat{g}_t))$  measures the fraction of the total volatility explained by the long term component;  $BIC = -2LOGL + p \log(T)$ , where LOGL is the log-likelihood of the model,  $p$  is the number of parameters, and  $T$  is the number of observations; The smallest BIC per economic indicator is highlighted in bold.

### 3.4.3 Out of sample forecast performance

We compare the predictive ability of symmetric and asymmetric GARCH MIDAS models with and without jump components, using RMSE and QLIKE of the  $k$ -day ahead forecast given by:

$$RMSE = \frac{1}{H} \sum_{h=1}^H \sqrt{\left(\hat{\sigma}_{T_h+k}^2 - (r_{T_h+k} - \mu)^2\right)^2}$$

$$QLIKE = \frac{1}{H} \sum_{k=1}^H \left( \log \hat{\sigma}_{T_h+k}^2 + \frac{(r_{T_h+k} - \mu)^2}{\log \hat{\sigma}_{T_h+k}^2} \right)$$

where we set  $H = 100$ , and  $T_h$  is the last day of  $h^h$  in-sample, obtained by applying a rolling window of length  $h$ , for  $h = 1, \dots, H$ , on the original in sample which ends on day  $T$ , to eliminate the impact of  $\hat{g}_T$  and  $\hat{\tau}_T$  on  $k$ -day forecasts which we compute using (3.4.1). We use  $(r_{T_h+k} - \mu)^2$  as a proxy of the true unknown volatility,  $\sigma_{T_h+k}^2$ , in day  $T_h + k$ , and we compute the forecast total volatility  $\hat{\sigma}_{T_h+k}^2$  using:

$$\begin{aligned} \hat{\sigma}_{T_h+k}^2 &= \hat{\tau}_{T_h+k} \hat{g}_{T_h+k} \\ &= \hat{\tau}_{T_h} \hat{g}_{T_h+k} \end{aligned} \tag{3.4.1}$$

where  $\hat{\tau}_{T_h+k}$  is kept equal to the estimate of  $\tau_{T_h}$ , and  $\hat{g}_{T_h+k}$  is the  $k$ -day forecast of the short-term volatility  $g_t$ .

We compute the 1-day ahead forecast,  $\hat{g}_{T_h+1}$ , using the specification of the short term volatility component, and its estimate  $\hat{g}_{T_h}$  and we compute the other  $k$ -day ahead forecasts recursively using:

GJR-GARCH-MIDAS:

$$\hat{g}_{T_h+1} = 1 - (\hat{\alpha} + \hat{\beta} + \hat{\gamma}/2) + \hat{\alpha} \frac{(r_{T_h} - \hat{\mu})^2}{\hat{\tau}_{T_h}} + \frac{1}{2} \hat{\gamma} \frac{(r_{T_h} - \hat{\mu})^2}{\hat{\tau}_{T_h}} I_{(r_{T_h} - \hat{\mu}) < 0} + \hat{\beta} \hat{g}_{T_h}$$

$$\hat{g}_{T_h+k} = 1 + (\hat{\alpha} + \hat{\beta} + \hat{\gamma}/2)^{k-1} \hat{g}_{T_h+1}$$

EGARCH-MIDAS:

$$\log(\hat{g}_{T_h+1}) = \hat{c}_0 + \hat{\gamma} \frac{(r_{T_h} - \hat{\mu})}{\sqrt{\hat{v}_{T_h} \hat{g}_{T_h}}} + \hat{\alpha} \left( \frac{|r_{T_h} - \hat{\mu}|}{\sqrt{\hat{v}_{T_h} \hat{g}_{T_h}}} - \sqrt{\frac{2}{\pi}} \right) + \hat{\beta} \log(\hat{g}_{T_h})$$

$$\hat{g}_{T_h+k} = \hat{g}_{T_h+k-1}^{\hat{\beta}} e^{\hat{c}_0 - \alpha \sqrt{\frac{2}{\pi}} \{e^{0.5\hat{\delta}_1^2} \Phi(\hat{\delta}_1) + e^{0.5\hat{\delta}_2^2} \Phi(\hat{\delta}_2)\}}$$

where  $\hat{\delta}_1 = \hat{\alpha} + \hat{\gamma}$ ,  $\hat{\delta}_2 = \hat{\alpha} - \hat{\gamma}$ , and  $\Phi(x)$  is cdf of  $N(0,1)$ . We also compute the cumulative forecast up to day  $k$  by accumulating the recursively determined  $k$ -day forecast for  $k = 1, \dots, 20$  days.

We assess the forecasting performance of the alternative GARCH-MIDAS models and their jump augmented extensions using GARCH-MIDAS as a benchmark model. We compute QLIKE (RMSE) loss as the ratio of QLIKE (RMSE) of the alternative models and their jump extensions to QLIKE (RMSE) of GARCH-MIDAS, and select the model with the smallest QLIKE (RMSE) loss as the preferred specification.

Tables 3.4.4–3.4.5 report RMSE and QLIKE losses for the  $k$ -day ahead forecast of the total volatility with  $k = [1, 5, 10, 15, 20]$  using in-sample period, 01/9/2000 to 31/7/2019. We consider  $EER_{US}$ ,  $GOP$ ,  $OP_{OPEC}$ , and  $OS_{OPEC}$  growth as the macroeconomic variable respectively when forecasting the long term volatility because they were found to be most influential in terms of the in-sample fit for WTI daily returns volatility.

Table 3.4.4 reports QLIKE loss results. For all forecast horizons, EGARCH-MIDAS-J outperforms all the alternative models across all economic indicators. Next, we turn to RMSE loss results in Table 3.4.5. EGARCH-MIDAS-J still outperforms all other models across all economic variables.

Overall, we confirm the best out-of-sample forecasting performance is achieved by the EGARCH-MIDAS-J model. Again, this suggests that the joint modelling of the leverage effect in the short term volatility, the long term volatility and rare events through jump will be important in capturing the salient time-varying volatility patterns of the daily WTI returns.

Table 3.4.4: QLIKE LOSS of daily volatility forecast

Macro	Model	1	5	10	15	20
<i>EER<sub>US</sub></i>	GJR-GARCH-MIDAS	1.078	1.124	1.076	1.096	1.078
	EGARCH-MIDAS	0.969	0.971	0.991	0.992	1
	GARCH-MIDAS-J	0.911	0.954	0.926	0.855	0.859
	GJR-GARCH-MIDAS-J	0.985	1.04	0.993	0.919	0.918
	EGARCH-MIDAS-J	<b>0.845</b>	<b>0.824</b>	<b>0.789</b>	<b>0.53</b>	<b>0.533</b>
<i>GOP</i>	GJR-GARCH-MIDAS	0.994	0.992	0.991	0.981	0.973
	EGARCH-MIDAS	0.968	0.949	0.986	1.05	0.947
	GARCH-MIDAS-J	0.98	1.039	0.988	0.923	0.935
	GJR-GARCH-MIDAS-J	0.925	0.923	0.927	0.909	0.906
	EGARCH-MIDAS-J	<b>0.871</b>	<b>0.857</b>	<b>0.826</b>	<b>0.542</b>	<b>0.543</b>
<i>OP<sub>OPEC</sub></i>	GJR-GARCH-MIDAS	1.106	1.157	1.104	1.095	1.082
	EGARCH-MIDAS	0.964	1.02	0.975	1.039	1.01
	GARCH-MIDAS-J	0.941	0.936	0.939	0.916	0.918
	GJR-GARCH-MIDAS-J	0.986	1.051	0.999	0.904	0.902
	EGARCH-MIDAS-J	<b>0.945</b>	<b>0.929</b>	<b>0.887</b>	<b>0.541</b>	<b>0.542</b>
<i>OS<sub>OPEC</sub></i>	GJR-GARCH-MIDAS	1.05	1.099	1.071	1.161	1.164
	EGARCH-MIDAS	0.938	0.992	0.971	1.03	1.033
	GARCH-MIDAS-J	0.943	0.941	0.957	0.933	0.926
	GJR-GARCH-MIDAS-J	0.941	0.939	0.944	0.907	0.908
	EGARCH-MIDAS-J	<b>0.677</b>	<b>0.699</b>	<b>0.687</b>	<b>0.577</b>	<b>0.581</b>

Note: This table reports QLIKE loss of the  $k$ -day total volatility forecast for  $k = 1, 5, 10, 15, 20$  using *EER<sub>US</sub>*, *GOP*, *OP<sub>OPEC</sub>* and *OS<sub>OPEC</sub>* as explanatory variables when forecasting the long term volatility. QLIKE loss is the ratio of QLIKE of GARCH-MIDAS-J, GJR-GARCH-MIDAS, GJR-GARCH-MIDAS-J, EGARCH-MIDAS and EGARCH-MIDAS-J to GARCH-MIDAS. The preferred model is the one with the smallest QLIKE loss which is highlighted in bold.

Table 3.4.5: RMSE LOSS of daily volatility forecast

Macro	Model	1	5	10	15	20
<i>EER<sub>US</sub></i>	GJR-GARCH-MIDAS	1.004	1.002	1.004	0.916	0.944
	EGARCH-MIDAS	0.993	0.993	0.995	0.911	0.931
	GARCH-MIDAS-J	0.993	0.993	0.996	0.88	0.884
	GJR-GARCH-MIDAS-J	0.984	0.977	0.981	0.899	0.922
	EGARCH-MIDAS-J	<b>0.966</b>	<b>0.967</b>	<b>0.966</b>	<b>0.774</b>	<b>0.805</b>
<i>GOP</i>	GJR-GARCH-MIDAS	1	0.998	0.999	0.925	0.949
	EGARCH-MIDAS	0.996	1	1.002	0.923	0.949
	GARCH-MIDAS-J	0.991	0.989	0.989	0.917	0.894
	GJR-GARCH-MIDAS-J	0.989	0.986	0.988	0.867	0.891
	EGARCH-MIDAS-J	<b>0.988</b>	<b>0.982</b>	<b>0.984</b>	<b>0.792</b>	<b>0.825</b>
<i>OP<sub>OPEC</sub></i>	GJR-GARCH-MIDAS	0.996	0.993	0.994	0.98	0.902
	EGARCH-MIDAS	0.993	0.99	0.989	0.932	0.969
	GARCH-MIDAS-J	1.004	1.006	1.007	1.045	1.047
	GJR-GARCH-MIDAS-J	0.994	0.991	0.992	0.84	0.863
	EGARCH-MIDAS-J	<b>0.989</b>	<b>0.981</b>	<b>0.984</b>	<b>0.767</b>	<b>0.796</b>
<i>OS<sub>OPEC</sub></i>	GJR-GARCH-MIDAS	1.002	1.002	1.008	1.151	1.199
	EGARCH-MIDAS	0.998	0.995	0.997	0.991	0.989
	GARCH-MIDAS-J	0.991	0.993	0.996	0.919	0.945
	GJR-GARCH-MIDAS-J	0.987	0.986	0.991	0.902	0.926
	EGARCH-MIDAS-J	<b>0.983</b>	<b>0.978</b>	<b>0.984</b>	<b>0.839</b>	<b>0.867</b>

Note: This table reports RMSE loss of the  $k$ -day total volatility forecast for  $k = 1, 5, 10, 15, 20$  using *EER<sub>US</sub>*, *GOP*, *OP<sub>OPEC</sub>* and *OS<sub>OPEC</sub>* as explanatory variables when forecasting the long term volatility. RMSE loss is the ratio of RMSE of GARCH-MIDAS-J, GJR-GARCH-MIDAS, GJR-GARCH-MIDAS-J, EGARCH-MIDAS and EGARCH-MIDAS-J to GARCH-MIDAS. The preferred model is the one with the smallest RMSE loss which is highlighted in bold.



### 3.4.4 Conclusion

We have proposed the Bayesian MCMC methodology to estimating asymmetric GARCH-MIDAS models that also include jump components, which are supposed to capture the presence of rare events. Via simulation studies we clearly showed that when the simulated data contain jump components, the QML estimates become unreliable or computationally infeasible. Still, the proposed MCMC approach can be easily conducted and produce relatively accurate estimates.

We have demonstrated the usefulness of the MCMC approach by analysing the WTI returns data. In sum, we document evidence that the joint modelling of the leverage effect, the long term volatility and rare events through jump will be important in capturing the salient time-varying volatility patterns of the daily WTI returns. Overall, we find that EGARCH-MIDAS-J is the most preferred model in terms of the in-sample fit and out-of-sample forecasting. This finding sheds further lights on the mixed evidence reported by several existing studies that applied QML estimates of GARCH-MIDAS models to daily WTI return data.

## 3.5 Appendix 2

### 3.5.1 Derivation of the proposal density of Alternative GARCH-MIDAS models

Consider the general GARCH-MIDAS type model:

$$r_t = \mu + \sqrt{g_t \tau_t} \varepsilon_t \quad (3.5.1)$$

$$\log(\tau_t) = m + \theta \sum_{k=1}^K w_k(\omega) X_{t-k} \quad (3.5.2)$$

where  $\varepsilon_t \sim N(0, 1)$ ,  $X$  is a macroeconomic variable, and  $g_t$  is expressed as:

For GARCH-MIDAS:

$$g_t = 1 - \alpha - \beta + \alpha \frac{(r_{t-1} - \mu)^2}{\tau_{t-1}} + \beta g_{t-1} \quad (3.5.3)$$

where  $\alpha > 0$ ,  $0 < \beta < 1$ , and  $\alpha + \beta < 1$

For GJR-GARCH-MIDAS:

$$g_t = 1 - \alpha - \beta + \alpha \frac{(r_{t-1} - \mu)^2}{\tau_{t-1}} + \gamma \frac{(r_{t-1} - \mu)^2}{\tau_{t-1}} I_{r_{t-1} - \mu < 0} + \beta g_{t-1} \quad (3.5.4)$$

where  $\beta > 0$ , and  $\alpha + \beta + \gamma/2 < 1$

For EGARCH-MIDAS:

$$\log(g_t) = c_0 + \alpha \left( \frac{|r_{t-1} - \mu|}{\sqrt{\tau_{t-1} g_{t-1}}} - \sqrt{\frac{2}{\pi}} \right) + \gamma \frac{r_{t-1} - \mu}{\sqrt{\tau_{t-1} g_{t-1}}} + \beta \log(g_{t-1}) \quad (3.5.5)$$

where  $|\beta| < 1$

The Log-likelihood function of the general model is:

$$\begin{aligned} \text{Log}L &= -\frac{1}{2} \sum_{t=1}^T \left\{ \sqrt{2\pi} + \log(g_t \tau_t) + \frac{(r_{t-1} - \mu)^2}{g_{t-1} \tau_{t-1}} \right\} \\ &\propto -\frac{1}{2} \sum_{t=1}^T \left\{ \log(g_t) + \log(\tau_t) + \frac{(r_{t-1} - \mu)^2}{g_{t-1} \tau_{t-1}} \right\} \end{aligned} \quad (3.5.6)$$

The posterior,  $p(\Theta_i | \Theta_{-i}, \mathbf{r})$ , of any parameter  $\Theta_i$  which can be any single individual parameter or a subset of the parameters of the model, is:

$$p(\Theta_i | \Theta_{-i}, \mathbf{r}) = \left( \prod_{t=1}^T \frac{1}{\sqrt{2\pi} \sqrt{g_t \tau_t}} \right) e^{-\frac{1}{2} \sum_{t=1}^T \frac{(r_{t-1} - \mu)^2}{g_{t-1} \tau_{t-1}}} \pi(\Theta_i) \quad (3.5.7)$$

where  $\pi(\Theta_i)$  is the prior density of  $\Theta_i$ ,  $r_0 = \bar{r}$ ,  $g_0 = 1$ . Since  $p(\Theta_i | \Theta_{-i}, \mathbf{r})$  is a density,  $\int_{-\infty}^{+\infty} p(\Theta_i | \Theta_{-i}, \mathbf{r}) d\Theta_i = 1$ , the analytic expression of the posterior is determined, up to a constant, by keeping only the terms of (3.5.7) that depend on  $\Theta_i$  after having replaced  $g_t$  and  $\tau_t$  in (3.5.7) by their expressions in function of the parameters.

**Posterior distributions of the parameters of EGARCH-MIDAS:**

The parameters of EGARCH-MIDAS, defined by (3.5.1, 3.5.2, and 3.5.5), are  $\Theta = (\mu, (\alpha, \beta, \gamma), (m, \theta, \omega))$ . We derive their posterior densities from (3.5.7), as follows:

**Posterior of  $\mu$ :** Using  $\pi(\mu) \sim N(\mu_0, \sigma_0^2)$ , and the fact that  $\tau_t$  does not depend of  $\mu$ , (3.5.7) becomes:

$$\begin{aligned} p(\mu | \Theta_{-\mu}, \mathbf{r}) &\propto \left( \prod_{t=1}^T \frac{1}{\sqrt{g_t}} \right) e^{-\frac{1}{2} \sum_{t=1}^T \frac{(r_{t-1} - \mu)^2}{g_{t-1}} + \frac{(\mu - \mu_0)^2}{\sigma_0^2}} \\ &\propto \left( \prod_{t=1}^T \frac{1}{\sqrt{g_t}} \right) e^{-\frac{1}{2} \left\{ \sum_{t=1}^T \frac{(r_{t-1} - \mu)^2}{g_{t-1}} + \frac{(\mu - \mu_0)^2}{\sigma_0^2} \right\}} \\ &\propto \left( \prod_{t=1}^T \frac{1}{\sqrt{g_t}} \right) e^{-\frac{1}{2} \left\{ \mu^2 \left( \sum_{t=1}^T \frac{1}{g_{t-1}} + \frac{1}{\sigma_0^2} \right) - 2\mu \left( \sum_{t=1}^T \frac{r_{t-1}}{g_{t-1}} - \mu_0 \right) \right\}} \end{aligned} \quad (3.5.8)$$

From (3.5.5),  $\prod_{t=1}^T \frac{1}{\sqrt{g_t}}$  is also a function of  $\mu$ , and therefore (3.5.8) cannot be the expression of a normal density or any other known family of densities. Hence, we simulate draws from  $p(\mu | \Theta_{-\mu}, \mathbf{r})$  using Metropolis-Hasting method of subsection 3.2.1, and considering a normal proposal density  $N(\bar{\mathbf{r}}, s^2/T)$  where  $\bar{\mathbf{r}}$  and  $s^2$  are the sample mean and sample variance of the returns.

**Posterior of the parameters  $\boldsymbol{\theta}_s = (\alpha, \log(\beta), \gamma)$ ,  $\boldsymbol{\theta}_L = (m, \theta)$ , and  $\omega$ :**

Since  $\alpha$ , and  $\gamma$  are real numbers, and  $0 < \beta < 1$ , we use the prior  $\pi(\boldsymbol{\theta}_s) \sim N_3(\boldsymbol{\theta}_{s,0}, \Sigma_{s,0})$  and  $\pi(\boldsymbol{\theta}_L) \sim N_2(\boldsymbol{\theta}_{L,0}, \Sigma_{L,0})$ , and  $\pi(\omega) \sim U([1, 50])$  where  $\boldsymbol{\theta}_{s,0} = (0, \log(0.9), 0)$ ,  $\Sigma_{s,0}$  is the 3 dimensional Identity Matrix,  $\boldsymbol{\theta}_{L,0} = (0, 0)'$ , and  $\Sigma_{L,0}$  is  $I_2$ . From (3.5.7), the posteriors  $p(\boldsymbol{\theta}_s | \mathbf{r}, \mu, \boldsymbol{\theta}_L, \omega)$ ,  $p(\boldsymbol{\theta}_L | \mathbf{r}, \mu, \boldsymbol{\theta}_s, \omega)$ , and  $p(\omega, | \mathbf{r}, \mu, \boldsymbol{\theta}_s, \boldsymbol{\theta}_L)$  cannot be expressed in the form of known density because:

$$p(\boldsymbol{\theta}_s | \mathbf{r}, \mu, \boldsymbol{\theta}_L, \omega) = \left( \prod_{t=1}^T \frac{1}{\sqrt{2\pi} \sqrt{g_t \tau_t}} \right) e^{-\frac{1}{2} \sum_{t=1}^T \frac{(r_{t-1} - \mu)^2}{g_{t-1} \tau_{t-1}}} \pi(\boldsymbol{\theta}_s) \quad (3.5.9)$$

$$p(\boldsymbol{\theta}_L | \mathbf{r}, \mu, \boldsymbol{\theta}_s, \omega) = \left( \prod_{t=1}^T \frac{1}{\sqrt{2\pi} \sqrt{g_t \tau_t}} \right) e^{-\frac{1}{2} \sum_{t=1}^T \frac{(r_{t-1} - \mu)^2}{g_{t-1} \tau_{t-1}}} \pi(\boldsymbol{\theta}_L) \quad (3.5.10)$$

$$p(\omega | \mathbf{r}, \mu, \boldsymbol{\theta}_s, \boldsymbol{\theta}_L) = \left( \prod_{t=1}^T \frac{1}{\sqrt{2\pi} \sqrt{g_t \tau_t}} \right) e^{-\frac{1}{2} \sum_{t=1}^T \frac{(r_{t-1} - \mu)^2}{g_{t-1} \tau_{t-1}}} 1[0.50] \quad (3.5.11)$$

Since the term  $\prod_{t=1}^T \frac{1}{\sqrt{2\pi} \sqrt{g_t \tau_t}}$  is a function of  $\boldsymbol{\theta}_s$ ,  $\boldsymbol{\theta}_L$ , and  $\omega$ , the posteriors cannot be expressed as a multivariate normal density or a Uniform density. We simulate draws of  $\boldsymbol{\theta}_s$ ,  $\boldsymbol{\theta}_L$ , and  $\omega$  using Metropolis-Hasting, Random Walk, or Adaptive random walk which we described in section 3.2.1. Draws of  $\omega$  can be simulated using GRIDDY-GIBBS procedure which can also be employed if the parameters of the short and long term components are estimated individually at the cost of increasing the number of iterations of the MCMC algorithm. Next, we discuss the derivation of parameters  $\mu_s^*$ ,  $\Sigma_s^*$ ,  $\mu_L^*$ ,  $\Sigma_L^*$ , proposal normal densities  $q(\boldsymbol{\theta}_s)$ , and  $q(\boldsymbol{\theta}_L)$ , employing (3.2.24) and (3.2.25), 2<sup>nd</sup> order Taylor expansion of the posterior densities  $\boldsymbol{\theta}_s$ , and  $\boldsymbol{\theta}_L$  which requires the computation of their gradients. From (3.5.5) and (3.5.6), we have:

$$\text{Log}(p(\Theta | \mathbf{r}, \Theta_{-i})) \propto -\frac{1}{2} \sum_{t=1}^T \left\{ \log(g_t) + \log \tau_t + \frac{(r_t - \mu)^2}{g_t \tau_t} \right\} + \log(\pi(\Theta))$$

where  $\Theta$  is either  $\theta_s$  or  $\theta_L$ . Then,

$$\begin{aligned}
 \frac{\delta}{\delta\Theta} \text{Log}p(\Theta | \mathbf{r}, \Theta_{-i}) &\propto -\frac{1}{2} \sum_{t=1}^T \left\{ \frac{\delta \log g_t}{\delta\Theta} + \frac{\delta \log \tau_t}{\delta\Theta} + \frac{\delta}{\delta\Theta} \frac{(r_t - \mu)^2}{g_t \tau_t} \right\} + \frac{\delta \log \pi(\Theta)}{\delta\Theta} \\
 &\propto -\frac{1}{2} \sum_{t=1}^T \left\{ \frac{\delta \log g_t}{\delta\Theta} + \frac{\delta \log \tau_t}{\delta\Theta} - \frac{(r_t - \mu)^2}{g_t^2 \tau_t^2} \left\{ \tau_t \frac{\delta g_t}{\delta} + g_t \frac{\delta \tau_t}{\delta} \right\} \right\} + \frac{\delta \log \pi(\Theta)}{\delta\Theta} \\
 &\propto -\frac{1}{2} \sum_{t=1}^T \left\{ \frac{\delta \log g_t}{\delta\Theta} + \frac{\delta \log \tau_t}{\delta\Theta} - (r_t - \mu)^2 \left\{ \frac{1}{g_t^2 \tau_t} \frac{\delta g_t}{\delta} + \frac{1}{g_t \tau_t^2} \frac{\delta \tau_t}{\delta} \right\} \right\} + \frac{\delta \log \pi(\Theta)}{\delta\Theta} \\
 &\propto -\frac{1}{2} \sum_{t=1}^T \left\{ \frac{\delta \log g_t}{\delta\Theta} + \frac{\delta}{\delta\Theta} - (r_t - \mu)^2 \frac{\delta \log \tau_t}{\delta\Theta} \left\{ \frac{1}{g_t \tau_t} \frac{\delta \log g_t}{\delta} + \frac{1}{g_t \tau_t} \frac{\delta \log \tau_t}{\delta} \right\} \right\} + \frac{\delta \log \pi(\Theta)}{\delta\Theta} \\
 &\propto -\frac{1}{2} \sum_{t=1}^T \left\{ 1 - \frac{(r_t - \mu)^2}{g_t \tau_t} \right\} \left\{ \frac{\delta \log g_t}{\delta\Theta} + \frac{\delta \log \tau_t}{\delta\Theta} \right\} + \frac{\delta \log \pi(\Theta)}{\delta\Theta}
 \end{aligned} \tag{3.5.12}$$

where  $\frac{\partial \log(\pi(\Theta))}{\partial \Theta} = -(\Theta - \Theta_0)' \Sigma_{\Theta_0}^{-1}$

To compute the value of the gradient (3.5.12), we need to compute  $\frac{\delta}{\delta\Theta} \log(\tau_t)$  and  $\frac{\delta}{\delta\Theta} \log(g_t)$  by employing (3.5.2) and (3.5.5): Replacing  $\Theta$  by  $\theta_s$  and  $\theta_L$ , we have  $\frac{\delta}{\delta\theta_s} \log(\tau_t) = 0$ ,  $\frac{\delta}{\delta\theta_L} \log(\tau_t) = [1, \sum_{k=1}^K w_k X_{t-k}^{(1)}, \dots, \sum_{k=1}^K w_k X_{t-k}^{(p)}]'$

Replacing  $\beta$  by  $e^{\gamma_2}$  in (3.5.5), we can derive :

$$\frac{\delta}{\delta\alpha} \log(g_t) = \frac{\delta}{\delta\alpha} c_0 + \left( \frac{|r_{t-1} - \mu|}{\sqrt{g_{t-1} \tau_{t-1}}} - \sqrt{\frac{2}{\pi}} \right) + \left\{ -0.5\alpha \frac{|r_{t-1} - \mu|}{\sqrt{g_{t-1} \tau_{t-1}}} - 0.5\gamma \frac{(r_{t-1} - \mu)}{\sqrt{g_{t-1} \tau_{t-1}}} + e^{\gamma_2} \right\} \frac{\delta}{\delta\alpha} \log(g_{t-1}) \tag{3.5.13}$$

$$\begin{aligned}
 \frac{\delta}{\delta\gamma_2} \log(g_t^*) &= \frac{\delta}{\delta\gamma_2} c_0 - 0.5 \alpha \frac{|r_{t-1} - \mu|}{\sqrt{g_{t-1} \tau_{t-1}}} \frac{\delta}{\delta\gamma_2} \log(g_{t-1}) - 0.5\gamma \frac{(r_{t-1} - \mu)}{\sqrt{g_{t-1} \tau_{t-1}}} \frac{\delta}{\delta\gamma_2} \log(g_{t-1}) + e^{\gamma_2} \left( 1 + \frac{\delta}{\delta\gamma_2} \log(g_{t-1}) \right) \\
 &= \frac{\delta}{\delta\gamma_2} c_0 + e^{\gamma_2} + \left\{ -0.5 \alpha \frac{|r_{t-1} - \mu|}{\sqrt{g_{t-1} \tau_{t-1}}} - 0.5\gamma \frac{(r_{t-1} - \mu)}{\sqrt{g_{t-1} \tau_{t-1}}} + e^{\gamma_2} \right\} \frac{\delta}{\delta\gamma_2} \log(g_{t-1})
 \end{aligned} \tag{3.5.14}$$

$$\begin{aligned}
 \frac{\delta}{\delta\gamma} \log(g_t) &= \frac{\delta}{\delta\gamma} c_0 - 0.5 \alpha \frac{|r_{t-1} - \mu|}{\sqrt{g_{t-1} \tau_{t-1}}} \frac{\delta}{\delta\gamma} \log(g_{t-1}) + \frac{r_{t-1} - \mu}{\sqrt{g_{t-1} \tau_{t-1}}} - 0.5\gamma \frac{r_{t-1} - \mu}{\sqrt{g_{t-1} \tau_{t-1}}} \frac{\delta}{\delta\gamma} \log(g_{t-1}) + e^{\gamma_2} \frac{\delta}{\delta\gamma} \log(g_{t-1}) \\
 &= \frac{\delta}{\delta\gamma} c_0 + \frac{r_{t-1} - \mu}{\sqrt{g_{t-1} \tau_{t-1}}} + \left\{ -0.5\alpha \frac{|r_{t-1} - \mu|}{\sqrt{g_{t-1} \tau_{t-1}}} - 0.5\gamma \frac{r_{t-1} - \mu}{\sqrt{g_{t-1} \tau_{t-1}}} + e^{\gamma_2} \right\} \frac{\delta}{\delta\gamma} \log(g_{t-1})
 \end{aligned} \tag{3.5.15}$$

Notice: we have expressed  $\frac{\delta}{\delta\alpha} \log(g_t)$  in function of  $\frac{\delta}{\delta\alpha} \log(g_{t-1})$ ,  $\frac{\delta}{\delta\gamma_2} \log(g_t)$  in terms of  $\frac{\delta}{\delta\gamma_2} \log(g_{t-1})$ , and  $\frac{\delta}{\delta\gamma} \log(g_t)$  in terms of  $\frac{\delta}{\delta\gamma} \log(g_{t-1})$ . Then, by employing (3.5.12) and  $\frac{\delta}{\delta\theta_s} \log(\tau_t) = 0$ , the gradient of the log-posterior  $\frac{\delta}{\delta\theta_s} \log(p(\theta_s | \mathbf{r}, \mu, \theta_L))$ , can be computed recursively.

Hence, the parameter  $\mu_s^*$  and  $\Sigma_s^*$  of the proposal density  $q(\theta_s)$  will be computed using (3.2.24) and (3.2.25) where  $\tilde{\theta}_s$  is an approximate value of  $\theta_s$  which maximizes  $p(\theta_s | \mathbf{r}, \mu, \theta_L)$ , and the 3x3 Hessian matrix

$$\left[ \frac{\partial \log(p(\boldsymbol{\theta}_s | \mathbf{r}, \boldsymbol{\mu}, \boldsymbol{\theta}_L))}{\partial \boldsymbol{\theta}_{s,i} \partial \boldsymbol{\theta}_{s,j}} \right] \text{ is } \frac{\delta}{\delta \boldsymbol{\theta}_s} \text{Log}(p(\boldsymbol{\theta}_s | \mathbf{r}, \boldsymbol{\mu}, \boldsymbol{\theta}_L))' \frac{\delta}{\delta \boldsymbol{\theta}_s} \text{Log}(p(\boldsymbol{\theta}_s | \mathbf{r}, \boldsymbol{\mu}, \boldsymbol{\theta}_L))$$

Similarly, the gradient  $\frac{\delta}{\delta \boldsymbol{\theta}_L} \text{Log}(p(\boldsymbol{\theta}_L | \mathbf{r}, \boldsymbol{\mu}, \boldsymbol{\theta}_s))$  will be computed by plugging in (3.5.12),  $\frac{\delta}{\delta \boldsymbol{\theta}_L} \log(g_t)$  and  $\frac{\delta}{\delta \boldsymbol{\theta}_L} \log(\tau_t)$  which are given by:

$$\frac{\delta}{\delta \boldsymbol{\theta}_L} \log(\tau_t) = \left[ 1, \sum_{k=1}^K w_k(\boldsymbol{\omega}) X_{t-k} \right] \quad (3.5.16)$$

and from (3.5.5),

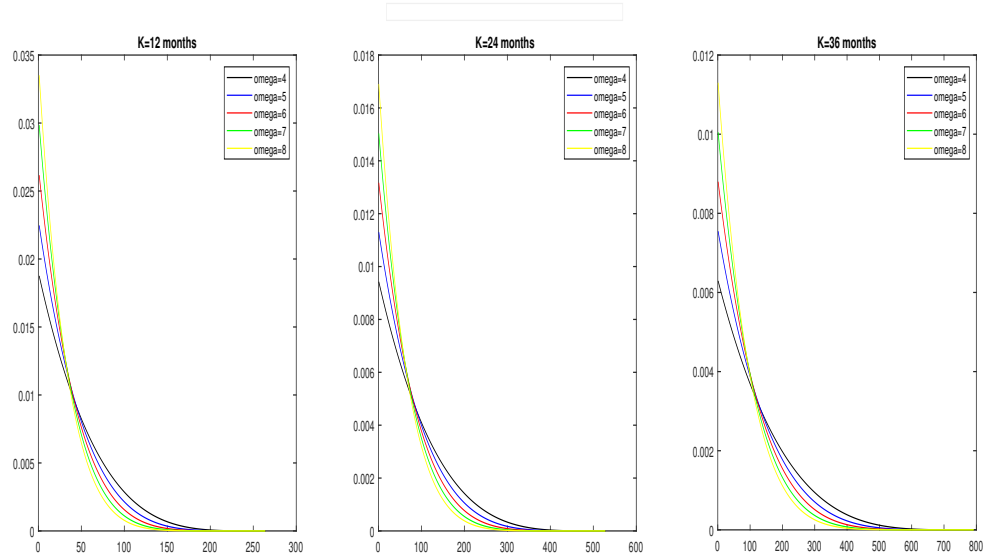
$$\begin{aligned} \frac{\delta}{\delta \boldsymbol{\theta}_L} \log(g_t) &= \frac{\delta}{\delta \boldsymbol{\theta}_L} c_0 + \alpha |r_{t-1} - \mu| \frac{\delta}{\delta \boldsymbol{\theta}_L} \left\{ \frac{1}{\sqrt{g_{t-1} \tau_{t-1}}} \right\} + \gamma (r_{t-1} - \mu) \left\{ \frac{\delta}{\delta \boldsymbol{\theta}_L} \left\{ \frac{1}{\sqrt{g_{t-1} \tau_{t-1}}} \right\} \right\} + e^{\gamma_2} \frac{\delta}{\delta \boldsymbol{\theta}_L} \log(g_{t-1}) \\ &= -0.5\alpha \frac{|r_{t-1} - \mu|}{\sqrt{g_{t-1} \tau_{t-1}}} \left\{ \frac{\delta}{\delta \boldsymbol{\theta}_L} \log(g_{t-1}) + \frac{\delta}{\delta \boldsymbol{\theta}_L} \log(\tau_{t-1}) \right\} - 0.5\gamma \frac{(r_{t-1} - \mu)}{\sqrt{g_{t-1} \tau_{t-1}}} \left\{ \frac{\delta}{\delta \boldsymbol{\theta}_L} \log(g_{t-1}) + \frac{\delta}{\delta \boldsymbol{\theta}_L} \log(\tau_{t-1}) \right\} + e^{\gamma_2} \frac{\delta}{\delta \boldsymbol{\theta}_L} \log(g_{t-1}) \\ &= \left\{ -0.5\alpha \frac{|r_{t-1} - \mu|}{\sqrt{g_{t-1} \tau_{t-1}}} - 0.5\gamma \frac{(r_{t-1} - \mu)}{\sqrt{g_{t-1} \tau_{t-1}}} + e^{\gamma_2} \right\} \frac{\delta}{\delta \boldsymbol{\theta}_L} \log(g_{t-1}) + \left\{ -0.5\alpha \frac{|r_{t-1} - \mu|}{\sqrt{g_{t-1} \tau_{t-1}}} - 0.5\gamma \frac{(r_{t-1} - \mu)}{\sqrt{g_{t-1} \tau_{t-1}}} \right\} \frac{\delta}{\delta \boldsymbol{\theta}_L} \log \tau_{t-1} \end{aligned}$$

**Posterior of the weighting parameter  $\boldsymbol{\omega}$ :** we suggest to use Griddy-Gibbs method in which a draw  $\boldsymbol{\omega}^{(j)}$  is given by  $\boldsymbol{\omega}^{(j)} = F^{-1}(u)$  where  $F(x)$  is an estimate of  $\int_1^x p(\boldsymbol{\omega} | \boldsymbol{\mu}, \boldsymbol{\theta}_s, \boldsymbol{\theta}_L) d\boldsymbol{\omega}$ . A good estimate  $F(x)$  is the cumulative area below  $p(\boldsymbol{\omega} | \boldsymbol{\mu}, \boldsymbol{\theta}_s, \boldsymbol{\theta}_L)$  from 1 to  $x$  which can be estimated numerically by:

$$F(x) = \frac{\sum_{i=1}^J p(\boldsymbol{\omega}(i) | \boldsymbol{\mu}, \boldsymbol{\theta}_s, \boldsymbol{\theta}_L)}{\sum_{i=1}^B p(\boldsymbol{\omega}(i) | \boldsymbol{\mu}, \boldsymbol{\theta}_s, \boldsymbol{\theta}_L)}$$

where  $J = \max\{i \text{ such that } \boldsymbol{\omega}(i) < x\}$ ,  $\boldsymbol{\omega}(1), \dots, \boldsymbol{\omega}(B)$  is sequence of  $B$  grid points in the support of  $\boldsymbol{\omega}$ ,  $[1, 50]$ . Since the weighting function  $w(k, \boldsymbol{\omega})$  does not change rapidly as illustrated in the below graphs, we use  $B = 100$ .

Figure 3.2: Plot of Beta weighting function



Note: This Figure illustrates the weighting function, when  $K=(12,24,36)$ , for different values of  $\boldsymbol{\omega}$  where as  $\boldsymbol{\omega}$  increase the weighting function becomes steeper.

### Posterior distributions of the parameters of GJRGARCH-MIDAS

Let  $\Theta = (\mu, \boldsymbol{\theta}_s, \boldsymbol{\theta}_L, \omega)$  where  $\boldsymbol{\theta}_s = (\alpha, \beta, \gamma)$  is the parameter vector of the short term Unit GJR-GARCH(1,1) specification given in (3.5.4), and  $\boldsymbol{\theta}_L = (m, \theta)$  and  $\omega$  are the parameters of the long term volatility component given in (3.5.2). The derivation of the posterior density of  $\mu, \boldsymbol{\theta}_s, \boldsymbol{\theta}_L$ , and  $\omega$  can be computed, by employing, (3.5.4) and (3.5.7) as done for EGAECH-MIDAS.

**Posterior of  $\mu$ :** Assuming a Prior  $N(0, 1)$ , (3.5.8) is valid for GJRGARCH-MIDAS, and therefore we simulate draws from  $p(\mu | \Theta_{-\mu}, \mathbf{r})$  by employing Metropolis-Hasting method, and considering a normal proposal density  $N(\bar{\mathbf{r}}, s^2/T)$  where  $\bar{\mathbf{r}}$  and  $s^2$  are the sample mean and sample variance of the returns.

**Posterior of  $\boldsymbol{\theta}_s = (\alpha, \beta, \gamma)$ :** Since  $\alpha > 0$  and  $\beta > 0$ , we simulate  $\boldsymbol{\theta}_s^* = (\gamma_1, \gamma_2, \gamma)$  where  $\gamma_1 = \log(\alpha)$ , and  $\gamma_2 = \log(\beta)$ , and we assume the prior for  $\boldsymbol{\theta}_s^* \sim N_3(\boldsymbol{\theta}_{s0}^*, I_3)$  where  $I_3$  is the 3-dimensional Identity matrix, and  $\boldsymbol{\theta}_{s0}^* = (0.05, 0.90, 0)$ . Using (3.5.12), and expressing  $g_t$  of (3.5.4) as a function of  $\boldsymbol{\theta}_s^* = (\gamma_1, \gamma_2, \gamma)$ , we get the gradient of  $p(\boldsymbol{\theta}_s^* | \mathbf{r}, \mu, \boldsymbol{\theta}_L, \omega)$ :

$$\frac{\delta}{\delta \boldsymbol{\theta}_s^*} \text{Log}(p(\boldsymbol{\theta}_s^* | \mathbf{r}, \mu, \boldsymbol{\theta}_L, \omega)) \propto -\frac{1}{2} \sum_{t=1}^T \left\{ 1 - \frac{(r_t - \mu)^2}{g_t \tau_t} \right\} \left\{ \frac{\delta \text{Log} g_t}{\delta \boldsymbol{\theta}_s^*} + \frac{\delta \text{Log} \tau_t}{\delta \boldsymbol{\theta}_s^*} \right\} + \frac{\delta \text{Log} \pi(\boldsymbol{\theta}_s^*)}{\delta \boldsymbol{\theta}_s^*}$$

where,  $\frac{\delta \text{Log} \pi(\boldsymbol{\theta}_s^*)}{\delta \boldsymbol{\theta}_s^*} = -(\boldsymbol{\theta}_s^* - \boldsymbol{\Theta}_{s0})' \Sigma_{\boldsymbol{\Theta}_{s0}}^{-1}$ , and  $\frac{\delta \text{Log} \tau_t}{\delta \boldsymbol{\theta}_s^*} = 0$ , and

$$g_t = 1 - e^{\gamma_1} - e^{\gamma_2} - \gamma/2 + e^{\gamma_1} \frac{(r_{t-1} - \mu)^2}{\tau_{t-1}} + \gamma \frac{(r_{t-1} - \mu)^2}{\tau_{t-1}} I_{\{r_{t-1} - \mu < 0\}} + e^{\gamma_2} g_{t-1} \quad (3.5.17)$$

Then,

$$\frac{\delta \text{Log} p(\boldsymbol{\theta}_s^* | \mathbf{r}, \mu, \boldsymbol{\Theta}_L, \omega)}{\delta \boldsymbol{\theta}_s^*} \propto -\frac{1}{2} \sum_{t=1}^T \left( 1 - \frac{(r_t - \mu)^2}{g_t \tau_t} \right) \frac{\delta g_t}{g_t \delta \boldsymbol{\theta}_s^*} - (\boldsymbol{\theta}_s^* - \boldsymbol{\Theta}_{s0})' \Sigma_{\boldsymbol{\Theta}_{s0}}^{-1}$$

where, employing (3.5.17), we compute  $\frac{\delta g_t}{\delta \boldsymbol{\theta}_s^*}$  recursively using:

$$\frac{\delta g_t}{\delta \boldsymbol{\theta}_s^*} = \begin{bmatrix} \frac{\delta g_t}{\delta \gamma_1} \\ \frac{\delta g_t}{\delta \gamma_2} \\ \frac{\delta g_t}{\delta \gamma} \end{bmatrix} = \begin{bmatrix} e^{\gamma_1} \left( -1 + \frac{(r_{t-1} - \mu)^2}{\tau_{t-1}} \right) + e^{\gamma_2} \frac{\partial g_{t-1}^*}{\partial \gamma_1} \\ e^{\gamma_2} (-1 + g_{t-1}^*) + e^{\gamma_2} \frac{\partial g_{t-1}^*}{\partial \gamma_2} \\ -\frac{1}{2} + \frac{(r_{t-1} - \mu)^2}{\tau_{t-1}} I_{\{r_{t-1} - \mu < 0\}} + e^{\gamma_2} \frac{\partial g_{t-1}^*}{\partial \gamma} \end{bmatrix} = \begin{bmatrix} e^{\gamma_1} \left( -1 + \frac{(r_{t-1} - \mu)^2}{\tau_{t-1}} \right) \\ e^{\gamma_2} (-1 + g_{t-1}^*) \\ -\frac{1}{2} + \frac{(r_{t-1} - \mu)^2}{\tau_{t-1}} I_{\{r_{t-1} - \mu < 0\}} \end{bmatrix} + e^{\gamma_2} \begin{bmatrix} \frac{\partial g_{t-1}^*}{\partial \gamma_1} \\ \frac{\partial g_{t-1}^*}{\partial \gamma_2} \\ \frac{\partial g_{t-1}^*}{\partial \gamma} \end{bmatrix}$$

Hence, we can compute the gradient and the Hessian of the log-posterior of  $\boldsymbol{\theta}_s^*$  from which we compute the mean and the covariance of the normal proposal density  $q(\boldsymbol{\theta}_s^*)$ .

**Posterior of  $\boldsymbol{\theta}_L$ :** As for EGARCH-MIDAS, the parameters of the proposal normal density can be computed using (3.5.12) i.e:

$$\frac{\delta \log p(\boldsymbol{\theta}_s^* | \mathbf{r}, \boldsymbol{\mu}, \boldsymbol{\theta}_s, \boldsymbol{\omega})}{\delta \boldsymbol{\theta}_L^*} \propto -\frac{1}{2} \sum_{t=1}^T \left( 1 - \frac{(r_t - \mu)^2}{g_t \tau_t} \right) \left( \frac{\delta g_t}{g_t \delta \boldsymbol{\theta}_L^*} + \frac{\delta \log \tau_t}{\delta \boldsymbol{\theta}_s^*} \right) - (\boldsymbol{\theta}_L - \boldsymbol{\theta}_{L0})' \boldsymbol{\Sigma}_{\boldsymbol{\theta}_{L0}}^{-1} \quad (3.5.18)$$

$\frac{\delta}{\delta \boldsymbol{\theta}_s^*} \log(\tau_t)$  is computed in (3.5.16), and from (3.5.17), we get:

$$\frac{\delta \log g_t}{\delta \boldsymbol{\theta}_L} = \frac{\delta g_t}{g_t \delta \boldsymbol{\theta}_L} = \frac{(r_{t-1} - \mu)^2}{g_t} \left( -\frac{e^\gamma}{\tau_{t-1}} + \gamma I_{\{r_{t-1} - \mu < 0\}} \right) \frac{\partial \log \tau_{t-1}}{\partial \boldsymbol{\theta}_L} + g_{t-1} e^{\gamma_2} \frac{\partial \log g_{t-1}}{\partial \boldsymbol{\theta}_L} \quad (3.5.19)$$

which can be computed recursively.

Then, the gradient  $\frac{\delta}{\delta \boldsymbol{\theta}_L} \text{Log}(p(\boldsymbol{\theta}_s | \mathbf{r}, \boldsymbol{\mu}, \boldsymbol{\Theta}_s, \boldsymbol{\omega}))$  can be evaluated by plugging the values of  $\frac{\delta}{\delta \boldsymbol{\theta}_s^*} \log(\tau_t)$  and  $\frac{\delta \log g_t}{\delta \boldsymbol{\theta}_L}$  in (3.5.19) and the Hessian is equal to the product of gradient and its transpose.

**Posterior of the weighting parameter  $\boldsymbol{\omega}$ :** we simulate draws of  $\boldsymbol{\omega}$  using exactly the same procedure which we discussed for EGARCH-MIDAS specification.

### Posterior distribution of the parameters of the jump component

When a jump component is added to the return specification i.e. the error  $e_t$  is a mixture of two normal variables  $N(0, \tau_t g_t)$  and  $N(\mu_z, \tau_t g_t + \sigma_z^2)$  with jump rate  $\kappa$ , where  $\mu_z$  and  $\sigma_z^2$  are the mean and variance of the size of the jump  $Z_t$  when it occurs ( $B_t = 1$ ), the likelihood function becomes:

$$L(\mathbf{r} | \Theta) = \prod_{t=1}^T \frac{1}{\sqrt{2\pi}} \left( \frac{(1 - \kappa)}{\sqrt{\tau_t g_t}} e^{-\frac{(r_t - \mu)^2}{2\tau_t g_t}} + \frac{\kappa}{\sqrt{\tau_t g_t + \sigma_z^2}} e^{-\frac{(r_t - \mu - \mu_z)^2}{2(\tau_t g_t + \sigma_z^2)}} \right)$$

and

$$\text{Log}L(\mathbf{r} | \Theta) = -2T \log(2\pi) - \frac{1}{2} (1 - \kappa) \sum_{t=1}^T \frac{(r_t - \mu)^2}{\tau_t g_t} - \frac{1}{2} \kappa \sum_{t=1}^T \frac{(r_t - \mu - \mu_z)^2}{(\tau_t g_t + \sigma_z^2)} \quad (3.5.20)$$

Then, the posterior distributions of the parameters  $\boldsymbol{\mu}$ ,  $\boldsymbol{\theta}_s$ , and  $\boldsymbol{\theta}_L$  of the short and long term components will be computed in the same way as done above with no difference on the derivation of the Gradient and the Hessian of the log-posteriors except that we employ (3.5.20) instead of (3.5.6) for their computation because  $\frac{\delta}{\delta \boldsymbol{\theta}_s^*} \log(\tau_t)$  and  $\frac{\delta \log g_t}{\delta \boldsymbol{\theta}_L}$  stays unchanged, as a consequence of capturing the jump component in the error term of the return. However, we need to add one block in our MCMC algorithm to simulate draws from the posteriors of  $(\mu_z, \sigma_z^2)$  and  $(\mu_z, \sigma_z^2, \kappa)$ . This block consists of drawing jointly  $(\mu_z, \sigma_z^2)$ , and then  $\kappa$ .

**Posterior of  $\boldsymbol{\delta} = (\mu_z, \log \sigma_z^2)$ :** We assume a bivariate normal prior  $\pi(\boldsymbol{\delta}) \sim N_2(\boldsymbol{\delta}_0, \boldsymbol{\Sigma}_0)$  where

$\Sigma_0 = \text{diagonal}(10, 1)$ ,  $\delta_0 = (0, \log 10)$  and prior  $\pi(\kappa) = U[0, 0.15]$ , as used by Chan and Grant (2016) in their GARCH(1,1)-J model. Hence, draws from the posteriors  $p(\boldsymbol{\delta} \mid \mathbf{r}, \Theta_{-i})$  and  $p(\boldsymbol{\kappa} \mid \mathbf{r}, \Theta_{-i})$  can be obtained by employing Metropolis-Hasting method using a bivariate normal proposal density  $q(\boldsymbol{\delta})$  and uniform proposal density  $q(\boldsymbol{\kappa}) = U[0, 0.15]$  where:

$$p(\boldsymbol{\delta} \mid \mathbf{r}, \mu, \boldsymbol{\theta}_s, \boldsymbol{\theta}_L, \omega, \kappa) \propto \text{Log}(L(\mathbf{r} \mid \mu, \boldsymbol{\theta}_s, \boldsymbol{\theta}_L, \omega, \boldsymbol{\delta}, \kappa))\pi(\boldsymbol{\delta})$$

where  $L(\mathbf{r} \mid \mu, \boldsymbol{\theta}_s, \boldsymbol{\theta}_L, \omega, \boldsymbol{\delta}, \kappa)$  is defined in (3.5.20). For GARCH(1,1), Chan and Grant (2016) used  $q(\boldsymbol{\delta}) \sim N_2(\bar{\mathbf{r}}, \Sigma_*)$  where  $\Sigma_* = \text{diag}(s, 1)$  and  $s$  is the standard deviation of the mean of  $\mathbf{r}$  but the mean and the covariance of  $\boldsymbol{\delta}$  can also be derived using 2nd order Taylor expansion of  $p(\boldsymbol{\delta} \mid \mathbf{r}, \mu, \boldsymbol{\theta}_s, \boldsymbol{\theta}_L, \omega, \kappa)$  using (3.2.24) and (3.2.25) which we employ in Chapter 4 for SV-MIDAS models.

**Remark:** As in Chapter 2, the summations of the parameters of the above posterior densities will be computed starting from  $t = 22K$  instead of  $t = 1$  if the required initial  $K$  monthly values of  $X_t$  are not available prior to the first month of the returns data.

### 3.5.2 Empirical results

The following plots illustrate movements of the macroeconomic variables

Figure 3.3: Crude Oil WTI daily Price for the period 2000-2021

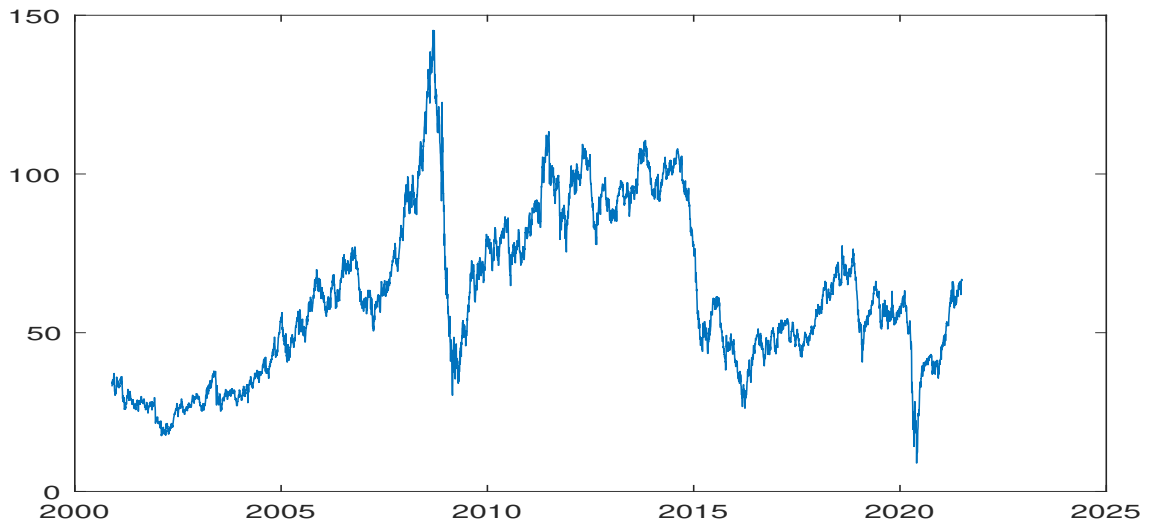




Figure 3.4: Industrial production of US and China, and CFNAI

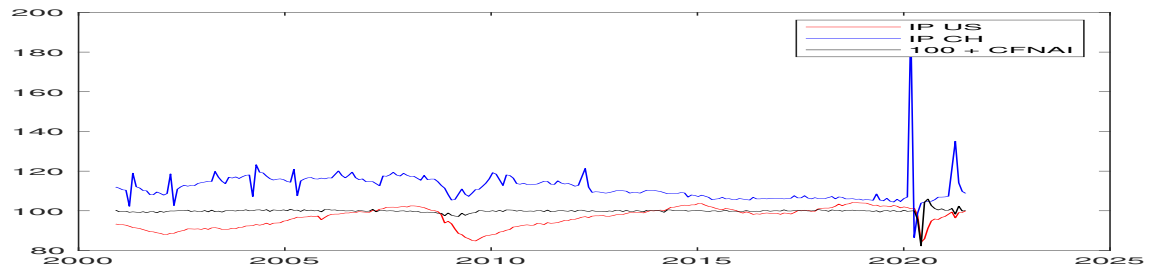


Figure 3.5: Effective Exchange rate of US and China

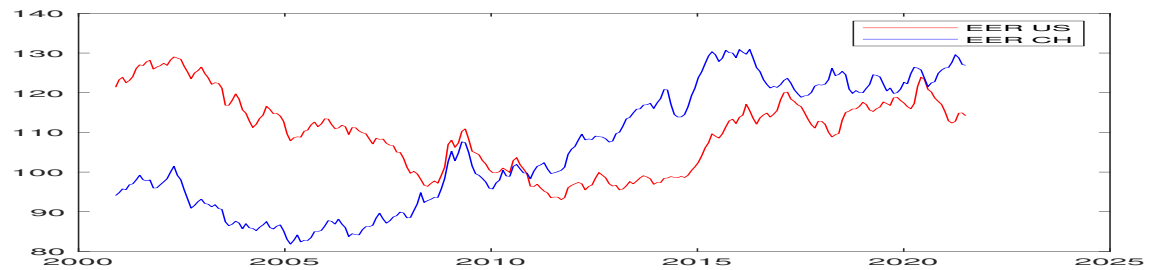


Figure 3.6: GEPU, EPU of US, EPU of China, and EPU of Russia

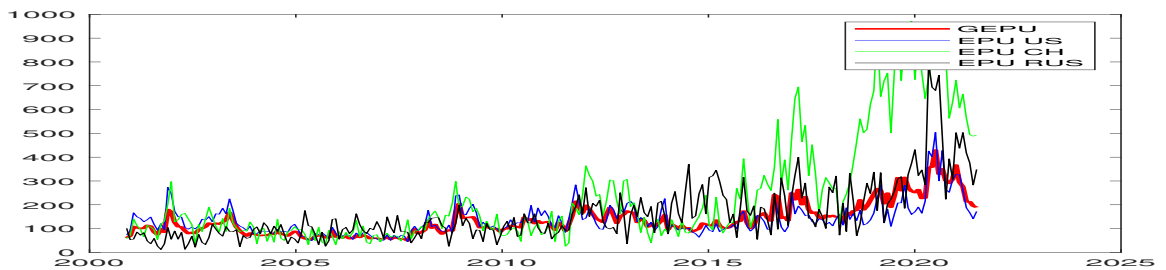
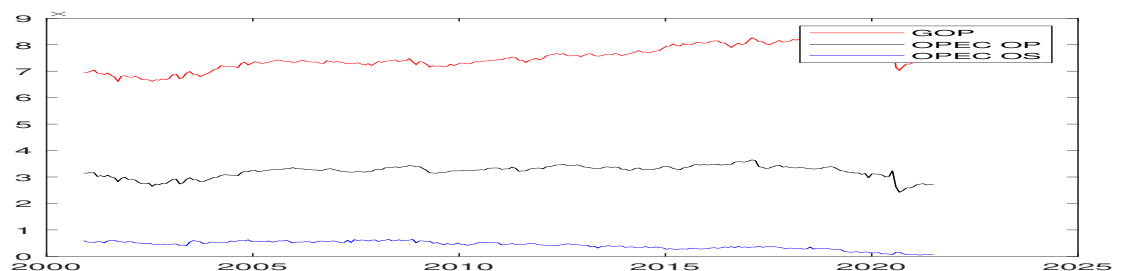


Figure 3.7: Global Oil Production, OPEC Oil Production, OPEC Oil supply



**Table 3.5.1: Estimation results of GARCH-MIDAS models for the period: 9.2000-8.2019**

Macro	Model	$\mu$	$\alpha_0$	$\alpha$	$\beta$	Lev	Persistence	M	$\theta$	$\omega$	$\mu_c$	$\sigma_c^2$	$\kappa$	BIC	LOGL	RMSE
<i>IP<sub>US</sub></i>	G-MIDAS	0.040 (0.040)	0.044	0.139 (0.013)	0.817 (0.016)		0.957	1.979 (0.077)	-0.327 (0.086)	14.352 (4.398)				19866	-9294	15.5
	G-MIDAS-J	0.065 (0.029)	0.023	0.149 (0.000)	0.828 (0.000)		0.977	0.990 (0.000)	-0.355 (0.000)	11.984 (2.636)	-0.016 (0.000)	24.631 (0.000)	0.048 (0.010)	19488	-9055	14.9
	GJR-MIDAS	-0.003 (0.041)	0.035	0.063 (0.010)	0.842 (0.013)	0.121 (0.016)	0.965	2.036 (0.135)	-0.306 (0.080)	13.342 (3.848)				19851	-9280	15.2
	GJR-MIDAS-J	0.044 (0.052)	0.048	0.044 (0.009)	0.848 (0.013)	0.119 (0.017)	0.952	0.816 (0.105)	-0.342 (0.093)	12.145 (3.747)	-0.022 (0.000)	24.096 (0.000)	0.049 (0.005)	19479	-9037	14.9
	EG-MIDAS	-0.020 (0.042)	0.002	0.196 (0.014)	0.969 (0.004)	-0.081 (0.008)	0.969	1.978 (0.066)	-0.382 (0.072)	16.311 (3.502)				19477	-9229	10.4
	EG-MIDAS-J	-0.019 (0.042)	0.002	0.194 (0.013)	0.968 (0.004)	-0.101 (0.008)	0.966	0.910 (0.066)	-0.376 (0.071)	13.359 (3.467)	-0.039 (0.000)	26.477 (0.000)	0.053 (0.005)	19453	-9036	9.2
<i>IP<sub>CH</sub></i>	G-MIDAS	0.032 (0.031)	0.025	0.117 (0.010)	0.858 (0.014)		0.975	2.061 (0.170)	-0.412 (0.073)	7.082 (1.349)				19859	-9291	10.7
	G-MIDAS-J	0.090 (0.039)	0.018	0.133 (0.000)	0.848 (0.000)		0.982	1.031 (0.000)	-0.440 (0.000)	5.000 (0.000)	-0.028 (0.000)	28.902 (0.000)	0.041 (0.009)	19505	-9064	9.3
	GJR-MIDAS	-0.037 (0.031)	0.019	0.073 (0.007)	0.854 (0.012)	0.109 (0.020)	0.981	2.309 (0.084)	-0.404 (0.051)	5.641 (1.312)				19858	-9283	10.6
	GJR-MIDAS-J	0.049 (0.057)	0.038	0.039 (0.009)	0.876 (0.014)	0.094 (0.015)	0.962	0.846 (0.093)	-0.412 (0.048)	7.938 (2.710)	-0.034 (0.000)	28.274 (0.000)	0.043 (0.005)	19455	-9024	9.0
	EG-MIDAS	0.019 (0.042)	0.002	0.218 (0.024)	0.958 (0.006)	-0.090 (0.008)	0.958	1.834 (0.041)	-0.315 (0.034)	5.455 (1.015)				19453	-9225	10.4
	EG-MIDAS-J	0.018 (0.041)	0.002	0.216 (0.024)	0.957 (0.006)	-0.112 (0.008)	0.972	0.844 (0.041)	-0.405 (0.034)	8.732 (1.005)	-0.016 (0.000)	32.589 (0.000)	0.048 (0.006)	19424	-9024	8.9
<i>EE<sub>RUS</sub></i>	G-MIDAS	0.047 (0.049)	0.036	0.138 (0.008)	0.827 (0.010)		0.965	2.111 (0.075)	-0.834 (0.074)	1.097 (0.314)				19863	-9293	11.4
	G-MIDAS-J	0.059 (0.037)	0.017	0.127 (0.000)	0.855 (0.000)		0.983	1.055 (0.000)	-0.883 (0.000)	13.264 (3.898)	0.000 (0.000)	39.842 (0.000)	0.034 (0.009)	19491	-9057	9.6
	GJR-MIDAS	-0.097 (0.019)	0.029	0.055 (0.008)	0.849 (0.010)	0.134 (0.015)	0.971	2.140 (0.076)	-0.838 (0.137)	2.000 (0.000)				19846	-9278	11.1
	GJR-MIDAS-J	-0.007 (0.048)	0.032	0.057 (0.010)	0.849 (0.012)	0.127 (0.017)	0.969	1.426 (0.272)	-0.794 (0.325)	2.751 (2.665)	-0.007 (0.043)	38.976 (67.157)	0.038 (0.032)	19496	-9061	9.8
	EG-MIDAS	0.162 (0.015)	0.001	0.174 (0.012)	0.984 (0.002)	-0.094 (0.004)	0.984	1.935 (0.223)	-0.794 (0.421)	2.388 (3.386)				19494	-9253	10.6
	EG-MIDAS-J	0.154 (0.014)	0.001	0.172 (0.012)	0.983 (0.002)	-0.118 (0.004)	0.967	0.890 (0.221)	-0.874 (0.417)	3.026 (3.352)	-0.016 (0.047)	41.590 (73.873)	0.043 (0.036)	19485	-9060	9.7
<i>EE<sub>RCH</sub></i>	G-MIDAS	0.040 (0.029)	0.027	0.128 (0.006)	0.846 (0.006)		0.973	2.245 (0.031)	-0.339 (0.080)	21.470 (3.998)				19887	-9305	11.3
	G-MIDAS-J	0.049 (0.039)	0.016	0.126 (0.000)	0.858 (0.000)		0.984	1.122 (0.000)	-0.364 (0.000)	8.136 (4.361)	-0.019 (0.000)	25.745 (0.000)	0.047 (0.006)	19458	-9040	9.7
	GJR-MIDAS	0.338 (0.048)	0.029	0.060 (0.009)	0.859 (0.010)	0.104 (0.014)	0.972	1.986 (0.099)	-0.372 (0.182)	9.777 (5.286)				19866	-9288	11.1
	GJR-MIDAS-J	0.028 (0.082)	0.039	0.037 (0.008)	0.874 (0.011)	0.100 (0.015)	0.961	0.893 (0.117)	-0.393 (0.126)	10.606 (4.433)	-0.025 (0.000)	25.186 (0.000)	0.048 (0.004)	19451	-9027	9.3
	EG-MIDAS	-0.036 (0.049)	0.001	0.190 (0.020)	0.978 (0.002)	-0.093 (0.007)	0.978	2.133 (0.082)	-0.237 (0.074)	20.413 (6.291)				19449	-9233	10.3
	EG-MIDAS-J	-0.034 (0.048)	0.001	0.189 (0.020)	0.978 (0.002)	-0.116 (0.007)	0.959	0.981 (0.081)	-0.432 (0.073)	11.666 (6.228)	-0.033 (0.000)	25.470 (0.000)	0.062 (0.005)	19430	-9027	9.2
<i>GE<sub>PU</sub></i>	G-MIDAS	0.039 (0.035)	0.032	0.122 (0.010)	0.846 (0.011)		0.968	1.997 (0.118)	0.046 (0.024)	8.032 (5.162)				19882	-9302	11.2
	G-MIDAS-J	0.066 (0.043)	0.018	0.132 (0.000)	0.849 (0.000)		0.982	0.998 (0.000)	0.054 (0.000)	12.506 (3.930)	-0.010 (0.000)	28.740 (0.000)	0.045 (0.006)	19452	-9037	9.6
	GJR-MIDAS	-0.015 (0.041)	0.028	0.055 (0.009)	0.859 (0.009)	0.117 (0.015)	0.972	2.049 (0.117)	0.054 (0.017)	8.161 (4.845)				19862	-9286	11.0
	GJR-MIDAS-J	0.034 (0.049)	0.044	0.039 (0.009)	0.867 (0.010)	0.101 (0.015)	0.956	0.806 (0.126)	0.070 (0.048)	3.365 (2.241)	-0.016 (0.000)	28.115 (0.000)	0.046 (0.010)	19447	-9021	9.2
	EG-MIDAS	0.137 (0.000)	0.001	0.166 (0.013)	0.982 (0.003)	-0.093 (0.008)	0.982	2.022 (0.159)	0.011 (0.009)	13.089 (5.250)				19445	-9243	10.6
	EG-MIDAS-J	0.130 (0.000)	0.001	0.165 (0.013)	0.981 (0.003)	-0.116 (0.008)	0.966	0.930 (0.157)	0.077 (0.009)	3.701 (5.197)	-0.029 (0.000)	31.429 (0.000)	0.044 (0.010)	19451	-9020	9.1
<i>EP<sub>USA</sub></i>	G-MIDAS	0.045 (0.038)	0.028	0.129 (0.008)	0.844 (0.010)		0.972	2.090 (0.092)	0.014 (0.008)	8.237 (4.437)				19884	-9303	11.4
	G-MIDAS-J	0.074 (0.041)	0.018	0.127 (0.000)	0.855 (0.000)		0.983	1.045 (0.000)	0.015 (0.000)	7.223 (3.885)	-0.001 (0.000)	27.694 (0.000)	0.046 (0.011)	19508	-9065	9.7
	GJR-MIDAS	-0.018 (0.041)	0.026	0.058 (0.009)	0.857 (0.011)	0.117 (0.014)	0.974	2.060 (0.105)	0.004 (0.009)	8.449 (4.349)				19863	-9286	11.1
	GJR-MIDAS-J	-0.008 (0.072)	0.043	0.037 (0.008)	0.866 (0.011)	0.109 (0.015)	0.957	0.995 (0.204)	0.137 (0.036)	2.437 (1.903)	-0.007 (0.000)	27.092 (0.000)	0.047 (0.009)	19454	-9024	9.1
	EG-MIDAS	0.027 (0.046)	0.001	0.269 (0.030)	0.977 (0.004)	-0.091 (0.007)	0.977	2.339 (0.132)	0.017 (0.040)	3.305 (1.389)				19452	-9224	10.4
	EG-MIDAS-J	0.026 (0.045)	0.001	0.266 (0.029)	0.976 (0.004)	-0.114 (0.007)	0.967	1.076 (0.131)	0.150 (0.039)	2.680 (1.375)	-0.033 (0.000)	31.597 (0.000)	0.043 (0.010)	19418	-9023	9.1
<i>EP<sub>UCH</sub></i>	G-MIDAS	0.017 (0.041)	0.028	0.131 (0.008)	0.841 (0.010)		0.972	2.143 (0.095)	-0.060 (0.007)	6.609 (5.037)				19886	-9304	11.4
	G-MIDAS-J	0.063 (0.041)	0.018	0.130 (0.000)	0.852 (0.000)		0.982	1.071 (0.000)	-0.090 (0.000)	10.555 (4.432)	-0.021 (0.000)	34.893 (0.000)	0.036 (0.005)	19450	-9036	9.6
	GJR-MIDAS	-0.010 (0.036)	0.028	0.058 (0.009)	0.857 (0.011)	0.115 (0.015)	0.972	2.026 (0.120)	-0.085 (0.003)	8.472 (4.406)				19863	-9286	11.1
	GJR-MIDAS-J	0.037 (0.045)	0.037	0.039 (0.008)	0.870 (0.009)	0.108 (0.014)	0.963	0.693 (0.172)	-0.078 (0.008)	7.747 (4.900)	-0.027 (0.000)	34.135 (0.000)	0.039 (0.007)	19452	-9039	9.4
	EG-MIDAS	0.040 (0.015)	0.001	0.280 (0.002)	0.975 (0.001)	-0.082 (0.002)	0.975	2.955 (0.037)	0.039 (0.002)	1.003 (0.053)				19450	-9224	10.4
	EG-MIDAS-J	0.038 (0.015)	0.001	0.277 (0.002)	0.974 (0.001)	-0.102 (0.002)	0.976	1.359 (0.037)	-0.086 (0.002)	8.521 (0.052)	-0.017 (0.000)	35.178 (0.000)	0.048 (0.008)	19413	-9039	9.3
<i>GOP</i>	G-MIDAS	0.064 (0.041)	0.030	0.122 (0.008)	0.848 (0.010)		0.970	1.967 (0.065)	0.496 (0.091)	11.382 (4.855)				19883	-9303	11.4
	G-MIDAS-J	0.085 (0.044)	0.022	0.147 (0.000)	0.831 (0.000)		0.978	0.983 (0.000)	0.670 (0.000)	6.707 (5.089)	-0.059 (0.000)	32.859 (0.000)	0.042 (0.004)	19455	-9039	9.8
	GJR-MIDAS	-0.031 (0.041)	0.026	0.053 (0.009)	0.863 (0.009)	0.117 (0.013)	0.974	2.033 (0.077)	0.805 (0.100)	11.321 (4.267)				19860	-9284	11.1
	GJR-MIDAS-J	0.034 (0.049)	0.038	0.034 (0.007)	0.878 (0.009)	0.100 (0.013)	0.962	0.705 (0.111)	0.866 (0.147)	9.589 (4.097)	-0.065 (0.000)	32.145 (0.000)	0.044 (0.009)	19451	-9022	9.4
	EG-MIDAS	-0.025 (0.052)	0.001	0.165 (0.015)	0.982 (0.003)	-0.090 (0.010)	0.982	2.100 (0.080)	0.266 (0.113)	12.768 (4.024)				19449	-9230	10.3
	EG-MIDAS-J	-0.024 (0.052)	0.001	0.164 (0.015)	0.981 (0.003)	-0.113 (0.010)	0.973	0.966 (0.079)	0.953 (0.112)	10.548 (3.984)	-0.021 (0.000)	33.348 (0.000)	0.057 (0.010)	19430	-9022	9.3
<i>OS<sub>OPEC</sub></i>	G-MIDAS	0.071 (0.042)	0.027	0.129 (0.007)	0.844 (0.009)		0.973	2.111 (0.084)	0.243 (0.113)	7.151 (4.508)				19884	-9303	11.6
	G-MIDAS-J	0.099 (0.037)	0.021	0.146 (0.000)	0.833 (0.000)		0.979	1.056 (0.000)	0.291 (0.000)	10.335 (4.035)	-0.064 (0.000)	39.778 (0.000)	0.012 (0.010)	19500	-9061	9.9
	GJR-MIDAS	-0.010 (0.036)	0.029	0.051 (0.009)	0.862 (0.010)	0.116 (0.012)	0.971	1.973 (0.082)								

Table 3.5.2: MCMC and QML Estimates for the period: 4.2000-8.2021

Macroeconomic variable	Model	Method	$\mu$	$\sigma_\mu$	$\sigma$	$\beta$	Lev	Persistence	$\theta$	$\theta^2$	$\theta^3$	$\mu$	$\sigma^2$	$\kappa$	BIC	Local	RMSF	
IP <sub>3</sub>	G-MIDAS	QMLE	0.008	0.000	0.073	0.023	0.000	1.000	-0.242	0.080	0.000	0.000	0.000	0.000	22362	-1155	85.3	
		QMLE	(0.022)		(0.002)	(0.002)			(0.203)	(0.253)	(16.546)							
		MCMC	0.039	0.033	0.113	0.854	0.067	1.876	0.967	1.876	-0.296	6.922	0.051	0.000	0.000	21209	-1066	84.6
	G-MIDAS-J	MCMC	0.047	0.020	0.133	0.847	0.080	0.980	0.980	0.571	-0.356	5.347	-0.027	26.773	0.063	20549	-10374	82.3
		QMLE	(0.063)		(0.000)	(0.000)			(0.000)	(0.000)	(1.288)	(0.000)	(0.000)	(0.010)				
		MCMC	0.049	0.000	0.056	0.918	0.053	1.000	1.000	0.024	0.003	0.000	0.000	0.000	22314	-1127	96.6	
	GJR-MIDAS	QMLE	-0.018	0.016	0.054	0.876	0.109	0.984	0.984	2.252	0.225	5.000	0.000	0.000	21187	-1051	83.5	
		QMLE	(0.013)		(0.009)	(0.014)			(0.000)	(0.000)	(0.000)	(0.000)	(0.000)	(0.010)				
		MCMC	0.025	0.020	0.030	0.898	0.103	0.980	0.980	0.744	-0.391	8.140	-0.045	28.534	0.067	20446	-10308	81.7
	EG-MIDAS	QMLE	-0.028	-0.001	0.186	0.969	-0.080	0.969	0.969	1.957	-0.259	49.677	0.000	0.000	22084	-1107	86.1	
		QMLE	(0.043)		(0.002)	(0.000)	(0.003)			(0.112)	(0.015)	(8.404)						
		MCMC	0.069	0.001	0.211	0.978	-0.063	0.978	0.978	1.755	-0.246	3.152	0.000	0.000	20652	-10479	83.1	
EG-MIDAS-J	MCMC	0.068	0.001	0.190	0.966	-0.113	0.966	0.966	0.655	-0.406	3.152	-0.043	29.419	0.066	20405	-10289	81.6	
	QMLE	(0.050)		(0.004)	(0.009)	(0.012)			(0.055)	(0.050)	(0.990)	(0.000)	(0.000)	(0.010)				
	MCMC	0.044	0.038	0.122	0.859	0.000	0.962	0.962	1.866	-0.284	2.750	0.000	0.000	22114	-11031	99.6		
G-MIDAS	QMLE	0.049	0.024	0.122	0.858	0.000	0.976	0.976	2.102	-0.290	14.314	0.000	0.000	21238	-1081	83.9		
	QMLE	(0.040)		(0.008)	(0.010)				(0.092)	(0.075)	(3.785)							
	MCMC	0.078	0.032	0.110	0.855	0.000	0.968	0.968	0.690	-0.517	11.776	-0.039	31.415	0.056	20569	-10384	82.3	
GJR-MIDAS	QMLE	0.045	0.000	0.053	0.919	0.055	1.000	1.000	0.033	0.149	10.000	0.000	0.000	22098	-11019	96.2		
	QMLE	(0.023)		(0.002)	(0.002)	(0.006)			(0.248)	(0.024)	(1.008)							
	MCMC	-0.022	0.022	0.052	0.865	0.121	0.978	0.978	2.062	-0.253	1.455	0.000	0.000	21191	-10553	83.9		
EG-MIDAS	QMLE	0.046	0.026	0.037	0.881	0.112	0.974	0.974	0.913	-0.530	12.194	-0.019	36.239	0.056	20446	-10308	82.3	
	QMLE	(0.041)		(0.007)	(0.010)	(0.017)			(0.119)	(0.203)	(0.498)	(0.000)	(0.000)	(0.009)				
	MCMC	-0.024	-0.001	0.177	0.971	-0.072	0.971	0.971	1.878	-0.302	4.936	0.000	0.000	22071	-11001	84.6		
EG-MIDAS-J	MCMC	0.115	0.001	0.150	0.900	-0.074	0.984	0.984	1.742	-0.241	19.936	0.000	0.000	20672	-10489	83.2		
	QMLE	(0.043)		(0.002)	(0.000)	(0.003)			(0.111)	(0.003)	(0.527)							
	MCMC	0.113	0.001	0.135	0.972	-0.124	0.972	0.972	0.643	-0.531	19.936	-0.018	36.210	0.059	20406	-10289	81.6	
G-MIDAS	QMLE	0.021	0.000	0.073	0.927	0.000	1.000	1.000	-0.302	0.139	5.001	0.000	0.000	22356	-11152	85.8		
	QMLE	(0.022)		(0.002)	(0.002)				(0.186)	(0.268)	(9.435)							
	MCMC	0.041	0.028	0.130	0.842	0.000	0.972	0.972	2.102	-0.839	2.112	0.000	0.000	21259	-10566	84.0		
G-MIDAS-J	MCMC	0.056	0.033	0.104	0.862	0.000	0.967	0.967	1.011	-0.931	8.729	-0.012	43.307	0.049	20585	-10377	82.1	
	QMLE	(0.057)		(0.010)	(0.010)				(0.090)	(0.153)	(0.351)	(0.000)	(0.000)	(0.008)				
	MCMC	0.049	0.000	0.055	0.918	0.053	1.000	1.000	0.024	0.011	10.000	0.000	0.000	22133	-11126	96.6		
EG-MIDAS	QMLE	-0.022	0.022	0.056	0.855	0.134	0.979	0.979	2.282	-0.283	2.187	0.000	0.000	21813	-10549	84.2		
	QMLE	(0.040)		(0.007)	(0.010)	(0.015)			(0.111)	(0.151)	(0.745)							
	MCMC	0.005	0.017	0.052	0.861	0.141	0.983	0.983	1.560	-0.913	1.646	-0.018	42.532	0.046	20611	-10390	82.7	
EG-MIDAS-J	MCMC	-0.033	-0.003	0.174	0.979	-0.076	0.979	0.979	2.100	0.186	24.230	0.000	0.000	22143	-11022	85.1		
	QMLE	(0.042)		(0.010)	(0.009)	(0.015)			(0.108)	(0.306)	(0.011)	(0.000)	(0.000)	(0.006)				
	MCMC	-0.031	0.001	0.173	0.967	-0.131	0.967	0.967	1.019	-0.927	8.014	0.000	0.000	20550	-10332	82.0		
G-MIDAS	QMLE	0.018	0.000	0.073	0.927	0.000	1.000	1.000	-0.307	0.092	5.000	0.000	0.000	22360	-11154	85.6		
	QMLE	(0.021)		(0.002)	(0.002)				(0.229)	(0.261)	(13.741)							
	MCMC	0.036	0.039	0.130	0.831	0.000	0.961	0.961	1.899	-0.839	1.485	0.000	0.000	21239	-10576	87.2		
G-MIDAS-J	MCMC	0.056	0.025	0.101	0.813	0.000	0.975	0.975	0.050	0.068	(3.292)	0.000	0.000	20548	-10374	82.2		
	QMLE	(0.086)		(0.000)	(0.000)				(0.110)	(0.204)	(4.298)	-0.030	27.984	0.062	20548	-10374	82.2	
	MCMC	0.049	0.000	0.055	0.918	0.053	1.000	1.000	0.023	0.010	10.000	0.000	0.000	22133	-11127	96.5		
GJR-GARCH-MIDAS	QMLE	0.044	0.034	0.067	0.840	0.120	0.967	0.967	2.107	0.330	16.624	0.000	0.000	22305	-10560	86.3		
	QMLE	(0.023)		(0.005)	(0.003)	(0.006)			(0.206)	(0.099)	(120.713)							
	MCMC	0.049	0.000	0.055	0.918	0.053	1.000	1.000	0.000	0.000	(3.578)	0.000	0.000	20447	-10308	87.7		
GJR-MIDAS	QMLE	0.036	0.032	0.041	0.869	0.116	0.968	0.968	0.922	0.430	11.189	-0.039	25.289	0.060	20447	-10308	87.7	
	QMLE	(0.049)		(0.010)	(0.011)	(0.017)			(0.096)	(0.060)	(3.048)	(0.000)	(0.000)	(0.010)				
	MCMC	-0.035	0.001	0.179	0.978	-0.084	0.978	0.978	2.149	-0.670	1.001	0.000	0.000	22115	-11023	85.1		
EG-MIDAS	QMLE	-0.044	0.000	0.031	0.890	0.002	0.980	0.980	1.216	-0.143	11.189	0.000	0.000	20658	-10488	83.0		
	QMLE	(0.044)		(0.000)	(0.001)	(0.002)			(0.126)	(0.143)	(0.189)							
	MCMC	-0.040	0.002	0.194	0.971	-0.078	0.971	0.971	1.946	-0.373	15.725	0.000	0.000	20658	-10488	83.0		
EG-MIDAS-J	MCMC	-0.009	0.002	0.174	0.959	-0.128	0.959	0.959	0.846	-0.473	15.725	-0.037	28.300	0.078	20406	-10289	84.5	
	QMLE	(0.047)		(0.009)	(0.003)	(0.010)	(0.016)		(0.039)	(0.057)	(2.895)	(0.000)	(0.000)	(0.000)				
	MCMC	0.017	0.000	0.073	0.927	0.000	1.000	1.000	-0.031	0.119	5.000	0.000	0.000	22364	-11156	85.2		
G-MIDAS	QMLE	0.044	0.028	0.121	0.851	0.000	0.972	0.972	0.204	0.021	9.927	0.000	0.000	21239	-10576	87.2		
	QMLE	(0.043)		(0.012)	(0.014)				(0.106)	(0.017)	(4.875)							
	MCMC	-0.021	0.028	0.122	0.851	0.000	0.972	0.972	1.289	0.069	1.547	-0.021	31.239	0.061	20565	-10382	82.1	
G-MIDAS-J	MCMC	0.049	0.000	0.055	0.918	0.053	1.000	1.000	0.023	-0.009	10.000	0.000	0.000	22133	-11127	96.7		
	QMLE	(0.023)		(0.005)	(0.002)	(0.006)			(0.254)	(0.117)	(178.124)							
	MCMC	0.019	0.020	0.089	0.911	(0.013)	0.980	0.980	0.079	0.015	(4.736)	-0.034	34.072	0.056	20550	-10360	82.4	
GJR-MIDAS	QMLE	-0.026	0.000	0.185	0.971	-0.078	0.971	0.971	1.943	0.227	49.904	0.000	0.000	22089	-11010	86.1		
	QMLE	(0.043)		(0.002)	(0.000)	(0.003)			(0.116)	(0.013)	(14.945)							
	MCMC	-0.054	0.001	0.185	0.978	-0.079	0.978	0.978	2.128	0.020	12.559	0.000	0.000	20669	-10487	82.9		
EG-MIDAS	QMLE	0.041	0.000	0.039	0.903	0.007	0.966	0.966	0.073	0.088	(4.349)	0.000	0.000	20509	-10319	81.8		
	QMLE	(0.048)		(0.010)	(0.002)	(0.009)			(0.059)	(0.039)	(3.568)	(0.000)	(0.000)	(0.004)				
	MCMC	0.013	0.000	0.073	0.927	0.000	1.000	1.000	0.020	0.080	5.000	0.000	0.000	22357	-11153	85.9		
G-MIDAS	QMLE	0.001	0.029	0.122	0.849	0.000	0.971	0										

Table 3.5.3: QML Estimates of the models when MCMC estimates are used as initial values

Model	Macro	$\mu$	$\alpha$	$\beta$	lev	per	m	$\theta$	$\omega$	bic	logl	rmse
G-MIDAS	<i>IP<sub>US</sub></i>	0.033	0.119	0.830		0.949	1.835	-0.386	5.742	19927.44	-9838.20	18.64
	<i>IP<sub>CH</sub></i>	0.035	0.111	0.856		0.967	1.825	-0.232	8.649	19932.75	-9840.85	18.93
	<i>EER<sub>US</sub></i>	0.032	0.110	0.859		0.969	1.799	-0.602	1.001	19931.06	-9840.01	18.67
	<i>EER<sub>CH</sub></i>	0.035	0.116	0.848		0.963	1.874	-0.363	10.231	19913.42	-9831.18	18.54
	<i>GEP<sub>U</sub></i>	0.031	0.108	0.856		0.963	1.872	0.054	2.060	19934.80	-9841.87	18.57
	<i>EP<sub>UUS</sub></i>	0.034	0.110	0.859		0.969	1.824	-0.007	8.917	19936.94	-9842.94	18.61
	<i>EP<sub>UCH</sub></i>	0.032	0.104	0.866		0.970	1.856	0.002	49.985	19934.92	-9841.94	18.75
	<i>GOP</i>	0.034	0.100	0.870		0.971	1.787	0.421	49.944	19925.06	-9837.00	18.55
	<i>OP<sub>OPEC</sub></i>	0.032	0.105	0.858		0.963	1.747	0.222	2.281	19919.59	-9834.27	18.44
	<i>OS<sub>OPEC</sub></i>	0.031	0.107	0.861		0.968	1.954	-0.019	1.112	19929.80	-9839.38	18.76
GJR-MIDAS	<i>IP<sub>US</sub></i>	-0.002	0.050	0.871	0.089	0.966	1.816	-0.342	13.506	19908.07	-9824.26	16.34
	<i>IP<sub>CH</sub></i>	-0.015	0.057	0.884	0.089	0.985	2.215	-0.385	5.747	19917.43	-9828.94	16.36
	<i>EER<sub>US</sub></i>	-0.013	0.044	0.886	0.097	0.978	1.875	-0.676	1.874	19904.16	-9822.30	16.46
	<i>EER<sub>CH</sub></i>	0.012	0.049	0.878	0.084	0.969	1.759	-0.310	9.772	19910.24	-9825.34	16.40
	<i>GEP<sub>U</sub></i>	-0.005	0.048	0.883	0.084	0.973	1.804	0.027	8.165	19913.12	-9826.78	16.40
	<i>EP<sub>UUS</sub></i>	-0.010	0.048	0.883	0.087	0.974	1.794	-0.009	8.422	19911.01	-9825.72	16.36
	<i>EP<sub>UCH</sub></i>	-0.017	0.052	0.882	0.089	0.979	2.004	0.000	8.340	19915.45	-9827.95	16.35
	<i>GOP</i>	-0.007	0.044	0.888	0.083	0.973	1.732	0.713	12.242	19908.62	-9824.53	16.39
	<i>OP<sub>OPEC</sub></i>	-0.005	0.043	0.880	0.090	0.968	1.712	0.386	7.085	19902.41	-9821.42	16.39
	<i>OS<sub>OPEC</sub></i>	-0.013	0.051	0.884	0.090	0.980	2.049	-0.025	8.085	19914.09	-9827.27	16.40
EG-MIDAS	<i>IP<sub>US</sub></i>	-0.035	0.189	0.959	-0.068	0.959	1.806	-0.518	16.040	19711.65	-9821.79	15.79
	<i>IP<sub>CH</sub></i>	-0.025	0.174	0.973	-0.064	0.973	1.861	-0.367	5.352	19715.97	-9823.95	15.80
	<i>EER<sub>US</sub></i>	-0.015	0.166	0.974	-0.067	0.974	1.727	-0.717	2.388	19727.62	-9829.78	15.82
	<i>EER<sub>CH</sub></i>	-0.022	0.172	0.973	-0.065	0.973	1.843	-0.153	11.064	19724.12	-9828.03	15.84
	<i>GEP<sub>U</sub></i>	-0.031	0.169	0.974	-0.063	0.974	1.869	0.006	12.905	19723.08	-9827.51	15.82
	<i>EP<sub>UUS</sub></i>	-0.036	0.172	0.977	-0.064	0.977	1.924	0.017	3.325	19722.45	-9827.19	15.80
	<i>EP<sub>UCH</sub></i>	-0.033	0.178	0.973	-0.063	0.973	2.273	0.026	1.173	19722.29	-9827.11	15.82
	<i>GOP</i>	-0.034	0.170	0.975	-0.060	0.975	1.858	0.382	12.817	19717.36	-9824.64	15.79
	<i>OP<sub>OPEC</sub></i>	-0.021	0.171	0.974	-0.063	0.974	1.897	0.044	9.996	19722.66	-9827.29	15.82
	<i>OS<sub>OPEC</sub></i>	-0.025	0.170	0.974	-0.064	0.974	1.879	-0.051	7.712	19723.48	-9827.71	15.81

Notes: This table reports the estimation results of GARCH-MIDAS, GJR-GARCH-MIDAS, and EGARCH-MIDAS using QML estimation approach when MCMC estimates are selected as initial values.

Table 3.5.4: RMSE LOSS function 2000-2019

Macro	Model	1	5	10	15	20
<i>IP<sub>US</sub></i>	GJR-MIDAS	0.994	0.993	0.996	0.954	0.979
	EG-MIDAS	0.988	0.987	0.989	0.951	0.971
	G-MIDAS-J	1.003	1.007	1.011	1.01	1.005
	GJR-MIDAS-J	0.988	0.987	0.992	0.869	0.895
	EG-MIDAS-J	0.984	0.983	0.987	0.802	0.84
<i>IP<sub>CH</sub></i>	GJR-MIDAS	1	1	1	0.971	0.992
	EG-MIDAS	0.983	0.98	0.978	0.879	0.898
	G-MIDAS-J	0.992	0.991	0.991	0.872	0.864
	GJR-MIDAS-J	0.985	0.983	0.983	0.825	0.84
	EG-MIDAS-J	0.981	0.977	0.978	0.75	0.774
<i>EER<sub>US</sub></i>	GJR-MIDAS	1.004	1.002	1.004	0.916	0.944
	EG-MIDAS	0.993	0.993	0.995	0.911	0.931
	G-MIDAS-J	0.993	0.993	0.996	0.88	0.884
	GJR-MIDAS-J	0.984	0.977	0.981	0.899	0.922
	EG-MIDAS-JJ	0.966	0.967	0.966	0.774	0.805
<i>EER<sub>CH</sub></i>	GJR-MIDAS	0.987	0.984	0.984	0.872	0.882
	EG-MIDAS	0.988	0.985	0.984	0.895	0.928
	G-MIDAS-J	0.994	0.995	0.994	0.89	0.868
	GJR-MIDAS-J	0.986	0.983	0.983	0.775	0.785
	EG-MIDAS-J	0.98	0.972	0.973	0.718	0.737
<i>GEP<sub>U</sub></i>	GJR-MIDAS	0.995	0.994	0.995	0.937	0.964
	EG-MIDAS	0.97	0.97	0.969	0.934	0.988
	G-MIDAS-J	1.008	1.008	1.009	0.949	0.942
	GJR-MIDAS-J	0.992	0.991	0.993	0.886	0.907
	EG-MIDAS-J	0.98	0.974	0.978	0.78	0.81
<i>EPU<sub>USA</sub></i>	GJR-MIDAS	0.994	0.993	0.993	0.912	0.934
	EG-MIDAS	0.984	0.985	0.986	0.894	1.147
	G-MIDAS-J	0.992	0.993	0.994	0.931	0.919
	GJR-MIDAS-J	0.986	0.984	0.986	0.814	0.836
	EG-MIDAS-J	0.981	0.977	0.982	0.803	0.889
<i>EPU<sub>CH</sub></i>	GJR-MIDAS	0.989	0.986	0.986	0.9	0.92
	EG-MIDAS	0.983	0.986	0.991	1.157	1.247
	G-MIDAS-J	0.997	0.998	1	0.957	0.953
	GJR-MIDAS-J	0.983	0.98	0.981	0.816	0.834
	EG-MIDAS-J	0.97	0.964	0.967	0.779	0.806
<i>GOP</i>	GJR-MIDAS	1	0.998	0.999	0.925	0.949
	EG-MIDAS	0.996	1	1.002	0.923	0.949
	G-MIDAS-J	0.991	0.989	0.989	0.917	0.894
	GJR-MIDAS-J	0.989	0.986	0.988	0.867	0.891
	EG-MIDAS-J	0.988	0.982	0.984	0.792	0.825
<i>OP<sub>OPEC</sub></i>	GJR-MIDAS	0.996	0.993	0.994	0.98	0.902
	EG-MIDAS	0.993	0.99	0.989	0.932	0.969
	G-MIDAS-J	1.004	1.006	1.007	1.045	1.047
	GJR-MIDAS-J	0.994	0.991	0.992	0.84	0.863
	EG-MIDAS-J	0.989	0.981	0.984	0.767	0.796
<i>OS<sub>OPEC</sub></i>	GJR-MIDAS	1.002	1.002	1.008	1.151	1.199
	EG-MIDAS	0.998	0.995	0.997	0.991	0.989
	G-MIDAS-J	0.991	0.993	0.996	0.919	0.945
	GJR-MIDAS-J	0.987	0.986	0.991	0.902	0.926
	EG-MIDAS-J	0.983	0.978	0.984	0.839	0.867

Notes: GJR-MIDAS refers to GJR-GARCH-MIDAS, EG-MIDAS, refers to EGARCH-MIDAS, and G-MIDAS refers to GARCH-MIDAS. This table reports RMSE loss of the  $k$ -day total volatility forecast for  $k = 1, 5, 10, 15, 20$ . RMSE loss is the ratio of RMSE of the reported models in this table to RMSE of GARCH-MIDAS. The preferred model is the one with the smallest RMSE loss.

Table 3.5.5: QLIKE LOSS function 2000-2019

Macro	Model	1	5	10	15	20
<i>IP<sub>US</sub></i>	GJR-MIDAS	1.095	1.144	1.099	1.103	1.098
	EG-MIDAS	0.978	1.021	1.001	1.057	1.038
	G-MIDAS-J	0.966	0.964	1	0.879	0.885
	GJR-MIDAS-J	0.964	1.023	0.975	0.898	0.899
	EG-MIDAS-J	0.955	0.93	0.912	0.54	0.549
<i>IP<sub>CH</sub></i>	GJR-MIDAS	1.075	1.113	1.072	1.104	1.097
	EG-MIDAS	0.943	0.982	0.949	0.978	0.959
	G-MIDAS-J	0.948	0.946	0.971	0.847	0.855
	GJR-MIDAS-J	0.943	0.993	0.946	0.876	0.88
	EG-MIDAS-J	0.837	0.825	0.803	0.524	0.529
<i>EER<sub>US</sub></i>	GJR-MIDAS	1.078	1.124	1.076	1.096	1.078
	EG-MIDAS	0.969	0.971	0.991	0.992	1
	G-MIDAS-J	0.911	0.954	0.926	0.855	0.859
	GJR-MIDAS-J	0.985	1.04	0.993	0.919	0.918
	EG-MIDAS-J	0.845	0.824	0.789	0.53	0.533
<i>EER<sub>CH</sub></i>	GJR-MIDAS	1.058	1.098	1.057	1.052	1.049
	EG-MIDAS	0.958	1	0.971	1.005	0.984
	G-MIDAS-J	0.956	0.946	0.98	0.842	0.85
	GJR-MIDAS-J	0.968	1.023	0.983	0.858	0.857
	EG-MIDAS-J	0.786	0.782	0.765	0.524	0.524
<i>GEP<sub>U</sub></i>	GJR-MIDAS	1.032	1.08	1.036	1.046	1.062
	EG-MIDAS	0.886	0.928	0.901	0.971	0.992
	G-MIDAS-J	1.004	0.998	1.012	0.926	0.917
	GJR-MIDAS-J	0.908	0.965	0.921	0.844	0.863
	EG-MIDAS-J	0.722	0.737	0.725	0.535	0.543
<i>EPU<sub>USA</sub></i>	GJR-MIDAS	1.073	1.131	1.062	1.094	1.097
	EG-MIDAS	0.915	0.954	0.939	1.022	1.046
	G-MIDAS-J	0.941	0.942	0.977	0.871	0.884
	GJR-MIDAS-J	0.921	0.999	0.935	0.855	0.867
	EG-MIDAS-J	0.778	0.839	0.882	0.587	0.626
<i>EPU<sub>CH</sub></i>	GJR-MIDAS	1.057	1.094	1.056	1.075	1.072
	EG-MIDAS	0.902	0.935	0.941	1.036	1.038
	G-MIDAS-J	0.942	0.938	0.946	0.876	0.88
	GJR-MIDAS-J	0.93	0.979	0.933	0.864	0.872
	EG-MIDAS-J	0.645	0.647	0.649	0.562	0.561
<i>GOP</i>	GJR-MIDAS	0.994	0.992	0.991	0.981	0.973
	EG-MIDAS	0.968	0.949	0.986	1.05	0.947
	G-MIDAS-J	0.98	1.039	0.988	0.923	0.935
	GJR-MIDAS-J	0.925	0.923	0.927	0.909	0.906
	EG-MIDAS-J	0.871	0.857	0.826	0.542	0.543
<i>OP<sub>OPEC</sub></i>	GJR-MIDAS	1.106	1.157	1.104	1.095	1.082
	EG-MIDAS	0.964	1.02	0.975	1.039	1.01
	G-MIDAS-J	0.941	0.936	0.939	0.916	0.918
	GJR-MIDAS-J	0.986	1.051	0.999	0.904	0.902
	EG-MIDAS-J	0.945	0.929	0.887	0.541	0.542
<i>OS<sub>OPEC</sub></i>	GJR-MIDAS	1.05	1.099	1.071	1.161	1.164
	EG-MIDAS	0.938	0.992	0.971	1.03	1.033
	G-MIDAS-J	0.943	0.941	0.957	0.933	0.926
	GJR-MIDAS-J	0.941	0.939	0.944	0.907	0.908
	EG-MIDAS-J	0.677	0.699	0.687	0.577	0.58

Notes: GJR-MIDAS refers to GJR-GARCH-MIDAS, EG-MIDAS, refers to EGARCH-MIDAS, and G-MIDAS refers to GARCH-MIDAS. This table reports QLIKE loss of the  $k$ -day total volatility forecast for  $k = 1, 5, 10, 15, 20$ . QLIKE loss is the ratio of QLIKE of the reported models in this table to QLIKE of GARCH-MIDAS. The preferred model is the one with the smallest QLIKE loss.

Table 3.5.6: and MCMC estimates of GARCH-MIDAS -DGP GARCH-MIDAS-J

	$\mu$	$\alpha$	$\beta$	m	$\theta$	$\omega$
Low	0	0.08	0.9	0.1	0.6	10
G-MIDAS-QMLE	0.003 (0.027)	0.080 (0.006)	0.889 (0.007)	0.337 (0.143)	0.071 (0.240)	19.973 (69.261)
G-MIDAS-MCMC	0.002 (0.036)	0.086 (0.008)	0.893 (0.011)	1.023 (0.136)	0.181 (0.114)	10.315 (4.044)
Medium	0	0.05	0.92	0.1	0.3	10
G-MIDAS-QMLE	-0.003 (0.030)	0.051 (0.004)	0.918 (0.006)	0.070 (0.090)	0.130 (0.050)	15.238 (20.847)
G-MIDAS-MCMC	-0.006 (0.036)	0.052 (0.005)	0.914 (0.009)	0.243 (0.072)	0.126 (0.081)	8.555 (3.208)
Large	0	0.08	0.85	-0.1	-0.45	10
G-MIDAS-QMLE	-0.006 (0.025)	0.086 (0.007)	0.831 (0.011)	0.037 (0.035)	-0.142 (0.019)	18.285 (6.303)
G-MIDAS-MCMC	-0.010 (0.039)	0.087 (0.008)	0.832 (0.016)	0.077 (0.056)	-0.148 (0.056)	9.571 (3.306)

MCMC estimates obtained by simulating 40000 iterations, and 15000 burnins. Standard deviations are given in brackets. Low, Medium, and Large, represents Low, Medium, and large breaks in the simulated volatility.

Table 3.5.7: QML and MCMC estimates of GJR-GARCH-MIDAS - DGP GJR-GARCH-MIDAS-J

Parameter	$\mu$	$\alpha$	$\beta$	$\gamma$	m	$\theta$	$\omega$
Low	0	0.05	0.85	0.1	-0.1	0.3	10
GJR-MIDAS-QMLE	-0.003 (0.022)	0.054 (0.007)	0.846 (0.008)	0.147 (0.015)	0.853 (0.179)	0.101 (0.040)	14.226 (24.214)
GJR-MIDAS-MCMC	-0.005 (0.0364)	0.0601 (0.0009)	0.8461 (0.0009)	0.13 (0.0017)	0.7161 (0.067)	0.203 (0.0828)	8.5048 (2.3883)
Medium	0	0.06	0.85	0.1	-0.1	0.3	10
GJR-MIDAS-QMLE	-0.001 (0.023)	0.047 (0.008)	0.840 (0.012)	0.114 (0.015)	0.958 (0.076)	0.184 (0.042)	25.085 (60.019)
GJR-MIDAS-MCMC	0.005 (0.038)	0.057 (0.009)	0.834 (0.013)	0.099 (0.013)	0.921 (0.066)	0.170 (0.070)	11.626 (3.375)
Large	0	0.06	0.85	0.1	-0.1	-0.45	10
GJR-MIDAS-QMLE	0.012 (0.019)	0.084 (0.009)	0.779 (0.014)	0.126 (0.017)	0.771 (0.075)	-0.225 (0.028)	28.668 (14.334)
GJR-MIDAS-MCMC	-0.010 (0.036)	0.062 (0.007)	0.846 (0.009)	0.085 (0.010)	0.755 (0.061)	-0.269 (0.072)	6.279 (2.079)

MCMC estimates obtained by simulating 40000 iterations, and 15000 burnins. Standard deviations are given in brackets. Low, Medium, and Large, represents Low, Medium, and Large breaks in the simulated volatility.

Table 3.5.8: QML and MCMC estimates of EGARCH-MIDAS - DGP EGARCH-MIDAS-J

	$\mu$	c	$\beta$	$\gamma$	$\alpha$	m	$\theta$	$\omega$
Medium	0		0.9	-0.1	0.05	-0.1	0.4	5
EG-MIDAS-QMLE	-0.020 (0.025)	0.001 (3.090)	0.878 (0.026)	-0.060 (0.025)	-0.019 (0.012)	0.598 (3.576)	0.235 (0.016)	10.422 (2.126)
EG-MIDAS-MCMC	-0.019 (0.025)	0.008 (0.982)	0.885 (0.027)	-0.072 (0.035)	0.030 (0.019)	0.489 (0.017)	0.279 (0.012)	9.235 (0.893)
Large	0		0.9	-0.05	0.05	-0.1	-0.45	10
EG-MIDAS-QML	-0.004 (0.017)	0.001 (0.011)	0.913 (0.009)	-0.073 (0.008)	-0.004 (0.010)	0.401 (0.101)	-0.321 (0.011)	30.013 (9.631)
EG-MIDAS-MCMC	-0.009 (0.030)	0.006 (0.001)	0.933 (0.012)	-0.063 (0.007)	0.016 (0.009)	0.693 (0.076)	-0.321 (0.043)	15.836 (2.901)

MCMC estimates obtained by simulating 40000 iterations, and 15000 burnins. Standard deviations are given in brackets. Low, Medium, and Large, represents Low, Medium, and large breaks in the simulated volatility.





# Bayesian MCMC Approach to Heston-SV-MIDAS Models with Jump

## 4.1 Introduction

Continuous time stochastic volatility (SV) models have been popular in modeling volatility of high frequency financial asset. The standard SV model specifies that the logged volatility follows a latent AR(1) process while the SV-L is an extension by incorporating the leverage effect through the correlation between the error term in the return equation and the error term in the volatility equation. These models have been used as an approximation to the continuous-time stochastic diffusion model (Hall and White (1987)) and their econometrics are described in Taylor (1986).

Men et al. (2016) showed that the SV models better capture the stylised properties of financial asset returns, especially when GARCH models tend to produce extremely high persistence. Furthermore, the SV model with normal errors seems to provide the better fit than GARCH with heavy tailed error distribution, see also Broto and Ruiz (2004) and Carnero et al. (2003)).

The SV models have been estimated using classical methods (Method of Moment and Maximum Likelihood estimation). However, these estimation methods tend to become complicated because the time-varying volatility is unknown and stochastic. This led to the extensive developments of the Markov Chain Monte Carlo Method (MCMC) algorithm, which was proposed by Jacquier et al. (1994). Unfortunately, Jacquier et al. (1994) method has a very limited success in improving the performance of the Heston Model as stated by Shephard and Kim (1994) because it updates the latent volatility, one at a time. This single-move sampler typically requires a large number of iterations before the MCMC estimate converges. Therefore, various MCMC extensions have been proposed in order to speed up the convergence of the algorithm. In the literature, SV-L model has been estimated mostly by Bayesian MCMC approach due to its statistical efficiency, convenience of implementation, and flexibility of modelling complex model. A number of extensions have also been proposed to improve the model fit, e.g. Chan and Grant (2016).

The discrete version of the continuous-time Heston (1993) model is similar to the SV-L model, though the variance,  $\sigma_t^2$ , also has a volatility equal to  $\sigma_{t-1}^2$ . The other feature is that the variance

of the return is equal to  $\sigma_{t-1}^2$ , not  $\sigma_t^2$ , which may better describe the impact of leverage effect as Black (1976) argued that future volatility may be negatively correlated with returns. The Heston model has been routinely applied in options pricing.

The Heston (1993) model, models volatility clustering and the leverage effect using SQR structure. However, Jones(2003), and Ait Sahalia (2007) recognized that the SQR model cannot capture important stylized facts which led Bates (2001), Andersen, Benzoni and Lund (2002), and Broadie, Chernov and Johannes (2007) to improve the Heston Model by adding jump components in the return and/or in the volatility equation. The resulting jump augmented models outperform the standard SV models in terms of the in-sample fit, but not necessarily in terms of out-of-sample forecasting. This motivated Heston (1997) and Christofferson et al. (2007) to develop alternative models such as 3/2 Heston model where the variance of the volatility is  $\sigma_{t-1}^{3/2}$  instead of  $\sigma_{t-1}$ . Grasselli (2017) proposes the 4/2 Heston model whose volatility is expressed as the sum of volatility of Heston model and that of 3/2 Heston Model. Other extensions have also been proposed, in the literature, such as switching regime Heston model and Heston-STAR model of Stramer et al. (2017).

In this study, we aim to extend the SV, SVL, and Heston models to SV-MIDAS, SVL-MIDAS, Heston-MIDAS and their jump augmented models by modelling the total volatility,  $\sigma_t^2$  as a product of a long term volatility component,  $\tau_t$  (summarizing the impact of the macroeconomic variables), and a short term volatility component,  $g_t$  (following the SV model). To this end, we develop the Bayesian MCMC estimation algorithm. In particular, we suggest a procedure for choosing the tuning parameter (variance) in the crucial step of the Metropolis-Hastings algorithm using random-walk process, to improve the efficiency and speed up the convergence of the MCMC algorithm, for simulating the posteriors of the volatility sequence.

We note that the parameters of alternative SV-MIDAS models and their jump augmented extensions can be directly estimated, using the Bayesian MCMC algorithm, from their posterior distributions, as their likelihood function can be expressed using known densities such as normal density, log normal density, and inverse gamma density, unlike alternative GARCH-MIDAS models parameters which are estimated using Metropolis-Hastings approach.

We confirm the reliability of the Bayesian MCMC approach via a comprehensive simulation study. First, we investigate the validity of the bayesian MCMC estimates of alternative SV-MIDAS models when generated dataset does not contain outliers. Second, we investigate the accuracy of the bayesian MCMC estimates when alternative jump augmented SV-MIDAS models are applied to generated dataset with outliers. Our findings suggest the reliability of the Bayesian MCMC approach in capturing different levels of leverage effect (low, medium, and high), in capturing the correct impact of the important parameter  $\psi$  that defines the impact of the macroeconomic variable (MIDAS regression), and in capturing different levels of outliers successfully through the jump component in the extended models.

In the empirical study, we model WTI returns using the proposed SV-MIDAS models and their jump augmented extensions by employing 10 economic indicators known for their impact on WTI returns volatility. Our results suggest that Heston-MIDAS-J, SVL-MIDAS-J are the favoured models according to DIC<sup>1</sup>. Also, we note that unlike the Heston model (benchmark), Heston-MIDAS was able to detect a negative leverage effect comparable to SVL-MIDAS model.

This Chapter is organized as follows: In Section 2 we describe the SV, SV-L and Heston models, and develop their MIDAS extensions. Section 3 presents the Bayesian MCMC estimation algorithms. In Section 4, we investigate the finite sample performance of the proposed MCMC approach via extensive simulation experiments. Section 5 provides an empirical application to WTI returns. Section 6 concludes.

## 4.2 The Models

Taylor(1994) proposed the following stochastic volatility (SV) model:

$$r_t = \mu + e^{h_t/2} \varepsilon_t \quad (4.2.1)$$

$$h_t = \alpha_0 + \phi (h_{t-1} - \alpha_0) + \sigma_h \eta_t \quad (4.2.2)$$

$$h_0 \sim N\left(\alpha_0, \frac{\sigma_h^2}{1 - \phi^2}\right)$$

where  $\mu$ ,  $\alpha_0$ ,  $\phi$ , and  $\sigma_h$  are the parameters, and  $\varepsilon_t$  and  $\eta_t$  are *iid*  $N(0, 1)$ . The volatility persistence parameter  $\phi$  satisfies  $|\phi| < 1$  to ensure weak stationarity. In the SV model,  $r_t \sim N(\mu, e^{h_t})$ , and  $\varepsilon_t$  and  $\eta_t$  are independent.

To accommodate the leverage effect, the stochastic volatility with leverage (SV-L) model allows the error terms,  $\varepsilon_{t+1}$  and  $\eta_t$  to be correlated, i.e.  $(\varepsilon_{t+1}, \eta_t)$  follows a bivariate normal distribution with mean 0 and variance  $\Sigma = \begin{bmatrix} 1 & \rho \\ \rho & 1 \end{bmatrix}$ . The leverage effect is present if  $\rho$  is negative, which can be seen from the expression of  $E(h_{t+1} | r_t)$  given by (Men et al. (2017))

$$E(h_{t+1} | r_t) = \alpha_0 (1 - \phi) + \frac{\alpha_0 \phi}{1 + \phi} + \rho \sigma_h e^{(-\sigma_h^2/4(1-\sigma_h^2)^2 + \alpha_0 \sigma_h/(1-\phi^2)) r_t} \quad (4.2.3)$$

Alternatively, Jackier et al. (2004) assumes that  $(\varepsilon_t, \eta_t)$  are correlated instead of  $(\varepsilon_{t+1}, \eta_t)$ . However, the leverage effect is not guaranteed to exist in this formulation because Asai et al. (2006) showed:

$$\frac{dh_{t+1}}{dr_t} = \frac{\rho \sqrt{\sigma_h} e^{h_{t+1}/e^{h_t}}}{(1 + 0.5\rho \sqrt{\sigma_h} \varepsilon_{t+1})}$$

<sup>1</sup>DIC is a Bayesian method for model comparison Shriener (2009). Following Spiegelhalter et al. (2002)  $DIC = D(y, \hat{\Theta}) + 2pD$ , where  $D(y, \hat{\Theta}) = 2\log(p(y|\hat{\Theta}))$ , and  $pD = \text{var}(D(y, \hat{\Theta}))$ .

whose sign can be negative if  $\rho > 0$  and  $\varepsilon_{t+1} < -2/\rho\sqrt{\sigma_h}$ . This can occur if the returns data contain large outliers because  $\rho\sqrt{\sigma_h}$  is usually quite small. For this reason we use the first formulation.

Heston (1993) proposed the continuous time Heston model which is defined by

$$\frac{dS_t}{S_t} = \mu dt + \sqrt{g(t)} dW(t) \quad (4.2.4a)$$

$$dg(t) = \kappa(\theta - g(t))dt + \sigma_g\sqrt{g(t)}dB(t) \quad (4.2.4b)$$

where  $S(t)$  is the price at time  $t$ ,  $W(t)$  and  $B(t)$  are correlated Weiner processes,  $\rho dt = \text{cor}(dW(t), dB(t))$ , and  $\mu$ ,  $\kappa$ ,  $\theta$ , and  $\sigma_v$  are the parameters.  $\theta$  is the long term mean of  $g(t)$ , and  $\kappa$  measures the speed of reversion of  $g(t)$  to  $\theta$  ( $1 - \kappa$  is the persistence rate). The leverage effect is present when  $\rho < 0$ . (4.2.4b) is known as the Square Root (SQR) volatility model. If  $g(t)$  is constant, the Heston model, (4.2.4), nests the popular options pricing model of Black and Scholes (1973).

Using Ito's formula, we can easily derive that the model of  $\log(S_t)$  is:

$$d\log(S_t) = (\mu - 0.5g(t))dt + \sqrt{g(t)} dW(t) \quad (4.2.5)$$

$$dg(t) = \kappa(\theta - g(t))dt + \sigma_g\sqrt{g(t)}dB(t) \quad (4.2.6)$$

Using Euler-Maruyama discretization, the model of daily returns is expressed as:

$$r_t = \mu - 0.5g_{t-1} + \sqrt{g_{t-1}}\varepsilon_t^s \quad \text{for } t = 1, \dots, T \quad (4.2.7)$$

$$g_t = g_{t-1} + \kappa(\theta - g_{t-1}) + \sigma_g\sqrt{g_{t-1}}\eta_t \quad (4.2.8)$$

If one is interested in modelling returns data rather than options evaluation, Eraker et al. (2003) derived the following discrete version of the Heston model directly from (4.2.4):

$$r_t = \mu + \sqrt{g_{t-1}}\varepsilon_t^s \quad (4.2.9)$$

$$g_t = g_{t-1} + \kappa(\theta - g_{t-1}) + \sigma_g\sqrt{g_{t-1}}\eta_t \quad (4.2.10)$$

where the Ito's formula is ignored and  $\frac{dS_t}{S_t} = \frac{d\log(S_t)}{dt}$  is used. The main difference between SV-L and reduced-form Heston model (HRM) is that the variance of the volatility of HRM, (4.2.10), depends on  $g_{t-1}$  whereas the variance  $\sigma_h^2$ , (4.2.2), of the log-volatility in the SV-L model is constant.

Several extensions have also been proposed to improve the empirical performance of the Heston model. For example, Bates (2001) included a Jump component in the return equation. Heston (1997) replaced the volatility innovation  $\sigma_g\sqrt{g_{t-1}}\eta_t$  by  $\sigma_g g_{t-1}^{3/2}\eta_t$  and called it 3/2 He-

ston Model, which had been extended by Christoffersen (2010) as follows:

$$r_t = \mu - 0.5g_{t-1} + \sqrt{g_{t-1}}\varepsilon_t^s \quad (4.2.11)$$

$$g_t = v_{t-1} + kg_{t-1}^a (\theta - g_{t-1}) + \sigma_g g_{t-1}^b \eta_t \quad (4.2.12)$$

where  $\mu$ ,  $\theta$ ,  $\alpha$ ,  $k$ ,  $\sigma_g$ , are the main parameters.  $a$  and  $b$  are chosen by the user such that  $a \in \{0, 1\}$  and  $b \in \{\frac{1}{2}, 1, 3/2\}$ . It also nests the SV-L model by imposing  $a = b = 0$ . This model also includes the discrete version of the original Heston model ( $a = 0$  and  $b = \frac{1}{2}$ ), and 3/2 Heston model ( $a = 0$  and  $b = \frac{3}{2}$ ). Christoffersen et al. (2008) reported that Heston Model cannot capture important stylised facts of Option pricing, and illustrated its inappropriateness for SP500 by fitting the volatility specification (4.2.8) to realised volatility using high frequency data. Moreover, they claim that the main issue is not the existence of jumps in returns or in the volatility but in the non-appropriateness of the specification (4.2.8) which fails to capture observed rapid fluctuations of the volatility. This led them to use non affine diffusion process (4.2.12)

Due to the success and popularity of GARCH-MIDAS model of Engle et al. (2013) in improving the performance of GARCH type models which are, in general, outperformed by SV models, we develop the SV-MIDAS model by using multiplicative volatility component model, i.e.  $v_t = \tau_t e^{h_t}$ :

$$r_t = \mu + \sqrt{\tau_t} e^{\frac{h_t}{2}} \varepsilon_t \quad (4.2.13)$$

$$h_t = \alpha_0 + \phi (h_{t-1} - \alpha_0) + \sigma_h \eta_t \quad (4.2.14)$$

$$\log(\tau_t) = m + \psi \sum_{k=1}^K w_k X_{t-k}$$

$$h_0 \sim N\left(\alpha_0, \frac{\sigma_h^2}{1 - \phi^2}\right)$$

where  $h_t = \log(g_t)$  is the logged short term volatility component,  $\varepsilon_t$  and  $\eta_t$  are uncorrelated. The SV-L-MIDAS model is defined by (4.2.13-4.2.14), where we allow  $\varepsilon_{t+1}$  and  $\eta_t$  to be correlated, i.e.  $\rho = \text{corr}(\varepsilon_{t+1}, \eta_t)$ .

Similarly, we define the Heston-MIDAS models:

Heston-MIDAS(1):

$$r_t = \mu - 0.5\tau_{t-1}g_{t-1} + \sqrt{\tau_{t-1}}\sqrt{g_{t-1}}\varepsilon_t \quad (4.2.15)$$

$$g_t = g_{t-1} + \kappa(\theta - g_{t-1}) + \sigma_g \sqrt{g_{t-1}}\eta_t \quad (4.2.16)$$

$$\log(\tau_t) = m + \psi \sum_{k=1}^K w_k X_{t-k}$$

Heston-MIDAS(2):

$$r_t = \mu - 0.5\tau_{t-1}g_{t-1} + \sqrt{\tau_{t-1}}\sqrt{g_{t-1}}\varepsilon_t \quad (4.2.17)$$

$$g_t = g_{t-1} + \kappa g_{t-1}^a (\theta - g_{t-1}) + \sigma_g g_{t-1}^b \eta_t \quad (4.2.18)$$

$$\log(\tau_t) = m + \psi \sum_{k=1}^K w_k X_{t-k}$$

where  $(a, b)$  is chosen by the user from  $\{0, 1\} \times \{0, \frac{1}{2}, 1, \frac{3}{2}\}$

Heston-MIDAS(3):

$$r_t = \mu + \sqrt{\tau_{t-1}} \sqrt{g_{t-1}} \varepsilon_t \quad (4.2.19)$$

$$g_t = g_{t-1} + \kappa g_{t-1}^a (\theta - g_{t-1}) + \sigma_g g_{t-1}^b \eta_t \quad (4.2.20)$$

$$\log(\tau_t) = m + \psi \sum_{k=1}^K w_k X_{t-k}$$

Heston-MIDAS(4):

$$r_t = \mu - \beta \tau_{t-1} g_{t-1} + \sqrt{\tau_{t-1}} \sqrt{g_{t-1}} \varepsilon_t \quad (4.2.21)$$

$$g_t = g_{t-1} + \kappa g_{t-1}^a (\theta - g_{t-1}) + \sigma_g g_{t-1}^b \eta_t \quad (4.2.22)$$

$$\log(\tau_t) = m + \psi \sum_{k=1}^K w_k X_{t-k}$$

where  $\rho = \text{corr}(\varepsilon_t, \eta_t)$ . Note that Heston-MIDAS(1) is the original Heston model of Heston (1993) with MIDAS regression, Heston-MIDAS(2) is Christofferson (2007) with MIDAS regression which includes the Heston 3/2 model of Heston (1997), where  $g_t$  does not follow *SQR* specification. Heston-MIDAS(3) is a proposed version of Heston model by Eraker et al. (2003) with MIDAS regression when  $a = 0$  and  $b = \frac{1}{2}$ , and Heston-MIDAS(4) presents the general model which nests all the proposed models.

### 4.2.1 Bayesian Estimation of SV-MIDAS models

The Bayesian estimation of SV-MIDAS models needs to deal with the stochastic short term volatility component ( $h_t = \log(g_t)$ ), which will be simulated instead of being computed by plugging the updated values of the parameters as in GARCH-MIDAS models. In other words, posterior draws of the parameter vector  $\mathbf{h} = (h_0, h_1, \dots, h_T)'$ , are also obtained together with draws from the posteriors of the individual parameters  $\theta_i$ 's of the model. For SVL-MIDAS, the posterior density of each parameter  $\theta_i$  of the model is computed using

$$p(\theta_i | \mathbf{r}, \mathbf{h}, \Theta_{-\theta_i}) \propto L(\mathbf{r}, \mathbf{h} | X, \theta_i, \Theta_{-\theta_i}) \pi(\theta_i)$$

where  $L(\mathbf{r}, \mathbf{h} | X, \theta_i, \Theta_{-\theta_i})$  is the likelihood,  $\pi(\theta_i)$  is the prior density of  $\theta_i$ , and  $\Theta_{-\theta_i}$  is the set of all the parameters of the model except  $\theta_i$ . We propose the following MCMC algorithm for SVL-MIDAS:

- i. Choose initial parameter values  $\Theta^{(0)} = (\mu^{(0)}, \alpha_0^{(0)}, \phi^{(0)}, \sigma_h^{(0)}, \rho^{(0)}, \boldsymbol{\theta}_L^{(0)})$  where  $\boldsymbol{\theta}_L^{(0)} = (m^{(0)}, \psi^{(0)}, \omega^{(0)})$ , and initial short term volatility  $\mathbf{h}^{(0)}$ .
- ii. Simulate  $\mu^{(1)}$  from  $p(\mu | \Theta_{-\mu}, \mathbf{r}, \mathbf{h}^{(0)})$  where  $\Theta_{-\mu} = (\alpha_0^{(0)}, \phi^{(0)}, \sigma_h^{(0)}, \rho^{(0)}, \boldsymbol{\theta}_L^{(0)})$

- iii. Simulate  $\rho^{(1)}$  from  $p(\rho | \Theta_{-\rho}, \mathbf{r}, \mathbf{h}^{(0)})$  where  $\Theta_{-\rho} = (\mu^{(1)}, \alpha_0^{(0)}, \phi^{(0)}, \sigma_h^{(0)}, \boldsymbol{\theta}_L^{(0)})$
- iv. Simulate  $\sigma_h^{2(1)}$  from  $p(\sigma_h^2 | \Theta_{-\sigma_h^2}, \mathbf{r}, \mathbf{h}^{(0)})$  where  $\Theta_{-\sigma_h^2} = (\mu^{(1)}, \alpha_0^{(0)}, \phi^{(0)}, \rho^{(1)}, \boldsymbol{\theta}_L^{(0)})$
- v. Simulate  $\phi^{(1)}$  from  $p(\phi | \Theta_{-\phi}, \mathbf{r}, \mathbf{h}^{(0)})$  where  $\Theta_{-\phi} = (\mu^{(1)}, \alpha_0^{(0)}, \sigma_h^{(1)}, \rho^{(1)}, \boldsymbol{\theta}_L^{(0)})$
- vi. Simulate  $\alpha_0^{(1)}$  from  $p(\alpha_0 | \Theta_{-\alpha_0}, \mathbf{r}, \mathbf{h}^{(0)})$  where  $\Theta_{-\alpha_0} = (\mu^{(1)}, \phi^{(1)}, \sigma_h^{(1)}, \rho^{(1)}, \boldsymbol{\theta}_L^{(0)})$
- vii. Simulate  $\mathbf{h}^{(1)}$  from  $p(\mathbf{h} | \Theta^*, \mathbf{r})$  where  $\Theta^* = (\mu^{(1)}, \alpha_0^{(1)}, \phi^{(1)}, \sigma_h^{(1)}, \rho^{(1)}, \boldsymbol{\theta}_L^{(0)})$
- viii. Simulate  $\boldsymbol{\theta}_L^{(1)}$  from  $p(\boldsymbol{\theta}_L | \Theta_{-\boldsymbol{\theta}_L}, \mathbf{r}, \mathbf{h}^{(1)})$  where  $\Theta_{-\boldsymbol{\theta}_L} = (\mu^{(1)}, \phi^{(1)}, \sigma_h^{(1)}, \rho^{(1)}, \alpha_0^{(1)})$

Repeat steps ii-viii a large number of times.

We propose the following MCMC algorithm for simulating draws from the posterior distribution of the parameter vector  $\Theta$  of Heston-MIDAS model where  $\Theta = (\mu, \kappa, \theta, \sigma_g, \rho, \boldsymbol{\theta}_L)'$  and  $\boldsymbol{\theta}_L = (m, \psi, \omega)$ :

- i. Choose initial values  $\Theta^{(0)}$  and initial short term volatility  $\mathbf{g}^{(0)}$ .
- ii. Simulate  $\mu^{(1)}$  from  $p(\mu | \Theta_{-\mu}, \mathbf{r}, \mathbf{g}^{(0)})$  where  $\Theta_{-\mu} = (\kappa^{(0)}, \theta^{(0)}, \sigma_g^{(0)}, \rho^{(0)}, \boldsymbol{\theta}_L^{(0)})$
- iii. Simulate  $\rho^{(1)}$  from  $p(\rho | \Theta_{-\rho}, \mathbf{r}, \mathbf{g}^{(0)})$  where  $\Theta_{-\rho} = (\mu^{(1)}, \kappa^{(0)}, \theta^{(0)}, \sigma_g^{(0)}, \boldsymbol{\theta}_L^{(0)})$
- iv. Simulate  $\sigma_g^{2(1)}$  from  $p(\sigma_g^2 | \Theta_{-\sigma_g^2}, \mathbf{r}, \mathbf{g}^{(0)})$  where  $\Theta_{-\sigma_g^2} = (\mu^{(1)}, \kappa^{(1)}, \theta^{(0)}, \rho^{(0)}, \boldsymbol{\theta}_L^{(0)})$
- v. Simulate  $\theta^{(1)}$  from  $p(\theta | \Theta_{-\theta}, \mathbf{r}, \mathbf{g}^{(0)})$  where  $\Theta_{-\theta} = (\mu^{(1)}, \kappa^{(1)}, \sigma_g^{(1)}, \rho^{(0)}, \boldsymbol{\theta}_L^{(0)})$
- vi. Simulate  $\kappa^{(1)}$  from  $p(\kappa | \Theta_{-\kappa}, \mathbf{r}, \mathbf{g}^{(0)})$  where  $\Theta_{-\kappa} = (\mu^{(1)}, \theta^{(1)}, \sigma_g^{(1)}, \rho^{(1)}, \boldsymbol{\theta}_L^{(0)})$
- vii. Simulate  $\mathbf{g}^{(1)}$  from  $p(\mathbf{g} | \Theta^*, \mathbf{r})$  where  $\Theta^* = (\mu^{(1)}, \kappa^{(1)}, \theta^{(1)}, \sigma_g^{(1)}, \rho^{(1)}, \boldsymbol{\theta}_L^{(0)})$
- viii. Simulate  $(\boldsymbol{\theta}_L^{(1)})$  from  $p(\boldsymbol{\theta}_L | \Theta_{-\boldsymbol{\theta}_L}, \mathbf{r}, \mathbf{g}^{(1)})$  where  $\Theta_{-\boldsymbol{\theta}_L} = (\mu^{(1)}, \kappa^{(1)}, \theta^{(1)}, \sigma_g^{(1)}, \rho^{(1)})$

Repeat steps ii-viii a large number of times.

#### 4.2.2 Prior and posterior distributions of the parameters of SV-L-MIDAS

Several prior densities of the parameter vector  $(\mu, \alpha_0, \phi, \sigma_h, \rho)'$  for SV-L model were proposed in the literature. We follow Chan and Grant(2016) and assume:

- i) Normal prior for  $\mu, \alpha_0$ , and  $\phi$  with means 0, 1, 0.9, and variance 10, 10, and 1, respectively. The prior of  $\phi$  is truncated such that  $|\phi| < 1$ .
- ii) Prior distribution of  $\sigma_h^2$  is the Inverse Gamma distribution  $IG(a, b)$  where  $a = 5$  and  $b = 0.16$ .
- iii) We assume a uniform distribution  $U_{[-1, 1]}$  for the prior of  $\rho$ .

For the parameters of the long term component  $\tau_t$ , we assume bivariate normal prior for  $(m, \psi)$  with mean  $(0, 0.3)$  and Variance matrix,  $I_2$ , and a normal prior for  $\omega$  with mean 10 and variance 400, truncated at 1 and 50.

The prior distributions of  $\mu$ ,  $\alpha_0$ ,  $\phi$ , and  $\sigma_h$  are conjugate. Therefore, it is straightforward to get draws from their posterior distributions. From Appendix A3.1 we report the following results:

**Posterior of  $\mu$ :** Given the prior,  $\pi(\mu) = N(\mu_0, \sigma_{\mu_0}^2)$ , the posterior of  $\mu$  is  $N(\mu_\mu, \sigma_\mu^2)$  where

$$\mu_\mu = \frac{\frac{1}{(1-\rho^2)} \sum_{t=1}^{T-1} e^{-h_t} \left( \frac{r_t}{\tau_t} - \rho \frac{(h_t - h_{t-1})e^{0.5h_t}}{\sqrt{\tau_t} \sigma_h} \right) + \frac{\mu_{\mu_0}}{\sigma_{\mu_0}^2}}{\left\{ \frac{1}{(1-\rho^2)} \sum_{t=1}^{T-1} \frac{1}{\tau_t} e^{h_t} + \frac{1}{\sigma_{\mu_0}^2} \right\}}$$

$$\sigma_\mu^2 = \frac{1}{\left\{ \frac{1}{(1-\rho^2)} \sum_{t=1}^{T-1} \frac{1}{\tau_t} e^{h_t} + \frac{1}{\sigma_{\mu_0}^2} \right\}}$$

**Posterior of  $\alpha_0$ :** Given the prior,  $\pi(\alpha_0) = N(\mu_{\alpha_0}^*, \sigma_{\alpha_0}^{*2})$ , the posterior distribution  $p(\alpha_0 | X, \mathbf{r}, \mathbf{h}, \Theta_{-\alpha_0})$  is  $N(\mu_{\alpha_0}, \sigma_{\alpha_0}^2)$  where

$$\sigma_{\alpha_0}^2 = \frac{1}{T \frac{(1-\phi)^2}{(1-\rho^2) \sigma_h^2} + \frac{T(1-\phi^2)}{\sigma_h^2} + \frac{1}{\sigma_{\alpha_0}^{*2}}}$$

$$\mu_{\alpha_0} = \frac{\frac{(1-\phi)\rho}{\sigma_h(1-\rho^2)} \sum_{t=1}^T \frac{(r_t - \mu)}{\sqrt{\tau_t} e^{0.5h_t}} - \frac{(1-\phi)\rho^2}{\sigma_h^2(1-\rho^2)} \sum_{t=0}^{T-1} (h_{t+1} - \phi h_t) T \frac{(1-\phi)}{\sigma_h^2} \sum_{t=0}^{T-1} (h_{t+1} - \phi h_t) + (1-\phi^2) \frac{h_1}{\sigma_h^2} + \frac{\mu_{\alpha_0}^*}{\sigma_{\alpha_0}^{*2}}}{T \frac{(1-\phi)^2}{(1-\rho^2) \sigma_h^2} + T \frac{(1-\phi^2)}{\sigma_h^2} + \frac{1}{\sigma_{\alpha_0}^{*2}}}$$

Note: we can set  $\alpha_0 = 0$  if we desire to obtain a unit variance short-term component  $g_t$ .

**Posterior of  $\phi$ :** Given the prior,  $\pi(\phi) = N(\mu_{\phi_0}, \sigma_{\phi_0}^2) 1_{(-1,1)}$ , the posterior,  $p(\phi | \mathbf{x}, \mathbf{r}, \mathbf{h}, \Theta_{-\phi})$  is truncated normal,  $N(\mu_\phi, \sigma_\phi^2) 1_{]-1,1[}$  where

$$\sigma_\phi^2 = \frac{1}{\frac{\rho^2}{\sigma_h^2(1-\rho^2)} \sum_{t=1}^T (h_t - \alpha_0)^2 + \frac{1}{\sigma_h^2} \sum_{t=1}^T (h_t - \alpha_0)^2 + \frac{1}{\sigma_{\phi_0}^2}}$$

$$\mu_\phi = \frac{-\frac{\rho}{(1-\rho^2) \sigma_h} \left( \sum_{t=1}^T \frac{(r_t - \mu)(h_t - \alpha_0)}{\sqrt{\tau_t} e^{0.5h_t}} - \frac{\rho}{\sigma_h} \sum_{t=1}^T (h_t - \alpha_0)^2 \right) + \frac{1}{\sigma_h^2} \sum_{t=0}^{T-1} (h_{t+1} - \alpha_0)(h_t - \alpha_0) + \frac{\mu_{\phi_0}}{\sigma_{\phi_0}^2}}{\frac{\rho^2}{\sigma_h^2(1-\rho^2)} \sum_{t=1}^T (h_t - \alpha_0)^2 + \frac{1}{\sigma_h^2} \sum_{t=1}^T (h_t - \alpha_0)^2 + \frac{1}{\sigma_{\phi_0}^2}}$$

**Posterior of  $\rho$**  Given the uniform prior  $U_{]-1,1[}$ , the prior  $\pi(\rho)$  is not conjugate because its posterior cannot be simplified further than

$$p(\rho | \mathbf{x}, \mathbf{r}, \mathbf{h}, \Theta_{-\rho}) \propto \exp(-0.5 \left\{ \sum_{t=1}^T \frac{(r_t - \mu - \frac{\rho}{\sigma_h} \sqrt{\tau_t} e^{0.5h_t} (h_{t+1} - \alpha_0 - \phi(h_t - \alpha_0)))^2}{(1-\rho^2) \tau_t e^{h_t}} \right\}) \times U_{]-1,1[} \quad (4.2.23)$$

For simulating draws from  $p(\rho | \mathbf{x}, \mathbf{r}, \mathbf{h}, \Theta_{-\rho})$  we adopt the Metropolis Hasting method using a normal proposal density and Random Walk or Griddy Gibbs sampler, which consists of approximating  $p(\rho | \mathbf{x}, \mathbf{r}, \mathbf{h}, \Theta_{-\rho})$  by adjacent lines over a grid  $\{\rho_0, \dots, \rho_L\}$  where  $\rho_0 = -1 + \delta$ ,  $\rho_L = 1 - \delta$  with  $L = 100$ , and  $\delta$  is a small positive random number. Hence, draws from



$p(\rho \mid \mathbf{x}, \mathbf{r}, \mathbf{h}, \Theta_{-\rho})$  are generated by simulating from its piece wise linear approximation whose ordinates  $\{y_0, \dots, y_L\}$  are given by

$$y_i = \exp \left( -0.5 \left\{ \sum_{t=1}^T \frac{\left( r_t - \mu - \frac{\rho}{\sigma_h} \sqrt{\tau_t} e^{0.5h_t} (h_{t+1} - \alpha_0 - \phi(h_t - \alpha_0)) \right)^2}{(1 - \rho^2) \tau_t e^{h_t}} \right\} \right) \text{ for } i = 1, \dots, L$$

**Posterior of  $\sigma_h^2$ :** For an inverse-Gamma prior,  $\pi(\sigma_h^2) = IG(a, b)$  is not conjugate because its posterior  $p(\sigma_h^2 \mid \mathbf{x}, \mathbf{r}, \mathbf{h}, \Theta_{-\sigma_h^2})$  can be expressed as

$$p(\sigma_h^2 \mid \mathbf{r}, \mathbf{h}, \Theta_{-\sigma_h^2}) \propto IG(a + (T + 1)/2, b + 0.5(T \sum_{t=0}^{T-1} ((h_{t+1} - \alpha_0 - \phi(h_t - \alpha_0))^2 + (1 - \phi^2)h_1))$$

where  $A = \exp(-0.5 \left\{ \sum_{t=0}^{T-1} \frac{\left( r_t - \mu - \frac{\rho}{\sigma_h} \sqrt{\tau_t} e^{0.5h_t} (h_{t+1} - \alpha_0 - \phi(h_t - \alpha_0)) \right)^2}{(1 - \rho^2) \tau_t e^{h_t}} \right\})$  cannot be expressed as  $e^{\frac{C}{\sigma_h^2}}$

where  $C$  is independent of  $\sigma_h^2$ . Then, we obtain draws from  $\sigma_h^2$  using Griddy-Gibbs sampler or Metropolis Hasting method. Since the support of  $\sigma_h^2$  is unknown, we prefer the Metropolis Hasting method using the proposal density,  $IG(a + (T + 1)/2, b + 0.5(T \sum_{t=0}^{T-1} ((h_{t+1} - \alpha_0 - \phi(h_t - \alpha_0))^2 + (1 - \phi^2)h_1))$ .

### Posterior of the parameter $\theta_L$ of the long term component

We use Metropolis Hasting method to draw  $(m, \psi)$  using a bivariate normal proposal density whose mean and variance covariance are computed using the 2nd order Taylor expansion of its posterior density, section 4.6.2 of Appendix 3, where:

$$\frac{\partial p(m, \psi \mid \Theta_{-(m, \psi)}, \mathbf{x}, \mathbf{r}, \mathbf{h})}{\partial m} = \left\{ -0.5 - \frac{1}{2(1 - \rho^2)} \left\{ - \sum_{t=1}^T \frac{(r_t - \mu)^2}{\tau_t e^{h_t}} + \frac{\rho}{2\sigma_h} \sum_{t=1}^T \frac{(r_t - \mu)}{\sqrt{\tau_t} e^{0.5h_t}} e^{h_t} \right\} \right\} + \frac{\partial \log(\pi(m, \psi))}{\partial m}$$

$$\frac{\partial p(m, \psi \mid \Theta_{-(m, \psi)}, \mathbf{x}, \mathbf{r}, \mathbf{h})}{\partial \psi} = -0.5 \prod_{t=1}^T \sum_{k=1}^K w_k X_{t-k} - \frac{1}{2(1 - \rho^2)} \left\{ \sum_{t=1}^T - \frac{(r_t - \mu)^2}{\tau_t e^{h_t}} \sum_{k=1}^K w_k X_{t-k} + \frac{\rho}{2\sigma_h} \sum_{t=1}^T \frac{(r_t - \mu)}{\sqrt{\tau_t} e^{0.5h_t}} \sum_{k=1}^K w_k X_{t-k} e^{h_t} \right\} + \frac{\partial \log(\pi(m, \psi))}{\partial \psi}$$

because  $\frac{\partial \log(\tau_t)}{\partial m} = 1$  and  $\frac{\partial \log \tau_t}{\partial \psi} = \sum_{k=1}^K w_k X_{t-k}$ .

The mean and variance matrix of the proposal bivariate normal density are computed using (3.5.17-3.5.18) of Chapter 3.

**Posterior of  $\mathbf{h}$ :** We consider 3 approaches for drawing from posterior of  $\mathbf{h}$ . The first approach is the Single-Move sampling by Kim et al. (1998), which consists of drawing each  $h_t$  for  $t = 2, \dots, T - 1$ , assuming the others  $h_{-t}$ 's are known and using the fact that

$$p(h_t \mid \Theta, \mathbf{r}, \mathbf{h}_{-t}) \propto p(h_t \mid \Theta, \mathbf{h}_{-t}) p(r_t \mid \Theta, h_t)$$

where  $p(h_t|\Theta, \mathbf{h}_{-t}) = p(h_t|\Theta, h_{t-1}, h_{t+1})$  (Kim et al. (1998))

$$p(h_t|\Theta, \mathbf{r}, \mathbf{h}_{-t}) \propto p(h_t|\Theta, h_{t-1}, h_{t+1}) p(r_t|\Theta, h_t)$$

The second approach is the block sampler by Omori and Watanabe (2008), which consists of dividing  $\mathbf{h}$  in the  $M$  groups  $\{\mathbf{h}_1, \dots, \mathbf{h}_M\}$  where each block  $\mathbf{h}_m = (h_{(m-1)L+1}, \dots, h_{mL})$ , for  $L = 100$ , is updated using draws from the posterior of the error block,  $\boldsymbol{\varepsilon}_m = (\varepsilon_{(m-1)L+1}, \dots, \varepsilon_{mL})$ , while assuming the other blocks are known. Using Bayes theorem, it is easily seen that

$$p(\boldsymbol{\varepsilon}_m|\boldsymbol{\varepsilon}_{-m}, \Theta, \mathbf{r}) \propto \prod_{t=(m-1)L+1}^{mL} p(r_t|\Theta, h_t, h_{t+1}, \tau_t) \times \prod_{s \neq m}^M p(\boldsymbol{\varepsilon}_s^h|\boldsymbol{\varepsilon}_{-s}^h, \Theta, \mathbf{r}) \quad (4.2.24)$$

where

$$r_t|\Theta, h_t, h_{t+1}, \tau_t \sim N\left(\mu + \frac{\rho}{\tau_t^d \sigma_h} \sqrt{\tau_t} e^{0.5h_t} (h_t - \varphi_h h_t + \alpha_0 (1 - \varphi_h)), (1 - \rho^2) \tau_t e^{h_t}\right)$$

Since the right hand side is unknown, they suggest to approximate  $p(\boldsymbol{\varepsilon}_m^h|\boldsymbol{\varepsilon}_{-m}^h, \Theta, \mathbf{r})$  by a multivariate normal distribution  $N(\boldsymbol{\mu}_m, \boldsymbol{\Sigma}_m)$  using the 2nd order Taylor expansion, i.e.  $\boldsymbol{\varepsilon}_m$  is drawn using Metropolis Hasting method as in Single move sampler.

The third approach is that of Eraker et al. (2003): Using the known property that for each  $t$ ,  $p(v_t|\mathbf{r}, \mathbf{g}_{-t}, \Theta) = p(g_t|\mathbf{r}, v_{t-1}, v_{t+1}, \Theta)$  where total volatility  $v_t = \tau_t e^{h_t}$ , we derive from Bayes theorem

$$p(v_t|\mathbf{r}, v_{t-1}, v_{t+1}, \Theta) \propto p(v_t, \mathbf{r}|v_{t-1}, \Theta) p(v_{t+1}, \mathbf{r}|v_t, \Theta)$$

If we denote  $g_t = e^{h_t}$ , the expression of  $p((r_t, g_t)|g_{t-1}, \Theta, \tau_t)$  and  $p((r_{t+1}, g_{t+1})|g_t, \Theta, \tau_{t+1})$  can be deduced as

$$p((r_t, g_t)|r_{t-1}, g_{t-1}, \Theta) = \frac{1}{2\pi \tau_{t-1} \sigma_g \sqrt{(1-\rho^2)g_{t-1}}} e^{-\frac{1}{2(1-\rho^2)}\{\varepsilon_{r_{t-1}}^2 - 2\rho\varepsilon_{r_{t-1}}\varepsilon_{g_{t-1}} + \varepsilon_{g_{t-1}}^2\}}$$

$$p((r_{t+1}, g_{t+1})|r_t, g_t, \Theta) = \frac{1}{2\pi \tau_t \sigma_g \sqrt{(1-\rho^2)g_t}} e^{-\frac{1}{2(1-\rho^2)}\{\varepsilon_{r_t}^2 - 2\rho\varepsilon_{r_t}\varepsilon_{g_t} + \varepsilon_{g_t}^2\}}$$

Using the fact  $\varepsilon_{r_t}^2|g_{t-1}$  does not depend on  $g_t$ , we derive:

$$p(g_t|\mathbf{r}, g_{t-1}, g_{t+1}, \Theta) \propto \frac{1}{\sqrt{\tau_{t-1}} \sigma_g \sqrt{(1-\rho^2)}} e^{-\frac{1}{2(1-\rho^2)}\{-2\rho\varepsilon_{r_{t-1}}\varepsilon_{g_t} + \varepsilon_{g_t}^2\}} \frac{1}{\tau_{t-1} \sigma_g \sqrt{(1-\rho^2)g_t}} e^{-\frac{1}{2(1-\rho^2)}\{\varepsilon_{r_{t-1}}^2 - 2\rho\varepsilon_{r_{t-1}}\varepsilon_{g_{t+1}} + \varepsilon_{g_{t+1}}^2\}}$$

$$\propto \frac{1}{\tau_{t-1} \sigma_g^2 (1-\rho^2) g_t} e^{-\frac{1}{2(1-\rho^2)}\{\varepsilon_{r_{t-1}}^2 - 2\rho(\varepsilon_{r_{t-1}}\varepsilon_{g_t} + \varepsilon_{r_{t-1}}\varepsilon_{g_{t+1}}) + \varepsilon_{g_t}^2 + \varepsilon_{g_{t+1}}^2\}}$$

We use Random Walk to simulate from  $p(g_t|\mathbf{r}, g_{t-1}, g_{t+1}, \Theta)$  i.e.:

For the  $j^{\text{th}}$  MCMC iteration, we simulate

$$g_t^* = g_t^{(j-1)} + cN(0, 1) \quad (4.2.25)$$

$g_t^*$  is accepted as  $g_t^{(j)}$  with probability  $\alpha$  defined by:

$$\alpha = \frac{p(g_t^* | \mathbf{r}, g_{t-1}, g_{t+1}, \Theta)}{p(g_t^{(j-1)} | \mathbf{r}, g_{t-1}, g_{t+1}, \Theta)}$$

where  $c$  is chosen by the user to achieve an acceptance rate of about 40-50% (Eraker (2003)). If  $g_t^*$  is not accepted, we take  $g_t^{(j)} = g_t^{(j-1)}$  for each  $t$ .

In (4.6.13) of Appendix 3, we propose to select  $c$  using the smoothing parameter of the kernel density estimate of the initial volatility  $\mathbf{g}^{(0)}$ .

### 4.2.3 Estimation of the Heston-MIDAS model

Along the similar lines in the SV-L MIDAS, we consider the following likelihood function and derive the posterior distributions of the parameters (see Appendix 3):

$$L(\mathbf{r}, \mathbf{g} | \Theta, \mathbf{x}) \propto \Omega^{-\frac{T}{2}} \left( \prod_{t=1}^T \frac{1}{\tau_{t-1} g_{t-1}} e^{-\frac{1}{2\Omega} \{ (\Omega + \psi^2) (\varepsilon_t^s)^2 - 2\Psi \varepsilon_t^s \varepsilon_t^g + (\varepsilon_t^g)^2 \}} \right) \quad (4.2.26)$$

where  $\varepsilon_t^s = \frac{(r_t - \mu + \beta \tau_{t-1} g_{t-1})}{\sqrt{\tau_{t-1} g_{t-1}}}$ ,  $\varepsilon_t^g = \frac{g_t - \kappa \theta - (1 - \kappa) g_{t-1}}{\sigma_g \sqrt{g_{t-1}}}$ ,  $\Omega = \sigma_g^2 (1 - \rho^2)$ , and  $\psi = \rho \sigma_g$ .

**Posterior distribution of  $\mu$ :** Given the prior,  $\mu \sim N(\mu_0, \sigma_0^2)$ , the posterior of  $\mu$  is also normal;  $N(\mu^*, \sigma_\mu^{*2})$  where

$$\mu^* = \frac{A \sum_{t=1}^T \frac{(r_t + \beta \tau_{t-1} g_{t-1})}{\tau_{t-1} g_{t-1}} - B \sum_{t=1}^T \frac{C_t}{g_{t-1}} + \mu_0 / \sigma_0^2}{D + 1 / \sigma_0^2} \quad \sigma_\mu^2 = 1 / (D + \frac{1}{\sigma_0^2})$$

where  $D = A \sum_{t=1}^T 1 / \tau_{t-1} g_{t-1}$ ,  $C_t = v_t - \kappa \theta - (1 - \kappa) g_{t-1}$ ,  $A = \frac{1}{1 - \rho^2}$ , and  $B = \rho / \sigma_v (1 - \rho^2)$ .

**Posterior distribution of  $\psi$  and  $\Omega$ :** Given the priors,  $\Omega \sim IG(\alpha_0, \beta_0)$  and  $\psi | \Omega \sim N(\psi_0, \sigma_{\psi_0}^2)$ , the posterior distributions of  $\Omega$  and  $\psi | \Omega$  are also  $IG(\alpha_*, \beta_*)$ , and  $N(\psi^*, \sigma_\psi^{*2})$  where<sup>2</sup>

$$\begin{aligned} \alpha_* &= \frac{T}{2} + \alpha_0 \\ \beta_* &= \beta_0 + \frac{1}{2} \sum_{t=1}^T (\varepsilon_t^y)^2 + \frac{1}{2} p_0 \psi_0^2 - \frac{1}{2} \frac{(P_0 \psi_0 + \sum_{t=1}^T \varepsilon_t^s \varepsilon_t^y)^2}{p_0 + \sum_{t=1}^T (\varepsilon_t^s)^2} \\ \psi^* &= \frac{P_0 \psi_0 + \sum_{t=1}^T \varepsilon_t^s \varepsilon_t^y}{P_0 \psi_0 + \sum_{t=1}^T (\varepsilon_t^s)^2} \\ \sigma_\psi^{*2} &= \frac{\Omega}{P_0 + \sum_{t=1}^T (\varepsilon_t^s)^2} \end{aligned}$$

<sup>2</sup>Draws of  $\rho$  are obtained from those of  $\psi$  and  $\sigma_g$  since  $\psi = \rho \sigma_g$ .

**Posterior distribution of  $\theta$ :** Given the prior  $\theta \sim N(\theta_0, \sigma_0^2)$ ,  $p(\theta | \Theta_{-\theta}, \mathbf{x}, \mathbf{r}, \mathbf{g})$  is  $N(\theta_*, \sigma_\theta^2)$  where

$$\theta_* = \frac{\frac{\kappa}{\Omega} \left( \sum_{t=1}^T \frac{A_t}{g_{t-1}} - \psi \sum_{t=1}^T \frac{B_t}{\sqrt{\tau_t} g_{t-1}} \right) + \theta_0 / \sigma_0^2}{D} \quad \sigma_\theta^2 = 1/D,$$

$$A_t = \frac{\kappa(v_t - v_{t-1} + \kappa g_{t-1})}{g_{t-1}}, B_t = (r_t - \mu + \beta g_{t-1} \tau_{t-1}), D = \frac{\kappa^2}{\Omega} \sum_{t=1}^T \frac{1}{g_{t-1}} + 1/\sigma_0^2.$$

Note: we set  $\theta = 1$  if we desire to obtain unit variance short term component  $g_t$ .

**Posterior distribution of  $\kappa$ :** Given the normal prior  $\kappa \sim N(\kappa_0, \sigma_\kappa^2)$ , its posterior distribution  $p(\kappa | \Theta_{-\kappa}, \mathbf{x}, \mathbf{r}, \mathbf{g})$  is normal with mean  $\kappa_*$  and variance  $\sigma_{\kappa^*}^2$ , where<sup>3</sup>

$$\kappa_* = \frac{\frac{1}{\Omega} \left( \sum_{t=1}^T \frac{A_t}{g_{t-1}} - \psi \sum_{t=1}^T \frac{B_t}{\tau_t g_{t-1}} \right) + \kappa_0 / \sigma_0^2}{D} \quad \sigma_{\kappa^*}^2 = 1/D,$$

$$A_t = (\theta - g_{t-1})(g_t - g_{t-1}); B_t = (r_t - \mu + \beta g_{t-1} \tau_t) (\theta - g_{t-1}), \text{ and } D = \frac{1}{\Omega} \sum_{t=1}^T \frac{(\theta - g_{t-1})^2}{g_{t-1}} + 1/\sigma_0^2.$$

#### Posterior of the parameters of the long term component:

The prior of  $m$  is not conjugate even in the simple case with  $(\beta = 0, c = \frac{1}{2}$  and  $d = 0)$  because, using (4.2.26) we easily deduce that

$$\begin{aligned} p(m | \mathbf{x}, \mathbf{r}, \mathbf{g}, \Theta_{-m}) &\propto \left( \prod_{t=1}^T \frac{1}{\tau_{t-1}^c g_{t-1}} \right) e^{-\frac{1}{2(1-\rho^2)} \sum_{t=1}^T \{ \varepsilon_{r_t}^2 - 2\rho \varepsilon_{r_t} \varepsilon_{g_t} \}} \pi(m) \\ &\propto e^{-\frac{1}{2(1-\rho^2)} \sum_{t=1}^T \left\{ \frac{(r_t - \mu)^2 e^{-m}}{g_{t-1}} - 2\rho \varepsilon_{g_t} \frac{(r_t - \mu) e^{-0.5m}}{\sqrt{g_{t-1}}} \right\} - 0.5Tm} \end{aligned} \quad (4.2.27)$$

$\varepsilon_{g_t}$  does not depend on  $m$  when  $d = 0$ , and  $\varepsilon_{r_t} = \frac{(r_t - \mu) e^{-0.5(m + \psi \sum_{k=1}^K w_k X_{t-k})}}{\sqrt{g_{t-1}}}$ ,  $\varepsilon_{r_t}^2 = \frac{(r_t - \mu)^2 e^{-(m + \psi \sum_{k=1}^K w_k X_{t-k})}}{g_{t-1}}$ , and  $\varepsilon_{g_t} = \frac{g_t - \kappa\theta - (1-\kappa)g_{t-1}}{\sigma_g \sqrt{g_{t-1}}}$ . Unfortunately,  $p(m | \mathbf{x}, \mathbf{r}, \mathbf{g}, \Theta_{-m})$  cannot be expressed as a known density because it involves  $e^{-m}$  and  $m$ . Similarly, we can show that

$$p(\psi | \mathbf{x}, \mathbf{r}, \mathbf{g}, \Theta_{-\psi}) \propto e^{-\frac{1}{2(1-\rho^2)} \sum_{t=1}^T \left\{ \frac{(r_t - \mu)^2 e^{-\psi \sum_{k=1}^K w_k X_{t-k}}}{g_{t-1}} - 2\rho \varepsilon_{g_t} \frac{(r_t - \mu) e^{-0.5\psi \sum_{k=1}^K w_k X_{t-k}}}{\sqrt{g_{t-1}}} \right\} - 0.5T\psi \sum_{k=1}^K w_k X_{t-k}} \pi(\psi) \quad (4.2.28)$$

For this, we decided to simulate  $j^{\text{th}}$  draw  $(m, \psi)^{(j)}$  using Adaptive Metropolis algorithm which consists of using the proposal  $f(m, \psi)$  defined by (Roberts and Rosenthal (2009))

$$f((m, \psi)) = \begin{cases} N_2 \left( (m, \psi)^{(j-1)}, \frac{0.1^2 I_2}{2} \right) & \text{if } j \leq 2 \\ (1 - \delta) N_2 \left( (m, \psi)^{(j-1)}, \frac{2.38^2 \Sigma^{(j)}}{2} \right) + \delta N_2 \left( (m, \psi)^{(j-1)}, \frac{0.1^2 I_2}{2} \right) & \text{if } 2 < j < j^* \\ N_2 \left( (m, \psi)^{(j-1)}, \Sigma^{(j^*)} \right) & \text{if } j > j^* \end{cases} \quad (4.2.29)$$

<sup>3</sup>In the implementation of MCMC, we use the truncated posterior normal distribution for these parameters  $\kappa$  and  $\theta$  as they are constrained to be non negative.

where  $j^*$  is the burnin,  $\delta = 0.05$  and  $\Sigma^{(j)}$  is the variance matrix of  $(m, \psi)^{(j)}$ 's for  $j < j^*$ . A draw  $(m, \psi)^*$  from  $f((m, \psi))$  is accepted as a draw  $(m, \psi)^{(j)}$  from the posterior  $p((m, \psi) | \mathbf{x}, \mathbf{r}, \mathbf{g}, \Theta_{-(m, \psi)})$  with probability  $\min(1, \frac{p((m, \psi)^* | \mathbf{x}, \mathbf{r}, \mathbf{g}, \Theta_{-(m, \psi)}) \pi((m, \psi)^*)}{p((m, \psi)^{(j)} | \mathbf{x}, \mathbf{r}, \mathbf{g}, \Theta_{-(m, \psi)}) \pi((m, \psi)^{(j)})})$ .

**Posterior of  $\omega$ :** Since  $\omega$  is bounded between 1 and 50, we use Griddy MCMC algorithm as follows:<sup>4</sup>

$$\begin{aligned} p(\omega | \mathbf{x}, \mathbf{r}, \mathbf{g}, \Theta_{-\omega}) &\propto e^{-\frac{1}{2(1-\rho^2)} \sum_{t=1}^T \{\varepsilon_{r_t}^2 - 2\rho\varepsilon_{r_t}\varepsilon_{g_t} + \varepsilon_{g_t}^2\}} 1_{[1,50]}(\omega) \\ &\propto e^{-\frac{1}{2(1-\rho^2)} \sum_{t=1}^T \{\varepsilon_{r_t}^2 - 2\rho\varepsilon_{r_t}\varepsilon_{g_t} + \varepsilon_{g_t}^2\}} 1_{[1,50]}(\omega) \end{aligned} \quad (4.2.30)$$

where  $\varepsilon_{r_t} = \frac{(r_t - \mu + \beta g_{t-1} e^{-c(m + \psi \sum_{k=1}^K w_k(\omega) X_{t-k}))}) e^{-c(m + \psi \sum_{k=1}^K w_k(\omega) X_{t-k})}}{\sqrt{g_{t-1}}}$ ,  $\varepsilon_{g_t} = \frac{(g_t - k\theta - (1-k)g_{t-1}) e^{-d(m + \psi \sum_{k=1}^K w_k(\omega) X_{t-k})}}{\sigma_g \sqrt{g_{t-1}}}$   
 $w_k(\omega) = \frac{(1 - \frac{k}{K})^{1-\omega}}{\sum_{k=1}^K (1 - \frac{k}{K})^{1-\omega}}$  and  $\pi(\omega)$  is U[1,50] using grids  $\omega_j = 1 + j/2$  for  $j = 1, \dots, 98$ , knowing that  $w_k(\omega)$  is not very sensitive to  $\omega$ .

#### 4.2.4 SVL-MIDAS, and Heston-MIDAS models with jump component

We extend the SVL-MIDAS and the general Heston-MIDAS(4) models by adding a jump component in the return equation to capture dynamics of rare events/spikes.

SVL-MIDAS-J model is given by:

$$\begin{aligned} r_t &= \mu + b_t z_t + \sqrt{\tau_t} e^{h_t/2} \varepsilon_{r_t} \\ h_t &= \alpha_0 + \phi(h_{t-1} - \alpha_0) + \sigma_h \eta_t \\ \log(\tau_t) &= m + \psi \sum_{k=1}^K w_k X_{t-k} \end{aligned} \quad (4.2.31)$$

where  $\rho = \text{corr}(\varepsilon_{t+1}, \eta_t)$ .

General Heston-MIDAS-J is defined by:

$$\begin{aligned} r_t &= \mu - \beta \tau_{t-1}^{2c} g_{t-1} + b_t z_t + \tau_{t-1}^c \sqrt{g_{t-1}} \varepsilon_{r_t} \\ g_t &= g_{t-1} + \kappa g_{t-1}^a (\theta - g_{t-1}) + \sigma_g g_{t-1}^b \eta_t \\ \log(\tau_t) &= m + \psi \sum_{k=1}^K w_k X_{t-k} \end{aligned} \quad (4.2.32)$$

where  $b_t$  is the indicator of the presence of a jump at time  $t$  i.e.  $b_t$  follows the Bernoulli distribution with parameter  $\lambda$ , and  $z_t | \{b_t = 1\}$  follows  $N(\mu_s, \sigma_s^2)$ . When there is a Jump at time  $t$ , i.e.  $b_t = 1$ ,  $\varepsilon_{r_t} = \frac{r_t - \tilde{\mu}_t - b_t z_t}{\tau_{t-1}^c \sqrt{g_{t-1}}}$ , and  $\tilde{\mu}_t = \mu + \beta \tau_{t-1}^{2c} g_{t-1}$  for Heston-MIDAS-J, and  $\varepsilon_{r_t} = \frac{r_t - \tilde{\mu}_t - b_t z_t}{\tau_{t-1}^c \sqrt{g_{t-1}}}$ , and  $\tilde{\mu}_t = \mu$  for SVL-MIDAS-J whereas  $\eta_t$  remains unchanged.

#### Posterior density of the jump size $z_t$ for SVL-MIDAS-J and Heston-MIDAS-J:

Given a normal prior,  $\pi(z_t) \sim N(\mu_s, \sigma_s^2)$ , the mean and variance of the normal posterior  $p_{z_t}(\cdot)$

<sup>4</sup>This is not time consuming as we can store  $\sum_{k=1}^K w_k(\omega_j) X_{t-k}$  for  $\omega_j = 1 + j/2$  for  $j = 1, \dots, 98$  before the start of the MCMC algorithm.

derived in Appendix (3) are given by

$$\mu_z = \frac{\frac{1}{(1-\rho^2)\tau_{t-1}^{2c}g_{t-1}^{2c}}(r_t - \tilde{\mu}_t) - \frac{\rho\varepsilon_{gt}}{(1-\rho^2)\tau_{t-1}^c g_{t-1}^c} + \frac{\mu_s}{\sigma_s^2}}{\frac{1}{(1-\rho^2)\tau_{t-1}^{2c}g_{t-1}^{2c}} + \frac{1}{\sigma_s^2}}$$

$$\sigma_z^2 = \frac{1}{\frac{1}{(1-\rho^2)\tau_{t-1}^c g_{t-1}^c} + \frac{1}{\sigma_s^2}}$$

where  $c = 1/2$  for SVL-MIDAS-J.

### Posterior density of the occurrence $b_t$ of jumps for SVL-MIDAS-J and Heston-MIDAS-J:

If we assume a Bernoulli prior  $Ber(\lambda_0)$ , then the posterior  $p_{b_t}(b_t | \Theta, \mathbf{x}, \mathbf{r}, \mathbf{z})$  is

$$p_{b_t}(b_t | \Theta, \mathbf{x}, \mathbf{r}, \mathbf{z}) \propto \left( \frac{\exp(-\frac{1}{2}A)\lambda_0}{1 - \lambda_0} \right)^{b_t} \propto \left( \frac{p}{1 - p} \right)^{b_t}$$

where  $p = \frac{1}{(1-\lambda_0)\exp(\frac{1}{2}A) + 1}$ , and  $A = \frac{1(z_t^2 - 2z_t(r_t - \tilde{\mu}))}{(1-\rho^2)\tau_{t-1}^{2c}g_{t-1}^{2c}} + \frac{2\rho z_t \varepsilon_{gt}}{\tau_{t-1}^c g_{t-1}^c}$  for Heston-MIDAS-J and  $A = \frac{1(z_t^2 - 2z_t(r_t - \tilde{\mu}))}{(1-\rho^2)\tau_{t-1}^{2c}g_{t-1}^{2c}} + \frac{2\rho z_t \varepsilon_{gt}}{\sqrt{\tau_{t-1}^{2c}g_{t-1}^{2c}}}$  for SVL-MIDAS-J.

### Posterior density of the rate $\lambda$ of occurrence of jumps:

If we assume the prior  $\pi(\lambda) \sim Beta(\alpha_{\lambda_0}, \beta_{\lambda_0})$ , the posterior is also  $Beta(\alpha_\lambda, \beta_\lambda)$  for both SVL-MIDAS-J and general Heston-MIDAS-J models where

$$\alpha_\lambda = \alpha_{\lambda_0} + \sum_{t=1}^T b_t$$

$$\beta_\lambda = \beta_{\lambda_0} + T - \sum_{t=1}^T b_t$$

### Posterior density of the parameters $\mu_s$ and $\sigma_s^2$ of Jump size $z_t$

Using normal prior  $N(m, M^2)$  for  $\mu_s$ , the posterior  $p_{\mu_s}(\mu_s | \mathbf{z}, \sigma_s^2)$  is normal with mean  $\mu_{\mu_s}$  and variance  $\sigma_{\mu_s}^2$  where

$$\mu_{\mu_s} = \frac{\frac{\sum_{t=1}^T z_t}{\sigma_s^2} + \frac{m}{M^2}}{\frac{T}{\sigma_s^2} + \frac{1}{M^2}}$$

$$\sigma_{\mu_s}^2 = \frac{1}{\frac{T}{\sigma_s^2} + \frac{1}{M^2}}$$

Assuming  $\pi(\sigma_s^2) \sim IG(\alpha_1, \beta_1)$  for  $\sigma_s^2$ , its posterior satisfies:

$$p_{\sigma_s^2}(\sigma_s^2 | \mathbf{z}, \mu_s) \propto \sigma_s^{-T} \exp\left(-\frac{\sum_{t=1}^T (z_t - \mu_s)^2}{2\sigma_s^2}\right) \pi(\sigma_s^2)$$

$$\propto (\sigma_s^2)^{-\alpha_1 - T/2 - 1} \exp\left(-\frac{\beta_1 + 0.5 \sum_{t=1}^T (z_t - \mu_s)^2}{\sigma_s^2}\right)$$

The posterior of  $\sigma_s^2$  follows  $IG(\alpha_2, \beta_2)$  where  $\alpha_2 = \alpha_1 + T/2$  and  $\beta_2 = \beta_1 + 0.5 \sum_{t=1}^T (z_t - \mu_s)^2$ .

### 4.2.5 Bayes Factor Analysis

The Bayesian approach enables us to identify the best model among  $N$  models  $M_i$ 's, which is useful in modelling data using SV-MIDAS type models when data from several different macroeconomic variables are available, where the best model is the one which has the largest posterior model probability  $p(M_i | \mathbf{r})$  which is defined by:

$$p(M_i | \mathbf{r}) = \frac{p(\mathbf{r} | M_i) \pi(M_i)}{\sum_{i=1}^N p(\mathbf{r} | M_i) \pi(M_i)} \quad (4.2.33)$$

where  $\pi(M_i)$  is the prior probability of model  $M_i$  such that  $\sum_{i=1}^N \pi(M_i) = 1$ , and  $p(\mathbf{r} | M_i)$  is the model likelihood which is defined, in turn, by:

$$p(\mathbf{r} | M_i) = \int_{\Theta_i} f(\mathbf{r} | \Theta_i, M_i) \pi(\Theta_i | M_i) d\Theta_i \quad (4.2.34)$$

When there is ground for assuming differences between  $\pi(M_i)$ 's, the comparison of two models  $M_i$  and  $M_j$  is done using the Bayes Factor:

$$B_{ij} = \frac{p(M_i | \mathbf{r})}{p(M_j | \mathbf{r})} \times \frac{\pi(M_j)}{\pi(M_i)} \quad (4.2.35)$$

Applying Bayes theorem, we can derive:

$$B_{ij} = \frac{p(\mathbf{r} | M_i)}{p(\mathbf{r} | M_j)} \quad (4.2.36)$$

Wasserman (1997) suggested the following guidelines for decision taking which is a slight modification of Jeffreys (1961).

Table 4.2.1: Jeffreys's scale of evidence for Bayes Factors

Bayes Factor	interpretation
$B_{ij} < \frac{1}{10}$	Strong evidence for $M_j$
$\frac{1}{10} < B_{ij} < \frac{1}{3}$	Moderate evidence for $M_j$
$\frac{1}{3} < B_{ij} < 1$	Weak evidence for $M_j$
$1 < B_{ij} < 3$	Weak evidence for $M_i$
$3 < B_{ij} < 10$	Moderate evidence for $M_i$
$B_{ij} > 10$	Strong evidence for $M_i$

Simple direct simulation methods for computing  $p(\mathbf{r} | M_i)$  by interpreting (4.2.35) as a mean: For example, using a simulated sample  $\{\Theta_i^{(1)}, \dots, \Theta_i^{(G)}\}$  from the prior distribution  $\pi(\Theta_i)$  of the

parameters of Model  $M_i$ , we can estimate, from (4.2.35),  $p(\mathbf{r}|M_i)$  by:

$$\hat{p}(\mathbf{r} | M_i) = \frac{1}{G} \sum_{k=1}^G f(\mathbf{r} | \Theta_i^{(k)}, M_i) \quad (4.2.37)$$

The main drawback of (4.2.37) is that most of the terms of the likelihood values  $f(r|\Theta_i^{(k)}, M_i)$ 's will be close to zeros due to peakedness of the likelihood function. This led Newton and Raftery (1994) to suggest to estimate it using Harmonic mean using a sample from the posterior distribution rather than the prior distribution i.e.:

$$\hat{p}(\mathbf{r} | M_i) = \left[ \frac{1}{G} \sum_{k=1}^G \frac{1}{f(r | \Theta_i^{(k)}, M_i)} \right]^{-1}$$

where  $\{\Theta_i^{(1)}, \dots, \Theta_i^{(G)}\}$  is simulated from the posterior  $p(\Theta_i | M_i)$ .

Chib and Jeliazkov (2001).proposed an indirect method for estimating model likelihoods from the MCMC output using the fact that the marginal likelihood  $p(\mathbf{r}|M_i)$  can be expressed as for every  $\Theta_i$ :

$$p(\mathbf{r} | M_i) = \frac{f(\mathbf{r} | \Theta_i, M_i)\pi(\Theta_i | M_i)}{p(\Theta_i | M_i)} \quad (4.2.38)$$

It is clear that the numerator of the right hand side of (4.2.38) can be computed easily in each iteration of the MCMC algorithm.

Since (4.2.38) is valid for every  $\Theta_i$ , they suggest to estimate  $p(\mathbf{r}|M_i)$  by

$$\hat{p}(\mathbf{r} | M_i) = \frac{f(\mathbf{r} | \Theta_i^*, M_i)\pi(\Theta_i^* | M_i)}{p(\Theta_i^* | M_i)} \quad (4.2.39)$$

where  $\Theta_i^*$  is the mode of the posterior  $p(\Theta_i | M_i)$ .

Finally, we report that the logarithm of Bayes Factor  $B_{ij}$  is asymptotically equivalent to Schwarz information criterion (SIC/BIC) proposed by Schwarz (1978). Kass and Raftery,( 1995) showed that:

$$\frac{(BIC_i - BIC_j) - \log(B_{ij})}{\log(B_{ij})} \sim 0 \quad (4.2.40)$$

when  $T$  is large. Hence,  $\log(B_{ij})$  can be aproximated by  $\Delta BIC = BIC_i - BIC_j$ .

### 4.3 Monte Carlo Simulation

We conduct two experiments to investigate the finite sample performance of the Bayesian MCMC estimation by using two data generating processes (DGP) with and without jump com-



ponents in a data-oriented manner where  $r_t$  represents the value of the return on  $t^{th}$  day, for  $t = 1, \dots, T$ , of the simulated return data. For each  $t$ , we denote by  $n$ , for  $n = 1, \dots, N$ , the month to which day  $t$  belongs to, and we denote by  $i$ , for  $i = 1, \dots, 22$  working days, its index in the month. In other words, the day  $t$  is described by  $(i, n)$  i.e.  $t = 22(n - 1) + i$ .

### Experiment 1: the DGP with no jump components

First, we generate a sample of  $(180 + K)$  monthly observations with  $K = 24$  for an artificial macroeconomic variable,<sup>5</sup> which follows an AR(1) process:

$$x_n = \varphi x_{n-1} + \varepsilon_n, \quad \varepsilon_n \sim N(0, 1), \quad n = 1, \dots, 180 + K$$

where we set  $\varphi = 0.95$  and  $x_0 = 0$ . Second, we generate the 180 monthly observations of the long term volatility,  $\tau_n$  by

$$\log(\tau_n) = m + \psi \sum_{k=1}^K w_k X_{n-k} \quad n = 1, \dots, 180$$

where  $w(k, \omega)$  is the Beta weighting function. We set  $m = (-0.1, 0.1)$  and consider several values of  $\psi = (-0.25, -0.4, 0.25, 0.4)$  and  $\omega = (5, 10)$ . Third, we generate the  $22 \times 180$  daily observations of the short-term volatility,  $g_t$  by

$$\text{SV-L-MIDAS: } \log(g_{i,n}) = \alpha_0 + \theta(\log(g_{i-1,n}) - \alpha_0) + \sigma_g \eta_{i-1,n}$$

$$\text{Heston-MIDAS: } g_{i,n} = g_{i-1,n} + k g_{i-1,n}^a (\theta - g_{i-1,n}) + \sigma_g g_{i-1,n}^b \eta_{i,n}$$

To investigate if the parameter estimates are sensitive to the initial values, our MCMC algorithms used the same initial values for  $\rho^{(0)}$ ,  $m^{(0)}$ ,  $\psi^{(0)}$ , and initial short-term component vector  $\mathbf{g}^{(0)}$  equal to the volatility  $\mathbf{v}$  of EGARCH(1,1), scaled by  $v(1)$  to approximate an initial unit short term volatility. We set the true values of the parameters for Heston-MIDAS as follow:  $a = 0, b = \frac{1}{2}, \mu = 0, \kappa = (0.03, 0.05, 0.07), \theta = (0.9, 0.95, 0.98), \rho = (-0.2, -0.1, 0, 0.1)$ , and  $\Sigma_v = (0.02, 0.04)$ . For SV-L-MIDAS:  $\mu = 0, \alpha_0 = (0.03, 0.05, 0.07), \theta = (0.9, 0.95, 0.98), \rho = (-0.2, -0.1, 0, 0.1)$ , and  $\Sigma_v = 0.02, 0.04$  Finally, we generate daily returns,  $r_t$  by:

$$\text{SV-L-MIDAS: } r_{i,n} = \mu + \sqrt{\tau_n g_{i-1,n}} \varepsilon_{i,n}^s$$

$$\text{Heston-MIDAS: } r_{i,n} = \mu - \beta \tau_n g_{i-1,n} + \sqrt{\tau_n} \sqrt{g_{i-1,n}} \varepsilon_{i,n}^s \text{ where } \rho = \text{cor}(\varepsilon_{i,n}^s, \eta_{i,n}).$$

Table 4.3.1 reports the results of experiment 1, parameter estimates of SV-L-MIDAS model, for 200 data sets using 40000 iterations and 10000 burnins. We note that our MCMC algorithm produces accurate parameter estimates of both the short term and the long term volatility components parameters, and  $\rho$  including for the case where the short term component is highly

<sup>5</sup>we generate  $(180 + K)$  samples for  $x_n$  due to the  $K$  lagged values of  $x_n$  used in modelling  $\log \tau_n$ .

persistent ( $\theta = 0.98$ ). These parameter estimates were obtained using the same initial values of the parameters  $\theta^{(0)} = 0.9$ ,  $\rho^{(0)} = 0$ ,  $m^{(0)} = 0$ ,  $\psi^{(0)} = 0$  (corresponding to  $\tau_t = 1$  for every  $t$ , and no asymmetry), and initial short-term component vector  $\mathbf{g}^{(0)}$  equal to the volatility  $\mathbf{v}$  of EGARCH(1,1), scaled by  $v(1)$  to approximate an initial unit short term volatility. Our algorithm updated the parameters from their initial values to the correct value independently of the difference between their true and initial values.

Table 4.3.2 reports the Bayesian MCMC estimates of the general Heston-MIDAS model for 200 data sets using 40000 iterations only and 10000 burnins. We note that our MCMC algorithm succeeds in producing accurate parameter estimates of both the short term and the long term components of the model as well as that of  $\rho$  when the return equation includes a volatility feedback component  $-0.5\tau_n g_{i-1,n}$ . Our MCMC  $\hat{\beta}$  is accurate when  $\beta = 0.5$ , and  $\beta = 0$ . In fact  $\hat{\beta}$  is accurate for other true values of  $\beta$  i.e. our MCMC algorithm is applicable for Heston-In Mean-MIDAS. As in experiment 1, we used the same initial values of the parameters  $\kappa^{(0)} = 0.05$ ,  $\beta^{(0)} = 0$ ,  $m^{(0)} = 0$ ,  $\psi^{(0)} = 0$ , and  $\omega^{(0)} = 5$ . The initial short term volatility  $\mathbf{g}^{(0)}$  is the volatility of EGARCH(1,1) scaled by  $g_1$ , and we used the kernel smoothing parameter,  $c = 1.06std(\mathbf{g}^{(0)})T^{-0.2}$ , as the tuning parameter of the random walk procedure in drawing the short term volatilities  $g_t$ 's. The accuracy of the estimates with 40000 iterations indicates that our MCMC algorithm is not sensitive to the choice of the initial values of the parameters; the preference of using EGARCH(1,1) volatility over simulated from truncated normal as done in literature; and the kernel smoothing parameter is a good choice over the tuning parameter  $c$  of random walk which is selected in adhoc manner in the literature. It is worth noting that unit short term volatility component Heston is obtained in a straightforward way by fixing  $\theta = 1$  as the case in GARCH-MIDAS because the specification is not described using its logarithm.

In sum, we establish that Bayesian MCMC can produce relatively precise estimates for SV-L-MIDAS, and Heston-MIDAS for the different values of  $\theta$ , and  $\rho$ .

Table 4.3.1: Bayesian MCMC estimates of the SV-L-MIDAS model

Parameters	$\mu$	$\rho$	$\alpha_0$	$\theta$	$\sigma_v^2$	$m$	$\psi$	$\omega$
TRUE	0	-0.10	0.03	0.90	0.04	0.10	-0.40	5.00
Estimate	-0.011 (0.017)	-0.097 (0.075)	0.024 (0.020)	0.910 (0.020)	0.039 (0.010)	0.048 (0.151)	-0.389 (0.063)	6.036 (3.021)
TRUE	0	0.10	0.03	0.98	0.04	-0.10	0.40	10.00
Estimate	-0.002 (0.006)	0.111 (0.035)	0.030 (0.016)	0.981 (0.014)	0.043 (0.005)	0.069 (0.064)	0.410 (0.034)	10.494 (6.457)
TRUE	0	0.00	0.07	0.90	0.02	-0.10	0.25	10.00
Estimate	0.001 (0.006)	-0.001 (0.014)	0.070 (0.034)	0.908 (0.052)	0.023 (0.005)	-0.136 (0.164)	0.273 (0.034)	10.739 (6.454)
TRUE	0	-0.20	0.05	0.95	0.04	0.10	-0.25	5.00
Estimate	0.001 (0.007)	-0.214 (0.092)	0.019 (0.094)	0.948 (0.000)	0.042 (0.008)	0.146 (0.130)	-0.233 (0.044)	5.800 (3.604)

Note: This table reports the parameter estimates of 4 DGP's using SV-L-MIDAS (4.2.13-4.2.14). Each DGP is created using different  $\rho$  values for the parameters of the short term and long term volatility components. Standard deviation are reported in brackets.

Table 4.3.2: Bayesian MCMC estimates of the Heston-MIDAS model

Parameters	$\mu$	$\beta$	$\rho$	$\kappa$	$\theta$	$\sigma_v^2$	$m$	$\psi$	$\omega$
TRUE	0	0.00	-0.20	0.00	1	0.04	0.10	-0.40	10.00
Estimate	-0.011 (0.017)	0.000 (0.001)	-0.171 (0.075)	0.006 (0.072)	1	0.042 (0.010)	0.078 (0.154)	-0.387 (0.093)	10.360 (3.021)
TRUE	0	0.50	0.20	0.05	1	0.04	0.10	0.40	10.00
Estimate	0.029 (0.020)	0.492 (0.079)	0.210 (0.079)	0.056 (0.078)	1	0.040 (0.010)	0.137 (0.133)	0.408 (0.106)	11.230 (3.166)
TRUE	0	0.00	0.00	0.03	1	0.04	-0.10	0.25	5.00
Estimate	-0.004 (0.019)	0.000 (0.001)	0.003 (0.070)	0.028 (0.099)	1	0.041 (0.008)	-0.136 (0.212)	0.263 (0.096)	6.099 (2.422)
TRUE	0	0.50	-0.10	0.07	1	0.03	-0.10	-0.25	5.00
Estimate	-0.004 (0.009)	0.490 (0.083)	-0.073 (0.032)	0.069 (0.050)	1	0.031 (0.004)	-0.091 (0.106)	-0.267 (0.044)	5.574 (1.868)

Note: This table reports the parameter estimates of 4 DGP's using Heston-MIDAS (4.2.21-4.2.22). Each DGP is created using different values for the parameters of the short term and long term volatility components. Standard deviations are reported in brackets. We set  $\theta = 1$  for ensuring the short term component  $g_t$  is unit variance.

### Experiment 2: the DGP with jump component

We now generate daily return data with jump component as follows:

$$\text{SV-L-MIDAS-J: } r_{i,n} = \mu + B_{i,n}Z_{i,n} + \sqrt{\tau_n g_{i-1,n}} \varepsilon_{i,n}^s$$

$$\text{Heston-MIDAS-J: } r_{i,n} = \mu - \beta \tau_n g_{i-1,n} + B_{i,n}Z_{i,n} + \sqrt{\tau_n} \sqrt{g_{i-1,n}} \varepsilon_{i,n}^s$$

where  $B_t$  follows a Bernoulli distribution with rate  $\lambda$ , and  $Z_t$  follows  $N(\mu_s, \sigma_s^2)$ . We consider  $\lambda = (2\%, 5\%, 8\%, 10\%)$  and  $\sigma_s^2 = (9, 25, 36, 49)$  to generate the low, medium, and high jumps.

Table 4.3.3 reports the simulation results when the data is generated from SV-L-MIDAS-J model. The Bayesian MCMC algorithm accurately estimated the true values of the parameters of the short term and long term components of the volatility, and the jump component for different cases of rare events (Low, Medium, High, and rare High).

Table 4.3.4 reports the the parameter estimates of the jump augmented general Heston-MIDAS model. We note that our MCMC algorithm produces accurate estimates of the parameters. The mean,  $\mu_s$  and variance,  $\sigma_s^2$ , of the jump size are accurately estimated.

As in experiment 1, the parameter estimates are also accurate for the case where the short term component is highly persistent,  $\kappa = 0.02$ , and when the frequency of jump occurrence is small,  $\lambda = 0.02$ .

In sum, the Bayesian MCMC algorithm accurately estimates our SV-MIDAS models with and without jump component.

Table 4.3.3: Bayesian MCMC estimates of the SV-L-MIDAS-J model

Parameters	$\mu$	$\rho$	$\alpha_0$	$\theta$	$\sigma_v^2$	$m$	$\psi$	$\omega$	$\mu_z$	$\sigma_z^2$	$\lambda$
TRUE	0	-0.10	0.03	0.90	0.04	0.10	-0.40	5.00	0.03	9.00	0.10
Estimate	0	-0.09	0.03	0.90	0.04	0.08	-0.41	5.72	0.03	11.31	0.10
	(0.074)	(0.074)	(0.023)	(0.018)	(0.002)	(0.138)	(0.073)	(1.213)	(0.014)	(3.983)	(0.020)
TRUE	0	0.10	0.03	0.98	0.04	-0.10	0.40	10.00	0.03	25.00	0.08
Estimate	-0.001	0.110	0.031	0.972	0.044	0.096	0.438	9.939	0.031	26.081	0.077
	(0.005)	(0.035)	(0.014)	(0.013)	(0.005)	(0.059)	(0.073)	(4.801)	(0.021)	(11.061)	(0.011)
TRUE	0	0.00	0.07	0.90	0.02	-0.10	0.25	10.00	-0.03	36.00	0.05
Estimate	0.001	0.000	0.071	0.923	0.024	-0.133	0.278	11.392	-0.029	35.632	0.047
	(0.006)	(0.015)	(0.033)	(0.053)	(0.015)	(0.156)	(0.032)	(3.054)	(0.019)	(9.962)	(0.007)
TRUE	0	-0.20	0.05	0.95	0.04	0.10	-0.25	5.00	-0.03	49.00	0.02
Estimate	0.001	-0.210	0.043	0.941	0.039	0.109	-0.249	6.077	-0.034	47.067	0.017
	(0.009)	(0.072)	(0.008)	(0.005)	(0.009)	(0.124)	(0.064)	(0.590)	(0.033)	(0.184)	(0.007)

Note: This table reports the parameter estimates of 4 DGP's using SV-L-MIDAS-J (4.2.31). Each DGP is created using different values for the parameters of the short term and long term volatility components. Standard deviations are reported in brackets.

Table 4.3.4: Bayesian MCMC estimates of the Heston-MIDAS-J model

Parameters	$\mu$	$\beta$	$\rho$	$\kappa$	$\theta$	$\sigma_v^2$	$m$	$\psi$	$\omega$	$\mu_z$	$\sigma_z^2$	$\lambda$
TRUE	0	0.00	-0.20	0.00	1	0.04	0.10	-0.40	10.00	0.03	9.00	0.10
Estimate	0	0.00	-0.18	0.00	1	0.04	0.11	-0.38	11.08	0.03	10.40	0.11
	(0.013)	(0.001)	(0.055)	(0.052)		(0.011)	(0.104)	(0.012)	(4.023)	(0.015)	(4.908)	(0.021)
TRUE	0	0.50	0.20	0.05	1	0.04	0.10	0.40	10.00	0.03	25.00	0.08
Estimate	0.009	0.499	0.210	0.053	1	0.040	0.120	0.408	10.531	0.037	24.408	0.078
	(0.024)	(0.089)	(0.089)	(0.058)		(0.018)	(0.135)	(0.135)	(2.946)	(0.023)	(10.461)	(0.017)
TRUE	0	0.00	0.00	0.03	1	0.02	-0.10	0.25	5.00	-0.03	36.00	0.05
Estimate	-0.005	0.001	0.002	0.031	1	0.024	-0.149	0.246	5.994	-0.036	37.263	0.050
	(0.009)	(0.001)	(0.064)	(0.049)		(0.011)	(0.135)	(0.083)	(1.852)	(0.022)	(9.996)	(0.008)
TRUE	0	0.50	-0.10	0.07	1	0.02	-0.10	-0.25	5.00	-0.03	49.00	0.02
Estimate	0.003	0.489	-0.103	0.067	1	0.023	-0.111	-0.257	6.079	-0.040	48.267	0.018
	(0.011)	(0.077)	(0.035)	(0.050)		(0.011)	(0.160)	(0.089)	(2.054)	(0.024)	(0.144)	(0.009)

Note: This table reports the parameter estimates of 4 DGP's using Heston-MIDAS-J (4.2.32). Each DGP is created using different values for the parameters of the short term and long term volatility components. Standard deviations are reported in brackets. We set  $\theta = 1$  for ensuring the short term component  $g_t$  is unit variance.

## 4.4 Empirical Application

We aim to address the important issues of leverage effects and rare events by applying the jump-augmented SV-L-MIDAS, and Heston-MIDAS to an analysis of time-varying volatility patterns of WTI daily returns over the period 09/2000-8/2019. To examine the impacts of macroeconomic conditions on the long-run volatility, we consider a range of economic indicators: industrial production ( $IP$ ) of USA and China; economic policy uncertainty ( $EPU$ ) of USA and China; effective exchange rate ( $EER$ ) of USA and China; global economic policy uncertainty ( $GEPU$ ); OPEC oil production ( $OP_{OPEC}$ ), OPEC oil supply ( $OS_{OPEC}$ ), and global oil production ( $GOP$ ) as a proxy of overall economic indicator. We use the growth rate constructed by  $100\log(X_t/X_{t-1})$ . We also evaluate the relative performance of SV-MIDAS-J, SV-L-GARCH-MIDAS-J and Heston-MIDAS-J models in terms of in-sample fit and bayes factor analysis.

In fact, WTI returns had been modelled by standard SV models. Chan and Grant(2016) applied SV, SVL, SV-J, SV-M (in Mean), GARCH-M to weekly WTI returns in the period 1997-2014:

They found the inclusion of  $\lambda \sigma_t^2$  in the return equation of SV-M and GARCH-M is not significant and found  $\hat{\beta}$  is -0.02 with standard deviation 0.02 which is far from the fixed value  $-1/2$  of Heston Model, and  $\hat{\mu}_{SV-M} = 0.47$  whereas  $\hat{\mu}_{SV} = 0.17$ .

#### 4.4.1 Benchmark estimation results

We report the MCMC parameter estimates of SV, SV-L, SV-J, and SV-L-J in Table 4.4.1 which indicate that SVL and SVL-J suggest the presence of the leverage effect, and its inclusion in the model improves the fit according to DIC and RMSE. Our results for SV, SVL, and SV-J are similar to those of Chan and Grant (2016). Moreover, according to DIC and RMSE, inclusion of Jump component improved the fit of SV-J whereas it did not for SVL-J which is due to the fact that  $\hat{\mu}_z = 0.043$  (which is small).

Table 4.4.1: Parameter estimates of SV models

Model	$\mu$	$\alpha_0$	$\phi$	$\sigma_v^2$	$\rho$	$\lambda$	$\mu_z$	$\sigma_z^2$	DIC	RMSE
SV	0.077 (0.027)	1.415 (0.119)	0.978 (0.004)	0.028 (0.003)					20165.43	15.180
SV-L	0.035 (0.027)	1.395 (0.12)	0.981 (0.004)	0.022 (0.004)	-0.365 (0.061)				20141.63	12.975
SV-J	0.094 (0.029)	1.334 (0.146)	0.986 (0.003)	0.018 (0.003)		0.028 (0.013)	-1.739 (0.313)	16.458 (6.167)	20106.15	13.311
SV-L-J	0.032 (0.028)	1.403 (0.124)	0.982 (0.004)	0.021 (0.003)	-0.386 (0.063)	0.053 (0.035)	0.043 (0.087)	12.797 (5.978)	20093.44	12.970

Note: This table reports the estimation results of Stochastic volatility (SV), asymmetric Stochastic volatility (SV-L), Stochastic volatility with jump (SV-J), and asymmetric stochastic volatility with jump (SV-L-J) models. DIC is a Bayesian method for model comparison developed by Spiegelhalter et al. (2002) where  $DIC = D(y, \hat{\Theta}) + 2pD$ , where  $D(y, \hat{\Theta}) = 2\log(p(y|\hat{\Theta}))$ , and  $pD = var(D(y, \hat{\Theta}))$ . Standard deviations are reported brackets.

We turn to the estimation results for Heston model with and without Jump component in return equation. According to both RMSE and DIC, we note that inclusion of the jump component improves the fit of each of the models, and SV, and SV-L models produce a high persistence parameter  $\hat{\phi}$  and  $1 - \hat{\kappa}$  between 0.978 and 0.988. Also, DIC and RMSE suggest that SV-L outperforms the other 2 models (without jump component) SV, and Heston.

Furthermore, SV-L model produces a significant negative  $\hat{\rho}$ , indicating the presence of a leverage effect in the volatility of WTI returns. However, the Heston Model produces a significant but positive  $\hat{\rho} = 0.255$ . We also validate our MATLAB code by reproducing very similar parameter estimates to those of Brooks and Prokopczuk (2013) for WTI returns, and those of Eraker et al. (2003).

We also note including of the leverage effect in SV-L model, did not alter the parameter estimates of SV model but both RMSE and DIC indicate the out-performance of SV-L on SV. Surprisingly, the original Heston model produced a significant but positive correlation, indicating inverse leverage effect, and produces  $\hat{\mu} = 1.73$ .

Table 4.4.2: Parameter estimates of Heston models

Model	$\mu$	$\theta$	k	$\sigma_v^2$	$\rho$	$\lambda$	$\mu_z$	$\sigma_z^2$	DIC	RMSE
Heston	1.735 (0.079)	3.708 (0.154)	0.063 (0.009)	0.056 (0.022)	0.255 (0.056)				20177.24	17.394
Heston-J	1.468 (0.063)	3.009 (0.202)	0.016 (0.004)	0.008 (0.011)	0.072 (0.091)	0.13 (0.015)	0.032 (0.065)	10.275 (0.293)	20109.14	14.152

Note: This table reports the estimation results of Heston model of Heston (1993) where  $\beta = 1/2$ , and Heston-J of Bates (1999). DIC is a Bayesian method for model comparison developed by Spiegelhalter et al. (2002) where  $DIC = D(y, \hat{\Theta}) + 2pD$ , where  $D(y, \hat{\Theta}) = 2\log(p(y|\Theta))$ , and  $pD = \text{var}(D(y, \hat{\Theta}))$ . Standard deviations are reported brackets.

Tables 4.4.3–4.4.4, reports the MCMC parameter estimates of Heston-MIDAS and its jump augmented extension, and SV-L-MIDAS and its jump augmented extension using the important economic indicator  $OP_{OPEC}$ . By comparing these models with their respective benchmark models, we find that the use of MIDAS regression improved the persistence of SV-L-MIDAS and Heston-MIDAS as  $\hat{\phi}$  and  $1 - \hat{\kappa}$  are much lower than those of the SV-L and Heston models. Also, we note that Heston-MIDAS was able to capture a negative leverage effect unlike its benchmark model Heston.

Table 4.4.3: MCMC parameter estimates of Heston-MIDAS models -  $OP_{OPEC}$ 

Model	$\hat{\mu}^*$	$\hat{\kappa}$	$\hat{\rho}$	$\hat{\sigma}_v^2$	$\hat{\mu}_j$	$\hat{\sigma}_j^2$	$\hat{\lambda}$	m	$\psi$	$\omega$	DIC
H-MIDAS	0.082 (0.040)	0.022 (0.001)	-0.174 (0.072)	0.044 (0.002)				1.655 (0.174)	0.413 (0.173)	8.289 (2.365)	20038
H-MIDAS-J	0.066 (0.032)	0.065 (0.004)	-0.230 (0.086)	0.018 (0.001)	-0.036 (0.036)	50.515 (0.775)	0.029 (0.015)	0.880 (0.092)	0.505 (0.249)	7.618 (2.174)	19646

Note: This table reports the estimation results of H-MIDAS which refer to Heston-MIDAS model (3.2.21-3.2.22), and H-MIDAS-J which refer to Heston-MIDAS-J (4.2.32) using  $OP_{OPEC}$  as the explanatory variable for modelling the long term component of the volatility. DIC is a Bayesian method for model comparison developed by Spiegelhalter et al. (2002) where  $DIC = D(y, \hat{\Theta}) + 2pD$ , where  $D(y, \hat{\Theta}) = 2\log(p(y|\Theta))$ , and  $pD = \text{var}(D(y, \hat{\Theta}))$ . Standard deviations are reported brackets.

Table 4.4.4: MCMC parameter estimates of SV-L-MIDAS models -  $OP_{OPEC}$ 

Model	$\hat{\mu}$	$\hat{\alpha}_0$	$\hat{\phi}$	$\hat{\rho}$	$\hat{\sigma}_v^2$	$\hat{\mu}_j$	$\hat{\sigma}_j^2$	$\hat{\lambda}$	m	$\psi$	$\omega$	DIC
SVL-M	0.097 (0.048)	1.436 (1.402)	0.980 (0.019)	-0.173 (0.051)	0.028 (0.001)				1.765 (0.185)	0.405 (0.168)	8.716 (2.487)	20057
SVL-M-J	0.099 (0.049)	1.391 (1.360)	0.902 (0.018)	-0.240 (0.057)	0.028 (0.001)	-0.037 (0.036)	46.773 (0.718)	0.031 (0.016)	0.706 (0.074)	0.506 (0.084)	7.845 (2.238)	19659

Note: This table reports the estimation results of SVL-M which refers to SVL-MIDAS (4.2.13-4.2.14), and SVL-M-J which refers to SVL-MIDAS-J (4.2.31) using  $OP_{OPEC}$  as the explanatory variable for modelling the long term component of the volatility. DIC is a Bayesian method for model comparison developed by Spiegelhalter et al. (2002) where  $DIC = D(y, \hat{\Theta}) + 2pD$ , where  $D(y, \hat{\Theta}) = 2\log(p(y|\Theta))$ , and  $pD = \text{var}(D(y, \hat{\Theta}))$ . Standard deviations are reported brackets.

## 4.4.2 In-sample fit comparison

In Table 4.4.5 we summarise the in-sample estimation results for SV-MIDAS, SV-L-MIDAS, and Heston-MIDAS models and their jump-augmented extensions where we reproduce the long

term estimate,  $\hat{\psi}$ , and DIC from Tables (4.6.1-2) in Appendix 3. We summarise the main findings as follows:

First, DIC convincingly selects MIDAS models with jump components over MIDAS models without jump components. Overall, Heston-MIDAS-J is the most preferred model across 7 macroeconomic variables  $IP_{US}$ ,  $IP_{CH}$ ,  $EER_{CH}$ ,  $EPU_{US}$ ,  $EPU_{CH}$ ,  $GOP$  and  $OP_{OPEC}$ , while SV-L-MIDAS-J is preferred for 3 macroeconomic variables  $EER_{US}$ ,  $GEP_{US}$ , and  $OS_{OPEC}$ .

Second, the jump augmented MIDAS models produced significant long term coefficients ( $\psi$ ) with predicted signs for all macroeconomic variables. They also tend to produce slightly large magnitudes than MIDAS models without jump components.

Third, we evaluate the relative importance of each macroeconomic variable by employing VR that measures the fraction of the total volatility explained by the long term component. Notice that jump-augmented MIDAS models produced a larger VR than MIDAS models without jump components, suggesting that if we ignore the presence of rare events or outliers, then the long term variance is likely to be under-estimated.

Focusing on Heston-MIDAS-J estimation results, we find that the most influential variable is the  $OP_{OPEC}$ , that explains 45.7% of the total volatility for WTI returns. The second-most influential variable is  $GOP$  growth, that explains 39.2% of the total volatility, followed by  $OS_{OPEC}$  (41.15%) and  $EER_{US}$  (38.16%). This highlights the dominant position of the OPEC in the global oil industry.

Table 4.4.5: Estimation results of the impact of economic indicators on WTI returns volatility

Panel A: The summary of Bayesian estimates of SV-MIDAS, SVL-MIDAS, and Heston-MIDAS									
	SV-MIDAS			SVL-MIDAS			H-MIDAS		
Macro	$\hat{\theta}$	DIC	VR	$\hat{\theta}$	DIC	VR	$\hat{\theta}$	DIC	VR
$IP_{US}$	-0.337***	20064	15.5 %	-0.309***	20049	17.8 %	-0.385***	20052	18.9 %
$IP_{CH}$	-0.424***	20057	14.2 %	-0.408***	20056	16.4 %	-0.318***	20027	17.4 %
$EER_{US}$	-0.859***	20061	17.0 %	-0.847***	20044	19.5 %	-0.802***	20070	20.7 %
$EER_{CH}$	-0.349***	20085	9.1 %	-0.376***	20064	10.5 %	-0.24***	20023	11.1 %
GEPUS	0.047***	20080	11.7 %	0.055***	20060	13.5 %	0.011***	20020	14.3 %
$EPU_{US}$	0.015***	20082	14.2 %	0.004	20061	16.4 %	0.017	20026	17.4 %
$EPU_{CH}$	-0.061***	20084	8.7 %	-0.086**	20061	10.0 %	-0.08***	20024	10.6 %
GOP	0.51***	20081	18.0 %	0.813***	20058	20.7 %	0.269***	20023	22.0 %
$OP_{OPEC}$	0.25***	20082	19.6 %	0.405***	20057	22.5 %	0.413**	20038	23.9%
$OS_{OPEC}$	-0.039*	20081	14.9 %	-0.065*	20051	17.1 %	-0.068**	20034	18.1 %

Panel B: The summary of Bayesian estimates of SV-M-J,SVL-M-J, and H-M-J									
	SV-MIDAS-J			SVL-MIDAS-J			H-MIDAS-J		
Macro	$\hat{\theta}$	DIC	VR	$\hat{\theta}$	DIC	VR	$\hat{\theta}$	DIC	VR
$IP_{US}$	-0.358***	19682	26.1 %	-0.345***	19654	30.5 %	-0.387***	<b>19647</b>	32.4 %
$IP_{CH}$	-0.445***	19699	20.2 %	-0.416***	19629	23.5 %	-0.417***	<b>19617</b>	25.0 %
$EER_{US}$	-0.892***	19685	30.7 %	-0.802***	<b>19671</b>	35.9 %	-0.9***	19680	38.1 %
$EER_{CH}$	-0.368***	19652	19.6 %	-0.397***	19625	22.9 %	-0.445***	<b>196241</b>	24.3 %
GEPUS	0.055***	19646	25.1 %	0.07**	<b>19622</b>	29.3 %	0.079***	19645	31.1 %
$EPU_{US}$	0.015***	19703	28.7 %	0.138***	19628	33.6%	0.155***	<b>19612</b>	35.6 %
$EPU_{CH}$	-0.091***	19644	15.9 %	-0.079***	19626	18.6 %	-0.089***	<b>19624</b>	19.7 %
GOP	0.676***	19649	33.1 %	0.875***	19625	38.8 %	0.981***	<b>19604</b>	41.1 %
$OP_{OPEC}$	0.294***	19695	36.8 %	0.506***	19659	43.1 %	0.505***	<b>19624</b>	45.7 %
$OS_{OPEC}$	-0.07***	19682	31.2 %	-0.076**	<b>19635</b>	36.6 %	-0.085**	19644	38.8 %

Notes:  $\hat{\theta}$  indicate the impact of the macroeconomic variable on  $\tau_t$ ; \*\*\*, \*\*, and \* indicate 1%, 5%, and 10% significance level;  $VR = var(\log(\hat{\tau}_t))/var(\log(\hat{\tau}_t\hat{g}_t))$  measures the fraction of the total volatility explained by the long term component; DIC is a Bayesian method for model comparison developed by Spiegelhalter et al. (2002) where  $DIC = D(y, \hat{\Theta}) + 2pD$ , where  $D(y, \hat{\Theta}) = 2\log(p(y|\hat{\Theta}))$ , and  $pD = var(D(y, \hat{\Theta}))$ ; Panel A reports Bayesian MCMC estimates of the impact of economic indicators on WTI long term component of the volatility using alternative SV-MIDAS(4.2.13-4.2.14) where  $\rho = 0$ , SVL-MIDAS (4.2.13-4.2.14), and Heston-MIDAS(4.2.21-4.2.22); Panel B reports Bayesian MCMC estimates of the impact of economic indicators on WTI long term component of the volatility using alternative SV-MIDAS-J(4.2.31), SVL-MIDAS-J(4.2.31), and Heston-MIDAS-J(4.2.32).

### 4.4.3 Bayes factor analysis

Table 4.4.6 reports the logarithm of the Bayes factor, using (4.3.40), for all models compared to SV-MIDAS across all macroeconomic variables. Form this table we note that, Heston-MIDAS-J and SV-L-MIDAS-J are selected as the models with the better fit to WTI returns for all macroeconomic variables followed by SV-MIDAS-J model. Note that Heston-MIDAS-J is the overall better model as it is selected across 7 macroeconomic variables, and SV-L-MIDAS-J for 3 macroeconomic variables. Also, Heston-MIDAS-J and SV-L-MIDAS-J produced comparable Bayes factor results with slight preference of Heston-MIDAS-J.



Table 4.4.6: log Bayes factor results

Macro	SV-MIDAS-J	SV-L-MIDAS	SV-L-MIDAS-J	Heston-MIDAS	Heston-Midas-J
<i>IP<sub>US</sub></i>	7.381	4.994	7.821	4.301	<b>7.854</b>
<i>IP<sub>CH</sub></i>	7.315	5.027	7.832	4.422	<b>7.876</b>
<i>EER<sub>US</sub></i>	7.568	4.543	<b>7.898</b>	4.257	7.711
<i>EER<sub>CH</sub></i>	5.643	3.542	7.711	3.487	<b>7.931</b>
GEP <sub>U</sub>	6.501	4.411	<b>7.689</b>	4.312	7.612
<i>EPU<sub>US</sub></i>	6.941	4.884	7.854	5.302	<b>8.701</b>
<i>EPU<sub>CH</sub></i>	7.843	6.501	9.009	6.721	<b>10.043</b>
GOP	6.798	5.522	8.723	5.621	<b>9.262</b>
<i>OP<sub>OPEC</sub></i>	7.667	5.324	9.427	5.39	<b>9.933</b>
<i>OS<sub>OPEC</sub></i>	6.721	5.192	<b>7.843</b>	4.389	7.722

Notes: This table reports the log Bayes factor results for SV-MIDAS-J (4.2.31), SV-L-MIDAS (4.2.13-4.2.14), SV-L-MIDAS-J (4.2.31), Heston-MIDAS (4.2.21-4.2.22), and Heston-Midas-J (4.2.32) where SV-MIDAS (4.2.13-4.2.14) is used as a benchmark model  $M_i$ . The higher the log of the Bayes factor the better the model. The highest log Bayes factor is highlighted in bold for each macroeconomic variable.

#### 4.4.4 Out-Sample fit comparison

Now we investigate the out sample forecast performance of alternative SV-MIDAS models and their jump augmented extensions with different low-frequency macroeconomic indicators.

Following Shang and Zheng (2018), we use the rolling window approach to compute the results of the out-sample forecasts. Specifically, using the data samples of a fixed window, we estimate the model parameters and compute the one step ahead forecast values of daily volatility. We set a forecast horizon from 2/9/2000 to 30/8/2019. We use the RMSE and QLIKE ratios to evaluate the performance of the out sample forecasts of the models.

Table 4.4.7 reports RMSE loss results. For all forecast horizons, Jump and Leverage augmented model, SVL-MIDAS-J and Heston-MIDAS-J, outperforms all the alternative models across all economic indicators.

Next, we turn to QLIKE loss results in Table 4.4.8. Heston-MIDAS-J and SVL-MIDAS-J still outperforms all other models across all economic variables.

Overall, we confirm that the best out-of-sample forecasting performance is achieved by the Heston-MIDAS-J model. Again, this suggests that the joint modelling of the leverage effect in the short term volatility, the long term volatility and rare events through jump will be important in capturing the salient time-varying volatility patterns of the daily WTI returns. Lastly, our out of sample investigation gave the same conclusion as the Bayes factor and DIC analysis.

Table 4.4.7: RMSE LOSS of daily volatility forecast

Macro	Model	1	5	10	15	20
<i>EER<sub>US</sub></i>	SVL-MIDAS	0.984	0.982	0.984	0.898	0.925
	Heston-MIDAS	0.983	0.980	0.981	0.891	0.881
	SV-MIDAS-J	0.935	0.933	0.935	0.853	0.879
	SVL-MIDAS-J	<b>0.897</b>	<b>0.896</b>	<b>0.897</b>	<b>0.819</b>	<b>0.844</b>
	Heston-MIDAS-J	0.906	0.904	0.906	0.821	0.851
<i>GOP</i>	SVL-MIDAS	0.974	0.972	0.974	0.889	0.916
	Heston-MIDAS	0.973	0.970	0.971	0.882	0.872
	SV-MIDAS-J	0.925	0.924	0.925	0.844	0.870
	SVL-MIDAS-J	0.907	0.905	0.907	0.827	0.853
	Heston-MIDAS-J	<b>0.888</b>	<b>0.887</b>	<b>0.888</b>	<b>0.810</b>	<b>0.835</b>
<i>OP<sub>OPEC</sub></i>	SVL-MIDAS	0.954	0.953	0.954	0.871	0.897
	Heston-MIDAS	0.954	0.951	0.952	0.864	0.855
	SV-MIDAS-J	0.907	0.905	0.907	0.827	0.852
	SVL-MIDAS-J	0.889	0.887	0.889	0.811	0.835
	Heston-MIDAS-J	<b>0.870</b>	<b>0.869</b>	<b>0.870</b>	<b>0.794</b>	<b>0.818</b>
<i>OS<sub>OPEC</sub></i>	SVL-MIDAS	0.973	0.972	0.973	0.888	0.915
	Heston-MIDAS	0.973	0.970	0.971	0.882	0.872
	SV-MIDAS-J	0.925	0.923	0.925	0.844	0.870
	SVL-MIDAS-J	<b>0.888</b>	<b>0.886</b>	<b>0.888</b>	<b>0.810</b>	<b>0.835</b>
	Heston-MIDAS-J	0.896	0.895	0.896	0.817	0.842

Note: This table reports RMSE loss of the  $k$ -day total volatility forecast for  $k = 1, 5, 10, 15, 20$  using *EER<sub>US</sub>*, *GOP*, *OP<sub>OPEC</sub>* and *OS<sub>OPEC</sub>* as explanatory variables when forecasting the long term volatility. RMSE loss is the ratio of RMSE of SVL-MIDAS (4.2.13-4.2.14), Heston-MIDAS (4.2.21-4.2.22), SV-MIDAS-J (4.2.31), SVL-MIDAS-J (4.2.31), and Heston-MIDAS-J (4.2.32), to SV-MIDAS (4.2.13-4.2.14). The preferred model is the one with the smallest RMSE loss which is highlighted in bold.

Table 4.4.8: QLIKE LOSS of daily volatility forecast

Macro	Model	1	5	10	15	20
<i>EER<sub>US</sub></i>	SVL-MIDAS	0.971	0.972	0.972	0.973	0.979
	Heston-MIDAS	0.961	0.965	0.966	0.970	0.971
	SV-MIDAS-J	0.941	0.954	0.946	0.955	0.959
	SVL-MIDAS-J	<b>0.915</b>	<b>0.924</b>	<b>0.919</b>	<b>0.908</b>	<b>0.893</b>
	Heston-MIDAS-J	0.925	0.932	0.929	0.919	0.901
<i>GOP</i>	SVL-MIDAS	0.972	0.948	0.988	0.981	0.973
	Heston-MIDAS	0.968	0.949	0.986	0.983	0.967
	SV-MIDAS-J	0.952	0.941	0.948	0.923	0.935
	SVL-MIDAS-J	0.925	0.923	0.927	0.909	0.906
	Heston-MIDAS-J	<b>0.871</b>	<b>0.862</b>	<b>0.872</b>	<b>0.871</b>	<b>0.888</b>
<i>OP<sub>OPEC</sub></i>	SVL-MIDAS	0.982	0.957	0.998	0.991	0.983
	Heston-MIDAS	0.978	0.958	0.996	0.993	0.977
	SV-MIDAS-J	0.962	0.950	0.957	0.932	0.944
	SVL-MIDAS-J	0.934	0.932	0.936	0.918	0.915
	Heston-MIDAS-J	<b>0.880</b>	<b>0.871</b>	<b>0.881</b>	<b>0.880</b>	<b>0.897</b>
<i>OS<sub>OPEC</sub></i>	SVL-MIDAS	0.962	0.938	0.978	0.971	0.963
	Heston-MIDAS	0.958	0.939	0.976	0.973	0.957
	SV-MIDAS-J	0.942	0.931	0.938	0.914	0.925
	SVL-MIDAS-J	<b>0.862</b>	<b>0.853</b>	<b>0.863</b>	<b>0.862</b>	<b>0.879</b>
	Heston-MIDAS-J	0.871	0.858	0.870	0.869	0.887

Note: This table reports QLIKE loss of the  $k$ -day total volatility forecast for  $k = 1, 5, 10, 15, 20$  using *EER<sub>US</sub>*, *GOP*, *OP<sub>OPEC</sub>* and *OS<sub>OPEC</sub>* as explanatory variables when forecasting the long term volatility. QLIKE loss is the ratio of QLIKE of SVL-MIDAS (4.2.13-4.2.14), Heston-MIDAS (4.2.21-4.2.22), SV-MIDAS-J (4.2.31), SVL-MIDAS-J (4.2.31), and Heston-MIDAS-J (4.2.32) to SV-MIDAS (4.2.13-4.2.14). The preferred model is the one with the smallest QLIKE loss which is highlighted in bold.

## 4.5 Conclusion

In this chapter, we extended the family of two multiplicative component models by developing SV-MIDAS, SVL-MIDAS, and different Heston-MIDAS models which are competitors of GARCH-MIDAS type models. The fact that all models produce comparable long term component, we recommend to the user to apply the model whose uni-component volatility model produces a better in sample fit. Based on the recognized preference of SV and SVL models over GARCH type models, we conjecture that their MIDAS version will outperform GARCH-MIDAS type models in empirical studies. It will also be interesting to investigate if Heston-MIDAS model can easily be used in option pricing.

## 4.6 Appendix 3

### 4.6.1 Posteriors of parameter of Heston-MIDAS Models with no Jump component

We report the derivation of the posterior distributions of the parameters of the General Heston-MIDAS Model which nests several variants of the original Model of Heston(1993) which had

been studied in the literature.

Consider the General discrete Heston-MIDAS(4) Model:

$$r_t = \mu + \beta g_{t-1} \tau_{t-1}^{2c} + \tau_t^c \sqrt{g_{t-1}} \varepsilon_{r_t} \quad (4.6.1a)$$

$$g_t = k\theta + (1-k)g_{t-1} + \tau_t^d \sqrt{g_{t-1}} \sigma_g \varepsilon_{g_t} \quad (4.6.1b)$$

$$\log(\tau_t) = m + \psi \sum_{j=1}^K w_j x_{t-j} \quad (4.6.1c)$$

where  $\varepsilon_{r_t}$ 's and  $\varepsilon_{g_t}$ 's are  $iidN(0, 1)$  with  $\rho = cor(\varepsilon_{r_t}, \varepsilon_{g_t})$ ,  $X$  is a macroeconomic variable, and  $w_j$ 's are the beta weighting series of length  $K$  such that  $\sum_{j=1}^K w_j = 1$ .

#### Particular cases:

- Heston model ( HFM) ( Heston (1993), Christoffersen et al. (2010)):  $\beta = -\frac{1}{2}, c = d = 0$
- Heston Model (HRM) ( EJP(2003), Li et al.(2011), among others) :  $\beta = 0, c = d = 0$
- Heston Model (HGM) (Andersen et al. (2002), Pan(2002) Jones(2003) Eraker( 2004) , Hurn et al. (2012)):  $c = d = 0$ , and  $\beta$  is to be estimated
- When  $c = \frac{1}{2}$  and  $d = 0$ , Midas component is included only in returns volatility

The MCMC algorithm for estimating the parameter vector,  $\Theta = (\mu, \beta, k, \theta, \sigma_g^2, \rho, m, \psi)$ , can easily be set up once we compute the close form of the joint posterior distribution of  $p(\Theta | \mathbf{r}, \mathbf{g}, \mathbf{x})$  which satisfies:

$$p(\Theta | \mathbf{r}, \mathbf{g}, \mathbf{x}) \propto L(\mathbf{r}, \mathbf{g} | \Theta, \mathbf{x}) \pi(\Theta) \quad (4.6.2)$$

where  $\mathbf{x}$  is the macroeconomic data, and  $\pi(\Theta)$  is the prior density of  $\Theta$  which can be expressed as the product of the priors of the individual parameters if we assume their independence, and  $L(\mathbf{r}, \mathbf{g} | \Theta, \mathbf{x})$  is the joint likelihood function by considering  $\mathbf{g}$  is latent.

#### Expression of the likelihood function $L(\mathbf{r}, \mathbf{g} | \Theta, \mathbf{x})$

Using the recursive description of  $r_t$  and  $v_t$ , the likelihood function is expressed as:

$$L(\mathbf{r}, \mathbf{g} | \Theta, \mathbf{x}) = \prod_{t=1}^T f((r_t, g_t) | \Theta, \mathbf{x}) = \prod_{t=1}^T f((r_t, g_t) | r_{t-1}, g_{t-1}, \mathbf{x}, \Theta) \quad (4.6.3)$$

where  $(r_t, g_t) | r_{t-1}, g_{t-1}, \mathbf{x}, \Theta$  follows a bivariate normal distribution with parameters:  $\mu_{(r_t, g_t)} = ((\mu + \beta g_{t-1} \tau_{t-1}^{2c}), k\theta + (1-k)g_{t-1})'$  and  $\Sigma_t = g_{t-1} \begin{bmatrix} \tau_{t-1}^{2c} & \rho \tau_{t-1}^{c+d} \sigma_g \\ \rho \tau_{t-1}^{c+d} \sigma_g & \tau_{t-1}^{2d} \sigma_g^2 \end{bmatrix}$

Plugging  $\mu_{(r_t, g_t)}$  and  $\Sigma_t$  in the expression of the density of bivariate normal  $X$  with mean  $\mu_x$ , and variance-covariance matrix  $\Sigma$ ,  $f(x) = \frac{1}{2\pi\sqrt{|\Sigma|}} \exp(-\frac{1}{2}(x - \mu_x)' \Sigma^{-1} (x - \mu_x))$ , and using the fact that

$$|\Sigma_t| = g_{t-1}^2 \tau_{t-1}^{2c+2d} \sigma_g^2 (1-\rho^2), \text{ and } \Sigma_t^{-1} = \frac{1}{\tau_{t-1}^{2c+2d} g_{t-1}^2 \sigma_g^2 (1-\rho^2)} \begin{pmatrix} \tau_{t-1}^{2d} \sigma_g^2 & -\rho \sigma_g \tau_{t-1}^{c+d} \\ -\rho \sigma_g \tau_{t-1}^{c+d} & \tau_{t-1}^{2c} \end{pmatrix}, \text{ we}$$

obtain:

$$f((r_t, g_t) | r_{t-1}, g_{t-1}, \mathbf{x}, \Theta) = \frac{1}{2\pi \tau_{t-1}^{c+d} \sigma_g \sqrt{(1-\rho^2)} g_{t-1}} e^{-\frac{1}{2(1-\rho^2)} \{\varepsilon_{r_t}^2 - 2\rho \varepsilon_{r_t} \varepsilon_{g_t} + \varepsilon_{g_t}^2\}} \quad (4.6.4a)$$

$$\varepsilon_{r_t} = \frac{r_t - \mu - \beta g_{t-1} \tau_{t-1}^{2c}}{\tau_{t-1}^c \sqrt{g_{t-1}}} \quad (4.6.4b)$$

$$\varepsilon_{g_t} = \frac{g_t - k\theta - (1-k)g_{t-1}}{\tau_{t-1}^d \sigma_g \sqrt{g_{t-1}}} \quad (4.6.4c)$$

and the likelihood  $L((\mathbf{r}, \mathbf{g}) | \Theta, \mathbf{x})$  is given by:

$$L((\mathbf{r}, \mathbf{g}) | \Theta, \mathbf{x}) = \left( \frac{1}{2\pi \sigma_g \sqrt{(1-\rho^2)}} \right)^T \left( \prod_{t=1}^T \frac{1}{\tau_{t-1}^{c+d} g_{t-1}} \right) e^{-\frac{1}{2(1-\rho^2)} \sum_{t=1}^T \{\varepsilon_{r_t}^2 - 2\rho \varepsilon_{r_t} \varepsilon_{g_t} + \varepsilon_{g_t}^2\}} \quad (4.6.5)$$

**The posterior Distribution of  $\mu$ :** If we assume prior  $\mu \sim N(\mu_0, \sigma_0^2)$ , we show that the density of the posterior distribution  $p_\mu(\mu | \mathbf{r}, \mathbf{g}, \Theta_{-\mu}, \mathbf{x})$  is also a normal distribution  $N(\mu^*, \sigma_\mu^{*2})$

Applying (4.6.2) for the parameter  $\mu$  only i.e.:  $p_\mu(\mu | \mathbf{r}, \mathbf{g}, \mathbf{x}, \Theta_{-\mu}) \propto L(\mathbf{r}, \mathbf{g} | \Theta_{-\mu}, \mathbf{x}) \pi(\mu)$ ,  $\pi(\mu)$  is its prior density, and using (4.6.5), we get:

$$p_\mu(\mu | \mathbf{r}, \mathbf{g}, \mathbf{x}, \Theta_{-\mu}) \propto e^{-\frac{1}{2(1-\rho^2)} \sum_{t=1}^T \{\varepsilon_{r_t}^2 - 2\rho \varepsilon_{r_t} \varepsilon_{g_t} + \varepsilon_{g_t}^2\}} \exp\left(-\frac{(\mu - \mu_0)^2}{2\sigma_0^2}\right)$$

Since  $\varepsilon_{g_t}$  does not depend on  $\mu$ , then:

$$p_\mu(\mu | \mathbf{r}, \mathbf{g}, \mathbf{x}, \Theta_{-\mu}) \propto e^{-\frac{1}{2(1-\rho^2)} \sum_{t=1}^T \{\varepsilon_{r_t}^2 - 2\rho \varepsilon_{r_t} \varepsilon_{g_t} + \varepsilon_{g_t}^2\}} \exp\left(-\frac{(\mu - \mu_0)^2}{2\sigma_0^2}\right)$$

Using (4.6.4a) and (4.6.4b), we derive that:

$$\varepsilon_{r_t}^2 = \frac{(r_t - \mu - \beta g_{t-1} \tau_{t-1}^{2c})^2}{\tau_{t-1}^{2c} g_{t-1}} = \frac{1}{\tau_{t-1}^{2c}} \left\{ \mu^2 + (r_t - \beta g_{t-1} \tau_{t-1}^{2c})^2 - 2(r_t + 0.5g_{t-1} \tau_{t-1}^{2c})\mu + (r_t - \beta 0.5g_{t-1} \tau_{t-1}^{2c})^2 \right\}$$

$$\varepsilon_{r_t} \varepsilon_{g_t} = \frac{(r_t - \mu - \beta g_{t-1} \tau_{t-1}^{2c})(g_t - k\theta - (1-k)g_{t-1})}{\sigma_g \tau_{t-1}^{c+d} g_{t-1}}$$

By including all the terms of  $\varepsilon_{r_t}^2$ ,  $\varepsilon_{r_t} \varepsilon_{g_t}$ , and  $\varepsilon_{g_t}^2$  that do not depend on  $\mu$  in the proportionality term, we get:

$$p_\mu(\mu | \mathbf{r}, \mathbf{g}, \mathbf{x}, \Theta_{-\mu}) \propto e^{-\frac{1}{2(1-\rho^2)} \sum_{t=1}^T \left\{ \frac{1}{\tau_{t-1}^{2c} g_{t-1}} [\mu^2 - 2(r_t - \beta g_{t-1} \tau_{t-1}^{2c})\mu] + 2\mu \frac{\rho}{\sigma_g \tau_{t-1}^{c+d} g_{t-1}} (g_t - k\theta - (1-k)g_{t-1}) \right\}} e^{-\frac{(\mu - \mu_0)^2}{2\sigma_0^2}}$$

The right hand side of the above expression can be expressed as  $e^{-\frac{1}{2\sigma_\mu^{*2}}(\mu-\mu^*)^2}$  where

$$\sigma_\mu^{*2} = \frac{1}{\frac{1}{(1-\rho^2)} \sum_{t=1}^T \frac{1}{\tau_{t-1}^{2c} g_{t-1}} + \frac{1}{\sigma_0^2}}$$

$$\mu^* = \frac{\frac{1}{(1-\rho^2)} \left\{ \sum_{t=1}^T \frac{(r_t - \beta g_{t-1} \tau_{t-1}^{2c})}{\tau_{t-1}^{2c} g_{t-1}} - \frac{\rho}{\sigma_v} \sum_{t=1}^T \frac{(g_t - k\theta - (1-k)g_{t-1})}{\tau_t^{c+d} g_{t-1}} \right\} + \frac{\mu_0}{\sigma_0^2}}{\frac{1}{(1-\rho^2)} \sum_{t=1}^T \frac{1}{\tau_{t-1}^{2c} g_{t-1}} + \frac{1}{\sigma_0^2}}$$

**Posterior Distribution of  $\theta$ :** As for  $\mu$ , we assume a normal prior for  $\theta$ ,  $N(\theta_0, \sigma_0^2)$ , and from (4.6.2), and (4.6.5), the posterior  $p_\theta(\theta | \mathbf{r}, \mathbf{g}, \mathbf{x}, \Theta_{-\theta})$  is:

$$p_\theta(\theta | \mathbf{r}, \mathbf{g}, \mathbf{x}, \Theta_{-\theta}) \propto \left( \prod_{t=1}^T \frac{1}{\tau_{t-1}^{c+d} g_{t-1}} \right) e^{-\frac{1}{2(1-\rho^2)} \sum_{t=1}^T \{ \varepsilon_{r_t}^2 - 2\rho \varepsilon_{r_t} \varepsilon_{g_t} + \varepsilon_{g_t}^2 \}} e^{-\frac{(\theta - \theta_0)^2}{2\sigma_0^2}}$$

If we keep only the terms that depend on  $\theta$ , we get

$$p_\theta(\theta | \mathbf{r}, \mathbf{g}, \mathbf{x}, \Theta_{-\theta}) \propto e^{-\frac{1}{2(1-\rho^2)} \sum_{t=1}^T \{ -2\rho \varepsilon_{r_t} \varepsilon_{g_t} + \varepsilon_{g_t}^2 \}} e^{-\frac{(\theta - \theta_0)^2}{2\sigma_0^2}}$$

Plugging the expression of  $\varepsilon_{g_t}$ , and keeping only the terms which depend on  $\theta$ , we obtain:

$$p_\theta(\theta | \mathbf{r}, \mathbf{g}, \mathbf{x}, \Theta_{-\theta}) \propto e^{-\frac{1}{2(1-\rho^2)} \sum_{t=1}^T \left\{ -2\rho \varepsilon_{r_t} \frac{g_t - k\theta - (1-k)g_{t-1}}{\tau_{t-1} \sigma_g \sqrt{g_{t-1}}} + \frac{(g_t - k\theta - (1-k)g_{t-1})^2}{\tau_{t-1}^{2d} \sigma_g^2 g_{t-1}} \right\} - \frac{(\theta - \theta_0)^2}{2\sigma_0^2}}$$

$$\propto e^{-\frac{1}{2} \left\{ \left( \frac{1}{(1-\rho^2)} \sum_{t=1}^T \frac{k^2}{\tau_{t-1}^{2d} \sigma_g^2 g_{t-1}} + \frac{1}{\sigma_0^2} \right) \theta^2 - 2\theta \left( \frac{1}{(1-\rho^2)} \sum_{t=1}^T \frac{-\rho k \varepsilon_{r_t}}{\tau_{t-1}^d \sigma_g \sqrt{g_{t-1}}} + \sum_{t=1}^T \frac{k(g_t - (1-k)g_{t-1})}{\tau_{t-1}^{2d} (1-\rho^2) \sigma_g^2 g_{t-1}} + \frac{\theta_0}{\sigma_0^2} \right) \right\}}$$

Hence, the posterior distribution of  $\theta$  is also normal with mean  $\theta^*$  and variance  $\sigma_\theta^2$ :

$$\sigma_\theta^2 = \frac{1}{\frac{1}{(1-\rho^2)} \sum_{t=1}^T \frac{k^2}{\tau_{t-1}^{2d} \sigma_g^2 g_{t-1}} + \frac{1}{\sigma_0^2}}$$

$$\theta^* = \frac{\frac{k}{\sigma_g (1-\rho^2)} \left\{ \sum_{t=1}^T \frac{-\rho \varepsilon_{r_t}}{\tau_{t-1}^d \sqrt{g_{t-1}}} + \frac{1}{\sigma_g^2} \sum_{t=1}^T \frac{((g_t - (1-k)g_{t-1}))}{\tau_{t-1}^{2d} g_{t-1}} \right\} + \frac{\theta_0}{\sigma_0^2}}{\frac{k^2}{2\sigma_g^2 (1-\rho^2)} \sum_{t=1}^T \frac{1}{\tau_{t-1}^{2d} g_{t-1}} + \frac{1}{\sigma_0^2}}$$

**Posterior Distribution of  $\kappa$ :** using prior  $\kappa \sim N(\kappa_0, \sigma_\kappa k^2)$ , we derive using the same previous approach that the posterior distribution  $p(\kappa | \mathbf{r}, \mathbf{g}, \Theta_{-\kappa})$  follows the normal distribution with mean  $\kappa_*$  and variance  $\sigma_{\kappa_*}^2$  because after omitting the terms that do not depend on  $\kappa$ , we

obtain:

$$p(\kappa | \mathbf{r}, \mathbf{g}, \mathbf{x}, \Theta_{-\kappa}) \propto e^{-\frac{1}{2(1-\rho^2)} \sum_{t=1}^T \left\{ -2\rho \varepsilon_{r_t} \frac{g_t - \kappa\theta - (1-\kappa)g_{t-1}}{\tau_{t-1}^d \sigma_g \sqrt{g_{t-1}}} + \frac{(g_t - \kappa\theta - (1-\kappa)g_{t-1})^2}{\tau_{t-1}^{2d} \sigma_g^2 g_{t-1}} \right\} - \frac{(\kappa - k_0)^2}{2\sigma_\kappa^2}}$$

The right hand side expression can be expressed as

$$\begin{aligned} p(\kappa | \mathbf{r}, \mathbf{g}, \mathbf{x}, \Theta_{-\kappa}) &\propto e^{-\frac{1}{2(1-\rho^2)} \sum_{t=1}^T \left\{ -2\rho \varepsilon_{r_t} \frac{\kappa(-\theta + g_{t-1})}{\tau_{t-1}^d \sigma_g \sqrt{g_{t-1}}} + \frac{\kappa^2(\theta - g_{t-1})^2}{\tau_{t-1}^{2d} \sigma_g^2 g_{t-1}} \frac{-2\kappa(\theta - g_{t-1})(g_t - g_{t-1})}{\tau_{t-1}^{2d} \sigma_g^2 g_{t-1}} \right\} - \frac{(\kappa - k_0)^2}{2\sigma_\kappa^2}} \\ &\propto e^{-\frac{1}{2} \left\{ \kappa^2 \left( \frac{1}{(1-\rho^2)} \sum_{t=1}^T \frac{(\theta - g_{t-1})^2}{\tau_{t-1}^{2d} \sigma_g^2 g_{t-1}} + \frac{1}{\sigma_\kappa^2} \right) - 2\kappa \left( \frac{1}{(1-\rho^2)} \sum_{t=1}^T \left( \rho \frac{\varepsilon_{r_t}(-\theta + g_{t-1})}{\tau_{t-1}^d \sigma_g \sqrt{g_{t-1}}} + \frac{(\theta - g_{t-1})(g_t - g_{t-1})}{\tau_{t-1}^{2d} \sigma_g^2 g_{t-1}} \right) + \frac{k_0}{\sigma_\kappa^2} \right) \right\}} \end{aligned}$$

Hence,

$$\begin{aligned} \sigma_{\kappa^*}^2 &= \frac{1}{\frac{1}{(1-\rho^2)} \sum_{t=1}^T \frac{(\theta - g_{t-1})^2}{\tau_{t-1}^{2d} \sigma_g^2 g_{t-1}} + \frac{1}{\sigma_\kappa^2}} \\ \kappa_* &= \frac{\frac{1}{(1-\rho^2)} \sum_{t=1}^T \left( \rho \frac{\varepsilon_{r_t}(-\theta + g_{t-1})}{\tau_{t-1}^d \sigma_g \sqrt{g_{t-1}}} + \frac{(\theta - g_{t-1})(g_t - g_{t-1})}{\tau_{t-1}^{2d} \sigma_g^2 g_{t-1}} \right) + \frac{k_0}{\sigma_\kappa^2}}{\frac{1}{(1-\rho^2)} \sum_{t=1}^T \frac{(\theta - g_{t-1})^2}{\tau_{t-1}^{2d} \sigma_g^2 g_{t-1}} + \frac{1}{\sigma_\kappa^2}} \end{aligned}$$

**Posterior distribution of  $\rho$  and  $\sigma_g^2$ :** If we assume  $\pi(\rho) = U(-1, 1)$ , its posterior density  $p(\rho | \mathbf{r}, \mathbf{g}, \mathbf{x}, \Theta_{-\rho})$  is defined by

$$\begin{aligned} p(\rho | \mathbf{r}, \mathbf{g}, \mathbf{x}, \Theta_{-\rho}) &\propto \left( \prod_{t=1}^T \frac{1}{\tau_{t-1}^{c+d} g_{t-1}} \right) e^{-\frac{1}{2(1-\rho^2)} \sum_{t=1}^T \{ \varepsilon_{r_t}^2 - 2\rho \varepsilon_{r_t} \varepsilon_{g_t} + \varepsilon_{g_t}^2 \}} \frac{1}{2} 1_{[-1,1]}(\rho) \\ &\propto e^{-\frac{1}{2(1-\rho^2)} \sum_{t=1}^T \{ \varepsilon_{r_t}^2 - 2\rho \varepsilon_{r_t} \varepsilon_{g_t} + \varepsilon_{g_t}^2 \}} 1_{[-1,1]}(\rho) \end{aligned}$$

Unfortunately,  $p(\rho | \mathbf{r}, \mathbf{g}, \mathbf{x}, \Theta_{-\rho})$  does not belong to a known family. For this, simulation from  $p(\rho | \mathbf{r}, \mathbf{g}, \mathbf{x}, \Theta_{-\rho})$  is either done using Griddy MCMC method, or by using Eraker(2004) transformation. Griddy-Gibbs MCMC approach consists of approximating the total integral of  $f(\rho) = e^{-\frac{1}{2(1-\rho^2)} \sum_{t=1}^T \{ \varepsilon_{r_t}^2 - 2\rho \varepsilon_{r_t} \varepsilon_{g_t} + \varepsilon_{g_t}^2 \}} 1_{[-1,1]}(\rho)$  by the area below the step functions  $f(a_j)$ 's on grids  $[a_{j-1}, a_j]$  where  $a_j = a_{j-1} + \Delta$  in  $[-1, 1]$  for  $j = 1, \dots, N$  i.e.

$$A = \int_{-1}^1 f(\rho) d\rho = \Delta \sum_{j=1}^N f(a_j) = \Delta \sum_{j=1}^N f(\rho) = \Delta \sum_{j=1}^N e^{-\frac{1}{2(1-a_j^2)} \sum_{t=1}^T \{ \varepsilon_{r_t}^2 - 2 a_j \varepsilon_{r_t} \varepsilon_{g_t} + \varepsilon_{g_t}^2 \}}$$

In each MCMC iteration, we simulate  $u$  from  $U[0, A]$ , then we identify the interval  $[f(a_{j^*-1}), f(a_{j^*})]$  which includes  $u$ , and take  $a_{j^*-1}$  as a simulated value of  $\rho$  if  $\Delta$  is small, or simulate it from  $U[a_{j-1}, a_j]$ .

The numerical integration of Griddy MCMC method can be avoided by using Eraker(2003) transformation  $(\gamma, \Omega)$ , where  $\gamma = \rho \sigma_g$  and  $\Omega = \sigma_g^2(1 - \rho^2)$ . Using this transformation, we can

easily show that the likelihood function  $L((\mathbf{r}, \mathbf{g}) | \Theta, \mathbf{x})$  of (4.6.5) is expressed as:

$$L((\mathbf{r}, \mathbf{g}) | \Theta, \mathbf{x}) = \left( \frac{1}{2\pi\Omega} \right)^T \left( \prod_{t=1}^T \frac{1}{\tau_{t-1}^{c+d} g_{t-1}} \right) e^{-\frac{1}{2\Omega} \sum_{t=1}^T \{(\Omega + \gamma^2) \varepsilon_{r_t}^2 - 2\gamma \varepsilon_{r_t} \varepsilon_{g_t} + \varepsilon_{g_t}^2\}} \quad (4.6.6)$$

The advantage of using  $(\gamma, \Omega)$  is that their prior distributions are conjugate when they are  $\Omega \sim IG(\alpha_0, \beta_0)$  and  $\gamma | \Omega \sim N(\gamma_0, \frac{\Omega}{2})$ . In this case, the joint posterior of  $(\gamma, \Omega)$  is expressed as:

$$\begin{aligned} p(\gamma, \Omega | \mathbf{r}, \mathbf{g}, \Theta_1) &\propto L(\mathbf{r} | \Theta_1, \mathbf{g}) \pi(\gamma | \Omega) \pi(\Omega) \\ &\propto L(\mathbf{r} | \Theta_1, \mathbf{g}) \sqrt{\frac{2}{\Omega}} \exp\left(-\frac{(\gamma - \gamma_0)^2}{\Omega}\right) \frac{\beta^{\alpha_0}}{\Gamma(\alpha_0)} \Omega^{-\alpha_0 - 1} \exp\left(-\frac{\beta_0}{\Omega}\right) \end{aligned} \quad (4.6.7)$$

where  $\Theta_1 = (\mu, \beta, \theta, \kappa, m, \psi)$

By grouping the terms of the right hand side of (4.6.7), we can easily derive that the posterior of  $\Omega$  is  $IG(\alpha_*, \beta_*)$  and that of  $\psi | \Omega$  is  $N(\psi^*, \sigma_\psi^{*2})$  where

$$\begin{aligned} \alpha_* &= \frac{T}{2} + \alpha_0 \text{ and } \beta_* = \beta_0 + \frac{1}{2} \sum_{t=1}^T (\varepsilon_t^g)^2 + \psi_0^2 - \frac{1}{2} \frac{(2\psi_0 + \sum_{t=1}^T \varepsilon_t^r \varepsilon_t^g)^2}{2 + \sum_{t=1}^T (\varepsilon_t^r)^2} \\ \psi^* &= \frac{2\psi_0 + \sum_{t=1}^T \varepsilon_t^r \varepsilon_t^g}{2\psi_0 + \sum_{t=1}^T (\varepsilon_t^r)^2} \text{ and } \sigma_\psi^{*2} = \frac{\Omega}{2 + \sum_{t=1}^T (\varepsilon_t^r)^2} \end{aligned}$$

Hence, draws of  $\rho$  and  $\sigma_g^2$  will be computed from those of  $\Omega$  and  $\gamma$  using the above Eraker's transformations.

Note: Since we do not know the range of  $\sigma_g^2$ , we did not use griddy MCMC method but we used Eraker transformation approach to simulate from its posterior.

### Posterior of the parameters $(m, \psi, \omega)$ of long term component $\tau$ :

The prior of  $m$  is not conjugate even in the simple case ( $\beta = 0, c = \frac{1}{2}$ , and  $d = 0$ ) because, using (4.6.5) and (4.6.1c) we easily deduce that:

$$\begin{aligned} p(m | \mathbf{r}, \mathbf{g}, \mathbf{x}, \Theta_{-m}) &\propto \left( \prod_{t=1}^T \frac{1}{\tau_{t-1}^c g_{t-1}} \right) e^{-\frac{1}{2(1-\rho^2)} \sum_{t=1}^T \{\varepsilon_{r_t}^2 - 2\rho \varepsilon_{r_t} \varepsilon_{g_t}\}} \pi(m) \\ &\propto e^{-\frac{1}{2(1-\rho^2)} \sum_{t=1}^T \left\{ \frac{(r_t - \mu)^2 e^{-m}}{g_{t-1}} - 2\rho \varepsilon_{g_t} \frac{(r_t - \mu) e^{-0.5m}}{\sqrt{g_{t-1}}} \right\} - 0.5Tm} \end{aligned} \quad (4.6.8)$$

since  $\varepsilon_{g_t}$  does not depend on  $m$ ,  $\varepsilon_{g_t} = \frac{g_t - \kappa\theta - (1-\kappa)g_{t-1}}{\sigma_g \sqrt{g_{t-1}}}$ , and  $\varepsilon_{r_t} = \frac{(r_t - \mu) e^{-0.5(m + \psi \sum_{k=1}^K w_k x_{t-k})}}{\sqrt{g_{t-1}}}$ ,  
 $\varepsilon_{r_t}^2 = \frac{(r_t - \mu)^2 e^{-(m + \psi \sum_{k=1}^K w_k x_{t-k})}}{g_{t-1}}$ .

Unfortunately,  $p(m | \mathbf{r}, \mathbf{g}, \mathbf{x}, \Theta_{-m})$  cannot be expressed as a known density because it involves  $e^{-m}$  and  $m$ .



Similarly, we can show that

$$p(\boldsymbol{\psi} | \mathbf{r}, \mathbf{g}, \mathbf{x}, \Theta_{-\boldsymbol{\psi}}) \propto e^{-\frac{1}{2(1-\rho^2)} \sum_{t=1}^T \left\{ \frac{(r_t - \mu)^2 e^{-\psi \sum_{k=1}^K w_k x_{t-k}}}{g_{t-1}} - 2\rho \varepsilon_{g_t} \frac{(r_t - \mu) e^{-0.5\psi \sum_{k=1}^K w_k x_{t-k}}}{\sqrt{g_{t-1}}} \right\} - 0.5T \psi \sum_{k=1}^K w_k x_{t-k}} \pi(\boldsymbol{\psi}) \quad (4.6.9)$$

For this, we decided to simulate  $j^{\text{th}}$  draw  $(m, \boldsymbol{\psi})^{(j)}$  using Adaptive Metropolis algorithm which consists of using the proposal  $f((m, \boldsymbol{\psi}))$  which is defined by (Roberts and Rosenthal (2009)) as:

$$f((m, \boldsymbol{\psi})) = \begin{cases} N_2 \left( (m, \boldsymbol{\psi})^{(j-1)}, \frac{0.1^2 I_2}{k} \right) & \text{if } j \leq 2 \\ (1 - \delta) N_2 \left( (m, \boldsymbol{\psi})^{(j-1)}, \frac{2.38^2 \Sigma^{(j)}}{k} \right) + \delta N_2 \left( (m, \boldsymbol{\psi})^{(j-1)}, \frac{0.1^2 I_2}{k} \right) & \text{if } 2 < j < j^* \\ N_2 \left( (m, \boldsymbol{\psi})^{(j-1)}, \Sigma^{(j^*)} \right) & \text{if } j > j^* \end{cases} \quad (4.6.10)$$

where  $k$  is the number of parameters i.e.  $k = 2$ ,  $j^*$  is the burnin,  $\delta = 0.05$ ,  $I_2$  is the identity matrix, and  $\Sigma^{(j)}$  is the variance covariance matrix of  $(m, \boldsymbol{\psi})^{(j)}$ 's for  $j < j^*$ .

A draw  $(m, \boldsymbol{\psi})^*$  from  $f((m, \boldsymbol{\psi}))$  is accepted as a draw  $(m, \boldsymbol{\psi})^{(j)}$  from the posterior  $p(m, \boldsymbol{\psi} | \mathbf{r}, \mathbf{g}, \mathbf{x}, \Theta_{-(m, \boldsymbol{\psi})})$  with probability  $\min(1, \frac{p((m, \boldsymbol{\psi})^* | \mathbf{r}, \mathbf{g}, \mathbf{x}, \Theta_{-(m, \boldsymbol{\psi})}) \pi((m, \boldsymbol{\psi})^*)}{p((m, \boldsymbol{\psi})^{(j)} | \mathbf{r}, \mathbf{g}, \mathbf{x}, \Theta_{-(m, \boldsymbol{\psi})}) \pi((m, \boldsymbol{\psi})^{(j)})})$

**Posterior of  $\omega$ :** Since  $\omega$  is bounded between 1 and 50, we use Griddy MCMC algorithm as described for  $\rho$  where

$$p(\omega | \mathbf{r}, \mathbf{g}, \mathbf{x}, \Theta_{-\omega}) \propto e^{-\frac{1}{2(1-\rho^2)} \sum_{t=1}^T \{ \varepsilon_{r_t}^2 - 2\rho \varepsilon_{r_t} \varepsilon_{g_t} + \varepsilon_{g_t}^2 \}} 1_{[1, 50]}(\omega) \quad (4.6.11) \\ \propto e^{-\frac{1}{2(1-\rho^2)} \sum_{t=1}^T \{ \varepsilon_{r_t}^2 - 2\rho \varepsilon_{r_t} \varepsilon_{g_t} + \varepsilon_{g_t}^2 \}} 1_{[1, 50]}(\omega)$$

where  $\varepsilon_{r_t} = \frac{(r_t - \mu + \beta g_{t-1} e^{-c(m + \psi \sum_{k=1}^K w_k(\omega) x_{t-k}))}) e^{-c(m + \psi \sum_{k=1}^K w_k(\omega) x_{t-k})}}{\sqrt{g_{t-1}}}$ ,  $\varepsilon_{g_t} = \frac{(g_t - \kappa \theta - (1 - \kappa) g_{t-1}) e^{-d(m + \psi \sum_{k=1}^K w_k(\omega) x_{t-k})}}{\sigma_g \sqrt{g_{t-1}}}$

$w_k(\omega) = \frac{(1 - \frac{k}{K})^{1-\omega}}{\sum_{k=1}^K (1 - \frac{k}{K})^{1-\omega}}$  and  $\pi(\omega)$  is  $U[1, 50]$  using grids  $\omega_j = 1 + j/2$  for  $j = 1, \dots, 98$ , knowing that  $w_k(\omega)$  is not very sensitive to  $\omega$  ( see Chapter 1).

Note: This is not time consuming as we can store  $\sum_{k=1}^K w_k(\omega_j) x_{t-k}$  for  $\omega_j = 1 + j/2$  for  $j = 1, \dots, 98$  before the start of the MCMC algorithm.

### Posterior of short term volatility $\mathbf{g}$ :

Using the known property that for each  $t$ ,  $p(g_t | \mathbf{r}, \mathbf{x}, \mathbf{g}_{-t}, \Theta) = p(g_t | \mathbf{r}, \mathbf{x}, g_{t-1}, g_{t+1}, \Theta)$ , we derive from Bayes theorem that

$$p(v_t | \mathbf{r}, \mathbf{x}, g_{t-1}, g_{t+1}, \Theta) \propto p(g_t, \mathbf{r} | g_{t-1}, \mathbf{x}, \Theta) p(g_{t+1}, \mathbf{r} | g_t, \mathbf{x}, \Theta)$$

where the expression of  $p(g_t, \mathbf{r} | g_{t-1}, \mathbf{x}, \Theta)$  and  $p(g_{t+1}, \mathbf{r} | g_t, \mathbf{x}, \Theta)$  can be deduced from (4.6.4a) i.e.

$$p((r_t, g_t) | r_{t-1}, g_{t-1}, \mathbf{x}, \Theta) = \frac{1}{2\pi \tau_{t-1}^{c+d} \sigma_g \sqrt{(1-\rho^2)g_{t-1}}} e^{-\frac{1}{2(1-\rho^2)} \{ \varepsilon_{r_{t+1}}^2 - 2\rho \varepsilon_{r_t} \varepsilon_{g_t} + \varepsilon_{g_t}^2 \}}$$

$$p((r_{t+1}, g_{t+1}) | r_t, g_t, \mathbf{x}, \Theta) = \frac{1}{2\pi \tau_{t-1}^{c+d} \sigma_g \sqrt{(1-\rho^2)g_t}} e^{-\frac{1}{2(1-\rho^2)} \{ \varepsilon_{r_{t+1}}^2 - 2\rho \varepsilon_{r_{t+1}} \varepsilon_{g_{t+1}} + \varepsilon_{g_{t+1}}^2 \}}$$

Using the fact  $\varepsilon_{r_t}^2 | g_{t-1}$  does not depend on  $g_t$ , we derive that:

$$p(g_t | \mathbf{r}, \mathbf{x}, g_{t-1}, g_{t+1}, \Theta) \propto \frac{1}{\tau_{t-1}^{c+d} \sigma_g \sqrt{(1-\rho^2)}} e^{-\frac{1}{2(1-\rho^2)} \{ -2\rho \varepsilon_{r_t} \varepsilon_{g_t} + \varepsilon_{g_t}^2 \}} \frac{1}{\tau_{t-1}^{c+d} \sigma_g \sqrt{(1-\rho^2)g_t}} e^{-\frac{1}{2(1-\rho^2)} \{ \varepsilon_{r_{t+1}}^2 - 2\rho \varepsilon_{r_{t+1}} \varepsilon_{g_{t+1}} + \varepsilon_{g_{t+1}}^2 \}}$$

$$\propto \frac{1}{\tau_{t-1}^{2c+2d} \sigma_g^2 (1-\rho^2)g_t} e^{-\frac{1}{2(1-\rho^2)} \{ \varepsilon_{r_{t+1}}^2 - 2\rho (\varepsilon_{r_t} \varepsilon_{g_t} + \varepsilon_{r_{t+1}} \varepsilon_{g_{t+1}}) + \varepsilon_{g_t}^2 + \varepsilon_{g_{t+1}}^2 \}}$$

We use Random Walk to simulate from  $p(g_t | \mathbf{r}, \mathbf{x}, g_{t-1}, g_{t+1}, \Theta)$  i.e.:

For the  $j^{th}$  MCMC iteration, we simulate

$$g_t^* = g_t^{(j-1)} + cN(0, 1) \quad (4.6.12)$$

$g_t^*$  is accepted as  $g_t^{(j)}$  with probability  $\alpha$  defined by:

$$\alpha = \frac{p(g_t^* | \mathbf{r}, g_{t-1}, g_{t+1}, \Theta)}{p(g_t^{(j-1)} | \mathbf{r}, g_{t-1}, g_{t+1}, \Theta)}$$

where  $c$  is chosen by the user to achieve an acceptance rate of about 40-50% (EGP (2003)).

If  $g_t^*$  is not accepted, we take  $g_t^{(j)} = g_t^{(j-1)}$  for each  $t$ .

**Remark:** It is well recognized that the convergence of the MCMC algorithm depends crucially on the initial values  $\mathbf{g}^{(0)}$  and the choice of the meta parameter  $c$ . In the literature of Heston Model,  $\mathbf{g}^{(0)}$  is simulated from truncated normal  $N\left(\theta^{(0)}, \frac{(\sigma_g^{(0)})^2 \theta^{(0)}}{2}\right) 1_{g>0}$  for each  $g_t^{(0)}$  where  $\theta^{(0)}$  and  $\sigma_g^{(0)}$  are the initial values, based on Eraker(2001) which states that  $p(g_t | \mathbf{r}, \mathbf{x}, g_{t-1}, g_{t+1}, \Theta)$  can be approximated by  $N\left(\frac{g_{t-1}+g_{t+1}}{2}, \frac{\sigma_g^2(1-\rho^2)g_{t-1}}{2}\right)$ .

To improve the speed of MCMC convergence, we use the volatility of EGARCH(1,1) as  $\mathbf{g}^{(0)}$  which is more realistic than the above iid normally distributed using initial values of the parameters. Furthermore, we note that in the first iteration of the MCMC, (4.6.12) becomes:

$$g_t^* = g_t^{(0)} + g_t^{(0)} cN(0, 1)$$

and simulated  $g_t^*$  is a draw from the kernel density estimate of  $\mathbf{g}^0$  under the assumption that  $g_t^{(0)}$ 's are iid (Silverman(1981) which suggests to estimate/choose  $c$  as the optimal smoothing

parameter under normality which is defined by:

$$c = 1.06n^{-0.2}s \quad (4.6.13)$$

where  $s$  is the sample standard deviation of  $\mathbf{g}^{(0)}$  of size  $n$ .

Indeed, it can be updated, in a similar way as the adaptive approach, for each  $t$  by using  $c_t = s_t 1.06j^{-0.2}$ .

where  $s_t$  is the standard deviation of the previous draws  $g_t^{(i)}$  for  $i < j$

**Posterior distribution of  $\beta$ :** If we assume a normal prior  $N(\beta_0, \sigma_{\beta_0}^2)$ , the posterior is

$$p_{\beta}(\beta | \mathbf{r}, \mathbf{g}, \mathbf{x}, \Theta_{-\beta}) \propto e^{-\frac{1}{2(1-\rho^2)} \sum_{t=1}^T \{\varepsilon_{r_t}^2 - 2\rho\varepsilon_{r_t}\varepsilon_{g_t} + \varepsilon_{g_t}^2\}} \exp\left(-\frac{(\beta - \beta_0)^2}{2\sigma_{\beta_0}^2}\right)$$

Using the same steps as those used for the posterior of  $\mu$ , we show that  $p_{\beta}(\beta | \mathbf{r}, \mathbf{g}, \mathbf{x}, \Theta_{-\beta})$  is  $N(\beta_*, \sigma_{\beta_*}^2)$  where

$$\sigma_{\beta}^{*2} = \frac{1}{\frac{1}{(1-\rho^2)} \sum_{t=1}^T g_{t-1} \tau_{t-1}^{2c} + \frac{1}{\sigma_0^2}}$$

$$\mu_{\beta}^* = \frac{\frac{1}{(1-\rho^2)} \left\{ \sum_{t=1}^T (r_t - \mu) + \frac{\rho}{\sigma_g} \sum_{t=1}^T \tau_{t-1}^c \frac{(g_t - \kappa\theta - (1-\kappa)g_{t-1})}{\tau_{t-1}^d} \right\} + \frac{\beta_*}{\sigma_{\beta_*}^2}}{\frac{1}{(1-\rho^2)} \sum_{t=1}^T g_{t-1} \tau_{t-1}^{2c} + \frac{1}{\sigma_0^2}}$$

## 4.6.2 Posterior distribution of parameters of SVL-MIDAS Model with no Jump Component

Consider the SVL-MIDAS model which is defined by

$$r_t = \mu + \tau_t^c e^{h_t/2} \varepsilon_t^r \quad (4.6.14a)$$

$$h_{t+1} = \alpha_0 + \varphi(h_t - \alpha_0) + \sigma_h \tau_t^d \varepsilon_t^h \quad (4.6.14b)$$

$$\log(\tau_t) = m + \theta \sum_{k=1}^K w_k(\omega) X_{t-k} \quad (4.6.14c)$$

where  $|\varphi| < 1$ ,  $h_t = \log(g_t)$ ,  $\varepsilon_t^r$  and  $\varepsilon_t^h$  are  $N(0, 1)$  and  $cor(\varepsilon_t^r, \varepsilon_t^h) = \rho$ .

The Posterior distribution of the parameter vector  $\Theta = (\mu, \alpha_0, \varphi, \sigma_h, m, \theta, \omega)$  can be derived using the same approach as that used for Heston-MIDAS parameters, given in subsection 4.6.1 because the likelihood function is also expressed as:

$$L((\mathbf{r}, \mathbf{g}) | \Theta, \mathbf{x}) = \left( \frac{1}{2\pi \sigma_g \sqrt{(1-\rho^2)}} \right)^T \left( \prod_{t=1}^T \frac{1}{\tau_t^{c+d}} \right) e^{-\frac{1}{2(1-\rho^2)} \sum_{t=1}^T \{\varepsilon_{r_t}^2 - 2\rho\varepsilon_{r_t}\varepsilon_{g_t} + \varepsilon_{g_t}^2\}}$$

where

$$\varepsilon_{r_t} = \frac{r_t - \mu}{\tau_t^c e^{h_t/2}} \quad (4.6.15a)$$

$$\varepsilon_{g_t} = \frac{h_{t+1} - \phi h_{t1} - \alpha_0 (1 - \phi)}{\tau_t^d \sigma_g} \quad (4.6.15b)$$

In other words, the difference between the posterior distribution of the parameters of SVL-MIDAS and those of Heston-MIDAS models is in the expression of the errors terms  $\varepsilon_{r_t}^r$  and  $\varepsilon_{g_t}^h$ . Actually, the posteriors of SVL model are very known in the literature.

**Posterior distribution of  $\mu$ :** If  $\pi(\mu) = N(\mu_0, \sigma_{\mu 0}^2)$ , we can easily derive that the posterior  $p(\mu | \mathbf{r}, \mathbf{h}, \mathbf{x}, \Theta_{-\mu})$  is  $N(\mu_\mu, \sigma_\mu^2)$  where :

$$\mu_\mu = \frac{\frac{1}{(1-\rho^2)} \sum_{t=1}^T e^{-h_t} \left( \frac{r_t}{\tau_t^{c2}} - \rho \frac{eh e^{0.5h_t}}{\tau_t^{c+d} \sigma_h} \right) + \frac{\mu_{\mu 0}}{\sigma_{\mu 0}^2}}{\left\{ \frac{1}{(1-\rho^2)} \sum_{t=1}^T \frac{1}{\tau_t^{c2} e^{h_t}} + \frac{1}{\sigma_{\mu 0}^2} \right\}}$$

$$\sigma_\mu^2 = \frac{1}{\left\{ \frac{1}{(1-\rho^2)} \sum_{t=1}^T \frac{1}{\tau_t^{c2} e^{h_t}} + \frac{1}{\sigma_{\mu 0}^2} \right\}}$$

**Posterior distribution of  $\alpha_0$ :** If  $\pi(\alpha_0) = N(\mu_{h0}, \sigma_{\mu h0}^2)$ ,  $p(\alpha_0 | \mathbf{r}, \mathbf{h}, \mathbf{x}, \Theta_{-\alpha_0})$  is  $N(\mu_{\alpha_0}, \sigma_{\alpha_0}^2)$  where

$$\sigma_{\alpha_0}^2 = \frac{1}{T \frac{(1-\phi)^2}{(1-\rho^2) \sigma_h^2} + \frac{(1-\phi)^2}{\sigma_h^2} \sum_{t=1}^T \frac{1}{\tau_t^{2d}} + \frac{(1-\phi^2)}{\sigma_h^2 \tau_1^{2d}} + \frac{1}{\sigma_{\mu h0}^2}}$$

$$\mu_{\alpha_0} = \frac{\frac{(1-\phi_h)\rho}{\sigma_h(1-\rho^2)} \sum_{t=1}^T \frac{(r_t - \mu)}{\tau_t^c e^{0.5h_t}} - \frac{(1-\phi_h)\rho^2}{\sigma_h^2(1-\rho^2)} \sum_{t=0}^{T-1} \frac{(h_{t+1} - \phi_h h_t)}{\tau_t^{2d}} - \frac{(1-\phi)}{\sigma_h^2} \sum_{t=0}^{T-1} \frac{(h_{t+1} - \phi_h h_t)}{\tau_t^{2d}} + (1-\phi^2) \frac{h_1}{\sigma_h^2 \tau_1^{2d}} + \frac{\mu_{h0}}{\sigma_{\mu h0}^2}}{T \frac{(1-\phi)^2}{(1-\rho^2) \sigma_h^2} + \frac{(1-\phi)^2}{\sigma_h^2} \sum_{t=1}^T \frac{1}{\tau_t^{2d}} + \frac{(1-\phi^2)}{\sigma_h^2 \tau_1^{2d}} + \frac{1}{\sigma_{\mu h0}^2}}$$

**Posterior distribution of  $\phi$ :** If we assume  $\pi(\phi) = N(\mu_{\phi 0}, \sigma_{\phi 0}^2) 1_{(-1, 1)}$ , we have  $p(\phi | \mathbf{r}, \mathbf{h}, \mathbf{x}, \Theta_{-\phi})$  is  $N(\mu_\phi, \sigma_\phi^2) 1_{(-1, 1)}$  where

$$\sigma_\phi^2 = \frac{1}{\frac{\rho^2}{\sigma_h^2(1-\rho^2)} \sum_{t=1}^T (h_t - \alpha_0)^2 + \frac{1}{\sigma_h^2} \sum_{t=1}^T \frac{(h_t - \alpha_0)^2}{\tau_t^{2d}} + \frac{1}{\sigma_{\phi 0}^2}}$$

$$\mu_\phi = \frac{-\frac{\rho}{(1-\rho^2)\sigma_h} \left( \sum_{t=1}^T \frac{(r_t - \mu)(h_t - \alpha_0)}{\tau_t^c e^{0.5h_t}} - \frac{\rho}{\sigma_h} \sum_{t=1}^T (h_t - \alpha_0)^2 \right) + \frac{1}{\sigma_h^2} \sum_{t=0}^{T-1} \frac{(h_{t+1} - \alpha_0)(h_t - \alpha_0)}{\tau_t^{2d}} + \frac{\mu_{\phi 0}}{\sigma_{\phi 0}^2}}{\frac{\rho^2}{\sigma_h^2(1-\rho^2)} \sum_{t=1}^T (h_t - \alpha_0)^2 + \frac{1}{\sigma_h^2} \sum_{t=1}^T \frac{(h_t - \alpha_0)^2}{\tau_t^{2d}} + \frac{1}{\sigma_{\phi 0}^2}}$$

**Posterior distribution of  $\rho$ :** Using Uniform prior  $U(-1, 1)$ , the prior  $\pi(\rho)$  is not conjugate

because  $p(\rho \mid \mathbf{r}, \mathbf{h}, \mathbf{x}, \Theta_{-\rho})$  cannot be simplified further than

$$p(\rho \mid \mathbf{r}, \mathbf{h}, \mathbf{x}, \Theta_{-\rho}) \propto \exp\left(-0.5 \sum_{t=0}^{T-1} \frac{\left(r_t - \mu - \frac{\rho}{\sigma_h} \tau_t^c e^{0.5h_t} (h_{t+1} - \alpha_0 - \phi(h_t - \alpha_0))\right)^2}{(1 - \rho^2) \tau_t^{2c} e^{h_t}}\right) U(-1, 1)$$

We simulate draws of  $\rho$  by approximating  $p(\rho \mid \mathbf{r}, \mathbf{h}, \mathbf{x}, \Theta_{-\rho})$  by linear interpolation over grids as done for Heston-MIDAS model.

**Posterior of  $\sigma_h^2$ :** As done in the literature, we assume prior  $\pi(\sigma_h^2) = IG(a, b)$ , we can show that

$$\begin{aligned} p(\sigma_h^2 \mid \mathbf{r}, \mathbf{h}, \Theta_{-\sigma_h^2}) &\propto \exp\left(-\frac{0.5}{\sigma_h^2} \sum_{t=0}^{T-1} \frac{\left(r(t) - \mu - \frac{\rho}{\sigma_h} \tau_t^c e^{0.5h_t} (h_{t+1} - \alpha_0 - \phi(h_t - \alpha_0))\right)^2}{(1 - \rho^2) \tau_t^{2c} e^{h_t}} + \frac{(1 - \phi^2)}{\tau_1^{2d} \sigma_h^2}\right) \\ &\times \frac{b^a}{\Gamma(a) (\sigma_h^2)^{a+(T+1)/2}} e^{-\frac{(b+0.5 \sum_{t=0}^{T-1} \frac{(h_{t+1} - \alpha_0 - \phi(h_t - \alpha_0))^2}{\tau_t^{2d}})}{\sigma_h^2}} \\ &\propto \exp\left(-\frac{0.5}{\sigma_h^2} \sum_{t=0}^{T-1} \frac{\left(r(t) - \mu - \frac{\rho}{\sigma_h} \tau_t^c e^{0.5h_t} (h_{t+1} - \alpha_0 - \phi(h_t - \alpha_0))\right)^2}{(1 - \rho^2) \tau_t^{2c} e^{h_t}}\right) \\ &\times IG\left(a + (T + 1)/2, b + 0.5 \left(\sum_{t=0}^{T-1} \frac{(h_{t+1} - \alpha_0 - \phi(h_t - \alpha_0))^2}{\tau_t^{2d}} + \frac{(1 - \phi^2) h_1}{\tau_1^{2d}}\right)\right) \end{aligned}$$

Hence,  $p(\sigma_h^2 \mid \mathbf{r}, \mathbf{h}, \Theta_{-\sigma_h^2})$  is not an IG distribution because the first exponential term of the right hand side cannot be expressed as  $\exp(C/\sigma_h^2)$  where  $C$  is independent of  $\sigma_h^2$ . Since the support of  $\sigma_h^2$  is unknown, we use Metropolis Hasting method, as done for SVL in the literature, using the proposal density  $IG(a + (T + 1)/2, b + 0.5(\sum_{t=0}^{T-1} \frac{(h_{t+1} - \alpha_0 - \phi(h_t - \alpha_0))^2}{\tau_t^{2d}} + \frac{(1 - \phi^2) h_1}{\tau_1^{2d}}))$

**Posterior of the parameters  $(m, \psi, \omega)$  of long term component  $\tau$ :**

We draw  $(m, \psi, \omega)$  using Adaptive Metropolis method as done for Heston-MIDAS model in subsection 4.6.1.

### 4.6.3 Posterior distribution of the parameters $(\mu_z, \sigma_z, \lambda)$ of Jump component for SVL-MIDAS-J and Heston-MIDAS-J

In the literature, estimation of the parameters of jump component is the same for GARCH, GJRGARCH, EGARCH, SV, SVL, and Heston Models. In fact, the inclusion of the long-term component does not alter the approach for estimating  $(\mu_z, \sigma_z, \lambda)$  where  $(\mu_z, \sigma_z^2)$  are the mean and the variance of the jump size variable which is assumed normal, and  $\lambda$  is the rate of jump occurrence.

**Posterior density  $p_{z_t}(\cdot)$  of the Jump size  $z_t$ :**

Similar to Chapter 3, we assume a normal prior  $\pi(z_t) \sim N(\mu_s, \sigma_s^2)$  for the jump size  $z_t$ . When there is a Jump at time  $t$ , i.e.  $b_t = 1$ ,  $\varepsilon_t^r$  becomes

$$\varepsilon_{r_t} = \frac{r_t - \tilde{\mu}_t - b_t z_t}{\tau_{t-1}^c \sqrt{g_{t-1}}}, \quad \tilde{\mu}_t = \mu + \beta \tau_{t-1}^{2c} g_{t-1} \quad \text{for Heston-MIDAS-J} \quad (4.6.16a)$$

$$\varepsilon_{r_t} = \frac{r_t - \tilde{\mu}_t - b_t z_t}{\tau_t^c \sqrt{g_t}}, \quad \tilde{\mu}_t = \mu \quad \text{for SVL-MIDAS-J} \quad (4.6.16b)$$

where  $\tilde{\mu}_t = \mu$  for SVL-MIDAS-J model,  $\tilde{\mu}_t = \mu + \beta \tau_{t-1}^{2c} g_{t-1}$  for Heston-MIDAS-J, and  $\eta_t^g$  remains unchanged.

Thus, when  $b_t = 1$ , the posterior  $p_{z_t}(z_t | \Theta, \mathbf{r}, \mathbf{x}, \mathbf{g}, b_t = 1)$  satisfies

$$p_{z_t}(z_t | \Theta, \mathbf{x}, \mathbf{r}, \mathbf{g}, b_t = 1) = \mathbf{L}(\mathbf{r}, \mathbf{g} | \mathbf{x}, z_t, b_t = 1) \pi(z_t) \propto e^{-\frac{1}{2(1-\rho^2)} \sum_{t=1}^T \{\varepsilon_{r_t}^2 - 2\rho \varepsilon_{r_t} \varepsilon_{g_t}\}} \pi(z_t)$$

Keeping only the terms that depend on  $z_t$ , for Heston-MIDAS-J Model, we get:

$$p_{z_t}(z_t | \mathbf{x}, \Theta, \mathbf{r}, \mathbf{g}, b_t = 1) \propto \exp\left(-\frac{1}{2} \left( \frac{1}{(1-\rho^2) \tau_{t-1}^{2c} g_{t-1}} + \frac{1}{\sigma_s^2} \right) z_t^2 - 2z_t \left( \frac{1}{(1-\rho^2) \tau_{t-1}^{2c} g_{t-1}} (r_t - \tilde{\mu}_t) - \frac{\rho \varepsilon_{g_t}}{(1-\rho^2) \tau_{t-1}^c g_{t-1}} + \frac{\mu_s}{\sigma_s^2} \right)\right) \quad (4.6.17)$$

Hence, the mean and variance of the normal posterior  $p_{z_t}(\cdot)$  are

$$\mu_z = \frac{\frac{1}{(1-\rho^2) \tau_{t-1}^{2c} g_{t-1}} (r_t - \tilde{\mu}_t) - \frac{\rho \varepsilon_{g_t}}{(1-\rho^2) \tau_{t-1}^c g_{t-1}} + \frac{\mu_s}{\sigma_s^2}}{\frac{1}{(1-\rho^2) \tau_{t-1}^{2c} g_{t-1}} + \frac{1}{\sigma_s^2}}$$

$$\sigma_z^2 = \frac{1}{\frac{1}{(1-\rho^2) \tau_{t-1}^{2c} g_{t-1}} + \frac{1}{\sigma_s^2}}$$

When  $b_t = 0$ , the Likelihood  $\mathbf{L}(\mathbf{r}, \mathbf{g} | \Theta, \mathbf{x}, b_t = 0)$  will be independent of  $z_t$ , and therefore

$$p_{z_t}(z_t | \mathbf{x}, \Theta, \mathbf{r}, \mathbf{g}, b_t = 0) = \pi(z_t) \quad (4.6.18)$$

(4.6.17) indicates that draws of  $z_t$  is given only when  $b_t = 1$  whereas (4.6.18) reports that when  $b_t = 0$ ,  $z_t$  is drawn from the prior  $\pi(z_t) \sim N(\mu_s, \sigma_s^2)$  as done in the literature for SVL-J and Heston-J.

Note: For SVL-MIDAS-J Model the expression of  $\mu_z$  and  $\sigma_z^2$  are the same as above except that  $\tau_{t-1}$  and  $g_{t-1}$  are replaced by  $\tau_t$  and  $g_t$ .

**Posterior density of the occurrence  $b_t$  of jumps:** If we assume a Bernoulli prior  $Ber(\lambda_0)$ , then

$$p_{b_t}(b_t | \mathbf{x}, \Theta, \mathbf{r}, \mathbf{g}, z_t) \propto e^{-\frac{1}{2(1-\rho^2)} \sum_{t=1}^T \{\varepsilon_{r_t}^2 - 2\rho \varepsilon_{r_t} \varepsilon_{g_t}\}} \lambda_0^{b_t} (1 - \lambda_0)^{1-b_t}$$

Using the facts that  $b_t^2 = b_t$ ,  $\lambda_0^{J_t} (1 - \lambda_0)^{1-b_t} = \left( \frac{\lambda_0}{1-\lambda_0} \right)^{b_t} (1 - \lambda_0)$ , and algebraic calculations, we deduce that the posterior  $p_{b_t}(b_t | \mathbf{x}, \Theta, \mathbf{r}, \mathbf{g}, z_t)$  is also binomial distribution with parameter  $p$

because

$$p_{b_t}(b_t | \mathbf{x}, \Theta, \mathbf{r}, \mathbf{g}, z_t) \propto \left( \frac{\exp(-\frac{1}{2}A)\lambda_0}{1-\lambda_0} \right)^{b_t} \propto \left( \frac{p}{1-p} \right)^{b_t}$$

where  $p = \frac{1}{(1-\lambda_0)\exp(\frac{1}{2}A)+1}$ , and  $A = \frac{1(z_t^2 - 2z_t(r_t - \bar{\mu}))}{(1-\rho^2)\tau_{t-1}^2 g_{t-1}^2} + \frac{2\rho z_t \varepsilon_{g_t}}{\tau_{t-1}^2 g_{t-1}^2}$  for Heston-MIDAS-J and  $A = \frac{1(z_t^2 - 2z_t(r_t - \bar{\mu}))}{(1-\rho^2)\tau_t^2 g_t^2} + \frac{2\rho z_t \varepsilon_{g_t}}{\tau_t^2 g_t^2}$  for SVL-MIDAS-J

**Posterior density  $p_\lambda(\cdot)$  of the rate  $\lambda$  of occurrence of jumps:** Assuming  $\pi(\lambda)$  is  $Beta(\alpha_{\lambda_0}, \beta_{\lambda_0})$  we can show that the posterior  $p_\lambda(\cdot)$  is also  $Beta(\alpha_\lambda, \beta_\lambda)$  for both SVLJ-MIDAS and HGMJ-MIDAS models where

$$\alpha_\lambda = \alpha_{\lambda_0} + \sum_{t=1}^T b_t$$

$$\beta_\lambda = \beta_{\lambda_0} + T - \sum_{t=1}^T b_t$$

**Posterior density of the parameters  $\mu_s$  and  $\sigma_s^2$  of Jump size  $z_t$**

Using normal prior  $N(m, M^2)$  for  $\mu_s$ , and the fact  $z_t \sim N(\mu_s, \sigma_s^2)$ , from Bayes Theorem we deduce that the posterior  $p_{\mu_s}(\mu_s | \mathbf{z}, \sigma_s^2)$  satisfies:

$$p_{\mu_s}(\mu_s | \mathbf{z}, \sigma_s^2) \propto p_z(\mathbf{z} | \mu_s, \sigma_s^2) \pi_{\mu_s}(\mu_s)$$

Using the fact that  $z_t$ 's are independent, we deduce that

$$p_{\mu_s}(\mu_s | \mathbf{z}, \sigma_s^2) \propto \exp\left(-\frac{1}{2}\left\{\left(\frac{T}{\sigma_s^2} + \frac{1}{M^2}\right)\mu_s^2 - 2\mu_s\left(\frac{\sum_{t=1}^T z_t}{\sigma_s^2} + \frac{m}{M^2}\right)\right\}\right)$$

Hence, the posterior  $p_{\mu_s}(\cdot)$  is also normal with mean  $\mu_{\mu_s}$  and the variance  $\sigma_{\mu_s}^2$  of the posterior  $p_{\mu_s}(\cdot)$  are:

$$\mu_{\mu_s} = \frac{\frac{\sum_{t=1}^T z_t}{\sigma_s^2} + \frac{m}{M^2}}{\frac{T}{\sigma_s^2} + \frac{1}{M^2}}$$

$$\sigma_{\mu_s}^2 = \frac{1}{\frac{T}{\sigma_s^2} + \frac{1}{M^2}}$$

Similarly, as done in the literature, we assume  $\pi(\sigma_s^2) \sim IG(\alpha_1, \beta_1)$  for  $\sigma_s^2$ , and using Bayes theorem we can derive that its posterior satisfies:

$$p_{\sigma_s^2}(\sigma_s^2 | \mathbf{z}, \mu_s) \propto \sigma_s^{-T} \exp\left(-\frac{\sum_{t=1}^T (z_t - \mu_s)^2}{2\sigma_s^2}\right) \pi(\sigma_s^2)$$

$$\propto (\sigma_s^2)^{-\alpha_1 - T/2 - 1} \exp\left(-\frac{\beta_1 + 0.5 \sum_{t=1}^T (z_t - \mu_s)^2}{\sigma_s^2}\right)$$

Thus, the posterior of  $\sigma_s^2$  follows  $IG(\alpha_2, \beta_2)$  where  $\alpha_2 = \alpha_1 + T/2$  and  $\beta_2 = \beta_1 + 0.5 \sum_{t=1}^T (z_t - \mu_s)^2$

**Remark:** As in Chapter 2, the summations of the parameters of the above posterior densities will be computed starting from  $t = 22K$  instead of  $t = 1$  if the required initial  $K$  monthly values of  $X_t$  are not available prior to the first month of the returns data.

### 4.6.4 Empirical Results

Table 4.6.1: Bayesian MCMC Estimates of SV-MIDAS, SVL-MIDAS and their jump augmented extensions

Macro	Models	No-jump augmented models										jump augmented models										
		$\mu$	$\beta$	$\kappa$	$\sigma_s$	$\rho$	$m$	$\psi$	$\omega$	DIC	$\mu$	$\beta$	$\kappa$	$\sigma_s$	$\rho$	$m$	$\psi$	$\omega$	$\mu_s$	$\sigma_s$	$\lambda$	DIC
IPUs	SVL-MIDAS	0.030	1.439	0.970	0.030	-0.194	1.622	-0.309	14.680	20049.48	0.031	1.394	0.892	0.030	-0.218	1.649	-0.345	13.212	-0.044	30.448	0.040	19654.03
	SV-MIDAS	(0.038)	(1.413)	(0.020)	(0.009)	(0.048)	(0.070)	(0.063)	(3.853)		(0.039)	(1.371)	(0.018)	(0.009)	(0.054)	(0.028)	(0.032)	(3.467)	(0.072)	(0.203)	(0.009)	19682.51
IPCh	SVL-MIDAS	0.043	1.435	0.958	0.026	-0.215	1.504	-0.408	4.910	20056.3	0.044	1.390	0.882	0.027	-0.241	1.601	-0.416	4.419	-0.018	37.477	0.044	19629.64
	SV-MIDAS	(0.042)	(1.411)	(0.031)	(0.008)	(0.050)	(0.043)	(0.039)	(1.116)		(0.043)	(1.369)	(0.029)	(0.008)	(0.056)	(0.017)	(0.019)	(1.005)	(0.096)	(0.886)	(0.010)	19699.62
EERUs	SVL-MIDAS	0.037	1.439	0.985	0.030	-0.227	1.586	-0.847	2.149	20044.65	0.038	1.394	0.906	0.030	-0.254	1.635	-0.802	1.934	-0.018	47.829	0.040	19671.49
	SV-MIDAS	(0.034)	(1.416)	(0.012)	(0.010)	(0.026)	(0.234)	(0.212)	(3.725)		(0.035)	(1.373)	(0.011)	(0.011)	(0.029)	(0.094)	(0.106)	(0.952)	(0.081)	(0.758)	(0.067)	19685.55
EERCh	SVL-MIDAS	0.040	1.454	0.979	0.041	-0.222	1.749	-0.376	18.372	20064.83	0.041	1.407	0.901	0.042	-0.249	1.700	-0.397	16.535	-0.037	29.291	0.057	19625.66
	SV-MIDAS	(0.041)	(1.429)	(0.011)	(0.020)	(0.043)	(0.086)	(0.078)	(6.920)		(0.042)	(1.385)	(0.010)	(0.020)	(0.048)	(0.034)	(0.039)	(6.228)	(0.045)	(0.298)	(0.009)	19652.48
GEPUs	SVL-MIDAS	0.030	1.554	0.985	0.044	-0.172	1.723	-0.349	18.819	20085.45	0.036	1.489	0.935	0.039	-0.244	1.601	-0.368	17.878	-0.036	28.119	0.055	19652.48
	SV-MIDAS	(0.031)	(1.529)	(0.011)	(0.021)	(0.084)	(0.078)	(7.088)		(0.037)	(1.466)	(0.011)	(0.021)	(0.038)	(0.038)	(0.037)	(6.734)	(0.043)	(0.286)	(0.009)		
EPUUs	SVL-MIDAS	0.092	1.436	0.971	0.027	-0.219	1.578	0.055	15.361	20060.84	0.094	1.391	0.893	0.028	-0.246	1.631	0.070	13.825	-0.032	36.144	0.040	19622.18
	SV-MIDAS	(0.040)	(1.407)	(0.022)	(0.005)	(0.042)	(0.104)	(0.094)	(3.804)		(0.041)	(1.365)	(0.020)	(0.005)	(0.048)	(0.042)	(0.047)	(3.424)	(0.096)	(6.920)	(0.020)	19646.18
EPUCh	SVL-MIDAS	0.069	1.536	0.976	0.029	-0.155	1.555	0.047	15.735	20080.32	0.082	1.472	0.927	0.294	-0.244	1.601	0.055	14.949	-0.031	34.698	0.039	19628.35
	SV-MIDAS	(0.030)	(1.507)	(0.022)	(0.005)	(0.102)	(0.014)	(3.897)		(0.036)	(1.445)	(0.021)	(0.055)	(0.045)	(0.024)	(3.702)	(0.092)	(0.883)	(0.019)			
EPUUs	SVL-MIDAS	0.037	1.433	0.976	0.025	-0.197	1.423	-0.086	1.903	20061.73	0.038	1.388	0.908	0.026	-0.220	1.699	-0.079	1.712	-0.019	40.855	0.044	19626.51
	SV-MIDAS	(0.028)	(1.415)	(0.004)	(0.010)	(0.012)	(0.039)	(0.036)	(0.058)		(0.028)	(1.372)	(0.003)	(0.010)	(0.013)	(0.016)	(0.018)	(0.052)	(0.015)	(0.857)	(0.014)	19644.52
GOP	SVL-MIDAS	0.032	1.436	0.982	0.027	-0.216	1.722	0.813	11.491	20048.39	0.033	1.391	0.904	0.028	-0.242	1.689	0.875	10.342	-0.023	38.350	0.052	19625.49
	SV-MIDAS	(0.014)	(1.406)	(0.015)	(0.004)	(0.063)	(0.084)	(0.076)	(4.778)		(0.014)	(1.364)	(0.014)	(0.004)	(0.070)	(0.034)	(0.038)	(4.300)	(0.028)	(0.725)	(0.018)	19649.13
OPopec	SVL-MIDAS	0.024	1.536	0.988	0.029	-0.196	1.496	0.510	11.771	20081.63	0.029	1.472	0.938	0.293	-0.244	1.601	0.055	14.949	-0.031	34.698	0.039	19628.35
	SV-MIDAS	(0.036)	(1.502)	(0.019)	(0.002)	(0.183)	(0.118)	(2.548)		(0.043)	(1.440)	(0.018)	(0.015)	(0.081)	(0.079)	(2.420)	(0.034)	(0.689)	(0.015)			
OSopec	SVL-MIDAS	0.032	1.419	0.972	0.014	-0.216	1.748	-0.065	7.184	20051.13	0.033	1.378	0.935	0.014	-0.242	1.699	-0.076	6.466	-0.021	46.240	0.035	19635.73
	SV-MIDAS	(0.016)	(1.420)	(0.025)	(0.001)	(0.059)	(0.052)	(0.047)	(2.875)		(0.016)	(1.376)	(0.023)	(0.001)	(0.067)	(0.021)	(0.024)	(2.587)	(0.018)	(0.908)	(0.015)	19682.31

Note: This table reports the estimation results of SV-MIDAS models (3.2.13-3.2.14), and SV-MIDAS-J models (4.2.31) using 10 macroeconomic indicators as explanatory variables for modelling the long term component of the volatility. DIC is a Bayesian method for model comparison developed by Spiegelhalter et al. (2002) where  $DIC = D(y, \hat{\Theta}) + 2pD$ , where  $D(y, \hat{\Theta}) = 2\log(p(y|\Theta))$ , and  $pD = var(D(y, \hat{\Theta}))$ . No jump augmented models refer to the standard SV-MIDAS, and SVL-MIDAS models, and the jump augmented models refer to SV-MIDAS-J and SVL-MIDAS-J. Standard deviations are between brackets.

Table 4.6.2: Bayesian MCMC Estimates of General Heston-MIDAS and its jump augmented extension

Macro	Models	No-jump augmented models										jump augmented models										
		$\mu$	$\beta$	$\kappa$	$\sigma_s$	$\rho$	$m$	$\psi$	$\omega$	DIC	$\mu$	$\beta$	$\kappa$	$\sigma_s$	$\rho$	$m$	$\psi$	$\omega$	$\mu_s$	$\sigma_s$	$\lambda$	DIC
IPUs	SVL-MIDAS	0.025	-0.005	0.024	0.048	-0.274	1.521	-0.385	13.960	20052.68	0.020	-0.011	0.021	0.019	-0.328	0.809	-0.387	12.830	-0.044	32.884	0.046	19647.65
	SV-MIDAS	(0.032)	(0.011)	(0.008)	(0.015)	(0.068)	(0.065)	(0.065)	(3.664)		(0.026)	(0.015)	(0.024)	(0.006)	(0.081)	(0.035)	(0.094)	(3.367)	(0.072)	(0.220)	(0.009)	
IPCh	SVL-MIDAS	0.036	-0.006	0.021	0.043	-0.303	1.410	-0.318	4.669	20027.78	0.029	-0.012	0.062	0.017	-0.362	0.750	-0.417	4.291	-0.018	40.476	0.042	19617.91
	SV-MIDAS	(0.035)	(0.012)	(0.007)	(0.012)	(0.070)	(0.040)	(0.040)	(1.062)		(0.029)	(0.015)	(0.021)	(0.005)	(0.084)	(0.021)	(0.058)	(0.976)	(0.096)	(0.957)	(0.010)	
EERUs	SVL-MIDAS	0.031	-0.006	0.023	0.048	-0.319	1.487	-0.802	2.044	20070.48	0.025	-0.012	0.070	0.019	-0.382	0.791	-0.920	1.879	-0.018	51.655	0.038	19680.21
	SV-MIDAS	(0.029)	(0.006)	(0.009)	(0.017)	(0.036)	(0.219)	(0.218)	(3.542)		(0.023)	(0.008)	(0.028)	(0.007)	(0.044)	(0.117)	(0.314)	(3.255)	(0.082)	(0.818)	(0.064)	
EERCh	SVL-MIDAS	0.034	-0.006	0.032	0.066	-0.312	1.640	-0.240	17.471	20023.73	0.027	-0.012	0.097	0.026	-0.374	0.872	-0.445	16.057	-0.038	31.634	0.055	19624.01
	SV-MIDAS	(0.034)	(0.010)	(0.018)	(0.032)	(0.061)	(0.080)	(0.080)	(6.580)		(0.028)	(0.013)	(0.053)	(0.013)	(0.073)	(0.115)	(0.648)	(0.045)	(0.322)	(0.009)		
GEPUs	SVL-MIDAS	0.077	-0.006	0.022	0.044	-0.309	1.480	0.011	14.608	20029.19	0.063	-0.012	0.065	0.018	-0.369	0.787	0.079	13.426	-0.033	39.035	0.038	19645.24
	SV-MIDAS	(0.033)	(0.010)	(0.004)	(0.008)	(0.060)	(0.097)	(0.097)	(3.617)		(0.027)	(0.013)	(0.013)	(0.003)	(0.072)	(0.052)	(0.140)	(3.235)	(0.096)	(0.993)	(0.019)	
EPUUs	SVL-MIDAS	0.086	-0.006	0.027	0.054	-0.307	1.798	0.017	2.828	20026.47	0.070	-0.012	0.080	0.022	-0.367	0.956	0.155	2.600	-0.037	39.243	0.038	19612.17
	SV-MIDAS	(0.038)	(0.010)	(0.042)	(0.008)	(0.058)	(0.130)	(0.129)	(1.453)		(0.031)	(0.012)	(0.125)	(0.003)	(0.069)	(0.069)	(0.186)	(3.325)	(0.016)	(1.079)	(0.019)	
EPUCh	SVL-MIDAS	0.031	-0.005	0.020	0.040	-0.277	2.272	-0.080	1.809	20024.64	0.025	-0.011	0.059	0.016	-0.331	1.208	-0.089	1.663	-0.020	43.691	0.042	19624.12
	SV-MIDAS	(0.023)	(0.003)	(0.009)	(0.016)	(0.017)	(0.037)	(0.037)	(0.055)		(0.019)	(0.004)	(0.026)	(0.006)	(0.020)	(0.053)	(0.051)	(0.015)	(0.015)	(0.925)	(0.014)	
GOP	SVL-MIDAS	0.027	-0.006	0.022	0.044	-0.305	1.615	0.269	10.928	20023.55	0.022	-0.012	0.065	0.018	-0.365	0.859	0.981	10.043	-0.023	41.418	0.050	19604.25
	SV-MIDAS	(0.012)	(0.015)	(0.004)	(0.006)	(0.088)	(0.079)	(0.078)	(4.543)		(0.009)	(0.019)	(0.011)	(0.003)	(0.105)	(0.042)	(0.113)	(4.176)	(0.029)	(0.783)	(0.017)	
OPopec	SVL-MIDAS	0.082	-0.006	0.022	0.044	-0.317	1.655	0.413	8.289	20038.01	0.066	-0.012	0.065	0.018	-0.380	0.880	0.505	7.618	-0.037	50.515	0.029	19646.02
	SV-MIDAS	(0.040)	(0.012)	(0.001)	(0.072)	(0.174)	(0.173)	(2.365)		(0.032)	(0.015)	(0.004)	(0.001)	(0.086)	(0.092)	(0.249)	(2.174)	(0.036)	(0.775)	(0.015)		
OSopec	SVL-MIDAS	0.027	-0.006	0.011	0.023	-0.305	1.639	-0.068	6.832	20034.01	0.022	-0.012	0.033	0.009	-0.365	0.872	-0.085	6.279	-0.021	49.939	0.033	19644.05
	SV-MIDAS	(0.013)	(0.014)	(0.012)	(0.002)	(0.084)	(0.049)	(0.049)	(2.734)		(0.011)	(0.018)	(0.014)	(0.001)	(0.100)	(0.026)	(0.050)	(2.512)	(0.018)	(0.980)	(0.015)	

Note: This table reports the estimation results of Heston-MIDAS model (3.2.21-3.2.22), and Heston-MIDAS-J models (4.2.32) using 10 macroeconomic indicators as explanatory variables for modelling the long term component of the volatility. DIC is a Bayesian method for model comparison developed by Spiegelhalter et al. (2002) where  $DIC = D(y, \hat{\Theta}) + 2pD$ , where  $D(y, \hat{\Theta}) = 2\log(p(y|\Theta))$ , and  $pD = var(D(y, \hat{\Theta}))$ . No jump augmented model refers to the Heston-MIDAS, and the jump augmented model refers to Heston-MIDAS-J. Standard deviations are between brackets.



## 5.1 Conclusions

In the recent literature, the two- components volatility GARCH-MIDAS model of Engle et al (2013) has extensively been applied for modeling the volatility of assets return. In this thesis, we investigate its finite sample performance, and we extend it to incorporate the important asymmetry effect and jump component to capture the observed sample skewness and large kurtosis. The recognized outperformance of other uni-component volatility such as EGARCH and Stochastic Volatility models over GARCH model motivates us to develop EGARCH-MIDAS, SV-MIDAS, SVL-MIDAS and Heston -MIDAS models and their Jump augmented versions.

Results of Chapter 2 indicate that it is important to include the asymmetry effect in the model by using EGARCH-MIDAS and GJRGARCH-MIDAS models improves the in sample and out sample performance of GARCH-MIDAS. Furthermore, the three models produce comparable estimate of the long term volatility component and the short term component is the predominant component as far as in sample and out sample performance is concerned: Our simulation and empirical results indicate that whenever a uni-component model, EGARCH say, outperforms GARCH, EGARCH-MIDAS outperforms GARCH-MIDAS independently of the macroeconomic variable used in the specification of the long term volatility component. The other specificity of these models is that they are uni-component volatility models with time varying intercept whose variations depend on the macroeconomic variable, suggesting their power in capturing changes in the level of the return volatility. However, their estimation inherits the recognized drawbacks of Maximum Likelihood method of GARCH, GJR-GARCH, and EGARCH models specially when the data contains outliers or when the short term volatility is highly persistent. This led us to estimate them using Bayesian method which does not suffer from the convergence of the numerically computed parameter estimates to local maxima of the likelihood, and the computation of their confidence intervals do not require their asymptotic normality which has not been proved yet. Finally, our empirical study suggests that the most explanatory macroeconomic variable is not necessarily a country-specific macroeconomic indicator, and the macroeconomic variable which produces the best in sample fit, it also produces the best forecasts. Results of Chapter 3 indicate that our MCMC algorithms for estimating GARCH-MIDAS, GJR-GARCH-MIDAS, and EGARCH-MIDAS models compete with Maximum Likelihood Estimates(MLE) which are obtained from convergence to the global maximum

of the likelihood, corresponding to cases when the returns data does not contain outliers and when the short term volatility component is not highly persistent. However, MLE depend crucially on the initial values of the parameters which are used for numerical maximization of the likelihood, and they produce erroneous decision on the impact of the macroeconomic variable considered in the model of the long-term component. Hence, our MCMC algorithms are to be recommended to practitioners who are not familiar with Bayesian approach despite that MCMC estimates are computed using Metropolis-Hasting simulation Method due to the fact the posterior distributions of the parameters do not belong to known family of distributions from which draws can easily be obtained. Furthermore, our simulation study indicates that incorporating the jump component by modelling the error term by a mixture of the two normal terms, as done in the literature of jump augmented GARCH(1,1), produces accurate parameter estimates of the jump component. Our empirical study indicates that (Jump augmented) EGARCH-MIDAS is preferred to (Jump augmented) GARCH-MIDAS and GJR-GARCH-MIDAS models for modelling the volatility WTI returns, and  $OP_{OPEC}$  is the most explanatory macroeconomic variable.

In Chapter 4, we developed two components stochastic volatility models (SV-MIDAS, SVL-MIDAS, and Heston-MIDAS), and designed MCMC algorithm for estimating their parameters. Our Heston-MIDAS model competes with the recent extensions of Heston model which aim to capture changes in observed levels of volatility over long subperiods. The identifiability of the two volatility components of Heston-MIDAS is overcome by restricting  $\theta = 1$  to ensure the unconditional mean of the short term component is equal to one, and we use our scaling method of EGARCH-MIDAS for SV-MIDAS and SVL-MIDAS models since their short term component is also specified by log-volatility. The posterior distribution of the parameters belong to known families or can be approximated by normal distributions whose parameters are easily derived from their 2nd order Taylor expansions whereas we use random walk procedure for drawing from the posteriors of the latent short term volatilities  $g_t$ 's after having overcome the ad hoc choice of the standard deviation of gaussian perturbations by the smoothing parameter of the kernel density. Our simulation study indicates that our MCMC algorithms produce accurate parameter estimates of the three models, and convergence of the MCMC algorithm is fast for Heston and Heston-MIDAS by tuning the perturbation by the kernel smoothing parameter. Finally our empirical study of WTI returns confirms that the long term component estimate does not depend on the choice of the model of the short term component but the total volatility of the return does, and the most explanatory macroeconomic variable is also  $OP_{OPEC}$ .

In future work, we plan to extend our flexible Bayesian approach to replace the model of the long term component by more realistic models by including an auto-regressive component and/or adding a jump component to capture changes in the dynamics of the macroeconomic variable or financial variable used in the specification of the long term volatility component. We are planning to also incorporate the leverage effect of the long term component for stochastic volatility MIDAS models by considering stochastic long term specification whose error term will be correlated with that of the return. In other words, the leverage effect of the short term component is assessed by  $\rho_1 = corr(r_t, g_{t+1})$  whereas the leverage effect of the long term com-

ponent will be measured by  $\rho_2 = \text{corr}(r_t, \tau_{t+1})$ .

It is natural to model the long term component using more than one macroeconomic variable to better capture the impact of economic environment. The extension of our Bayesian method is trivial when the macroeconomic variables are not co-integrated. When this is not the case there is an issue of identification of the parameters of the macroeconomic variables due to co-integration. We will investigate whether if this issue can be overcome by selecting the parameters of their priors from their estimates when they are used individually (One macroeconomic is used).

Lastly, it will be interesting to extend our Bayesian approach to DCC-MIDAS model of Conrad et al. (2015) for modelling bi-variate returns by using spatial auto-regressive panel data models. It will also be very interesting to investigate if Heston-MIDAS can easily be used in option pricing by exploring the impact of the long term component on the characteristic function.



## References

- Abi Jaber, E. (2019). The characteristic function of Gaussian stochastic volatility models: an analytic expression. Available at: <https://arxiv.org/pdf/2009.10972.pdf>
- Adrian, T. and Rosenberg, J. (2008), Stock Returns and Volatility: Pricing the Short-Run and Long-Run Components of Market Risk. *The Journal of Finance*, 63, 2997-3030.
- Afees, A. Salisu, and Rangan, G. and Elie, B. and Qiang, J. (2020). Forecasting Oil Volatility Using a GARCH-MIDAS Approach: The Role of Global Economic Conditions, Working Papers 202051, University of Pretoria, Department of Economics.
- Ait-Sahalia, Y. and Kimmel, R. (2007). Maximum likelihood estimation of stochastic volatility models. *Journal of Financial Economics*, 83, 413-452.
- Amado, C. and Teräsvirta, T. (2013). Modelling volatility by variance decomposition. *Journal of Econometrics*, 175, 142-153.
- Amado, C. Silvennoinen, A. and Teräsvirta, T. (2018). Models with Multiplicative Decomposition of Conditional Variances and Correlations. CREATES Research Papers 2018-14, Department of Economics and Business Economics, Aarhus University.
- Amendola, A., Candila, V., Scognamillo, A., (2017). On the Influence of US Monetary Policy on Crude Oil Price Volatility. *Empirical Economics*, 52, 155-178.
- Andersen, T.G., L. Benzoni, and J. Lund. (2002). Estimating Jump-Diffusions for Equity Returns. *Journal of Finance*, 57, 1239-84.
- Anyfantaki, S. and Demos, A. (2014). Estimation and Properties of a Time-Varying EGARCH(1,1) in Mean Model. *Econometric Reviews*, 35, 293-310.
- Asgharian, H., Hou, A.J., Javed, F. (2013). The Importance of the Macroeconomic Variables in Forecasting Stock Return Variance: A GARCH-MIDAS Approach. *Journal of Forecasting*, 32, 600-612.
- Mubarak, A., and Giouvris, E. (2017). A Comparative GARCH Analysis of Macroeconomic Variables and Returns on modelling the kurtosis of FTSE 100 Implied Volatility Index. *Multinational Finance Journal*, 22, 119-172.
- Ardia, D. (2008) Bayesian Estimation of a Markov-Switching Threshold Asymmetric GARCH Model with Student-t Innovations. *Econometrics Journal*, 12, 105-126.
- Ausan, M. C., and Galeano, P. (2007). Bayesian estimation of the Gaussian mixture GARCH model. *Computational Statistics and Data Analysis*, 51, 2636-2652.
- Awartani, B. and Corradi, V. (2005). Predicting the Volatility of SP-500 Stock Index via GARCH Models: The Role of Asymmetries. *International Journal of Forecasting*, 21, 167-183.

- Bai, X., Russell, J. R., and Tiao, G. C. (2003). Kurtosis of GARCH and stochastic volatility models with non-normal innovations. *Journal of econometrics*, 114, 349-360.
- Bates, D. S., (2001), The market for crash risk, Working Paper No w8557, University of Iowa, Finance Department. Available at SSRN: <https://ssrn.com/abstract=287754>.
- Bauwens, L., and Lubrano, M. (1998). Bayesian inference on GARCH models using the Gibbs sampler. *The Econometrics Journal*, 1, 23-46.
- Black, F. and Scholes, M. (1976). The Pricing of Options and Corporate Liabilities. *The Journal of Political Economy*, 81, 637-654.
- Borup, D., and Jakobsen, J. S. (2019). Capturing volatility persistence: a dynamically complete realized EGARCH-MIDAS model. *Quantitative Finance*, 19, 1839-1855.
- Bollerslev, T. (1987). A conditionally heteroskedastic time series model for speculative prices and rates of return. *The review of economics and statistics*, 69, 542-547.
- Broadie, M., Chernov, M. and Johannes, M. (2007). Model Specification and Risk Premia: Evidence from Futures Options. *Journal of Finance*, 62, 1453-1490.
- Broto, C. and Ruiz, E. (2004) Estimation Methods for Stochastic Volatility Models: A Survey. *Journal of Economic Surveys*, 18, 613-649.
- Campbell, S. D., and Diebold, F. X. (2009). Stock Returns and Expected Business Conditions: Half a Century of Direct Evidence. *Journal of Business and Economic Statistics*, 27, 266-278.
- Carnero, M. A., Pena D., and Ruiz, E. (2003). Persistence and kurtosis in GARCH and stochastic volatility models *Journal of Financial Econometrics*, 2, 319-342.
- Chan, J. C., and Grant, A. L. (2016). Modeling energy price dynamics: GARCH versus stochastic volatility. *Energy Economics*, 54, 182-189.
- Chan, J. C., and Eisenstat, E. (2015). Marginal likelihood estimation with the Cross-Entropy method. *Econometric Reviews*, 34, 256-285.
- Chen, N., Roll, R. and Ross, S. (1986). Economic forces and the stock market. *Journal of Business*, 59, 383-403.
- Chen, L., Zerilli, P., and Baum, C. F. (2020). Leverage effects and stochastic volatility in spot oil returns: A Bayesian approach with VaR and CVaR applications. *Energy Economics*, 79, 111-129.
- Chib, S., and Greenberg, E. (1995). Understanding the metropolis-hastings algorithm. *The american statistician*, 49, 327-335.
- Chib, S., and Jeliazkov, I. (2001). Marginal likelihood from the Metropolis-Hastings output. *Journal of the American Statistical Association*, 96, 270-281.
- Chong, C.W., Ahmad, M.I. and Abdullah, M.Y. (1999), Performance of GARCH models in forecasting stock market volatility. *Journal of Forecasting*, 18, 333-343.
- Choudhry, T. and Wu, H. (2008) Forecasting ability of GARCH vs Kalman filter method: evidence from daily UK time-varying beta. *Journal of Forecasting*, 27, 670-689.
- Clements, A. (2007). SP 500 implied volatility and monetary policy announcements. *Finance Research Letters*, 4, 227-232.

- 
- Conrad, C., K. Loch, and D. Rittler (2014). On the macroeconomic determinants of long-term volatilities and correlations in U.S. stock and crude oil markets. *Journal of Empirical Finance*, 29, 26-40.
  - Conrad C. and Loch K., (2015), Anticipating Long-Term Stock Market Volatility, *Journal of Applied Econometrics*, 30, 1090-1114.
  - Conrad, C. and Kleen, O. (2018). Two Are Better Than One: Volatility Forecasting Using Multiplicative Component GARCH Models. *Journal of Applied Econometrics*, 35, 19-45.
  - Conrad, C. and Schienle M., (2018). "Testing for an omitted multiplicative long-term component in GARCH models." *Journal of Business and Economic Statistics*, 38, 229-242.
  - Corsi, F. (2009). A Simple Approximate Long-Memory Model of Realized Volatility. *Journal of Financial Econometrics*, 7, 174-196.
  - Christoffersen, P., Jacobs, K. and Mimouni, K. (2010). Volatility Dynamics for the SP500: Evidence from Realized Volatility, Daily Returns and Option Prices. *Review of Financial Studies*, 23, 3141-3189.
  - Cuervo, G. Helio S. and Achcar, J. (2014). Generalized linear models with random effects in the two-parameter exponential family. *Journal of Statistical Computation and Simulation*. 84, 513-525.
  - DiCiccio, T. J., Kass, R. E., Raftery, A., and Wasserman, L. (1997). Computing Bayes factors by combining simulation and asymptotic approximations. *Journal of the American Statistical Association*, 92, 903-915.
  - Efimova, O., and Serletis, A. (2014). Energy markets volatility modelling using GARCH. *Energy Economics*, 43, 264-273.
  - Engle, R. F. (1982). Autoregressive Conditional Heteroscedasticity with Estimates of the Variance of United Kingdom Inflation. *Econometrica*, 50, 987-1007.
  - Engle, R.F. and Lee, G. (1999) A Permanent and Transitory Component Model of Stock Return Volatility. *Cointegration, Causality and Forecasting: A Festschrift in Honor of Clive W.J. Granger*. Oxford University Press, New York.
  - Engle, R. F., and Rangel, J., (2008). The Spline-GARCH model for low frequency volatility and its global macroeconomic causes, *Review of Financial Studies*, 21, 1187-1222.
  - Engle, R. F., Ghysels, E. and Sohn, B. (2013) Stock market volatility and macroeconomic fundamentals. *Review of Economics and Statistics*, 95, 776-797.
  - Eraker, B., Johannes, M. and Polson, N. (2003) The Impact of Jumps in Volatility and Returns. *Journal of Finance*, 58, 1269-1300.
  - Ewing, B. and Malik, F. (2017). Modelling Asymmetric Volatility in Oil Prices under Structural Breaks. *Energy Economics*, 63, 227-233.
  - Fang T., Lee T., and Su Z. (2020). Predicting the long-term stock market volatility: A GARCH-MIDAS model with variable selection. *Empirical Finance*, 58, 36-49.
  - Feng, Y. (2004). Simultaneously Modelling Conditional Heteroskedasticity and Scale Change. *Econometric Theory*, 20, 563-596.

- Francq, C., Wintenberger, O. and Zakoian, J.M. (2013). GARCH Models Without Positivity Constraints: Exponential or Log-GARCH. *Journal of Econometrics*, 177, 34–46.
- Ghysels, E., Sinko, A. and Valkanov, R. (2006). MIDAS regression: further results and new directions. *Econometric Reviews*, 26, 53-90.
- Glosten, L.R., Jagannathan, R. and Runkle, D.E. (1993). On the Relation between the Expected Value and the Volatility of the Nominal Excess Return on Stocks. *The Journal of Finance*, 48, 1779-1801.
- Goldman, E. and Shen, X. (2018). Analysis of Asymmetric GARCH Volatility Models with Applications to Margin Measurement. Pace University Finance Research Paper No. 2018/03.
- Grasselli, M. (2017), The 4/2 stochastic volatility model: a unified approach for the heston and the 3/2 model. *Mathematical Finance*, 27, 1013-1034.
- Hafner C.M. and Linton, O. (2009). Efficient Estimation of a Multivariate Multiplicative Volatility Model, STICERD - Econometrics Paper Series 541, Suntory and Toyota International Centres for Economics and Related Disciplines, LSE.
- Han, H. and Kristensen, D. (2015) Asymptotic Theory for the QMLE in GARCH-X Models with Stationary and Non-stationary Covariates. *Journal of Business and Economic Statistics*, 32, 416-429.
- Han, X. and Lee, L.F. (2016): Bayesian Analysis of Spatial Panel Autoregressive Models With Time-Varying Endogenous Spatial Weight Matrices, Common Factors, and Random Coefficients. *Journal of Business and Economic Statistics*, 34, 642-660.
- Hansen, P. and Huang, Z., (2016). Exponential GARCH Modeling With Realized Measures of Volatility, *Journal of Business & Economic Statistics*, 34, 269-287.
- Harvey, A. and Shephard, N. (1996). Estimation of an Asymmetric Stochastic Volatility Model for Asset Returns. *Journal of Business and Economic Statistics*, 14, 429-434.
- Heston, S. (1993). A Closed-Form Solution for Options with Stochastic Volatility with Applications to Bond and Currency Options. *Review of Financial Studies*, 6, 327-343.
- Heston, S. (1997). A Simple New Formula for Options with Stochastic Volatility. OLIN-97-23. Available at SSRN: <https://ssrn.com/abstract=86074>
- Heynen, R. C. and Kat, H. M. (1994). Volatility prediction: A comparison of stochastic volatility, GARCH(1,1) and EGARCH(1,1) models. *Journal of Derivatives*, 2, 50-65.
- Hull, J. and White, A. (1987). The Pricing of Options on Assets with Stochastic Volatilities. *The Journal of Finance*, 42, 281-300.
- Jacquier, E., Doan, T., Polson, N., and Rossi, P. (1994). Bayesian Analysis of Stochastic Volatility Models. *Journal of Business and Economic Statistics*, 12, 371-89.
- Jeffreys, H. (1961). Small corrections in the theory of surface waves. *Geophysical Journal International*, 6, 115-117.
- Jones, C. (2003). The Dynamics of Stochastic Volatility: Evidence from Underlying and Options Markets. *Journal of Econometrics*, 16, 1-22.
- Kass, R. E., and Raftery, A. E. (1995). Bayes factors. *Journal of the american statistical association*, 90, 773-795.



- Khan, M. I., Yasmeen, T., Shakoor, A., Khan, N. B., and Muhammad, R. (2017). 2014 oil plunge: Causes and impacts on renewable energy. *Renewable and Sustainable Energy Reviews*, 68, 609-622.
- Kim, S., Shephard, N. and Chib, S. (1998) Stochastic Volatility: Likelihood Inference and Comparison with ARCH Models. *Review of Economics Studies*, 65, 361-393.
- Klein, T. and Walther, T. (2016). Oil price volatility forecast with mixture memory GARCH. *Energy Economics*, 58, 46-58.
- Koo, B., and Linton, O. (2015). Robust estimation of semiparametric multiplicative volatility models. *Econometric Theory*, 31, 671-702.
- Kyriakopoulou, D. (2015), Asymptotic Normality of the QML Estimator of the EGARCH(1,1) Model. Available at SSRN: <https://ssrn.com/abstract=2236055>.
- Lee, T. and Lee, S. (2009), Normal Mixture Quasi-maximum Likelihood Estimator for GARCH Models. *Scandinavian Journal of Statistics*, 36, 157-170.
- Fang L., Chen, B., Yu, H. and Qian, Y. (2017), The importance of global economic policy uncertainty in predicting gold futures market volatility: A GARCH-MIDAS approach, *Journal of Futures Markets*, 38, 56-63.
- Lin J., and Chang H.Y. (2020). Volatility transmission from equity, bulk shipping, and commodity markets to oil etf and energy fund a GARCH-MIDAS model. *Mathematics*, 8, 2-17.
- Lin, Z. (2018). Modelling and forecasting the stock market volatility of SSE Composite Index using GARCH models. *Future Generation Computer Systems*, 79, 960-972.
- Liu, H. C. and Hung, J. C, (2010) "Forecasting SP-100 Stock Index Volatility: The Role of Volatility Asymmetry and Distributional Assumption in GARCH Models," *Expert Systems With Applications*, 37(7). 4928-4934.
- Liu, J., Ma, F., Tang, Y., and Zhang, Y. (2019). Geopolitical risk and oil volatility: A new insight. *Energy Economics*, 84, 104548.
- Lumsdaine, R. (1995). Finite-sample properties of the maximum-likelihood estimator in garch(1,1) and igarch(1,1) models a monte carlo investigation. *Journal of Business and Economic Statistics*, 13, 1–10.
- Men Z., Yee E., Lien F.S., Wen D., and Chen Y., (2016). Short-term wind speed and power forecasting using an ensemble of mixture density neural networks. *Renewable Energy*, 87, 203-211.
- Men. Z., McLeish D., Kolkiewicz A.W., and Wirjanto T.S., (2017). Comparison of asymmetric stochastic volatility models under different correlation structures, *Journal of Applied Statistics*, 44, 1350–1368.
- Mi Z.F., Wei Y.M., Tang B.J., Cong R.G., Yu H., Cao H., and Guan D., (2017) .Risk assessment of oil price from static and dynamic modelling approaches. *Applied Econometrics*. 929-939.
- Mota, P.P. and Esquivel, M.L.,(2014). On a continuous time stock price model with regime switching, delay, and threshold. *Quantitative Finance*, 14, 1479–1488.
- Nakajima, J. (2012), Bayesian analysis of generalized autoregressive conditional heteroskedasticity and stochastic volatility: modeling leverage, jumps, heavy-tails for fi-

- nancial time series. *The Japanese Economic Review*, 63, 81-103.
- Nakatsuma, T. (2000). Bayesian analysis of ARMA-GARCH models: A Markov chain sampling approach. *Journal of Econometrics*, 95, 57-69.
  - Naimy V. Y., and Hayek M.R. (2018). Modelling and predicting the Bitcoin volatility using GARCH models. *International Journal of Mathematical Modelling and Numerical Optimisation*, 688, 855-866.
  - Nelson, D. B. (1991). Conditional heteroskedasticity in asset returns: A new approach. *Econometrica: Journal of the Econometric Society*, 59, 347-370.
  - Newton, M. A., and Raftery, A. E. (1994). Approximate Bayesian inference with the weighted likelihood bootstrap. *Journal of the Royal Statistical Society: Series B (Methodological)*, 56, 3-26.
  - Wintenberger, O. (2013), Continuous Invertibility and Stable QML Estimation of the EGARCH(1,1) Model, *Scandinavian Journal of Statistics*, 40, 846-867.
  - Olubusoye, O. E., Yaya, O. S., and Ojo, O. O. (2016). Misspecification of Variants of Autoregressive GARCH Models and Effect on In-Sample Forecasting. *Journal of Modern Applied Statistical Methods*, 15,350-361.
  - Omori, Y., and Watanabe, T. (2008). Block sampler and posterior mode estimation for asymmetric stochastic volatility models. *Computational Statistics and Data Analysis*, 52, 2892-2910.
  - Pan Z., Wang, C. W., and Libo Y., (2017). Oil price volatility and macroeconomic fundamentals: A regime switching GARCH-MIDAS model, *Journal of Empirical Finance*, 43, 130-142.
  - Roberts, G. O., Gelman, A., and Gilks, W. R. (1997). Weak Convergence and Optimal Scaling of Random Walk Metropolis Algorithms. *The Annals of Applied Probability*, 7, 110–120.
  - Roberts, G. O., and Smith, A. F. (1994). Simple conditions for the convergence of the Gibbs sampler and Metropolis-Hastings algorithms. *Stochastic processes and their applications*, 49, 207-216.
  - Roberts, G. O., and Rosenthal, J. S. (2009). Examples of adaptive MCMC. *Journal of computational and graphical statistics*, 18, 349-367.
  - Shephard N., and Kim S. (1994). *Stochastic Volatility: Likelihood Inference and Comparison with ARCH Models*, Review of Economic Studies, Oxford University Press, 65, 361-393.
  - Sachs R.V. and van Bellegem, S. (2004). Forecasting Economic Time Series with Unconditional Time-Varying Variance. *International Journal of Forecasting*, 20, 611– 627.
  - Salisu, A. A., and Isah, K. O. (2017). Revisiting the oil price and stock market nexus: A nonlinear Panel ARDL approach. *Economic Modelling*, 66, 258-271.
  - Salisu, A. A., and Fasanya, I. O. (2012). Comparative performance of volatility models for oil price. *International Journal of Energy Economics and Policy*, 2, 167-183.
  - Schwarz, G. (1978). Estimating the dimension of a model. *The annals of statistics*, 6, 461-464.

- 
- Stramer O., Shen, X. and Bognar, M. A. (2017). Bayesian inference for Heston-STAR models. *Statistics and Computing*, 27, 331-348.
  - Sun B, Yu H, Fang L (2018) The role of global economic policy uncertainty in long-run volatilities and correlations of U.S. industry-level stock returns and crude oil. *Plos one*, 13, 1-17.
  - Taylor S. J. (1986), *Modelling Financial Time Series*, Chichester.
  - Takaishi, T. (2011). Volatility estimation using a rational GARCH model. *Quantitative Finance and Economics*, 2, 127-136.
  - Teresiene, D. (2009). Lithuanian stock market analysis using a set of GARCH models. *Journal of Business Economics and Management*. 10. 349-360.
  - Van Bellegem S., and Sachs R.V., (2004), Forecasting economic time series with unconditional time-varying variance. *International Journal of Forecasting*, 20, 611-627.
  - Vogt, M, Walsh, C. (2018). Estimating nonlinear additive models with nonstationarities and correlated errors. *Scandinavian Journal of Statistics*. 46, 160-199.
  - Vogt, M. and Walsh, C. (2018). Estimating Nonlinear Additive Models with Non-stationarities and Correlated Errors *Scandinavian Journal of Statistics*, 46, 160-199.
  - Vrontos, I. D., Dellaportas, P., and Politis, D. N. (2000). Full Bayesian inference for GARCH and EGARCH models. *Journal of Business and Economic Statistics*, 18, 187-198.
  - Wang, F., and Ghysels, E. (2015). Econometric analysis of volatility component models. *Econometric Theory*, 31, 362-393.
  - Wang, J., Zhou, H., Hong, T., Li, X., and Wang, S. (2020). A multi-granularity heterogeneous combination approach to crude oil price forecasting. *Energy Economics*, 91, 104790.
  - Wasserman, L., DiCiccio, T. J., Kass, R. E., and Raftery, A. (1997). Computing Bayes Factors by Combining Simulation and Asymptotic Approximations. *Journal of the American Statistical Association*, 92, 903-915.
  - Wei, Y., Wang, Y., and Huang, D. (2010). Forecasting crude oil market volatility: Further evidence using GARCH-class models. *Energy Economics*, 32, 1477-1484.
  - Yi, A., Yang, M., and Li, Y. (2021). Macroeconomic Uncertainty and Crude Oil Futures Volatility- Evidence from China Crude Oil Futures Market. *Frontiers in Environmental Science*, 9, 21.
  - Yin, L. and Zhou, Y., (2016). What drives long-term oil market volatility Fundamentals versus speculation. *Economics - The Open-Access, Open-Assessment E-Journal*, Kiel Institute for the World Economy, 10, 1-26.
  - You, Y. and Liu, X., (2020), Forecasting short-run exchange rate volatility with monetary fundamentals: A GARCH-MIDAS approach, *Journal of Banking and Finance*, 116, e105849.
  - Yu, H., Fang, L., Sun, B. (2018). The role of global economic policy uncertainty in long-run volatilities and correlations of U.S. industry-level stock returns and crude oil. *PloS one*, 13, e0192305.

- 
- Zakoian. J.M. (1994). Threshold Heteroskedastic Models. *Journal of Economic Dynamics and Control*, 18, 931-955.
  - Zhang, Y., Ma, F., Shi, B., and Huang, D. (2018). Forecasting the prices of crude oil: An iterated combination approach. *Energy Economics*, 70, 472-483.
  - Zou, W. and Chen, J. (2013). Markov regime-switching model in crude oil market: Comparison of composite likelihood and full likelihood. *The Canadian Journal of Statistics*, 41, 717-724.